



## Innovative Superabsorbent Polymers for Crack Mitigation of Concrete Structures: From Laboratory to Construction Site

**José Roberto Tenório Filho**

Doctoral dissertation submitted to obtain the academic degree of  
Doctor of Civil Engineering

### **Supervisors**

Prof. Nele De Belie, PhD - Didier Snoeck, PhD

Department of Structural Engineering and Building Materials  
Faculty of Engineering and Architecture, Ghent University

June 2021



**GHENT  
UNIVERSITY**





## **Innovative Superabsorbent Polymers for Crack Mitigation of Concrete Structures: From Laboratory to Construction Site**

**José Roberto Tenório Filho**

Doctoral dissertation submitted to obtain the academic degree of  
Doctor of Civil Engineering

### **Supervisors**

Prof. Nele De Belie, PhD - Didier Snoeck, PhD

Department of Structural Engineering and Building Materials  
Faculty of Engineering and Architecture, Ghent University

June 2021

ISBN 978-94-6355-505-0

NUR 955

Wettelijk depot: D/2021/10.500/53



## **Members of the Examination Board**

### **Chair**

Prof. Em. Luc Taerwe, PhD, Ghent University

### **Other members entitled to vote**

Prof. Geert De Schutter, PhD, Ghent University

Prof. Konstantin Kovler, PhD, Technion Israel Institute of Technology, Israel

Prof. Romildo Dias Toledo Filho, PhD, Universidade Federal do Rio de Janeiro, Brazil

Prof. Kim Van Tittelboom, PhD, Ghent University

Prof. Sandra Van Vlierberghe, PhD, Ghent University

### **Supervisors**

Prof. Nele De Belie, PhD, Ghent University

Didier Snoeck, PhD, Ghent University



*De costas voltadas, não se vê o futuro  
Nem o rumo da bala, nem a falha do muro [...]*

*Pedro Abrunhosa*



## Acknowledgements

The journey to the conclusion of this PhD started years ago and could not have been concluded without the help and inspiration from many people. It only feels right to begin this book by sharing a part of that story and expressing my enormous gratitude to all of those people.

It all started with a curious teenager, back in 2009, wondering what would happen if one would add more sand or more cement to a concrete mixture. That curiosity grew bigger and bigger, and by 2011, it became a passion, when I gave my initial steps towards research in the first year of my Civil Engineering studies. That passion and curiosity were welcomed and further developed by my first ever supervisors, prof. Karol, prof. Silvia and prof. Suzann. They showed me that my passion could become my profession and became the first role-models of what kind of successful professional I would like to be. *Queridas professoras, orientadoras e meus grandes exemplos de sucesso profissional: a vocês, um imenso obrigado.*

In 2012, such passion and curiosity gave place to a dream, inspired by a name that kept showing up in most papers from my literature studies and that I had the chance to learn from in the first Brazilian Concrete Conference I attended. That was prof. Geert De Schutter, who first introduced me to labo Magnel-Vandepitte. On that day, I decided that I wanted to come to Ghent University. The moment then arrived in 2015 and here I was as an exchange student to live the most amazing experience of my life so far. At this same period, I met my second inspiration within Ghent University: prof. Nele De Belie, who guess what, became my PhD supervisor (but that is for later). She might not remember this, but on my first day at her course “Life cycle assessment of materials and structures” I had to ask her to sign my learning agreement to be officially allowed to follow her course. On that occasion, she looked at me and said “ah, there is someone wanting an autograph”. Yeah, well, I have to say that after that first lesson I did become a fan. *Bom, nesse capítulo da minha trajetória eu não posso deixar de agradecer a quem nem mesmo me conhece, mas que forneceram os meios que me permitiram viver esse sonho. Aos ex-presidentes do Brasil, Luiz Inácio Lula da Silva e Dilma*

*Rousseff: obrigado por enxergarem a educação, a ciência e a tecnologia como motores para o desenvolvimento do nosso país.*

After a lot of studying hours, wonderful people, tons of waffles (and many, MANY nights on the the amazing Overpoorstraat) it was time to go back home. A year after returning to Brazil to complete my studies, and now we are in 2017, Ghent University popped-up again: a short video of this impressive and innovative project (SMARTCAST) took me once again to the website of the University looking for more information about that super cool project (I mean, active control of concrete rheology during casting?! Who would not be mesmerized by that?). Well, to my disappointment I could not find more information about this project, but there was something else that definitely caught my attention on the website of Ghent University that day: **Doctoral (PhD) full time position in ‘Innovative SuperAbsorbent Polymers for crack mitigation and increased service life of concrete structures’**. You can already imagine that my first reaction was to ask google what were SuperAbsorbent Polymers. To my surprise, the first thing I saw was a cute baby wearing what seemed to be some very comfortable diapers. But wait, is that right? Are diapers saving the day in the concrete industry?? If that is not the coolest thing I had seen in my student life so far, I don’t know what would it be. To my surprise, the contact person of the project was prof. Nele De Belie.

On that day I thought, whoa, that would be a very nice opportunity to return to Ghent and finally do research there. But then, would I be ready to take on a PhD without having followed a master? (in Brazil we have a 5-years bachelor degree followed by an optional 2-years master for those who wish to give a step further into research). In the moment of doubt I’ve heard from a very wise friend: *Amigo, só vai. Se alguém consegue é tu! (the closest translation I can give: “Dear, go for it!”)*. *Por esse conselho de ouro, minha eterna gratidão à minha amiga Natália Vieira. Amiga, tu sabe né, é nós.* So yes, I sent an e-mail to prof. De Belie with some questions about the project. One day after my first message I also received an e-mail from this Dr. Didier Snoeck, welcoming my application for the position. A few months later, lots of anxiety and tons of e-mails, I finally received a message containing my name and the words “ranking”, “position 1”, “would you accept the position?”. That was all I could read

in that moment, and as you might be wondering, of course, I packed and moved (not right away though). Dear Dr. Snoeck, or Didier (as you became afterwards), in case you were not aware of that, in that day you changed my life. And for that, I will be forever grateful.

After a lot of celebration, tons of documents, tears and see-you-soon-hugs, I started my PhD in January 2018. From there, it has been the craziest of the rollercoasters with uncountable ups and downs and the most amazing people I could have asked for, to whom I would now like to express my gratitude. I will start with the whole C&E team and all of its members since I have arrived here, but specially: Adelaide, Natália, Bjorn, Judy, Puput, Juan Manuel, Yasmina and Vanessa for making our workplace such a joyful place to go to. Next, my office mates Laurence, Nicky and Didier (who would know it could be so funny to share the office with your supervisor). The amazing staff team of labo Magnel-Vandepitte, each and every one of which were a fundamental part of the results presented in this book. I would particularly like to say a huge thank you to Tommy, Tom, Dieter, Christel, Marijke and Jens for all the support in the lab over these years (I know you must hear that a lot, but still that is not enough: guys, you are life-savers!). To all the iSAP members for the unquestionable dedication to our project, the most fruitful discussions, and incredible effort to make everything work in the best of the ways. Namely, Luc, Stijn, Sandra, Kim and Els. The amazing team from InterBeton and Artes Depret for all the support during the on-site campaign, and specially Stefaan who was always so kind and helpful in my visits to Brugge and ZeeBrugge. To the jury members of my evaluation committee who so kindly contributed with the improvement of this work.

To all my friends, here and across the ocean, who stood by me every step of the way, for the good and the bad. Specially to Thais and Matheus: *meus pais me deram dois irmãos de sangue e a vida me deu vocês de brinde.*

*E pra finalizar, o agradecimento mais especial àqueles que me deram a vida, que a partilham comigo a cada momento, e que não se cansam de me dar o suporte incondicional que me trouxe até aqui. Mãe, Pai, Vó, Bela, Zé, vocês são minha estrutura e nenhum concreto jamais vai superar a resistência e a durabilidade dessa fundação chamada família.*



# Table of contents

Summary .....	i
Samenvatting.....	vii
Resumo .....	xiii
Chapter 1.     General introduction .....	1
1.1     Shrinkage cracking in concrete structures .....	2
1.2     Objectives of the thesis .....	7
1.3     Outline of the thesis .....	8
References.....	11
Chapter 2.     Superabsorbent polymers (SAPs) and their potential as an admixture for cementitious materials .....	13
2.1     General definition.....	14
2.2     Synthesis of SAPs.....	15
2.3     Most common applications.....	17
2.4     Applications of SAPs in cementitious materials .....	18
2.5     Sorption and desorption behavior .....	20
2.6     SAPs used in the research .....	23
2.6.1     Commercial SAPs.....	25
2.6.2     (In-house developed) Alginate-based SAPs.....	25
2.6.3     (In-house developed) Sulfonate-based SAPs.....	26
2.6.4     Water absorption of the SAPs in different fluids .....	29
2.7     Conclusions.....	36
References.....	38
Chapter 3.     The effects of SAPs on cement pastes.....	45
3.1     Introduction.....	47
3.2     Absorption capacity of SAPs in cement pastes .....	48

3.3	Development of autogenous shrinkage strain .....	55
3.4	Effects on the compressive strength .....	63
3.5	Desorption kinetics of SAPs and effects on the internal relative humidity (IRH) of cement pastes .....	69
3.6	Effects on the setting time and hardening of the cement pastes .....	74
3.7	Conclusions.....	80
	References .....	82
Chapter 4. Investigation of different approaches to determine the time-zero as start for autogenous shrinkage measurements in cement pastes .....		
4.1	Time-zero in literature: definition and measurement methods.....	89
4.2	Determination of the time-zero in this research.....	92
4.2.1	Mixture compositions.....	92
4.2.2	Measuring the autogenous shrinkage and setting/hardening of the mixtures .....	93
4.2.3	Build-up in the capillary pressure .....	93
4.2.4	Air void analysis .....	94
4.3	Results and discussion .....	95
4.3.1	Setting time .....	95
4.3.2	Transition point between fluid and solid state based on the rate of autogenous strain.....	96
4.3.3	Development of capillary pressure.....	98
4.3.4	Autogenous strain for different time-zeros.....	100
4.4	Practical issues and conclusions .....	105
	References .....	107
Chapter 5. The effects of SAPs on concrete mixtures under laboratory conditions .....		
		111

5.1	Introduction.....	113
5.2	Preliminary mix-design.....	117
5.2.1	Production of the reference mixture .....	117
5.2.2	Production of the SAP-containing mixtures and water absorption of SAPs in concrete .....	118
5.3	Effects of SAPs on the shrinkage of concrete mixtures.....	121
5.3.1	Manual measurements .....	121
5.3.2	Monitoring the deformation of concrete specimens with optical fiber (SOFO) sensors .....	128
5.4	Effects of SAPs on the compressive strength of concrete.....	136
5.5	Effects of SAPs on the scaling resistance of concrete under freeze-thawing with de-icing salts .....	139
5.6	Promotion of immediate sealing in cracked concrete .....	148
5.7	Conclusions.....	153
	References.....	156
Chapter 6. The use of SAPs for the construction of crack-free large- scale structures under realistic conditions .....		
6.1	Introduction.....	163
6.2	Mixing SAPs in concrete: from laboratory scale to the concrete plant .....	164
6.2.1	Concrete mixtures produced in the laboratory.....	164
6.2.2	Mixtures compositions produced in the concrete plant.....	167
6.2.3	Shrinkage measurements.....	170
6.2.4	Air void analysis .....	172
6.2.5	Compressive strength.....	177
6.2.6	Final remarks .....	178
6.3	Construction and monitoring of the large-scale demonstrator .....	180



6.3.1	Mixture composition and details of the walls .....	182
6.3.2	Characterization of the concrete mixtures.....	185
6.3.3	Monitoring of the walls .....	186
6.3.4	Results and discussion .....	192
6.4	Conclusions.....	226
	References .....	228
Chapter 7.	Final remarks and future aspects of the research.....	231
7.1	General conclusions.....	232
7.2	Prospects for future research.....	239
	Curriculum Vitae.....	241

## Summary

There is no doubt that concrete is one of the most used and diverse building materials ever created by mankind. Concrete is everywhere in our daily life and for some structures we have the feeling that they will remain there for a lifetime. That might not really be true. Despite its considerable strength and technological development, the durability of concrete is frequently endangered by cracks that may not even be visible to the human eye (at least, initially). As old as the material itself, cracks are almost inevitable and can develop in a concrete structure at a very early age. They are intrinsic to the material, as a consequence of the shrinkage that follows cement hydration and their growth can be enhanced by environmental factors. Through cracks, a preferential pathway is built for the ingress of a vast number of aggressive substances that in time become responsible for the most common problems affecting concrete structures: carbonation, sulfate-attack, acid-attack and ingress of chlorides, being the key factors leading to concrete degradation, corrosion of reinforcement, spalling of concrete layers and consequently the reduction of the service life of a structure. Until recently, cracks were only dealt with by means of repairs and maintenance after their appearance, always resulting in addition costs. *But is it possible to avoid cracks from forming in the first place?*

The answers is YES!

Most of the mechanisms behind the formation of shrinkage cracks in concrete can be related to water movement in the hydrating cement paste e.g. the loss of water in the capillary pores or at the structure's surface by means of drying (leading to drying and plastic shrinkage, respectively), and the consumption of water during hydration and development of tension in the capillary pores following self-desiccation (autogenous shrinkage). With advances in the field of concrete technology, shrinkage reducing admixtures have been developed and later on the concept of internal curing by adding water reservoirs in the mixture was introduced and explored (a clear example of that is the use of saturated light-weight aggregates). These solutions work to a certain extent, but other important questions might be raised. *What if cracks*

*occur nevertheless at a later age? Is it possible to make concrete mixtures, not only subjected to lower risk of early-age cracking, but also able to deal with future cracks by themselves?*

That question represents a very complex and dynamic context and the solution to that should be equally dynamic and versatile. One of the answers was found with the use of superabsorbent polymers.

Superabsorbent polymers, or SAPs, are present in our daily life since a very early-age. One of the most common uses for SAPs is the production of hygiene products such as diapers, but they can also be found in a diverse range of applications from the food industry to agriculture. SAPs are composed of a 3D network of polymeric chains connected by means of crosslinkers and possess an incredible ability to absorb and retain water (sometimes even up to 1500 times their own weight). Such polymers can be produced and adapted to be stable in diverse media, allowing them to keep absorbing and releasing water for infinite times, as long as water is available. With such features, this material figures as a very promising answer to the question above. Given its absorption and retaining ability, SAPs can be used to promote internal curing in cementitious systems, reducing significantly the incidence of early-age cracks. Additionally, should cracks occur at a later age, SAP particles present at the cracked surface can re-swell and provide instant sealing and potentially promote healing, given that certain conditions are met. In that context, SAPs have been intensively studied as a chemical admixture for cementitious materials for the past 20 years and promising results have been found.

In this thesis, ten different SAPs were studied with the main intent to reduce shrinkage cracking by means of internal curing and to provide concrete structures with the features of self-sealing and self-healing of cracks. Two commercially available SAPs based on acrylic acid, four “in-house” developed SAPs based on sulfonates and four also “in-house” developed SAPs based on alginates were used. The water kinetics of SAPs and their effects on cement paste and concrete were investigated and two SAPs, being one commercial and one “in-house” developed, were selected based on performance criteria and used for the construction of crack-free large scale walls built with reinforced concrete and monitored under realistic conditions for a period of eight months.

When tested in cement pastes the acrylic acid-based SAPs were found to have an absorption capacity of around 20 g of water per g of SAPs, with a controlled release taking place around the time when a solid skeleton is formed in the cement paste and autogenous shrinkage takes place. This controlled water release kept the internal relative humidity in the paste at higher levels for more than seven days and promoted a complete mitigation of autogenous shrinkage with limited reduction of compressive strength (below 20%) in comparison to a reference paste produced without SAPs. In contrast, the sulfonate-based SAPs presented an initially higher absorption capacity in cement paste, above 50 g/g and up to 180 g/g, and strong incontinent behavior that resulted initially in a partial reduction of autogenous shrinkage. Full mitigation demanded an increased amount of SAPs and water that resulted in a significant reduction of strength, up to 74% at the age of 28 days. An additional and innovative sulfonate-based SAP was developed with two types of crosslinkers, one of which being alkali-unstable. This double crosslinker feature enabled this new SAP to absorb a limited amount of water at the first stage (up to 13 g/g in cement paste) but with the potential for a considerable increase in absorption capacity upon hydrolysis of the alkali-unstable crosslinker when immersed in the alkaline environment of the cement paste. With this SAP, a full mitigation of shrinkage was achieved with a reduction of compressive strength below 30% at the age of 28 days. The alginate-based SAPs were used as promising alternative to reduce the negative effects of SAPs on the compressive strength. They presented a limited absorption capacity in cement paste (as low as 7 g/g). Amongst all tested SAPs the alginate SAPs promoted the lowest reduction of strength (between 10-18%) at 28 days. However, given their early release of water, only a partial mitigation of shrinkage was found, which gave no improvement over the addition of the same amount of water to a mixture without SAPs.

During the investigation of the effects of SAPs on cement pastes, a detailed study about the determination of the time-zero as starting point for the measurement of autogenous shrinkage was conducted. The so-called “knee-point” of the autogenous strain curve was then selected as the most appropriate moment to start the measurements of autogenous shrinkage. This point represents the moment of transition of the cement

paste from a fluid to solid state and can be directly derived from the autogenous shrinkage test (in this thesis performed with the use of corrugated tubes).

The inclusion of SAPs in concrete mixtures showed evidence that the absorption capacity of SAPs in cement pastes could be used as a very good approximation for their absorption in concrete mixtures. The kinetics of water release observed for the pastes and their effects on the promotion of internal curing, and reduction of autogenous shrinkage, as well as the effects on the compressive strength were also found to be valid for concrete mixtures. The commercial SAPs promoted a complete mitigation of autogenous shrinkage in the concrete mixtures with a reduction of compressive strength at 28 days limited to less than 20%. The reduction of strength was found to be more intense at early ages but not so prominent at later ages (as of 28 and 56 days). In addition to the mitigation of autogenous shrinkage, the compressive strength of the mixtures with commercial SAPs was found to be at the same level or higher than for a concrete mixture where additional water was added to the same amount as in the SAP mixtures. The amount of additional water used for mitigation of autogenous shrinkage in the mixtures with the commercial SAPs was in line with the amount of water theoretically needed to compensate for the chemical shrinkage of the cement type used as binder in the production of the concrete mixtures. The use of SAPs with limited addition of water and a controlled water release also increased the salt-scaling resistance of concrete subjected to freeze-thaw cycles substantially. That was found to be mostly related to the reduction of the distance between the capillary pores and the macro-pores left by SAPs after water release. The double crosslinker feature of the innovative sulfonate-based SAPs showed its most promising application for the promotion of immediate sealing of cracked concrete specimens. A reduction of 72% in the water permeability of cracked specimens was found for the mixture with the sulfonate-based SAP, against 45% with the commercial SAPs (both in comparison to a reference mixture with no SAPs). In terms of compressive strength, a very similar result was found for both SAP mixtures: 16% reduction for the commercial SAP and 18% reduction for the “in-house” developed SAP.

The inclusion of SAPs in the large-scale production of concrete mixtures in a concrete plant was possible without considerable changes to the existing mixing protocol. SAPs were easily transported together with other dry materials on a transporting belt normally used at concrete plants. To avoid moisture uptake during transportation and swelling prior to the mixing, SAPs were inserted in water-soluble bags that were completely destroyed during the mixing procedure and dissolved afterwards, enabling a homogenous distribution of SAPs over the concrete mass with very limited to almost no agglomeration. With one commercial and one sulfonate-based SAP and their combination, three walls with dimensions 14 m x 2.75 m x 0.8 m were built with reinforced concrete and were found to remain crack-free over the complete monitoring period of more than eight months. In contrast, two reference walls without SAPs and different water content (respectively same total and same effective water-to-cement ratio as the SAP mixtures) presented cracks already five days after casting. The use of optical fiber sensors and multi-reference electrodes embedded in the concrete (attached to the steel reinforcement) enabled the continuous and automated monitoring of both shrinkage deformation and corrosion potential in the walls. The total shrinkage strain measured by the optical fiber sensors was 63% lower in the wall with a combination of both SAPs than in the reference wall, at the age of 7 days. Furthermore, the strain level measured in the reference wall at the moment the first cracks were noticed (five days), was only recorded in the combined SAPs wall after 14 days. The multi-reference electrodes indicated a possible corrosion initiation near a cracked area of the reference wall around six months after casting. In contrast, no corrosion potential was measured in the SAP wall.

To conclude, the use of SAPs for the production of large-scale elements under realistic conditions was proven to be successful from different perspectives: 1) SAPs could be easily introduced in the mixing routine of concrete plants without the need of significant changes in the mixing protocols; 2) SAPs promoted a considerable reduction in the total shrinkage strain of the concrete, especially during the first seven days, enough to avoid the formation and development of cracks; 3) the addition of SAPs enabled the reduction of (minimally) 10% in the amount of shrinkage reinforcement, in comparison to one reference wall without

SAPs; 4) the effect of SAPs on the compressive strength of the structures was limited to a 17% decrease in strength; 5) the addition of SAPs would enable the concrete to self-seal and heal future cracks that might occur at later ages.

## Samenvatting

Het lijkt geen twijfel dat beton een van de meest gebruikte en diverse bouwmaterialen is die ooit door de mensheid zijn gemaakt. Beton is overal in ons dagelijks leven en bij sommige constructies hebben we het gevoel dat ze daar een leven lang zullen blijven. Dat is misschien niet helemaal waar. Ondanks zijn aanzienlijke sterkte en technologische ontwikkeling wordt de duurzaamheid van beton vaak in gevaar gebracht door scheuren die misschien niet eens zichtbaar zijn voor het menselijk oog (althans, in het begin). Zo oud als het materiaal zelf, zijn scheuren bijna onvermijdelijk en kunnen ze zich in een betonconstructie al op zeer jonge leeftijd ontwikkelen. Zij zijn intrinsiek aan het materiaal, als gevolg van de krimp die volgt op de cementhydratatie en hun groei kan worden versterkt door omgevingsfactoren. Via scheuren wordt een voorkeursroute aangelegd voor het binnendringen van een groot aantal agressieve stoffen die na verloop van tijd verantwoordelijk worden voor de meest voorkomende problemen in betonconstructies: carbonatatie, sulfaataantasting, zuuraantasting en het binnendringen van chloriden zijn de belangrijkste factoren die leiden tot degradatie van beton, corrosie van wapening, afbrokkeling van betonlagen en als gevolg de vermindering van de levensduur van een constructie. Tot voor kort werden scheuren alleen aangepakt door middel van reparaties en onderhoud na het ontstaan ervan, wat altijd extra kosten met zich meebracht. *Maar is het mogelijk om het ontstaan van scheuren in de eerste plaats te voorkomen?*

Het antwoord is JA!

De meeste mechanismen achter de vorming van krimpscheuren in beton kunnen in verband worden gebracht met de waterbeweging in de hydraterende cementpasta, b.v. het verlies van water in de capillaire poriën of aan het oppervlak van de structuur door droging (kenmerkend voor respectievelijk drogingskrimp en plastische krimp), en het verbruik van water tijdens de hydratatie en de ontwikkeling van spanning in de capillaire poriën ten gevolge van zelfdesiccatie (autogene krimp). Met de vooruitgang op het gebied van betontechnologie zijn krimpverminderende hulpstoffen ontwikkeld en later is het concept van interne nabehandeling door het toevoegen van waterreservoirs in het mengsel geïntroduceerd en onderzocht (een duidelijk voorbeeld daarvan



is het gebruik van verzadigde lichtgewicht toeslagmaterialen). Deze oplossingen werken tot op zekere hoogte, maar er kunnen andere belangrijke vragen worden gesteld. *Wat als er op latere leeftijd toch scheuren ontstaan? Is het mogelijk betonmengsels te maken die niet alleen minder risico lopen op scheuren op latere leeftijd, maar die ook toekomstige scheuren zelf kunnen helen?*

Die vraag is zeer complex en de oplossing moet even dynamisch en veelzijdig zijn. Een van de mogelijke antwoorden werd gevonden met het gebruik van superabsorberende polymeren.

Superabsorberende polymeren, of SAP's, zijn al sinds zeer jonge leeftijd aanwezig in ons dagelijks leven. Een van de meest gangbare toepassingen van SAP's is de productie van hygiëneproducten zoals luiers, maar ze zijn ook te vinden in een breed scala van toepassingen, van de voedingsindustrie tot de landbouw. SAP's bestaan uit een 3D-netwerk van polymere ketens die met elkaar verbonden zijn door middel van crosslinkers en ze bezitten een ongelooflijk vermogen om water te absorberen en vast te houden (soms zelfs tot 1500 maal hun eigen gewicht). Dergelijke polymeren kunnen zo worden geproduceerd en aangepast dat zij stabiel zijn in diverse media, waardoor zij oneindig lang water kunnen blijven absorberen en weer afgeven, zolang er water beschikbaar is. Met deze eigenschappen is dit materiaal een veelbelovend antwoord op de bovenstaande vraag. Gezien zijn absorptie- en retentievermogen kan SAP worden gebruikt om de interne nabehandeling in cementachtige systemen te bevorderen, waardoor het optreden van scheuren op jonge leeftijd aanzienlijk wordt verminderd. Mochten er op latere leeftijd scheuren ontstaan, dan kunnen de SAP-deeltjes die zich aan de scheurwand bevinden, opnieuw zwellen en zorgen voor een onmiddellijke afdichting. Ze kunnen ook een blijvende scheurdichting stimuleren, mits aan bepaalde voorwaarden wordt voldaan. In die context zijn SAP's de afgelopen 20 jaar intensief bestudeerd als chemisch hulpmiddel voor cementgebonden materialen en er zijn veelbelovende resultaten gevonden.

In dit proefschrift werden tien verschillende SAP's bestudeerd met als voornaamste doel krimpscheuren te verminderen door middel van interne nabehandeling en betonconstructies te voorzien van de

eigenschappen van zelfdichting en zelfheling van scheuren. Twee commercieel beschikbare SAP's op basis van acrylzuur, vier "in huis" ontwikkelde SAP's op basis van sulfonaten en vier eveneens "in huis" ontwikkelde SAP's op basis van alginaten werden gebruikt. De waterkinetiek van de SAP's en hun effecten op cementpasta en beton werden onderzocht en twee SAP's, één commerciële en een "in huis" ontwikkelde, werden geselecteerd op basis van prestatiecriteria en gebruikt voor de constructie van scheurvrije muren op grote schaal, gebouwd met gewapend beton en opgevolgd onder realistische omstandigheden gedurende een periode van acht maanden.

Bij testen in cementpasta's bleken de op acrylzuur gebaseerde SAP's een absorptiecapaciteit te hebben van ongeveer 20 g water per g SAP, waarbij een gecontroleerde waterafgifte plaatsvond rond het tijdstip waarop een vast skelet in de cementpasta wordt gevormd en autogene krimp optreedt. Door deze gecontroleerde afgifte van water bleef de interne relatieve vochtigheid gedurende meer dan zeven dagen op een hoger niveau en werd een volledige compensatie van de autogene krimp verkregen met een beperkte vermindering van de druksterkte (minder dan 20%) in vergelijking met een referentiepaste die zonder SAP's werd geproduceerd. Daarentegen vertoonden de SAP's op basis van sulfonaten aanvankelijk een hogere absorptiecapaciteit in cementpasta, meer dan 50 g/g en tot 180 g/g, en een sterk incontinent gedrag dat aanvankelijk resulteerde in een gedeeltelijke vermindering van de autogene krimp. Volledige mitigatie vereiste een grotere hoeveelheid SAP's en water, wat resulteerde in een aanzienlijke vermindering van de sterkte, tot 74% op een leeftijd van 28 dagen. Er werd een bijkomend innovatief SAP op basis van sulfonaten ontwikkeld met twee soorten crosslinkers, waarvan er één alkali-onstabiel is. Door deze dubbele crosslinker kon dit nieuwe SAP in het eerste stadium een beperkte hoeveelheid water absorberen (tot 13 g/g in cementpasta), maar met het potentieel voor een aanzienlijke toename van de absorptiecapaciteit na hydrolyse van de alkali-onstabiele crosslinker bij contact met het alkalische milieu van de cementpasta. Met dit SAP werd een volledige compensatie van de krimp bereikt met een vermindering van de druksterkte tot minder dan 30% op een leeftijd van 28 dagen. De op alginaten gebaseerde SAP's werden gebruikt als veelbelovend alternatief om de negatieve effecten van SAP's op de

druksterkte te verminderen. Zij vertoonden een beperkte absorptiecapaciteit in cementpasta (slechts 7 g/g). Van alle geteste SAP's veroorzaakten de alginaten SAP's de laagste reductie van de sterkte (tussen 10-18%) na 28 dagen. Gezien hun vroege afgifte van water werd echter slechts een gedeeltelijke vermindering van de krimp gevonden, die geen verbetering gaf ten opzichte van de toevoeging van dezelfde hoeveelheid water aan een mengsel zonder SAP's.

Tijdens het onderzoek naar de effecten van SAP's op cementpasta's werd een gedetailleerde studie uitgevoerd naar de bepaling van de tijd-nul als startpunt voor de meting van de autogene krimp. Het zogenaamde "kniepunt" van de autogene krimpcurve werd vervolgens gekozen als het meest geschikte moment om de metingen van de autogene krimp te starten. Dit punt vertegenwoordigt het moment van overgang van de cementpasta van een vloeibare naar een vaste toestand en kan rechtstreeks worden afgeleid uit de autogene krimpproef (in dit proefschrift uitgevoerd met behulp van gegolfde buizen).

De vochtopname van SAP's in betonmengsels toonde aan dat de absorptiecapaciteit van SAP's in cementpasta's kan worden gebruikt als een zeer goede benadering voor de absorptie ervan in betonmengsels. De kinetiek van de waterafgifte die voor de pasta's werd waargenomen en de effecten ervan op de bevordering van de interne nabehandeling en de vermindering van de autogene krimp, alsmede de effecten op de druksterkte, bleken ook geldig te zijn voor betonmengsels. De commerciële SAP's bevorderden een volledige compensatie van de autogene krimp in de betonmengsels met een vermindering van de druksterkte na 28 dagen beperkt tot minder dan 20%. De vermindering van de sterkte bleek intenser te zijn op jonge ouderdom, maar niet zo prominent bij latere leeftijden (vanaf 28 en 56 dagen). Naast de vermindering van de autogene krimp, bleek de druksterkte van de mengsels met commerciële SAP's op hetzelfde niveau of hoger te liggen dan voor een betonmengsel waar evenveel extra water werd toegevoegd als in de SAP-mengsels. De hoeveelheid extra water die werd gebruikt om de autogene krimp in de mengsels met de commerciële SAP's te beperken, was in overeenstemming met de hoeveelheid water die theoretisch nodig is om de chemische krimp te compenseren van de cementsoort die als bindmiddel werd gebruikt bij de productie van de

betonmengsels. Het gebruik van SAP's met beperkte toevoeging van water en een gecontroleerde waterafgifte verhoogde ook de weerstand tegen afschilfering van beton onderworpen aan vries-dooicycli aanzienlijk. Dit bleek vooral verband te houden met de verkleining van de afstand tussen de capillaire poriën en de macro-poriën die door de SAP's werden achtergelaten na het vrijkomen van water. De dubbele crosslinker eigenschap van de innovatieve op sulfonaat gebaseerde SAP's toonde zijn meest veelbelovende toepassing voor de onmiddellijke afdichting van gescheurde betonnen proefstukken. Een vermindering van 72% in de waterdoorlatendheid van gescheurde proefstukken werd gevonden voor het mengsel met het op sulfonaat gebaseerde SAP, tegenover 45% met de commerciële SAP's (beide in vergelijking met een referentiemengsel zonder SAP's). Wat betreft druksterkte werd een zeer vergelijkbaar resultaat gevonden voor beide SAP-mengsels: 16% reductie voor de commerciële SAP en 18% reductie voor de "in huis" ontwikkelde SAP.

De opname van SAP's in de grootschalige productie van betonmengsels in een betoncentrale was mogelijk zonder aanzienlijke wijzigingen in het bestaande mengprotocol. De SAP's konden gemakkelijk samen met andere droge materialen worden vervoerd op een transportband die normaal in betonfabrieken wordt gebruikt. Om vochtopname tijdens het transport en zwellings vóór het mengen te vermijden, werden de SAP's in wateroplosbare zakjes geplaatst die tijdens het mengen volledig vernietigd werden en nadien oplosten, waardoor een homogene verdeling van de SAP's over de betonmassa mogelijk werd met een zeer beperkte tot bijna geen agglomeratie. Met één commercieel en één sulfonaathoudend SAP en hun combinatie werden drie wanden met afmetingen 14 m x 2,75 m x 0,8 m met gewapend beton gebouwd en deze bleken scheurvrij te blijven gedurende de volledige monitoringsperiode van meer dan acht maanden. Daarentegen vertoonden twee referentiewanden zonder SAP en met verschillend watergehalte (respectievelijk dezelfde totale en dezelfde effectieve water-cement verhouding als de SAP-mengsels) al vijf dagen na het storten scheuren. Het gebruik van optische vezelsensoren en multi-referentie-elektroden ingebed in het beton (bevestigd aan de stalen wapening) maakte de continue en geautomatiseerde monitoring mogelijk van zowel krimpvorming als corrosiepotentiaal in de wanden. De totale krimp

gemeten door de optische vezelsensoren was 63% lager in de wand met een combinatie van beide SAP's dan in de referentiewand, op de leeftijd van 7 dagen. Bovendien werd het vervormingsniveau dat in de referentiewand werd gemeten op het moment dat de eerste scheuren werden opgemerkt (vijf dagen), in de gecombineerde SAP-wand pas na 14 dagen geregistreerd. De multi-referentie-elektroden wezen op een mogelijke corrosie-initiatie in de buurt van een gescheurd deel van de referentiewand ongeveer zes maanden na het gieten. Daarentegen werd geen corrosiepotentiaal waargenomen in de SAP-wand.

Concluderend kan worden gesteld dat het gebruik van SAP's voor de productie van grootschalige elementen onder realistische omstandigheden vanuit verschillende oogpunten succesvol is gebleken: 1) SAP's konden gemakkelijk worden ingevoerd in de mengroutine van betoncentrales zonder dat daarvoor significante veranderingen in de mengprotocollen nodig waren; 2) SAP's bevorderden een aanzienlijke vermindering van de totale krimp van het beton, vooral gedurende de eerste zeven dagen, voldoende om de vorming en ontwikkeling van scheuren te voorkomen; 3) de toevoeging van SAP's maakte het mogelijk de hoeveelheid krimpwapening met (minimaal) 10% te verminderen, in vergelijking met een referentiewand zonder SAP's; 4) het effect van SAP's op de druksterkte van de constructies bleef beperkt tot een afname van de sterkte met 17%; 5) de toevoeging van SAP's zou het beton in staat stellen zichzelf te helen en toekomstige scheuren die op latere leeftijd zouden kunnen ontstaan, te genezen.

## Resumo

Não há dúvidas de que o concreto é um dos materiais de construção mais utilizado e diversificado já desenvolvido pela humanidade. Estruturas de concreto estão presentes em grande parte do nosso cotidiano. Por vezes, a sua estabilidade e solidez geram a impressão de que essas estruturas estarão ali por toda a vida. No entanto, essa pode não ser a realidade. Apesar da considerável resistência e desenvolvimento tecnológico do material, a durabilidade do concreto é frequentemente ameaçada por fissuras, que podem nem ser visíveis ao olho humano (pelo menos, inicialmente). Tão antigas quanto o próprio material, as fissuras são quase inevitáveis e podem se desenvolver em uma estrutura de concreto em uma idade muito precoce. Elas são intrínsecas ao material, como consequência da retração que se segue à hidratação do cimento e seu crescimento pode ser potencializado por fatores ambientais. Através das fissuras, forma-se um caminho preferencial para o ingresso de um vasto número de substâncias agressivas que com o tempo se tornam responsáveis pelos problemas mais comuns que afetam as estruturas de concreto: carbonatação, ataque de sulfatos, ataque de ácidos e ingresso de cloretos, sendo os principais fatores que levam à degradação do concreto, corrosão das armaduras, destacamento das camadas de concreto e conseqüentemente a redução da vida útil de uma estrutura. Até recentemente, as fissuras só eram tratadas por meio de reparos e manutenção após seu surgimento, o que resulta sempre em custos adicionais. Seria então possível evitar a formação de fissuras?

A resposta é SIM!

A maioria dos mecanismos envolvidos na formação de fissuras de retração no concreto pode estar relacionada à água, especificamente a água dentro da pasta de cimento em hidratação durante as primeiras horas de vida de uma mistura cimentícia. Com os avanços no campo da tecnologia do concreto, foram desenvolvidos aditivos redutores de retração e, posteriormente, foi introduzido e explorado o conceito de cura interna pela adição de reservatórios de água na mistura, um exemplo é o uso de agregados leves saturados. Essas soluções funcionam até certo ponto, mas outras questões importantes podem e devem ser levantadas: E se, ainda assim, ocorrerem fissuras em uma idade posterior? É possível

fazer com que tais misturas de concreto não só possam estar sujeitas a um menor risco de fissuração precoce, como também possam lidar com futuras fissuras por si só?

Essa pergunta representa um problema bastante complexo. A boa notícia é que uma resposta promissora foi encontrada, através de uma solução extremamente simples, criativa e altamente inovadora: polímeros superabsorventes.

Os polímeros superabsorventes, ou PSAs, estão presentes em nosso cotidiano desde muito cedo. Um dos usos mais comuns para o material é a produção de produtos de higiene, como fraldas, mas eles também podem ser encontrados em uma gama diversificada de aplicações, desde a indústria alimentícia até a agricultura. Os PSAs são compostos de uma rede tridimensional de cadeias poliméricas, conectadas por meio de reticuladores e possuem uma incrível capacidade de absorver e reter água (às vezes até 1500 vezes seu próprio peso). Tais polímeros podem ser produzidos e adaptados para serem estáveis em diversos meios, permitindo-lhes continuar absorvendo e liberando água infinitas vezes, desde que haja água disponível. Com essas características, esse material é uma resposta muito promissora para a pergunta acima. Dada sua capacidade de absorção e retenção, os PSAs podem ser usados para promover a cura interna em sistemas cimentícios, reduzindo significativamente a incidência de fissuras nas primeiras idades. Além disso, caso ocorram em uma idade posterior, as partículas de PSAs presentes na superfície fissurada podem absorver água e aumentar em volume, fornecer selagem instantânea e potencialmente promover a auto-cicatrização, dado que certas condições sejam atendidas. Nesse contexto, os PSAs têm sido intensamente estudados como aditivo químico para materiais cimentícios nos últimos 20 anos e resultados promissores têm sido encontrados.

Nesta tese, dez diferentes PSAs foram estudados com o objetivo de reduzir as fissuras de retração por meio de cura interna e fornecer às estruturas de concreto as características de auto-selagem e auto-cicatrização de fissuras. Dois PSAs comercialmente disponíveis baseados em ácido acrílico, quatro PSAs desenvolvidos com base em sulfonatos e quatro PSAs desenvolvidos com base em alginatos foram utilizados. A

cinética da água nos PSAs e seus efeitos sobre a pasta de cimento e concreto foram investigados e dois PSAs, um comercial e um desenvolvido internamente, foram selecionados com base em critérios de desempenho e utilizados para a construção de paredes de concreto armado livre de fissuras, monitoradas sob condições reais por um período de oito meses.

Quando testados em pastas de cimento, os PSAs à base de ácido acrílico apresentaram uma capacidade de absorção de cerca de 20 g de água por g de PSAs, com uma liberação controlada ocorrendo em torno do momento em que um esqueleto sólido é formado na pasta de cimento e ocorre a retração autógena. Essa liberação controlada de água manteve níveis mais altos de umidade relativa interna por mais de sete dias e promoveu uma completa mitigação da retração autógena com redução limitada da resistência à compressão (abaixo de 20%) em comparação com uma pasta de referência produzida sem PSAs. Em contraste, os PSAs baseados em sulfonatos apresentaram uma capacidade de absorção inicialmente maior em pasta de cimento, acima de 50 g/g e alcançando até 180 g/g, e um forte comportamento incontinente, que resultou inicialmente em uma redução parcial da retração autógena. A mitigação total exigiu um aumento da quantidade de PSAs e de água que resultou em uma redução significativa da resistência à compressão (até 74% aos 28 dias de idade). Um PSA inovador baseado em sulfonatos foi desenvolvido com dois tipos de reticuladores, um dos quais é instável em ambiente alcalino. Esta característica de reticulador duplo permitiu que este novo PSA absorvesse uma quantidade limitada de água num estágio inicial (até 13 g/g em pasta de cimento), mas com potencial para um aumento considerável na capacidade de absorção graças à hidrólise do reticulador alcalinizável quando imerso no ambiente alcalino da pasta de cimento. Com este PSA, a retração autógena foi completamente eliminada com uma redução da resistência à compressão abaixo de 30% aos 28 dias de idade. Os PSAs baseados em alginato foram usados como alternativa promissora para reduzir os efeitos negativos dos PSAs sobre a resistência à compressão. Eles apresentaram uma capacidade de absorção limitada em pasta de cimento (tão baixa quanto 7 g/g). Entre todos os PSAs testados, os PSAs à base de alginato promoveram a menor redução de resistência à compressão (entre 10-18%) aos 28 dias.



Entretanto, dada sua liberação precoce de água, apenas uma atenuação parcial da retração foi encontrada, o que não resultou em nenhuma melhoria em relação à adição da mesma quantidade de água a uma mistura sem PSAs.

A inclusão de PSAs em misturas de concreto forneceu evidências de que a capacidade de absorção de PSAs em pastas de cimento poderia ser usada como uma aproximação precisa para sua absorção em misturas de concreto. A cinética de liberação de água observada para as pastas e seus efeitos na promoção da cura interna e na redução da retração autógena, assim como os efeitos na resistência à compressão, também foram considerados válidos para misturas de concreto. Os PSAs comerciais promoveram uma atenuação completa da retração autógena nas misturas de concreto com uma redução da resistência à compressão em 28 dias limitada a menos de 20%. A redução da resistência foi considerada mais intensa em idades iniciais, mas não tão proeminente em idades posteriores (a partir de 28 e 56 dias). Além da atenuação da retração autógena, verificou-se que a resistência à compressão das misturas com PSAs comerciais estava no mesmo nível ou maior do que uma mistura de concreto contendo a mesma quantidade total de água que as misturas com PSAs. A quantidade de água adicional utilizada para mitigação da retração autógena nas misturas com os PSAs comerciais se mostrou de acordo com a quantidade de água teoricamente necessária para compensar a retração química do tipo de cimento utilizado como aglomerante na produção das misturas de concreto estudadas. O uso de PSAs com adição limitada de água e uma liberação controlada também aumentou substancialmente a resistência ao gelo e degelo na presença de sais. Tal efeito foi associado principalmente à redução da distância entre os poros capilares e os macro poros deixados pelos PSAs após a liberação de água. A característica de duplo reticulador dos PSAs inovadores baseados em sulfonatos, mostrou sua aplicação mais promissora na promoção da selagem imediata de fissuras em peças de concreto. Uma redução de 72% na permeabilidade à água de corpo-de-prova fissurados foi obtida para a mistura com o PSA baseado em sulfonato, contra 45% com os PSAs comerciais (ambos em comparação com uma mistura de referência sem PSAs). Em termos de resistência à compressão, foi encontrado um resultado muito semelhante para ambas

as misturas com PSA: 16% de redução para o PSA comercial e 18% de redução para o PSA desenvolvido internamente.

A inclusão de PSAs na produção em larga escala de misturas de concreto em uma fábrica de concreto usinado se deu sem mudanças consideráveis no protocolo de mistura existente. Os PSAs foram facilmente transportados junto com outros materiais secos em uma esteira de transporte normalmente utilizada em escala industrial. Para evitar a absorção de umidade durante o transporte e a saturação antes da mistura, os PSAs foram inseridos em bolsas solúveis em água que foram completamente destruídas durante o procedimento de mistura e dissolvidas posteriormente, permitindo uma distribuição homogênea dos PSAs na massa de concreto (com quase nenhuma aglomeração). Com um PSA comercial e um baseado em sulfonato, três paredes com dimensões de 14 m x 2,75 m x 0,8 m foram construídas com concreto armado. As paredes permaneceram sem fissuras durante todo o período de monitoramento de mais de oito meses. Em contraste, duas paredes de referência sem PSAs e diferentes teores de água (respectivamente mesma relação água/cimento total e efetiva que nas misturas com PSA) apresentaram fissuras cinco dias após a concretagem. O uso de sensores de fibra ótica e eletrodos multireferência incorporados no concreto (fixados à armadura de aço) permitiu o monitoramento contínuo e automatizado tanto da deformação por retração quanto do potencial de corrosão nas paredes. A deformação de retração total medida pelos sensores de fibra ótica foi 63% menor na parede com uma combinação de ambos os PSAs do que na parede de referência, aos 7 dias de idade. Além disso, o nível de deformação medido na parede de referência no momento em que as primeiras fissuras foram notadas (cinco dias após a concretagem), só foi registrado na parede com a combinação dos PSAs 14 dias após a concretagem. Os eletrodos multireferência indicaram um possível início de corrosão nas imediações de uma área fissurada na parede de referência cerca de seis meses após a concretagem. Em contraste, nenhum potencial de corrosão foi indicado na parede com PSAs.

Para concluir, o uso de PSAs na produção de elementos em larga escala em condições reais foi comprovado com sucesso sob diferentes aspectos: 1) os PSAs foram facilmente introduzidos na rotina de mistura de usinas

de concreto sem a necessidade de mudanças significativas nos protocolos de mistura; 2) os PSAs promoveram uma redução considerável na deformação total de retração do concreto, especialmente durante os primeiros sete dias, o suficiente para evitar a formação e o desenvolvimento de fissuras; 3) a adição de PSAs permitiu a redução de (minimamente) 10% na quantidade de armadura de combate à retração, em comparação a uma parede de referência sem PSAs; 4) o efeito dos PSAs sobre a resistência à compressão das estruturas foi limitado a uma redução de 17% na resistência aos 28 dias; 5) a adição de PSAs pode ainda permitir que o concreto realize a auto-selagem e auto-cicatrização de fissuras que venham a ocorrer em idades posteriores.

## Chapter 1. General introduction

### 1.1 Shrinkage cracking in concrete structures

Most of the deteriorating mechanisms acting on concrete structures are related to the ingress of aggressive substances. Chemical concrete degradation, reinforcement corrosion and physical deterioration during freeze-thaw cycling are related to the ingress of substances such as chlorides, sulfates, acids, carbon dioxide and even water, amongst others. Even before reaching its hardened state, a cement-based composite is possibly subjected to the formation of cracks, especially due to the effects of early-age shrinkage. The formed porosity of the material and connectivity of the micro-cracks can become the perfect path for the ingress of those aggressive agents. There are four types of shrinkage deformations in this context: plastic, autogenous, drying, and carbonation shrinkage [1]. The resulting shrinkage cracking can be the effect of a single type or a combination.

Plastic shrinkage occurs in concrete at a very early age, when freshly cast and before setting. The underlying reason for plastic shrinkage is the loss of water from the surface from suction of underlying or adjacent drier layers or by evaporation of the exposed surface. If the amount of water available to replenish the moisture of the surface is less than the magnitude of water losses, plastic shrinkage will occur. The plastic shrinkage of concrete will be greater if the loss of water increases and is minimized by preventing the occurrence of evaporation after casting [1, 2]. The absence of the water film on top of the concrete surface leads to the development of water menisci. Capillary pressure rises due to surface tension and adhesive forces and shrinkage deformation along the exposed surface will be induced by inter-particle forces. Air penetrates the system when the water menisci can no longer bridge the cavities, which causes the capillary pressure to break down locally (Figure 1.1). Eventually, visible cracking will occur in the presence of movement restraint [1].

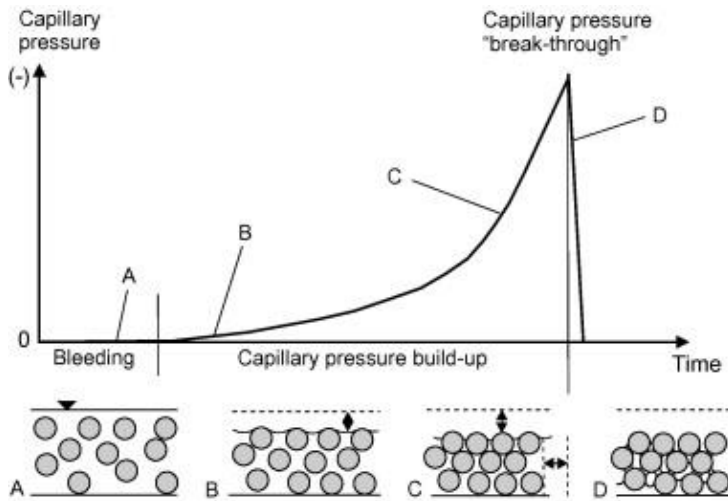


Figure 1.1 - Visualization of capillary pressure build-up, according to Slowik et al. [3].

Autogenous shrinkage is to this day a complex phenomenon, which is still not fully understood, but a general agreement exists about a close relationship between autogenous shrinkage and the internal relative humidity changes in the capillary pores of hardening cement paste [4-6]. Autogenous shrinkage can be described as the bulk deformation of a cementitious material system, which is sealed and under isothermal conditions. It takes place as a consequence of self-desiccation which is triggered by the internal consumption of water by further hydration of cement after formation of the initial structure of the cement matrix [1, 2, 7]. As hydration goes on in the cement paste, water is being consumed and hydration products are being formed, causing a refinement of the pore structure and formation of water menisci in the capillary pores. As hydration proceeds and more water is consumed, the curvature of the menisci decreases, increasing the tensile stresses in the pore fluid. In time, this increase in stresses gives place to the bulk shrinkage known as autogenous shrinkage. This process is illustrated in Figure 1.2

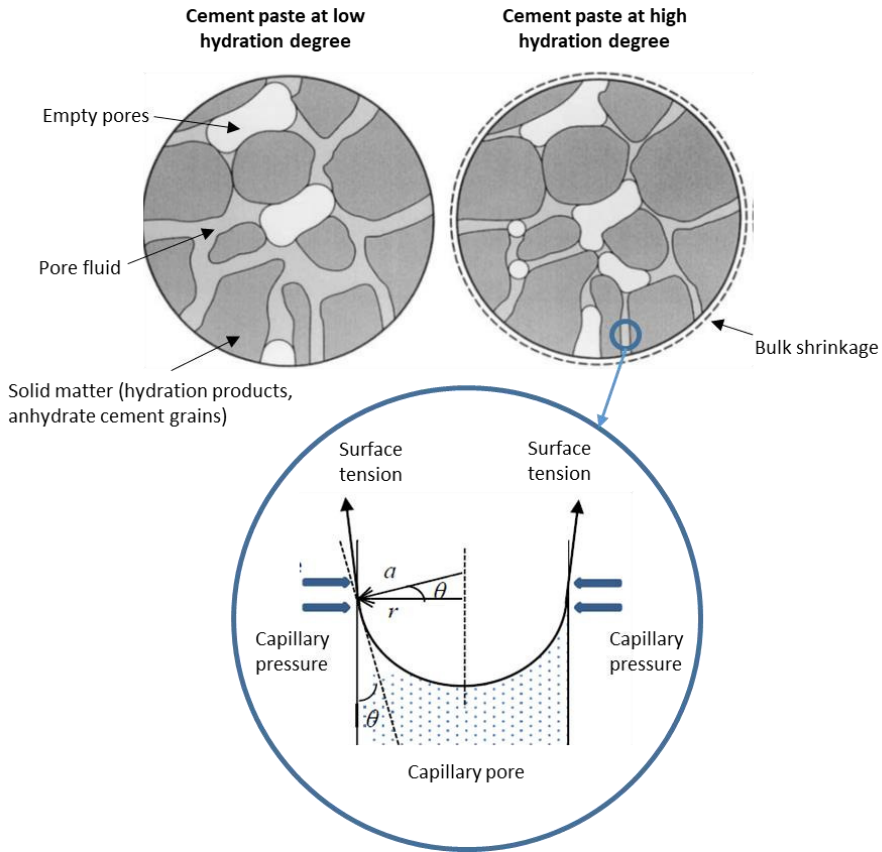


Figure 1.2 - Illustration of self-desiccation and autogenous shrinkage of hydrating cement paste. Adapted from Lyu [8] and Jensen and Hansen [9].

Based on the type of concrete, autogenous shrinkage occurs at different levels. It is more significant in (ultra-)high-performance concrete ((U)HPC) due to its low water-to-cement ratio ( $w/c < 0.4$ ). In ordinary concrete structures (with water-to-cement ratio above 0.42) it is not a very prominent phenomenon, but it may increase the risk of cracking, especially when supplementary cementitious materials are used [7, 10]. A higher  $w/c$  ratio can mitigate concrete cracking, but this results in a decrease of strength and impermeability [11]. This development of autogenous shrinkage can be avoided by internal or external water curing. However, since the dense microstructure of (U)HPC limits the water transport, autogenous shrinkage cannot be reduced significantly by external water curing.

Drying shrinkage is associated with the loss of internal water from the concrete to the environment by evaporation, since the concrete is exposed to a relative humidity below its saturation level [12]. This makes drying shrinkage almost inevitable, once concrete is exposed to a dry environment, where it will be in addition affected by conditions such as wind, air temperature, and sunlight [2, 7, 11]. First, the free water in the system evaporates from larger pores (larger than 50 nm). As the relative humidity decreases, the loss of water is intensified and reduces the thickness of the layer of adsorbed water. As evaporation proceeds and starts to take place in the smaller pores, the curvature of the water menisci begins to diminish until it is completely gone. From that moment on, the shrinkage occurs as a joint function of the superficial tension of the adsorbed water on the solid surface and the disjoining pressure, leading to the shrinkage of the whole system [12, 13].

Carbonation shrinkage occurs when concrete is exposed to carbon dioxide ( $\text{CO}_2$ ). Calcium hydroxide ( $\text{Ca}(\text{OH})_2$ ) of the hardened cement paste will react with the  $\text{CO}_2$  of the atmosphere in the presence of moisture. This reaction produces water that can eventually increase drying shrinkage [2, 12].

In Europe, costs related to repair works amount to half of the annual construction budget [14]. Additionally, indirect costs derived from traffic jams and interruptions of services can carry a severe economic penalty. More and more, contractors have been searching for a way to decrease shrinkage cracks, reduce costs of repair and maintenance, and obtain watertight structures. This is especially important for tunnel elements, underground parking garages, basements, liquid-containing structures, pavements, etc. Normally, contractors are often forced to apply crack repair right after construction, due to the formation of shrinkage cracks at early age. They also include a large amount of shrinkage reinforcement, needed to limit the observed shrinkage crack widths.

The shrinkage phenomenon, especially when referred to autogenous shrinkage, is inherent to the hydration process of the cementitious material and (among other factors) is a function of the water-to-cement ratio and curing conditions (temperature and humidity). In that regard,



the most common solution to reduce cracking associated with autogenous shrinkage is based on the use of internal curing agents.

In that context, this thesis investigates the use of superabsorbent polymers (SAPs) in concrete mixtures intended for the construction of reinforced concrete structures. The SAPs have been used as a smart material with the purpose of mitigating shrinkage cracking by means of internal curing, self-sealing cracks and reducing water permeability through cracks, with a possible self-healing afterwards.

## 1.2 Objectives of the thesis

This thesis was developed in the framework of the ICON project iSAP: Innovative SuperAbsorbent Polymers for crack mitigation and increased service life of concrete structures. The project was financed by SIM program SHE (Engineered Self-Healing Materials) and developed with the three industrial partners Artes Depret, InterBeton and Chemstream.

The thesis covers the use of commercial and “in-house” developed superabsorbent polymers (SAPs) for the production of crack-free reinforced concrete structures. The main objectives of the research were:

1. Gain more knowledge about the relation between the polymer structure of SAPs and their quantitative effect on internal curing and autogenous shrinkage mitigation;
2. Develop novel, superior superabsorbent polymers for internal curing / self-sealing / self-healing and compare their potential with benchmarked SAPs and commercial types;
3. Develop a three-step approach for obtaining crack free concrete by combining novel/commercial SAPs with optimal properties for each step: crack avoidance (internal curing) / rapid crack sealing / subsequent crack healing;
4. Illustrate the effectiveness of the developed SAP (combination) through:
  - a. reduction of the amount of autogenous shrinkage cracks (up to complete mitigation; reduction of observed cracking by 50%);
  - b. decrease in water permeability with a factor 1000 versus cracked (non-sealed) concrete;
  - c. full crack closure (by visual/microscopic observation).
5. Assess the effects of SAPs on several properties of concrete mixtures in fresh and hardened state;
6. Define measuring and monitoring protocols to study the amount of shrinkage and healing in real-size structures.
7. Demonstrate the general application of SAPs in concrete in-field with large-scale tests.

### 1.3 Outline of the thesis

The study was structured in four stages, which comprised: 1) the characterization and development of “in-house” SAPs; 2) application of SAPs in cement pastes; 3) application of SAPs in concrete mixtures at laboratory scale and 4) application of SAPs in large-scale structures under realistic conditions. This thesis is structured in this introductory chapter and six additional chapters, as described below.

Throughout the thesis, the values presented represent average values of three tested specimens. When different number of specimens were tested it will be indicated. The variability of the results is represented by the standard error of the average.

#### **Chapter 2 – Superabsorbent polymers (SAPs) and their potential as an admixture for cementitious materials**

In this chapter, the SAPs will be presented. An introduction will be given on the production processes and different applications of the SAPs. The stage 1 of the research will be described with the characterization of all the initially tested SAPs (commercial SAPs based on acrylate, alginate-based SAPs, and sulfonate-based SAPs). The concept of internal curing with SAPs is translated to a set of detailed product- and production-related requirements, which also define the constraints of the concrete technology and applications.

#### **Chapter 3 – The effects of SAPs on cement pastes**

This chapter will describe the stage 2 of the research. The effects of the SAPs on the workability, setting/hardening, mechanical properties, and autogenous shrinkage of cement pastes will be discussed. Focus is given to the kinetics of absorption and desorption by the SAPs and how they can affect the properties of the cement pastes. Based on the results of stage 2, some SAPs were selected for further investigation in concrete mixtures, as presented in Chapter 5.

**Chapter 4 – Investigation of different approaches to determine the time-zero as start for autogenous shrinkage measurements in cement pastes**

Different techniques to determine the time-zero for the autogenous shrinkage measurements in cement pastes with and without SAPs are investigated, exploring the influence of the different methods on the final values of the autogenous strain. The suitability of the different methods is discussed for the different paste compositions and a recommendation is provided especially for the case of SAPs.

**Chapter 5 – The effects of SAPs on concrete mixtures under laboratory conditions**

This chapter will describe the stage 3 of the research. It will present the preliminary study with SAPs for the mitigation of autogenous shrinkage and effects on the drying shrinkage in concrete, the effects on the compressive strength and the salt-scaling resistance under freeze-thaw cycles. Advanced optical fiber sensors are investigated as an alternative for the monitoring of shrinkage in large-scale elements. From the preliminary study and the initial mix design, optimized mixtures will be presented with fully in-house developed SAPs for the mitigation of autogenous shrinkage with minimum effect on the compressive strength and immediate sealing of cracks. The results of the compressive strength and the fitting of the SAP-modified concrete mixtures to the existing models for prediction of strength will be discussed.

**Chapter 6 – The use of SAPs for the construction of crack-free large-scale structures under realistic conditions.**

This chapter will be dedicated to the stage 4 of the research. The most promising SAPs studied in the previous chapters are used in the construction of large-scale structures under realistic conditions. It will comprise the report on the on-site and laboratory testing campaign. Details of the demonstrator and preliminary studies for the development of a large-scale mixing procedure including SAPs will be presented. The development of shrinkage strain and cracking of the structures will be discussed along with the results of a full laboratory characterization of the concrete mixtures.

## **Chapter 7 – Conclusions and future aspects of the research**

This chapter is dedicated to the main conclusions of the research and summary of contributions to the state-of-the art of the topic. Some aspects regarding the future research on the topic are enlisted.

## References

1. Mechtcherine, V., L. Dudziak, and S. Hempel. *Mitigating early age shrinkage of Ultra-High-Performance Concrete by using Super Absorbent Polymers (SAP)*. in *Creep, Shrinkage and Durability Mechanics of Concrete and Concrete Structures*. 2009. Ise-Shima, Japan: Taylor & Francis.
2. Brooks, J.J., 6 - *Shrinkage of Concrete*, in *Concrete and Masonry Movements*, J.J. Brooks, Editor. 2015, Butterworth-Heinemann. p. 137-185.
3. Slowik, V., M. Schmidt, and R. Fritzsche, *Capillary pressure in fresh cement-based materials and identification of the air entry value*. *Cement and Concrete Composites*, 2008. **30**(7): p. 557-565.
4. Wittmann, F., *Surface tension shrinkage and strength of hardened cement paste*. *Matériaux et Construction*, 1968. **1**(6): p. 547-552.
5. Powers, T.C., *The Properties of Fresh Concrete*. 1968: Wiley.
6. L'Hermite, R. *Volume Changes of Concrete*. in *Fourth international symposium on the chemistry of cement*. 1960. Washington, D.C, USA: United States. National Bureau of Standards.
7. Wu, L.M., et al., *Autogenous shrinkage of high performance concrete: A review*. *Construction and Building Materials*, 2017. **149**: p. 62-75.
8. Lyu, Y., *Autogenous Shrinkage of Cement-Based Materials: From the Fundamental Role of Self-Desiccation to Mitigation Strategies Based on Alternative Materials*, in *Faculty of Engineering and Architecture*. 2017, Ghent University: Ghent, Belgium.
9. Jensen, O.M. and P.F. Hansen, *Water-entrained cement-based materials I. Principles and theoretical background*. *Cement and Concrete Research*, 2001. **31**(4): p. 647-654.
10. Jiang, C.H., et al., *Autogenous shrinkage of high performance concrete containing mineral admixtures under different curing temperatures*. *Construction and Building Materials*, 2014. **61**: p. 260-269.
11. Jianxia, S., 6.14 - *Durability Design of Concrete Hydropower Structures*, in *Comprehensive Renewable Energy*, A. Sayigh, Editor. 2012, Elsevier: Oxford. p. 377-403.
12. Diniz, J.Z.F., J.F. Fernandes, and S.C. Kuperman, *Retração e Fluência*, in *Concreto: Ciência e tecnologia*, G.C. Isaia, Editor. 2011, Instituto Brasileiro do Concreto (IBRACON): São Paulo, Brasil. p. 673-703.
13. Isaia, G.C., *A água no concreto*, in *Concreto: Ciência e Tecnologia*, G.C. Isaia, Editor. 2011, Insituto Brasileiro do Concreto (IBRACON): São Paulo, Brasil. p. 311-346.
14. Cailleux, E.P., V. *Investigations on the development of self-healing properties in protective coatings for concrete and repair mortars*. in *2nd International Conference on Self Healing Materials*. 2009. Chicago, IL, USA.



## Chapter 2. Superabsorbent polymers (SAPs) and their potential as an admixture for cementitious materials

*And the SAP became this big!*  
*Unknown author*



## 2.1 General definition

Superabsorbent polymers (SAPs) consist of a natural and/or synthetic water-insoluble 3D network of polymeric chains crosslinked by chemical or physical bonding. They possess the ability to take up a significant amount of liquids from the environment (in amounts up to 1500 times their own weight) [1] and form an insoluble gel [2] (Figure 3.1). This amount of absorbed water can be released due to drying or osmotic pressure, consequently causing the SAPs to shrink in size [3, 4].

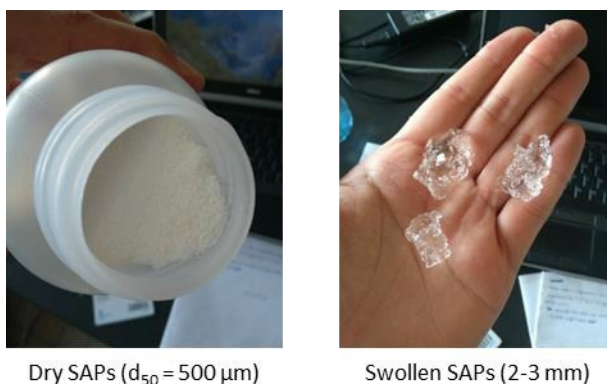


Figure 3.1 - SAP particles before and after swelling in demineralized water.

Depending of the type of electrical charges present in the side chains, non-ionic and ionic polymers can be distinguished [5]. In this classification, ionic polymers are polymers with positively or negatively charged atoms or associated groups of atoms, whereas non-ionic polymers possess no charged moieties [4, 6]. Commercially available SAPs are mostly synthetic ionic gels consisting of crosslinked polyacrylic acid, which are partially neutralized with hydroxides of alkali metals [2]. A common type of non-ionic polymer for SAPs is polyacrylamide [3]. The structure of SAPs is thus generally known and consists of organic materials. Upon swelling, SAPs do not dissolve due to the crosslinks between the polyelectrolytes. Crosslinks can be formed by multiple types of bonds. These bonds are either hydrogen, ionic or covalent bonds. The absorption capacity of the SAPs and the crosslinking density are inversely related and the crosslinking density is controlled in the production process of the SAP [1, 4, 7].

## 2.2 Synthesis of SAPs

Polymer synthesis plays an import role in the diversification of superabsorbent polymer application. There are multiple mechanisms to synthesize polymers, such as graft-copolymerization, photo-polymerization, condensation polymerization, ring-opening polymerization and radical polymerization [8]. SAPs are classically produced via free-radical-initiated polymerization of acrylic monomers [4, 9].

The free-radical polymerization process is highly exothermic and can be split into four parts, based on the reaction steps. The process starts with initiation, followed by propagation, chain transfer and termination [10]. Thermal or photochemical homolysis or a redox process generates free radicals from the initiator that initiates the polymerization. Following the initiation is a succession of quick propagation steps to form radical centers with a substituent. The radical center is moved to another molecule from the polymer end during the chain transfer, leaving the number of unpaired electrons unchanged. During the termination step the propagation of radical chain ends is deactivated [10]. The polymerization can be heterogeneous (emulsion, suspension) or homogeneous (bulk, solution) [11].

Suspension polymerization uses dispersed water-insoluble monomer particles, a dispersing medium, stabilizing agents and a monomer soluble initiator. The process itself is carried out in the droplets of liquid monomer, in which the droplets convert from a highly liquid state to hard solid polymer particle when a sufficiently high molecular weight is reached [12]. This transition from liquid to solid is known as the gel point. At this gel point, many properties of the polymer networks change and because those properties are mostly only useful after the transition, it is helpful to predict this gel point. This polymerization process typically results in spherical SAP particles [13]. The process of the emulsion polymerization differs only slightly from the suspension polymerization process as the emulsion polymerization system consists of a water-soluble initiator, emulsifier, monomer and a dispersing medium. However, the emulsion polymerization differs in the type of initiator and

the type and particle size of SAP. Emulsified monomer droplets are dispersed at the beginning of polymerization with the aid of a surfactant. The initiation is then induced by the initiator [14].

Bulk or mass polymerization is a process where the reaction mixture consists of a soluble initiator and vinyl monomers and thus no solvent or dispersant is involved. When adding this soluble radical initiator to the monomers in liquid state, the polymerization starts. This polymerization process results in blocks, which are crushed to obtain a desired particle size distribution [15], thus resulting in SAP particles with irregular shape [13, 15]. To obtain an appropriate balance between the requested properties of a SAP, the production process and its variables need to be optimized. For acrylic SAPs for example, the material properties are affected by the synthetic factors of the procedure. The effect of the variation in synthetic factor on the SAP material properties, given that the other factors remain constant, is shown in Table 3.1 [4].

Table 3.1 - Effect of the main synthetic factors affecting SAP material properties, adapted from [4]. + equals increasing effect, - equals decreasing effect.

Variation in synthetic factor	Absorption capacity	Absorption rate	Swollen gel strength	Soluble fraction
Increase in crosslinker concentration	-	-	+	-
Increase in initiator concentration	+	-	-	+
Increase in monomer concentration	-	+	-	+
Increase in reaction temperature	+	-	-	+
Increase in particles porosity	No effect	+	-	varied

## 2.3 Most common applications

SAPs were firstly developed in the late 1980s and their first application was in diapers. This market grew very quickly and today the main market for SAPs is still the hygiene industry, due to the application in diapers and adult care articles [16]. The biomedical field is part of this main market [2, 17] with application such as bandages, drug release/delivery, surgical sponges, tissue engineering [18] and contact lenses. The other part of the market comprises technical SAPs, which are all SAPs with exclusion of those applied in hygiene products, which can be based on AA and AM [16]. These other fields of application include but are not limited to the agricultural field, waste treatment, cable isolation and food packaging [16]. SAPs in the agriculture can be used in various ways. They can act as a controlled release system of nutrients or aid in germination and seedling establishment in the form of seed additives. Additionally, SAPs are used as soil amendments to increase the nutrient retention and water-holding capacity of soils [19].

Meyer [20] wrote the first patent in 1989 including SAPs in construction applications, as he worked with dry mortars containing superabsorbent polymers. The polymer addition would extend the working time of the composition, as well function as an aid against sagging. These products were never introduced into the market and at the end of the last century, the focus in construction applications shifted more towards internal curing of ultra-high performance concrete [16].

## 2.4 Applications of SAPs in cementitious materials

Up to now, the first and most reported application of SAPs in cementitious materials aimed at the reduction of autogenous shrinkage by means of internal curing. The work performed by Jensen and Hansen [21, 22] represented a very important landmark for the developments that followed their publication. In their work, the authors suggested the use of SAPs as internal curing agents for the mitigation of autogenous shrinkage in cement pastes and proposed a model to determine the correct amount of water needed for that, based on the theory of Powers [23]. From that moment on, several studies were performed further investigating the use of SAPs as internal curing agent in cement pastes, mortars and concrete [24-28]. Together with the use of SAPs for internal curing, questions were risen regarding the sorption and desorption kinetics of SAPs and its relation with the efficiency of the material as internal curing agent and the consequences of that for properties and very important advances were achieved: Schröfl et al. [15] investigated the effects of the molecular weight of different SAPs on their kinetics and introduced the concept of retentive and incontinent SAPs; Kang et al. [29-31] and Yang et al. [32] presented an in-depth discussion about the influences of mono- and multivalent ions on the sorption and desorption behavior of SAPs; Snoeck et al. [33] studied the water kinetics of SAPs during hydration of cement pastes by means of nuclear magnetic resonance (NMR) and identified the appropriate moment of water release for efficient internal curing of commercial acrylic-acid based SAPs.

Following that, several other routes started to be investigated as more opportunities were observed for the use of SAPs: 1) drying and plastic shrinkage of cementitious mixtures with SAPs were studied by Snoeck et al. [34], Mechtcherine and Dudziak [35], and Boshoff et al. [36]; 2) creep of concrete specimens produced with SAPs was studied by Assmann and Reinhardt [37] and more recently by Shen et al. [38], and Van Mullem [39]; 3) the use of SAPs to increase salt-scaling resistance of concrete mixtures was reported by Craeye et al. [40], Laustsen et al. [13], Mechtcherine et al. [41], and Monnig and Lura [42]; 4) the promotion of sealing and healing for cracked concrete was investigated by Snoeck et al. [43]; 5) Snoeck et al. [44] investigated the impact energy absorption in self-healing strain-hardening cementitious materials with superabsorbent

polymers; 6) the combined use of SAPs and supplementary cementitious materials and mineral admixtures was studied by Snoeck et al. [45], Liu et al. [46], Klemm et al. [47], and Lefever et al. [48, 49]; 7) Most recently, Van Der Putten et al. [50] extended the study of SAPs in cementitious mixtures aimed for 3D printing.

Most of the studies mentioned above made use of commercial SAPs based on acrylic acid. A few authors investigated the development and use of SAPs based on different types of chemistry: Mignon et al. [51, 52] investigated alginate based SAPs, Mannekens and Deroover [53] and De Meyst et al. [24] tested sulfonate based SAPs, and Wang et al. [54] studied amine- and ammonium-based pH-sensitive SAPs.

The wide range of possibilities for the application of SAPs in cementitious materials and the challenges still to overcome until the material can make its way into the market have motivated the creation of two technical committees by RILEM (The International Union of Laboratories and Experts in Construction Materials, Systems and Structures): TC 225-SAP “Application of Superabsorbent Polymers in Concrete Construction” and TC 260-RSC “Recommendations for Use of Superabsorbent Polymers in Concrete Construction”. The work developed during the time the two committees remained active resulted in the publication of very important recommendations for: characterization of SAPs prior to implementation in cementitious materials [55], using SAPs to mitigate autogenous shrinkage [56], and using SAPs to improve the freeze–thaw resistance of cementitious materials [57]. Additionally, a state-of-the-art report about the use of SAPs in cementitious materials was published in 2012 [1] and updated in 2021 [58].

## 2.5 Sorption and desorption behavior

The swelling of the SAPs is mainly driven by the osmotic pressure, which is proportional to the ion concentration in the aqueous solution [2, 16, 17, 32]. The three-dimensional polymer network forces the ions closely together in the SAP, resulting in a very high osmotic pressure [16]. When said SAP is immersed in a solution with lower concentration, osmotic pressure forms the driving force of the absorption [32]. As more water is absorbed by the SAP the charges within are diluted, resulting in an increased swelling and a reduction of the osmotic pressure. The swelling will be in equilibrium when all forces are even [16]. That is to say, when the elastic contractility of the three-dimensional polymer network equilibrates with the electrostatic repulsion between anion groups of the SAP [32]. The swollen SAPs will release water when they are exposed to a solution with a higher ion concentration.

The behavior of SAPs regarding absorbing, retaining and releasing fluids is key to their application in cementitious materials. The SAPs introduce water into the material, which is released after a certain period, mitigating autogenous shrinkage and self-desiccation as well as promoting self-healing [2, 43, 59, 60]. When cracks are formed, exposed SAPs can absorb water and re-swell, thus sealing the crack and preventing leakage [2, 61, 62].

When mixing concrete, the dry SAP particles will absorb a portion of the mixing water and swell. The SAPs will be finely distributed and form stable water reservoirs in the hardened cement paste. However, most of the absorbed solution will be drawn back into the capillary pores of the cement paste when the surrounding humidity drops. This can occur if hardened concrete is subjected to external drying or if mixing water is consumed by cement hydration to an extent that causes self-desiccation. Thus, the SAP particles will slowly release the absorbed water and shrink, leaving behind macro voids. These voids are distributed air-filled cavities. The SAPs can re-swell when the surrounding humidity increases again [2].

In terms of kinetics of water absorption and desorption, when placed in a cementitious environment, SAPs will have a lower absorption capacity

and swelling compared to immersion in pure or even demineralized water, as the concentration of cations in the pore solution is higher [32].

Di- and trivalent ions (e.g.  $\text{Ca}^{2+}$  and  $\text{Al}^{3+}$ ) influence the swelling of SAPs, especially those based on polyacrylates [2, 16, 29], because they form complexes with carboxylate groups and act as additional crosslinkers, thus reducing the absorption capacity [2, 16], which is called ionic crosslinking effect. To verify such effect, Yang et al (2019) [32] conducted a Fourier-transform infrared spectroscopy analysis (FTIR) to verify any possible changes in the chemical structure of their SAPs after contact with different fluids. For the case of SAPs immersed in alkaline environment, the authors found that the peak relative to the stretching vibration of  $-\text{COOH}$  groups disappeared after immersion of the SAPs in the solution, which can be considered as evidence of the complexation between the  $-\text{COOH}$  groups and the  $\text{Ca}^{2+}$  ions (Figure 3.2).

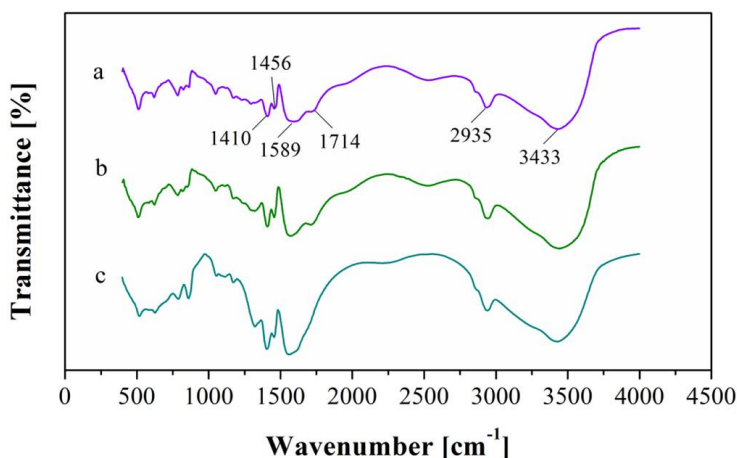


Figure 3.2 - The FTIR spectra of SAP-A (a) Dry state; (b) Dried at 50 °C after absorption in tap water; (c) Dried at 50 °C after absorption in saturated  $\text{Ca}(\text{OH})_2$  solution [32]. The peak at  $1714\text{ cm}^{-1}$  is due to the stretching vibration of  $-\text{COOH}$  group as a result of the complexation between  $\text{Ca}^{2+}$  and  $-\text{COOH}$  it disappears.

Other monomers can be introduced to avoid these formations, e.g. sulfonic acids as they do not contain ionic groups that form complexes with calcium or aluminum [16].

In [63], it was found that the equilibrium swelling ratio (ESR) of SAPs composed of poly(sodium acrylate-acrylamide) (PANa-PAM) copolymer



decreased in solutions containing  $\text{Ca}^{2+}$  or  $\text{Al}^{3+}$  ions. This can be explained by the Flory equation (equation 2.1)) [29].

$$q_m^{5/3} = \frac{\left[ \frac{i}{2v_u S^{*1/2}} \right]^2 + \left[ \left( \frac{1}{2} - \chi_1 \right) / v_1 \right]}{V_0 / v_e} \quad (2.1)$$

where  $q_m$  is the ESR,  $S^*$  is the ionic strength of the solution in which the SAP is immersed,  $v_1$  is the volume of solvent,  $v_e$  is the effective number of chains in the network,  $V_0$  is the volume of the un-swollen network,  $i/v_u$  is the concentration of fixed charge in the un-swollen network and  $\chi_1$  is the interaction parameter between the solvent and the network.

The ionic strength and the ESR are anti-correlated according to this equation, meaning that the absorption capacity of SAPs can vary depending on its crosslinking density (as represented by  $v_e$ ) and the ion composition of the solution [29]. The swelling capacity decreases with an increased crosslink density [2, 29, 30, 60, 64, 65]. To illustrate the effect of the crosslink density on the absorption capacity of the SAPs, Davis et al. (2020) [9] determined the absorption capacity of a polyacrylamide (PAM) SAP with three different weight percentages (wt.%) of crosslinkers in pore solutions. An increase of the absorption capacity was noted from 5.1 g/g to 20.6 g/g for a decreasing amount of wt.% of crosslinkers.

Not only the multivalent ions, but also monovalent ions can play an important role in the kinetics of sorption and desorption of SAPs, especially related to the retaining period.

The sorption capacity or swelling behavior as well as the kinetic behavior of a SAP thus greatly depends on its chemical composition [55].

## 2.6 SAPs used in the research

Most of the studies cited in section 2.4 have made use of synthetic and commercially available SAPs. These types of SAPs are usually powders that consist of a specific chemistry, particle size distribution (PSD) and show a specific swelling capacity in water. Most of them are built from the acrylic acid (AA) monomer, partially neutralized to its salt form ( $-\text{COO}^- \text{M}^+$ ), and acrylamide (AAm) [4]. These monomers are considered non-renewable materials that are dependent on the petroleum industry.

Other types of SAPs, so far not available at commercial scale, can also be used. The possibilities of changing the chemical composition of the SAPs enables one to fine-tune the desired properties of the material for a specific application. Thus, taking the most advantage of the material and reducing/avoiding possible negative. Previous studies [1, 24, 59, 61, 62, 66-69] have shown that incorporation of synthetic SAPs (based on acrylic acid, acrylamide, etc.) in paste/mortar samples resulted in regain of the water-tightness of cracks and could reduce autogenous shrinkage. However, the mechanical strength was severely reduced upon introduction of these SAPs.

Polysaccharides (e.g. alginate) have been reported as an alternative, as shown in several studies developed by Mignon et al. [6, 52, 69, 70], since the introduction of this type of SAPs resulted in a minimal effect on the compressive strength of cementitious materials. SAPs based on sulfonic acids have also been reported in literature as an interesting alternative for applications with cementitious materials. These type of SAPs are stronger in comparison to carboxylic acids and they lead to much higher osmotic forces to attract the water into the formed hydrogel network. Additionally, they are less influenced by changes in the pH of their environment, which is a benefit considering the alkaline environment inside a structure made of a cementitious matrix and possible changes upon development of cracks and ingress of aggressive agents. Besides, since crude oil is becoming more expensive and finite [71, 72] the use of polymers with alternative materials represent a cost-efficient and sustainable option.

In this research, 10 different SAPs were tested, including commercial SAPs and in-house developed SAPs. Different particle sizes were investigated and they will be specified when the respective tests are being described throughout the thesis. As already stated in the previous sections, different applications will require different properties from the SAPs, and this is directly related to their chemical composition, production process, and sometimes the particle size. Considering the main objective of the research being the combination of innovative SAPs for the production of concrete structures with the features of internal curing, self-sealing and self-healing of cracks, the following criteria were targeted for the production of the in-house developed SAPs and choice of commercially available ones:

- swelling capacity compatible with the complete closure of cracks up to 200-300  $\mu\text{m}$  width; advisable swelling ratio in demineralized water of 200-400 g/g SAP and limited swelling during mixing for sealing/healing; and in cement filtrate solution of 10-60 g/g SAP for internal curing purposes;
- reproducible characteristics of the SAPs;
- stability in different solutions (demineralized water, tap water, cement filtrate solution) and in an alkaline environment (pH 12-13) when mixed in a cementitious material;
- polymers with high enough glass transition temperature to be able to be ground ( $T_g$  of minimum 50°C, preferentially minimum 100°C);
- correct release of water after setting for internal curing to mitigate shrinkage without effect on setting of concrete;
- adjusted lab scale SAP synthesis protocols in order to obtain a successful upscaling with the infrastructure of the project partners;
- cost-effective and maximum additional cost of 15 €/m<sup>3</sup> of concrete;

Table 3.2 shows an overview of the SAPs initially studied in this research. More details will be provided in the following sections.

Table 3.2 - Overview of the studied SAPs. The type of chemistry, original design purpose and mean particle sizes are shown.

Name	Type of chemistry	Initial purpose	Mean particle size (d <sub>50</sub> ) in µm
SAPA	Acrylic acid	Internal curing	40
SAPB	Acrylic acid	Internal curing	360
SAPC1	Modified alginates	Self-healing	100
SAPC2	Modified alginates	Self-healing	100
SAPC3	Modified alginates	Self-healing	100
SAPC4	Modified alginates	Self-healing	100
SAPD1	Sulfonate-type	Internal curing	100
SAPD2.1	Sulfonate-type	Internal curing	100
SAPD2.2	Sulfonate-type	Internal curing	100
SAPD3	Sulfonate-type	Self- sealing/healing	100/300

2.6.1 Commercial SAPs

Two commercial SAPs based on acrylic acid chemistry were used. From now on, they will be referred to as SAPA and SAPB. SAPA, provided by BASF (Germany), is a copolymer of acrylamide and sodium acrylate produced through bulk polymerization. SAPB, made by SNF Floerger (France), is a crosslinked acrylate copolymer also produced through bulk polymerization. Due to commercial confidentiality, extra details about the production of both SAPs are not available.

2.6.2 (In-house developed) Alginate-based SAPs

Four alginate based SAPs were developed based on a modification of methacrylated alginate (algMOD) and redox polymerization.

A 2.5 m% aqueous sodium alginate solution was prepared and four equivalents MAAH with respect to the hydroxyl functionalities were added. The acidity of the mixture was constantly monitored and increased to pH 8 by adding a 5 M sodium hydroxide (NaOH) solution to improve reactivity. Moreover, the pH levels were monitored to avoid hydrolysis of the ester in the reaction product. After MAAH addition, the mixture was allowed to react overnight at room temperature. Afterwards, the modified alginate solution was combined with acrylic acid. Ammonium persulfate (APS) and N,N,N',N'-tetramethylene diamine (TEMED) were used to initiate the polymerization. APS was added at a concentration of 2 m% with respect to the total weight of the monomers. TEMED was added in a 1/1 vol% ratio with respect to APS. The polymerization was performed at 45°C during 24 h. Afterwards, the obtained SAPs were dried in an oven at 80°C. One of the SAPs was also purified in water for 24 h to investigate the possible effects of the presence of soluble materials in the performance of the final product. For one of the SAPs, a purification stage also took place during production to obtain a gel fraction of 100%. The composition of the various synthesized SAPs is shown in Table 3.3.

Table 3.3 - Composition of the various alginate-based SAPs produced by the <sup>3</sup>Polymer Chemistry & Biomaterials Group at Ghent University.

Name	AlgMOD/AA ratio (g/g)	APS	TEMED	Gel fraction (%)
SAPC1	1/7	2 m%	1/1 vol% APS	42.8 ± 0.9
SAPC2	1/7	2 m%	1/1 vol% APS	100%
SAPC3	1/4	2 m%	1/1 vol% APS	43.5 ± 3.3
SAPC4	1/10	2 m%	1/1 vol% APS	51.7 ± 1.3

### 2.6.3 (In-house developed) Sulfonate-based SAPs

An overview of the sulfonate-based SAPs is shown in Table 3.4. SAPs type 1 (SAPD1) and type 2 (SAPD2.1 and SAPD2.2) were initially designed for the promotion of internal curing. SAP type 3 (SAPD3) was developed with the purpose of self-sealing/healing.

Table 3.4 – Overview of the sulfonate based-SAPs produced by ChemStream bv.

Name	Composition	Alkali-stable CL (mol%)	Alkali-unstable CL (mol%)	% solubles
SAPD1	p[SVS-co-NaAMPS]	0.15	0	36
SAPD2.1	p[NaAMPS-co-ACMO(20) <sup>1</sup> ]	0.07	0	9
SAPD2.2	p[NaAMPS-co-ACMO(50) <sup>2</sup> ]	0.04	0	26
SAPD3	p[NaAMPS]	0.15	1	8

CL = crosslinker; <sup>1</sup> 20 mol% of ACMO; <sup>2</sup> 50 mol% of ACMO.

SAP type 1 is a SAP composed of 2 co-monomers NaAMPS (2-acrylamido-2-methyl-1-propanesulfonic acid sodium salt) and SVS (sodium vinyl sulfonate) that are lightly crosslinked to form a superabsorbent polymer that swells about 275 times its own weight in demineralized water. Both co-monomers contain the sodium salt form of a sulfonic acid group, which leads to a very densely charged hydrogel with great osmotic power for absorbing water. This type of SAP-composition is based on ChemStream’s prior art EP2835385 [73].

SAP type 2 is a SAP that is similar to SAP type 1, since it mainly consists of co-monomer NaAMPS, but it is ‘diluted’ with a non-charged or neutral monomer ACMO (acryloyl morpholino acrylate). The purpose of making SAP type 2 was to verify if the density of the charged sulfonate groups on the polymer SAP network has an influence on the behavior of the SAPs in the concrete mixtures and applications.

SAP type 3 is also very similar to SAP type 1, because it is solely composed of monomer NaAMPS. The difference however is defined by the use of a second alkali unstable crosslinker. In this case, the used SAP has a much lower initial swelling degree, but once the compound has been in the alkali environment of the cementitious materials for a few hours/days, the crosslinks that are constituted by the second crosslinker are hydrolyzed and the swelling potential of the SAP becomes much greater

again in situ. The idea behind this concept is to enable the use of higher dosages of SAPs without the need of higher amounts of additional water to compensate for the loss in workability, which normally leads to a significant increase in the air content in the hardened state of the concrete (due to the formation of macropores) and a resulting decrease in compressive strength. Once the alkali-unstable crosslinker is hydrolyzed, the SAP particles can swell more, which can be a benefit for the promotion of self-sealing of future cracks.

The dosage of stable and unstable crosslinkers was determined based on a preliminary study where different amounts of alkali-stable crosslinker were used. Figure 3.3 shows the effect of the total crosslinking amount on the absorption capacity of a NaAMPS-based SAP for both demineralized water and cement filtrate solution after three days of immersion, by means of the filtration method [55]. In the test performed with demineralized water it was noticed that an amount of crosslinking agent above 1 mol% did not promote a significant lowering in absorption capacity by the SAP. Based on that, a total amount of crosslinker of 1.15 mol% was chosen for the production of SAPD3.

The SAPs were prepared using a thermal bulk polymerization reaction in water, under inert atmosphere. After reaction, a bulky hydrogel is formed that has to be cut into smaller pieces and dried until all water is evaporated. A bulk polymerization reaction is very simple and convenient but is not a very controlled process. Therefore, it is always possible that some water-soluble fraction is still present in the end product containing unreacted monomers and/or not crosslinked linear oligomers. This soluble fraction is depicted in Table 3.4.

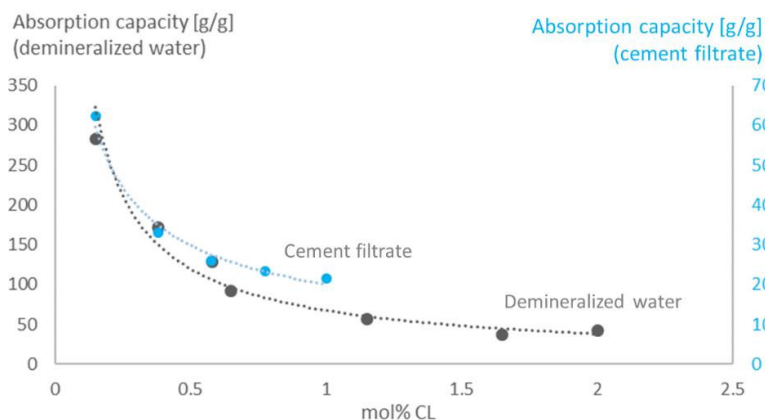


Figure 3.3 - Effect of the total crosslinking degree on the absorption capacity of NaAMPS-based SAP, measured after three days of immersion in the respective fluid (CL stands for crosslinker).

#### 2.6.4 Water absorption of the SAPs in different fluids

All SAPs were characterized in terms of absorption capacity in different fluids. Demineralized water and cement filtrate solution were used. A filtration test was performed in accordance with the recommendation from the RILEM technical committee 260-RSC on the use of SAPs [55]. In this test, a certain amount of dry SAPs is taken (in this research an amount of around 0.11 g was used), then, around 100 ml of the testing fluid are added to promote the swelling of the dry SAP particles. After specific swelling times, the mixture of swollen SAPs and remaining fluid is filtered and the absorption capacity is determined based on the amount of water absorbed by the dry SAPs. This test served as an preliminary assessment of the absorption capacity of SAPs. Some disadvantages of the method are described in [74]. Some limitations are also discussed in Chapter 3.

Given the double crosslinker nature of SAPD3, the absorption capacity in demineralized water was determined in two stages. In the first stage, the test was performed as described above. In the second stage, SAPD3 was tested after the hydrolysis of the alkali-unstable crosslinker. To do so, the SAP particles were tested in three different conditions: initial (before exposure to any alkaline environment), after 24 h and 72 h of continuous exposure to an alkaline environment (cement filtrate solution). The SAP



particles exposed to the cement filtrate solution were prepared as described below:

- SAPs were immersed in cement filtrate solution for 24 h/72 h and filtered afterwards;
- After filtration, the swollen SAPs were immersed in demineralized water for 24 h and filtered afterwards. This step was executed twice;
- Then, the swollen SAPs were oven-dried at 80°C for 24 h;
- The dry SAPs were then ready for determination of the absorption capacity after hydrolysis of the alkali-unstable crosslinker.

The cement filtrate solution was produced with demineralized water and cement (CEM III-B 42.5N – LH/SR) in a proportion of 1:5 (in mass). Both demineralized water and cement were continuously stirred at a very low speed during 24 h. Afterwards, the solution was filtered and it was ready to be used in the filtration test.

The absorption capacity of all SAPs after 10 min in demineralized water is shown in Figure 3.4. For the specific case of SAPD3, the absorption in demineralized water after the exposure to the alkaline environment of the cement filtrate solution is detailed in Figure 3.5.

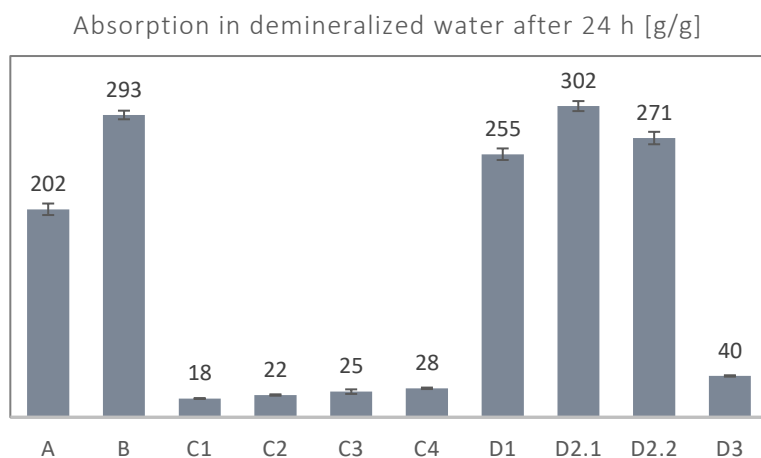


Figure 3.4 - Absorption capacity of all SAPs in demineralized water after 10 min of immersion.

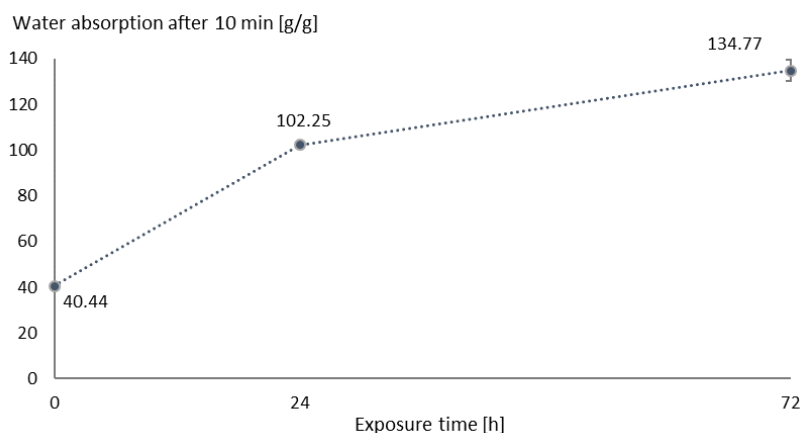


Figure 3.5 – Absorption of SAPD3 after 10 minutes of immersion in demineralized water measured after the exposure to the alkaline environment of the cement filtrate solution at 0, 24 and 72 hours.

The absorption capacity in demineralized water reveals some aspects regarding the possibly most suitable applications for the different SAPs. All SAPs initially thought to be used as internal curing agents present a much higher absorption capacity in comparison to the other SAPs, which were initially thought to be used for sealing and healing. Both commercial SAPs (SAPs A and B) and the sulfonate SAPs from type 1 and type 2 (SAPS D1, D2.1 and D2.2) have an absorption capacity above 200 g/g. For the commercial SAPs, no details regarding the chemical structure are known, which limits the discussion of the different behaviors to a probable difference in the amount of crosslinking, where a lower amount of crosslinking could be the reason why SAPB has a higher absorption capacity than SAPA.

As for the alginate-based SAPs, not much could be concluded with the absorption in demineralized water. Regarding the ratio of modified alginate and acrylic acid, no difference was observed in the absorption capacity of the SAPs when comparing the different ratios. The SAP with the lowest amount of modified alginates (SAPC4) had the same absorption capacity as the SAP with the highest amount of modified alginates in the composition (SAPC3). When it comes to the purification process and the influence of the gel fraction, no significant difference was found between SAPC1 and SAPC2.

The effect of the amount and type of crosslinking on the absorption capacity is very noticeable for the sulfonate SAPs. Starting with SAPD3, with a total crosslinking amount of 1.15 mol% (the highest amongst the sulfonates SAPs) a considerable lower absorption capacity was obtained compared to the other sulfonates SAPs.

Considering the degradation of the alkali-unstable crosslinker in SAPD3, a significant increase in water uptake was observed after immersion in cement filtrate. After 24 h of continuous exposure to the cement filtrate solution, the absorption capacity in demineralized water increased by a factor of 2.5. At the mark of 72 h of continuous exposure, the absorption capacity was 3.3 times higher than the initial one. Although there is a considerable increase, the value of the absorption capacity after 72 h of exposure is still lower than the expected value for a NaAMPS-based SAP with 0.15 mol% of crosslinker (see Figure 3.3). This indicates that the alkali-unstable crosslinker might not have degraded completely in the cement filtrate solution within the evaluated period. After 72 h, the increase in the water absorption seems to develop to a lower rate, indicating that it tends to stabilize shortly after that period. This could be an indication that the crosslinker would not completely hydrolyze in the cement filtrate solution, regardless of the time of exposure.

Apart from that, after some time a second process might start, namely extra complexation of the sulfonic acid groups with the high concentration of  $\text{Ca}^{2+}$  ions inside the pores. With this complexation, a counter reaction of extra ionic crosslinking can take place, which has the opposite effect to the hydrolysis of the second crosslinker.

The nature of the double crosslinking and its consequence to the effects of this SAP in the properties of cementitious materials will be further explored in Chapter 3 and Chapter 5.

Regarding SAPs type 2 and type 3 of the sulfonate group, with lesser crosslinking the type 2 SAPs present a slightly higher absorption capacity in comparison to SAP type 1 (SAPD1), which has the highest amount of crosslinking amongst the three (SAPD1, SAPD2.1 and SAPD2.2). As for SAPs D2.1 and D2.2, specifically, the influence of the dilution in the neutral monomer ACO (acryloyl morpholino acrylate) can also be seen.

The lesser the amount of ACO, the more densely charged is the polymer which leads to much higher osmotic forces to attract the water into the formed hydrogel network. Which explains why SAPD2.1 absorbs more water than SAPD2.2, despite the higher amount of crosslinking used in SAPD2.1

The absorption capacity of the SAPs in cement filtrate solution is depicted in Figure 3.6. As expected, the values of absorption are considerably lower than the ones found in demineralized water (Figure 3.4), which is due to a different concentration of ions in the cement filtrate solution in comparison to the demineralized water as it was also observed in several other studies [15, 29, 30, 32, 60].

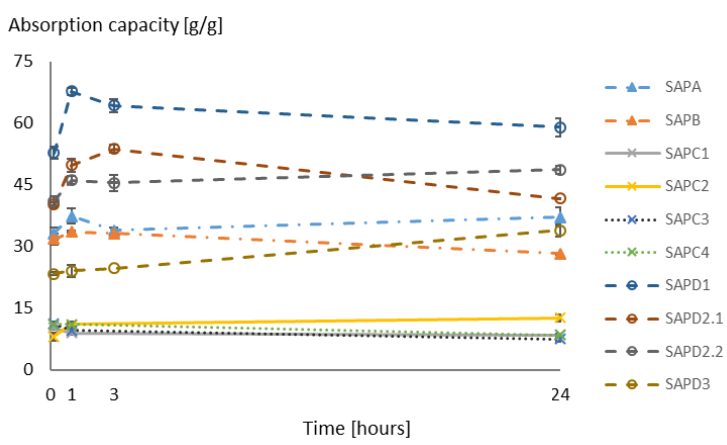


Figure 3.6 - Absorption capacity of all SAPs in cement filtrate solution measured after 10 min, 1 h, 3 h and 24 h. The commercial SAPs are represented by the triangular markers; the alginate SAPs are represented by the cross markers; the sulfonate SAPs are represented by the circular markers. The lines only represent a trend.

As it was the case for demineralized water, the different types of SAPs showed different behaviors with the cement filtrate solution. Overall, the sulfonate-based SAPs (with the exception of SAPD3) showed the highest absorption capacity of all SAPs. They were followed by the commercial SAPs, while the alginate-based SAPs had the lowest absorption capacity.

For the sulfonate-based SAPs, a significant increase in absorption capacity was found from 10 min up to 1 h after immersion in the cement filtrate solution, specifically for SAPs D1 and D2.1. For SAPD2.2, such increase was

not very pronounced and it might be related to the higher density of charges in SAPs D1 and D2.1 in comparison to SAPD2.2, which can be translated in much higher osmotic forces to attract the water into the formed hydrogel network. This potential increase in absorption capacity at early states could represent a negative impact on the workability of cementitious materials, specifically when considering applications where the material needs to be transported and it is not possible to proceed with immediate application right after the mixing process. As for SAPD3, a constant increase in the absorption capacity was noticed over time, which is related to the hydrolysis of the alkali-unstable crosslinker present in its composition (as already stated before).

The commercial SAPs absorb the cement filtrate at a very steady pace, without much significant increase at the early stages of testing. SAPB presents a small reduction in absorption at 24 h of immersion. This slightly different desorption can be explained by the differences in the chemical composition of both SAPs. Lee et al. (2018) [75] and Kang et al. (2018) [29] highlight that (poly) acrylate type SAP (SAPB) is more susceptible to  $\text{Ca}^{2+}$  complexation and therefore achieves a lower swelling ratio compared to acrylamide SAPs (SAPA) in calcium bearing solutions. Furthermore, the release of absorbed water is more rapid and recovery in swelling capacity of the first type is much slower than for the second.

With the lowest absorption capacity amongst all the tested SAPs, the alginate-based SAPs reveal a small influence of the purification process. SAPC2 is the only alginate-based SAP that shows an increased absorption at later stages, while all the others (SAPs C1, C3 and C4) present a slight reduction over time.

Except for SAPs C2 and D3, for all other cases where an increase in absorption capacity was noticed at early stages, it was followed by a decrease at 24 h, and the absorption capacity at that time was at the same level of the one measured after 10 min. It is already well established in literature that the swelling capacity of SAPs is mainly affected by ion concentration and cationic type [15, 29, 32, 63]. In the presence of high-valent cations, such as  $\text{Mg}^{2+}$ ,  $\text{Ca}^{2+}$  and  $\text{Al}^{3+}$  (abundant in the pore solution of cementitious materials), complexation will take place between such cations and the anionic groups in the SAPs. This complexation reduces the

electrostatic repulsion and the absorption capacity, potentially leading to water release.

## 2.7 Conclusions

The sorption and desorption behavior of SAPs in different solutions was investigated. The kinetics of the SAPs in cementitious media (in this case the cement filtrate solution) is dependent on the (cat/an)ion concentration of the solution. The multivalent and monovalent cations play a different but still both separately and combined important roles.

It is well known, and widely reported in literature, that upon contact with cementitious solutions the SAPs absorb  $\text{Ca}^{2+}$  ions while desorbing  $\text{Na}^+$  into the solution. In cement filtrate solutions, the ion concentration is relatively low (in comparison to a cement paste for example) due to the dilution effect caused by the considerably high water-to-cement ratio. In that case, the osmotic pressure (the driving force of absorption) is high and the SAPs immediately absorb a lot of fluid. Along with the fluid, the SAPs also absorb a lot of  $\text{Ca}^{2+}$ , which in time will cause charge-screening and strong complexation. This reduces the absorption capacity over time, and may impair the retention capacity of the SAP.

SAPs based on acrylic acid chemistry are very susceptible to this, mainly due to the density of anionic groups that will bridge with the  $\text{Ca}^{2+}$  to form new crosslinking. By analyzing the behavior of such type of SAP in a cement filtrate solution one might easily conclude that the SAP has some sort of incontinent behavior (as it was noticed for SAP B). This premature water release might be seen as a low efficacy of the SAPs when it comes to the mitigation of autogenous shrinkage, for example.

However, that is not really the case when it comes to SAPs in cement paste or concrete, for example. In such type of fluid, as Kang et al. (2018) showed it in [29], the presence of monovalent ions (such as  $\text{Na}^+$ ) is considerably higher than in the cement filtrate solution. This increased amount of monovalent ions contributes to an increased total ionic concentration of the fluid that will reduce the osmotic pressure and consequently the initial absorption capacity of the SAP. As the SAP is now absorbing less fluid at the beginning, it will also absorb less  $\text{Ca}^{2+}$ . The SAP will then be less susceptible to ionic crosslinking and its long-term absorption and retention capacity will not be affected. That is why, poly acrylic acids SAPs are very efficient in mitigating the autogenous

shrinkage of cement pastes and concrete, even though they might present a low retention capacity when tested in cement filtrate solution.

That will be further explored and discussed in Chapter 3.



## References

1. Mechtcherine, V. and H.W. Reinhardt, *Application of Super Absorbent Polymers (SAP) in Concrete Construction*, in *State-of-the-Art Report Prepared by Technical Committee 225-SAP*. 2012, RILEM. p. 165.
2. Wong, H.S., *Concrete with superabsorbent polymer*, in *Eco-Efficient Repair and Rehabilitation of Concrete Infrastructures*, R.E.M. F. Pacheco-Torgal, Xianming Shi, Nele De Belie, Kim Van Tittelboom, Andrés Sáez, Editor. 2018, Woodhead Publishing. p. 467-499.
3. Viktor, M., *Use of superabsorbent polymers (SAP) as concrete additive*. RILEM Technical Letters, 2016. **1**(0).
4. Zohuriaan-Mehr, M.J. and K. Kabiri, *Superabsorbent polymer materials: A review*. Iranian Polymer Journal, 2008. **17**(6): p. 451-477.
5. Tangkokiat, P., et al. *Characterization of Neutral Versus Anionic Superabsorbent Polymers (SAPs) in Ion-Rich Solutions for Their Use as Internal Curing Agents*. 2020. Cham: Springer International Publishing.
6. Mignon, A., et al., *Superabsorbent polymers: A review on the characteristics and applications of synthetic, polysaccharide-based, semi-synthetic and 'smart' derivatives*. European Polymer Journal, 2019. **117**: p. 165-178.
7. Jensen, O.M., *Use of Superabsorbent Polymers in Construction Materials*. Microstructure Related Durability of Cementitious Composites, Vols 1 and 2, 2008. **61**: p. 757-764.
8. H. Holback, Y.Y., K. Park, *Hydrogel swelling behavior and its biomedical applications*, in *Biomedical Hydrogels*, S. Rimmer, Editor. 2011, Woodhead Publishing. p. 3-24.
9. Barner-Kowollik, C., P. Vana, and T.P. Davis, *The Kinetics of Free-Radical Polymerization*, in *Handbook of Radical Polymerization*. 2002. p. 187-261.
10. Yamada, B. and P.B. Zetterlund, *General Chemistry of Radical Polymerization*, in *Handbook of Radical Polymerization*. 2002. p. 117-186.
11. Cunningham, M.F. and R. Hutchinson, *Industrial Applications and Processes*, in *Handbook of Radical Polymerization*. 2002. p. 333-359.
12. Yuan, H.G., G. Kalfas, and W.H. Ray, *SUSPENSION POLYMERIZATION*. Journal of Macromolecular Science, Part C, 1991. **31**(2-3): p. 215-299.
13. Laustsen, S., M.T. Hasholt, and O.M. Jensen, *Void structure of concrete with superabsorbent polymers and its relation to frost resistance of concrete*. Materials and Structures, 2015. **48**(1-2): p. 357-368.
14. Chern, C.S., *Emulsion polymerization mechanisms and kinetics*. Progress in Polymer Science, 2006. **31**(5): p. 443-486.
15. Schröfl, C., V. Mechtcherine, and M. Gorges, *Relation between the molecular structure and the efficiency of superabsorbent polymers (SAP) as concrete admixture to mitigate autogenous shrinkage*. Cement and Concrete Research, 2012. **42**(6): p. 865-873.

16. Friedrich, S., *Superabsorbent Polymers (SAP)*, in *Application of Super Absorbent Polymers (SAP) in Concrete Construction: State-of-the-Art Report Prepared by Technical Committee 225-SAP*, V. Mechtcherine and H.-W. Reinhardt, Editors. 2012, Springer Netherlands: Dordrecht. p. 13-19.
17. Peppas, N.A., B.V. Slaughter, and M.A. Kanzelberger, *9.20 - Hydrogels*, in *Polymer Science: A Comprehensive Reference*, K. Matyjaszewski and M. Möller, Editors. 2012, Elsevier: Amsterdam. p. 385-395.
18. Lee, K.Y. and D.J. Mooney, *Hydrogels for Tissue Engineering*. Chemical Reviews, 2001. **101**(7): p. 1869-1880.
19. Soh, S.K. and D.C. Sundberg, *Diffusion-controlled vinyl polymerization. I. The gel effect*. Journal of Polymer Science: Polymer Chemistry Edition, 1982. **20**(5): p. 1299-1313.
20. MEYER, W.C., *A POLYMERIC BLEND USEFUL IN THIN-BED MORTAR COMPOSITIONS*, E.P. Office, Editor. 1989.
21. Jensen, O.M. and P.F. Hansen, *Autogenous deformation and RH-change in perspective*. Cement and Concrete Research, 2001. **31**(12): p. 1859-1865.
22. Jensen, O.M. and P.F. Hansen, *Water-entrained cement-based materials I. Principles and theoretical background*. Cement and Concrete Research, 2001. **31**(4): p. 647-654.
23. Powers, T.C. *A Discussion of Cement Hydration in Relation to the Curing of Concrete*. in *Twenty-Seventh Annual Meeting of the Highway Research Board* 1947. Washington, D.C, USA: Highway Research Board.
24. De Meyst, L., et al., *Parameter Study of Superabsorbent Polymers (SAPs) for Use in Durable Concrete Structures*. Materials, 2019. **12**(9).
25. Justs, J., et al., *Internal curing by superabsorbent polymers in ultra-high performance concrete*. Cement and Concrete Research, 2015. **76**: p. 82-90.
26. Mechtcherine, V., et al., *Effect of internal curing by using superabsorbent polymers (SAP) on autogenous shrinkage and other properties of a high-performance fine-grained concrete: results of a RILEM round-robin test*. Materials and Structures, 2014. **47**(3): p. 541-562.
27. Craeye, B., M. Geirnaert, and G. De Schutter, *Super absorbing polymers as an internal curing agent for mitigation of early-age cracking of high-performance concrete bridge decks*. Construction and Building Materials, 2011. **25**(1): p. 1-13.
28. J. Piérard, V. Pollet, and N. Cauberg. *Mitigating autogenous shrinkage in HPC by internal curing using superabsorbent polymers*. in *International RILEM Conference on Volume Changes of Hardening Concrete: Testing and Mitigation*. 2006. Lyngby, Denmark: RILEM Publications SARL.

29. Kang, S.H., S.G. Hong, and J. Moon, *Importance of monovalent ions on water retention capacity of superabsorbent polymer in cement-based solutions*. Cement & Concrete Composites, 2018. **88**: p. 64-72.
30. Kang, S.H., S.G. Hong, and J. Moon, *Absorption kinetics of superabsorbent polymers (SAP) in various cement-based solutions*. Cement and Concrete Research, 2017. **97**: p. 73-83.
31. Sung-Hoon Kang, S.-G.H., Juhyuk Moon, *Absorption kinetics of superabsorbent polymers (SAP) in various cement-based solutions*. Cement and Concrete Research, 2017. **97**: p. 73-83.
32. Yang, J., et al., *Early-state water migration characteristics of superabsorbent polymers in cement pastes*. Cement and Concrete Research, 2019. **118**: p. 25-37.
33. Snoeck, D., L. Pel, and N. De Belie, *The water kinetics of superabsorbent polymers during cement hydration and internal curing visualized and studied by NMR*. Scientific Reports, 2017. **7**.
34. Snoeck, D., L. Pel, and N. De Belie, *Superabsorbent polymers to mitigate plastic drying shrinkage in a cement paste as studied by NMR*. Cement & Concrete Composites, 2018. **93**: p. 54-62.
35. Mechtcherine, V. and L. Dudziak, *Effects of Superabsorbent Polymers on Shrinkage of Concrete: Plastic, Autogenous, Drying*, in *Application of Super Absorbent Polymers (SAP) in Concrete Construction: State-of-the-Art Report Prepared by Technical Committee 225-SAP*, V. Mechtcherine and H.-W. Reinhardt, Editors. 2012, Springer Netherlands: Dordrecht. p. 63-98.
36. Boshoff, W., et al., *The effect of superabsorbent polymers on the mitigation of plastic shrinkage cracking of conventional concrete, results of an inter-laboratory test by RILEM TC 260-RSC*. Materials and Structures, 2020. **53**(4): p. 79.
37. Assmann, A. and H.W. Reinhardt, *Tensile creep and shrinkage of SAP modified concrete*. Cement and Concrete Research, 2014. **58**: p. 179-185.
38. Shen, D., et al., *Influence of super absorbent polymers on early-age behavior and tensile creep of internal curing high strength concrete*. Construction and Building Materials, 2020. **258**: p. 120068.
39. Van Mullem, T., *Development of standard testing methods to evaluate the self-healing efficiency of concrete*, in *Department of Structural engineering and building materials*. 2021, Ghent University.
40. Craeye, B., G. Cockaerts, and P. Kara De Maeijer, *Improving Freeze–Thaw Resistance of Concrete Road Infrastructure by Means of Superabsorbent Polymers*. Infrastructures, 2018. **3**(1): p. 4.
41. Mechtcherine, V., et al., *Effect of superabsorbent polymers (SAP) on the freeze-thaw resistance of concrete: results of a RILEM interlaboratory study*. Materials and Structures, 2017. **50**(1).

42. Monnig, S. and P. Lura, *Superabsorbent polymers - An additive to increase the freeze-thaw resistance of high strength concrete*. Advances in Construction Materials 2007, 2007: p. 351-358.
43. Snoeck, D., et al., *Self-healing cementitious materials by the combination of microfibres and superabsorbent polymers*. Journal of Intelligent Material Systems and Structures, 2014. **25**(1): p. 13-24.
44. Snoeck, D., T. De Schryver, and N. De Belie, *Enhanced impact energy absorption in self-healing strain-hardening cementitious materials with superabsorbent polymers*. Construction and Building Materials, 2018. **191**: p. 13-22.
45. Snoeck, D., O.M. Jensen, and N. De Belie, *The influence of superabsorbent polymers on the autogenous shrinkage properties of cement pastes with supplementary cementitious materials*. Cement and Concrete Research, 2015. **74**: p. 59-67.
46. Liu, J., et al., *The effect of SCMs and SAP on the autogenous shrinkage and hydration process of RPC*. Construction and Building Materials, 2017. **155**: p. 239-249.
47. Klemm, A.J. and K.S. Sikora, *The effect of Superabsorbent Polymers (SAP) on microstructure and mechanical properties of fly ash cementitious mortars*. Construction and Building Materials, 2013. **49**: p. 134-143.
48. Lefever, G., et al., *The Influence of Superabsorbent Polymers and Nanosilica on the Hydration Process and Microstructure of Cementitious Mixtures*. Materials, 2020. **13**(22): p. 5194.
49. Lefever, G., et al., *Combined use of superabsorbent polymers and nanosilica for reduction of restrained shrinkage and strength compensation in cementitious mortars*. Construction and Building Materials, 2020. **251**: p. 118966.
50. Van Der Putten, J., et al., *Early age shrinkage phenomena of 3D printed cementitious materials with superabsorbent polymers*. Journal of Building Engineering, 2021. **35**: p. 102059.
51. Mignon, A., et al., *Mechanical and self-healing properties of cementitious materials with pH-responsive semi-synthetic superabsorbent polymers*. Materials and Structures, 2017. **50**(6): p. 238.
52. Mignon, A., et al., *Alginate biopolymers: Counteracting the impact of superabsorbent polymers on mortar strength*. Construction and Building Materials, 2016. **110**: p. 169-174.
53. Mannekens, E. and G. Deroover. *The development of SAPs for reducing autogenous shrinkage and accomplishing self-healing and self-sealing properties in concrete*. in *Durable Concrete for Infrastructure under Severe Conditions: Smart Admixtures, Self-responsiveness and Nano-additions* 2019. Ghent, Belgium: MagneL Laboratory for Concrete Research.

54. Wang, C.Y., et al., *Self-healing cement composite: Amine- and ammonium-based pH-sensitive superabsorbent polymers*. Cement & Concrete Composites, 2019. **96**: p. 154-162.
55. Snoeck, D., C. Schröfl, and V. Mechtcherine, *Recommendation of RILEM TC 260-RSC: testing sorption by superabsorbent polymers (SAP) prior to implementation in cement-based materials*. Materials and Structures, 2018. **51**(5).
56. Wyrzykowski, M., et al., *Recommendation of RILEM TC 260-RSC: using superabsorbent polymers (SAP) to mitigate autogenous shrinkage*. Materials and Structures, 2018. **51**(5): p. 135.
57. Mechtcherine, V., et al., *Recommendations of RILEM TC 260-RSC for using superabsorbent polymers (SAP) for improving freeze–thaw resistance of cement-based materials*. Materials and Structures, 2019. **52**(4): p. 75.
58. Mechtcherine, V., et al., *Application of super absorbent polymers (SAP) in concrete construction—update of RILEM state-of-the-art report*. Materials and Structures, 2021. **54**(2): p. 80.
59. Snoeck, D., et al., *The effects of superabsorbent polymers on the microstructure of cementitious materials studied by means of sorption experiments*. Cement and Concrete Research, 2015. **77**: p. 26-35.
60. Jensen, O.M., *Water absorption of superabsorbent polymers in a cementitious environment*, in *International RILEM Conference on Advances in Construction Materials*, C.L.a.K.T. WAN, Editor. 2011, RILEM Publications SARL. p. 22 - 35.
61. Lee, H.X.D., H.S. Wong, and N.R. Buenfeld, *Potential of superabsorbent polymer for self-sealing cracks in concrete*. Advances in Applied Ceramics, 2010. **109**(5): p. 296-302.
62. Lee, H.X.D., H.S. Wong, and N.R. Buenfeld, *Self-sealing of cracks in concrete using superabsorbent polymers*. Cement and Concrete Research, 2016. **79**: p. 194-208.
63. Zhu, Q., C.W. Barney, and K.A. Erk, *Effect of ionic crosslinking on the swelling and mechanical response of model superabsorbent polymer hydrogels for internally cured concrete*. Materials and Structures, 2015. **48**(7): p. 2261-2276.
64. Reinhardt, H.-W. and A. Assmann, *Effect of Superabsorbent Polymers on Durability of Concrete*, in *Application of Super Absorbent Polymers (SAP) in Concrete Construction: State-of-the-Art Report Prepared by Technical Committee 225-SAP*, V. Mechtcherine and H.-W. Reinhardt, Editors. 2012, Springer Netherlands: Dordrecht. p. 115-135.
65. Davis, C.R., et al. *Altering the Crosslinking Density of Polyacrylamide Hydrogels to Increase Swelling Capacity and Promote Calcium Hydroxide Growth in Cement Voids*. 2020. Cham: Springer International Publishing.
66. Snoeck, D., et al., *Effect of high amounts of superabsorbent polymers and additional water on the workability, microstructure and strength of*

- mortars with a water-to-cement ratio of 0.50*. Construction and Building Materials, 2014. **72**: p. 148-157.
67. Ding, H., L. Zhang, and P. Zhang, *Factors Influencing Strength of Super Absorbent Polymer (SAP) Concrete*. Transactions of Tianjin University, 2017. **23**(3): p. 245-257.
68. Hong, G. and S. Choi, *Rapid self-sealing of cracks in cementitious materials incorporating superabsorbent polymers*. Construction and Building Materials, 2017. **143**: p. 366-375.
69. Mignon, A., et al., *Crack Mitigation in Concrete: Superabsorbent Polymers as Key to Success?* Materials, 2017. **10**(3).
70. Mignon, A., et al., *Mechanical and self-healing properties of cementitious materials with pH-responsive semi-synthetic superabsorbent polymers*. Materials and Structures, 2017. **50**(6).
71. Hua, S.B. and A.Q. Wang, *Synthesis, characterization and swelling behaviors of sodium alginate-g-poly(acrylic acid)/sodium humate superabsorbent*. Carbohydrate Polymers, 2009. **75**(1): p. 79-84.
72. Wu, L.Q., et al., *Utilizing renewable resources to create functional polymers: Chitosan-based associative thickener*. Environmental Science & Technology, 2002. **36**(15): p. 3446-3454.
73. Deroover, G. and E. Mannekens, *POLY-ELECTROLYTE POLYMER COMPOSITION AND ITS USE (EP 2835385 B1 20191225)*, E.P. Office, Editor. 2019: Belgium.
74. Zhao, S., O.M. Jensen, and M.T. Hasholt, *Measuring absorption of superabsorbent polymers in cementitious environments*. Materials and Structures, 2020. **53**(1): p. 11.
75. H.X.D. Lee, H.S.W., N.R. Buenfeld, *Effect of alkalinity and calcium concentration of pore solution on the swelling and ionic exchange of superabsorbent polymers in cement paste*. Cement and Concrete Composites, 2018. **88**: p. 150-164.



## Chapter 3. The effects of SAPs on cement pastes



This chapter was redrafted after:

Tenório Filho, J. R., Mannekens, E., Snoeck, D., & De Belie, N. (2019). Investigating the efficiency of “in-house” produced hydrogels as internal curing agents in cement pastes. In V. Caprai & H. J. H. Brouwers (Eds.), *PROCEEDINGS ICSBM 2019 VOLUME 5 - 2nd International Conference on Sustainable Building Materials* (pp. 37–43). Eindhoven, The Netherlands.

Tenório Filho, J. R., Snoeck, D., & De Belie, N. (2018). The effect of superabsorbent polymers on the cracking behavior due to autogenous shrinkage of cement-based materials. *Proceedings of the 60th Brazilian Concrete Conference*.

### 3.1 Introduction

As a first step towards the investigation of the effects of the different SAPs described in Chapter 2 on the properties of cementitious materials, a preliminary study was conducted on cement pastes. This study comprised the determination of the absorption capacity of the SAPs in the cementitious material and their performance regarding mitigation of autogenous shrinkage and compressive strength. The variation in the levels of internal relative humidity over time was monitored to provide a deeper insight into the effects of the SAPs on the internal curing of the cement pastes. Selected mixtures were also tested regarding the effects of the SAPs on the setting and hardening.

## 3.2 Absorption capacity of SAPs in cement pastes

The estimation of the absorption capacity with cement pastes was performed on the basis of comparative workability measured by means of a flow table test, similar to the one prescribed in the standard NBN EN 1015-3 [1] for mortars. Given the fluid consistency of the mixtures, the test was performed under a free flow, without the application of the prescribed beats to the apparatus plate.

Initially, a reference paste without SAPs and a water-to-cement ratio of 0.3 was produced. The workability of such paste was determined by means of the flow table test 10 min after the first contact of the dry materials with water. The test was performed in triplicates and the reference flow of the plain cement paste was determined as  $263 \pm 12$  mm. Afterwards, a new set of cement pastes was produced with a water-to-cement ratio of 0.354. For the plain cement paste with higher water content, the flow was  $353 \pm 15$  mm. New mixtures containing SAPs and water-to-cement ratio of 0.354 were then produced and the workability of all pastes was compared to the first reference ( $263 \pm 12$  mm).

The amount of SAPs in each paste was initially determined based on the absorption capacity of the SAPs in cement filtrate after 10 min, as determined in Chapter 2. Adjustments in the dosage of SAPs were continuously made until the workability of the SAP-containing paste was equal to that of the reference paste with water-to-cement ratio of 0.3. This approach has been widely reported in literature and mentioned as a practical and reliable method to estimate the absorption of SAPs in real cementitious materials [2-5].

Once the reference workability was achieved, the absorption capacity of each SAP was calculated considering the amount of absorbed water equivalent to an addition of 0.054 in the water to cement ratio of the pastes and the dosage of SAPs relative to the reference flow. The additional entrained water, defined as an additional water-to-cement ratio of 0.054, was determined based on the findings of Jensen and Hansen [6] as the theoretical amount of entrained water needed for full mitigation of autogenous shrinkage in cement pastes with a water-to-

cement ratio of 0.3. It is important to highlight that such approach was developed for ordinary Portland cement, but it was nevertheless used for a preliminary testing of the mixtures in this study.

All cement pastes were produced with blast furnace/Portland cement type CEM III-B 42.5N – LH/SR and a polycarboxylate superplasticizer at constant dosage of 0.3 m% in relation to the cement mass (Glenium 51, 35% conc., BASF, Germany). The mixing procedure was:

- 1) Cement and 90% of the water mixed for 60 s with low speed (140 rpm);
- 2) Mixing for 30 s at high speed (285 rpm);
- 3) Resting of the mixture for 90 s (with scrapping of material from the surface of the mixing bowl during the first 30 s of the pause);
- 4) Addition of the superplasticizer diluted in the remaining 10% of the mixing water and final mixing during 60 s at high speed (285 rpm).

Where SAPs were present, they were dry mixed with cement for 30 s before step 1 and the additional water was included in step 4. The mixing and the testing of the cement pastes were both performed in a room with controlled atmosphere ( $20 \pm 2$  °C and  $60 \pm 5\%$  RH).

The first SAP tested was the commercial SAPB. Given its absorption capacity of around 32 g/g in cement filtrate solution, a dosage of 0.17 m% of SAP over the cement mass was initially used in the production of the cement paste. The resulting flow was 300 mm (far more fluid than the reference mixture). New batches were produced with an increasing amount of SAPs, considering that the absorption capacity in cement filtrate solution was higher than the in the real cement paste. With the increasing amount of SAPs the flow was reduced (Figure 3.1). With the dosage of 0.25 m%, the mixture presented a flow compatible with that from the reference. The absorption of SAPB in the studied cement past was determined as 21 g/g.

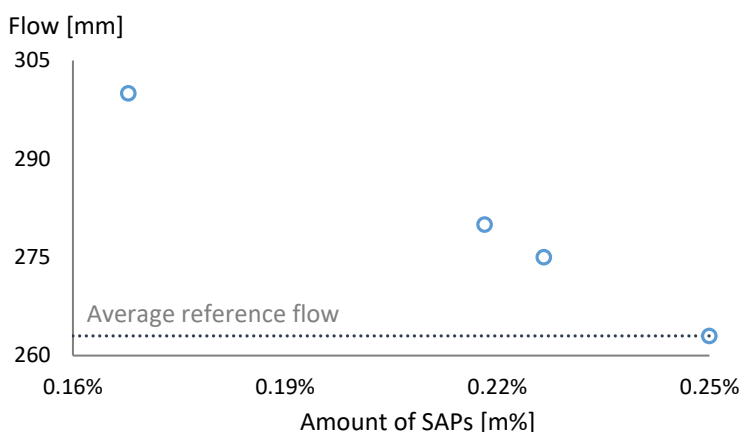


Figure 3.1 - Influence of the amount of SAPB on the free-flow of cement paste mixtures for a constant amount of superplasticizer and water. The flow value of the reference mixture is indicated.

For commercial SAPA, the absorption capacity in cement filtrate solution was 33 g/g, which would lead to a first dosage of 0.16 m% of SAP. Based on the experience with SAPB and considering that SAPA had a slightly higher absorption in cement filtrate, it was decided to start the tests with a dosage of 0.2 m%. That dosage resulted in a flow of 267.5 mm, which was considered compatible with that of the reference. The absorption capacity of SAPA in the cement paste was taken as 27 g/g. For both commercial SAPs, the absorption capacity in cement paste was lower than the one found in cement filtrate solution. As discussed in Chapter 2, the presence of multivalent ions, such as  $\text{Ca}^{2+}$ , is known to cause a complexation that can lead to further crosslinking inside the SAP particle, reducing its absorption capacity in time, especially for SAPs based on acrylic acid chemistry [7, 8].

With the alginate-based SAPs a flow compatible to that of the reference mixture was found for dosages of 0.77 m% for both SAPC1 and SAPC2, 0.64 m% for SAPC3 and 0.52 m% for SAPC4. Such dosages correspond to absorption capacities of 7 g/g, 7 g/g, 8.5 g/g and 10 g/g, respectively for SAPs C1, C2, C3 and C4.

For the sulfonate-based SAPs, starting with SAPD1, the absorption in cement filtrate taken as 53 g/g led to a dosage of SAPs around 0.1 m% for

the complete absorption of the additional entrained water. The sorption properties of this type of SAP are less sensitive to the  $\text{Ca}^{2+}$  dissolved in the liquid phase of the cement paste (the sulfonic group cannot be complexed with  $\text{Ca}^{2+}$ ) [9, 10], hence, the amount of 0.1 m% was initially tested. The mixture had a very plastic consistency and no flow was obtained in the flow table test, indicating that SAPD1 was absorbing more water than estimated in the cement filtrate solution. New batches were then produced with a decreasing amount of SAPs. At the dosage of 0.019 m% the required flow was achieved (Figure 3.2), with a corresponding absorption capacity of 284 g/g (higher than in demineralized water).

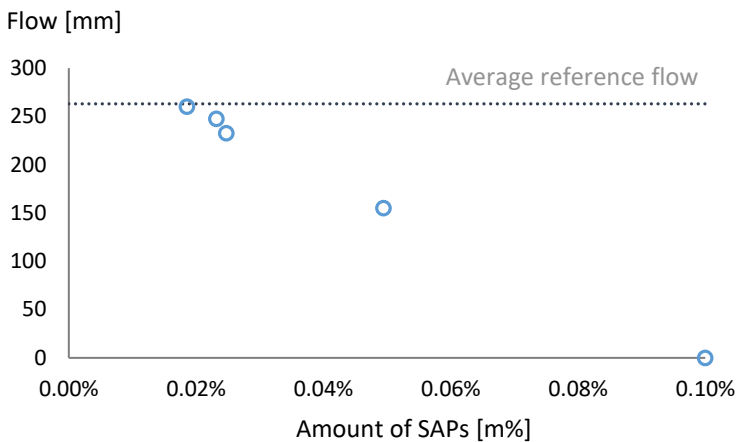


Figure 3.2 - Influence of the amount of SAPD1 in the free-flow of cement paste mixtures for a constant amount of superplasticizer and water. The flow value of the reference mixture is indicated.

For the type 2 sulfonate-based SAPs, both SAPD2.1 and SAPD2.2 absorbed around 40 g/g in cement filtrate solution. Based on that, an initial dosage of 0.135 m% of SAPs was used. That dosage resulted in an average flow of 270 mm and 273 mm, respectively for SAPD2.1 and SAPD2.2, which was considered compatible with the reference ( $263 \pm 12$  mm). The absorption capacity of both SAPs in cement paste was then defined as 40 g/g.

With the last of the sulfonate-based SAPs, SAPD3, an absorption capacity of around 23 g/g was found in cement filtrate solution. Based on that, an initial dosage of 0.23 m% of the said SAP was used for the production of the cement paste. A flow of 310 mm was measured, indicating that the

absorption of the SAP had been underestimated. A second paste was then produced with a dosage of 0.4 m%, giving a flow of 270 mm. with such dosage, the absorption capacity of SAPD3 in cement paste was determined as 13.5 g/g (which corresponds to a reduction of 41% in comparison to the absorption in cement filtrate solution).

Concerning the differences found in the absorption capacity of SAPs when tested in cement filtrate solution and real cement paste, the absorption can be more than double in the cement filtrate compared to when using the slump flow method which employs real cementitious materials [5, 11, 12]. Such differences indicate that the solution and conditions used in the filtration method are quite different from those of real cement-based materials. In fact, the total ion concentration of pore fluid with high water-to-cement ratio is usually lower than the one with low water-to-cement ratio, as a result of the water dilution of ions [13]. This is the case here for the cement pastes produced with a water-to-cement-ratio of 0.354 in contrast to the cement filtrate solution produced with a ratio of 5. In addition to that, the nature of the ion composition of the cementitious pore solution can also be changed due to the presence of superplasticizers, as described by Kang et al. in [14].

Now, specifically for SAPA and SAPB, the differences in the reduction of absorption capacity that were observed (18% and 37%, respectively) can be explained by their chemical composition. According to Lee et al. [15], SAPs produced from copolymers of acrylamide (SAPA) are less susceptible to  $\text{Ca}^{2+}$  complexation in comparison to SAPs produced from polyacrylate (SAPB), as it was already observed when these SAPs were immersed in cement filtrate solution (mentioned in Chapter 2).

For the alginate-based SAPs the difference in absorption when comparing the cement filtrate solution and the cement paste was not much significant, being the values in cement paste lower than those found for the cement filtrate solution. A reduction of 13% was found for both SAPC1 and SAPC2. While for SAPs C3 and C4 a reduction of 23% and 9% was found, respectively. The purification used in SAPC2 did not promote any difference in comparison to SAPC1 (which has the same chemical composition but higher gel fraction due to purification).

In the group of sulfonate-based SAPs three distinct behaviors were observed. For type 1 SAP (SAPD1) a considerable increase in absorption capacity was found in cement paste in comparison to cement filtrate solution, which was not expected. For the type 2 SAPs (SAPD2.1 and SAPD2.2) no change was obtained. As for the type 3 SAP (SAPD3) a reduction of around 41% was found. In terms of chemical composition, all sulfonated-based SAPs are partially composed of co-monomers NaAMPS (2-acrylamido-2-methyl-1-propanesulfonic acid sodium salt). In terms of the amount of alkali-stable crosslinker, both SAPs D1 and D3 have the same amount and differ in composition due to the presence of sodium vinyl sulfonate, which could be the reason of the unexpected higher absorption of SAPD1 in cement paste, considering the presence of the superplasticizer and a possible reaction between the sodium vinyl sulfonate in SAPD1 and the polycarboxylate-ether superplasticizer. As for the fact that SAPs type 2 presented no change in behavior when applied in cement paste, while SAPD3 presented a considerable reduction in absorption in cement paste, this could be explained by differences in the anionic concentration in the SAPs which could provoke a different response for both SAPs when immersed in the  $\text{Ca}^{2+}$  richer cement paste [16].

In the next subsections, to facilitate the identification of the different mixtures and dosage of SAPs, the following code will be used to designate the mixtures: P\_X(m%). Where P stands for paste, X represents the SAP which was used and the number in between parenthesis indicates the dosage of SAP. The reference mixtures will be identified as REF0.3 and REF0.354 where 0.3 and 0.354 represent the total water-to-cement ratio of the mixture. In all SAP-containing pastes the total water-to-cement ratio is 0.354 and it is composed of the mixing water (equivalent to a water-to-cement ratio of 0.3) and entrained water for internal curing (equivalent to a water-to-cement ratio of 0.054).



Table 3.1 – Summary of the paste mixtures with and without SAPs, initially defined based on the absorption capacity of the SAPs in cement paste. The effective water-to-cement ratio refers to the amount of water not stored in the SAPs.

Name	Dosage of SAP [m%]	Effective water-to-cement ratio [-]	Total water-to-cement ratio [-]
REF0.3	0	0.3	0.3
REF0.354	0	0.354	0.354
P_A(0.2)	0.2	0.3	0.354
P_B(0.25)	0.25	0.3	0.354
P_C1(0.77)	0.77	0.3	0.354
P_C2(0.77)	0.77	0.3	0.354
P_C3(0.64)	0.64	0.3	0.354
P_C4(0.52)	0.52	0.3	0.354
P_D1(0.019)	0.019	0.3	0.354
P_D2.1(0.135)	0.135	0.3	0.354
P_D2.2(0.135)	0.135	0.3	0.354
P_D3(0.4)	0.4	0.3	0.354

### 3.3 Development of autogenous shrinkage strain

The autogenous shrinkage was assessed according to the standard ASTM C1698–09 [17]. The test consists of the measurement of the deformation of cement pastes in corrugated tubes with a nominal length of  $425 \pm 5$  mm and a diameter of  $29 \pm 0.5$  mm. The tubes were filled vertically and in two layers, with the aid of a plastic funnel. After each layer, the tube was vibrated using a vibrating table to reduce the presence of air bubbles. The specimens were placed on metallic supports with one linear variable differential transducer (LVDT) with a range of 5 mm on one end (Figure 3.3). The other end was restrained in movement by a bolt connecting the tube to the metallic support. The measurements were performed continuously every 10 min for 7 days in a room with controlled atmosphere ( $20 \pm 2$  °C and  $60 \pm 5\%$  RH).

Even though the temperature variation inside the specimen might influence its shrinkage behavior, a previous study performed by Snoeck et al. [5] where tubes were immersed in a polyalkylene-glycol thermobath at 20 °C, and in parallel placed on a manual measuring bench in a temperature-controlled room, concluded that the increase in temperature did not have a significant effect and all results were comparable.

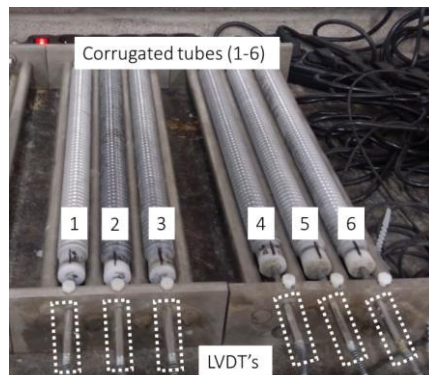


Figure 3.3 - Set up for the autogenous shrinkage measurement (LVDT's on the bottom of the image).

The shrinkage strain curves for all SAP-containing mixtures in comparison to the reference pastes without SAPs are depicted in Figure 3.4, Figure 3.5

and Figure 3.6. The curves represent the average strain values of triplicates for each mixture (positive values represent expansion and negative values represent shrinkage). They were grouped based on the different types of SAPs in order to improve the readability of the graphs. The choice of different y-axis for the alginate-based SAPs was chosen for the same reason. For the start of the measurements the so-called “knee-point” was chosen as time-zero. The point represents the moment of transition from a fluid to solid state of the cement paste. An elaborated discussion about different approaches for the choice of time-zero and the method for determining the “knee-point” will be presented in Chapter 4.

In comparison to the reference mixture with water-to-cement ratio 0.3, the addition of water without SAPs (REF0.354) promoted a considerable reduction in the shrinkage strain, although it was not enough to complete mitigate the shrinkage. As already stated by several authors, the release of water for internal curing and efficient reduction of shrinkage strain must happen around the time of setting of the mixture and continuously over a longer period [4, 5, 18-24]. By only using additional water, the extra water will be immediately available for cement hydration and will not contribute to the reduction of self-desiccation in the long term.

The addition of all types of SAPs promoted a considerable reduction of autogenous shrinkage strain over the whole time of testing. Such reduction, however, occurred to a different extent based on the type of SAPs and their kinetics of water release. In addition to that, for all mixtures where some additional water was used (with or without SAPs), a moderate and in some cases a more intense expansion was noticed at very early-ages. This can be attributed to the further hydration after setting that occurs due to the additional amount of water in the system and that causes a slight volume expansion in the pores. In literature, the same trend has been reported in [4, 25]. Some of the authors discuss a possible increased formation of portlandite and ettringite crystallization as mentioned in [26, 27].

The commercial (acrylic-acid-based) SAPA and SAPB promoted a complete mitigation of the shrinkage strain, starting from the very early-age and consistent during the whole monitoring period (Figure 3.4).

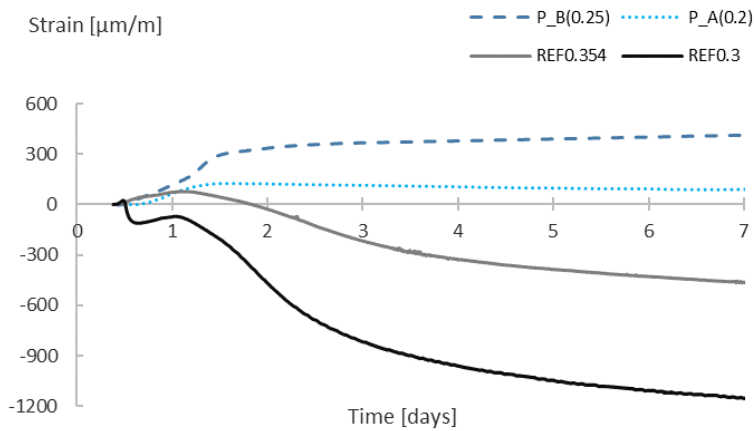


Figure 3.4 - Shrinkage strain of cement pastes with commercial SAPs in comparison to the reference mixtures. The legend is organized from the highest (positive) strain to the lowest (negative) strain after 7 days.

The shape of the curves for both SAPs indicate an expansion during the first hours of measurement. After reaching a maximum value (around 36 hours) that level of strain is kept constant. That could indicate that both SAPA and SAPB start releasing its stored water around the time of fluid to solid transition of the cement matrix (the “knee-point”), but do it gradually over a longer time period, which is reflected by the constant and positive strain over the 7 days of monitoring. In terms of kinetics, both SAPA and SAPB showed a very stable absorption with almost no desorption in the first 24 h of immersion in cement filtrate solution (Chapter 2).

The strain curves for the alginate-based SAPs are depicted in Figure 3.5. The first point to be noticed is that no significant differences were observed for the variations of these SAPs, reflecting the very similar behavior already observed in their absorption capacity measured in cement paste and cement filtrate solution (Chapter 2).

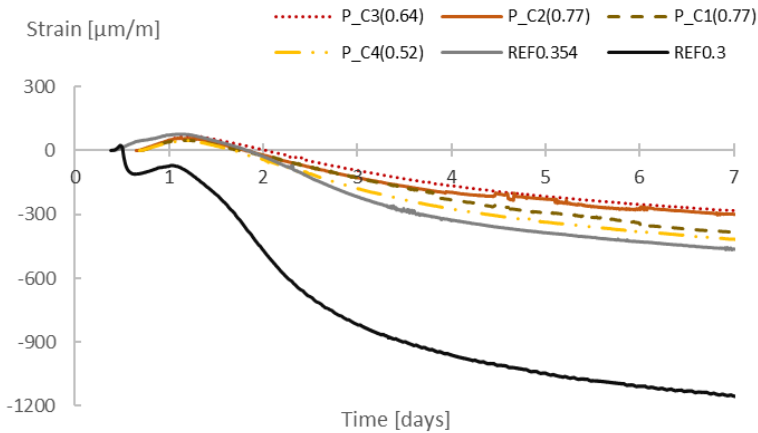


Figure 3.5 - Shrinkage strain of cement pastes with alginate-based SAPs in comparison to the reference mixtures. The legend is organized from the highest (positive) strain to the lowest (negative) strain after 7 days.

Although all the alginate-based SAPs promoted a significant reduction in strain in comparison to REF0.3 (64% to 74% after 7 days), overall, the strain for all SAPs (C1 to C4) develops in time almost parallel to REF0.354. Such behavior might be an indication that these SAPs are completely releasing their stored water right from the beginning. In that way, the water that was initially intended to be used for internal curing is actually being consumed in the hydration of the cement particles, already from the start. In practice, all the alginate-based SAPs mixtures work just as REF0.354, where additional water was used from the beginning. When the kinetics of these SAPs in cement filtrate solution were discussed in Chapter 2, a moderate desorption was observed, except for SAPC2. Although it was not much expressive (not much difference was found between the absorption capacity at 10 min and after 24 h), it could still be the case that upon contact with the cement paste, the alginate-based SAPs present an incontinent behavior. In the richer  $\text{Ca}^{2+}$  cement paste, because the calcium cation has a smaller size than the large polymer molecules, it can diffuse into the alginate solution, and according to the egg-box model mentioned by Smidsrød and Skjåk-Bræk in [28] this leads to further crosslinking processes.

As for the sulfonate-based SAPs, an intermediate trend was observed when compared to the previously discussed types. The strain development over time is shown in Figure 3.6.

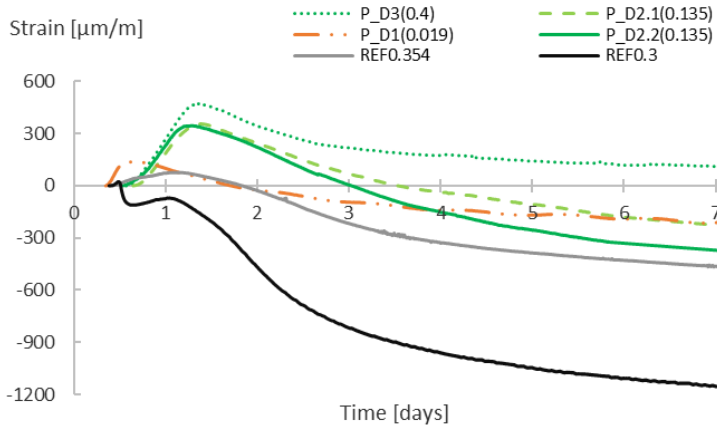


Figure 3.6 - Shrinkage strain of cement pastes with sulfonate-based SAPs in comparison to the reference mixtures. The legend is organized from the highest (positive) strain to the lowest (negative) strain after 7 days.

Despite of the fact that all sulfonate-based SAPs promoted a significant reduction in strain in comparison to REF0.3 (compatible with what was observed with the alginate-based SAPs), only SAPD3 was able to complete mitigate the shrinkage strain and keep constant and positive (meaning no shrinkage) values over time. For SAPs D1, D2.1 and D2.2, a considerable expansion was noticed with a peak around 36 h for SAPs D2.1 and D2.2 (more or less at the same time as SAPs A and B) and around 12 h for SAPD1. However, such expansion turned into further shrinkage right after the peak. From that moment on, those three SAP-mixtures performed in a way very similar to REF0.354. As it was already stated before, this could also be related to a strong and almost complete release of the stored water. In terms of kinetics in cement filtrate solution, all three SAPs (D1, D2.1 and D2.2) showed a strong absorption capacity at the first moments, followed by the beginning of a desorption trend (for SAPs D1 and D2.1).

As for SAPD3, an interesting behavior is noticed. Initially, there is an expansion followed by a decrease in the positive values of strain, very

similar to what happened with the other sulfonate-based SAPs. However, the shrinkage rate develops at a slower pace for SAPD3 and tends to stabilize, promoting a complete mitigation of the shrinkage during the 7 days of measurements. In terms of chemical composition, SAPD3 is the only SAP with the innovative double crosslinking feature, which enables it to absorb a very limited amount of water at first, but also promotes an increase in absorption capacity in time after exposure to alkaline environment. Regarding the kinetics of sorption, it was observed in Chapter 2 that the absorption capacity of SAPD3 increased in time in cement filtrate solution. The same can be expected to happen in cement paste, and probably at a faster pace, considering the higher concentration of calcium hydroxide in comparison to that of the cement filtrate solution. The distinct behavior observed for SAPD3 in the shrinkage strain curve might be an indication that, as the alkaline unstable crosslinker hydrolyses, SAPD3 might be reabsorbing the water that was initially released or even taking up extra water from the cementitious matrix. In this way, a cyclic equilibrium between desorption and further absorption is achieved, which enables a complete mitigation of shrinkage, even though there is an initial tendency of complete water release, as it happened for the other sulfonate-based SAPs.

From the results presented above, it was clear that the amount of additional water determined based on the work of Jensen and Hansen [6, 29] was enough to completely mitigate the autogenous shrinkage of the cement pastes with the effective water-to-cement ratio of 0.3, when SAPs with the appropriate kinetics were used. In order to further explore the internal curing effect of the sulfonate-based SAPs, it was decided to investigate how such SAPs would behave upon the use of higher dosages of SAPs and higher amount of additional water.

To do that, new cement paste mixtures were produced, as indicated in Table 3.2. First, the water absorption of the SAPs in the new cement pastes was measured by means of slump flow test as described before, then the autogenous shrinkage strain was measured with the corrugated tubes method.

Table 3.2 - Summary of the new paste mixtures with sulfonate-based SAPs. The amount of extra water added was defined based on the absorption capacity of the SAPs in cement paste and confirmed with a new round of the flow table test.

Name	Dosage of SAP [m%]	Effective water-to-cement ratio [-]	Total water-to-cement ratio [-]
P_D1(0.1)	0.1	0.3	0.45
P_D2.1(0.2)	0.2	0.3	0.39
P_D2.2(0.2)	0.2	0.3	0.39

At first, it was noticed that the water absorption of SAPD1 in the new cement pastes was not in accordance with the value found for the mixture previously studied (284 g/g). By increasing the SAP dosage, a different absorption capacity was found (150 g/g for a dosage of 0.1 m%). In contrast to that, the absorption capacity of SAPD2.1 and SAPD2.2 did not change significantly with the increasing dosage of SAP. For the dosage of 0.2 m% of both SAPs, an absorption of 45 g/g was found (comparable to the 40 g/g obtained with the dosage of 0.135 m% of SAPs D2.1 and D2.2). In light of the unexpected behavior of SAPD1, the absorption capacity of both SAPA and SAPB was also tested for cement pastes with 0.5 m% of each SAP and no difference was found in comparison to the absorption capacity in the cement pastes previously studied (P\_A(0.2) and P\_B(0.25)).

The shrinkage strain of the new cement paste mixtures is depicted in Figure 3.7. With the increased dosage of SAPs and additional water, all mixtures were free from shrinkage during the testing period. Unlike the previous cases, all SAP-containing mixtures now present a constant expansion trend. For SAPD1, the first expansion stage is followed by a reduction of the positive strain that in time presents a stable behavior where no shrinkage is taking place. Both SAPD2.1 and SAPD2.2 behave in a similar way but with a less pronounced increase and reduction of the positive strain.



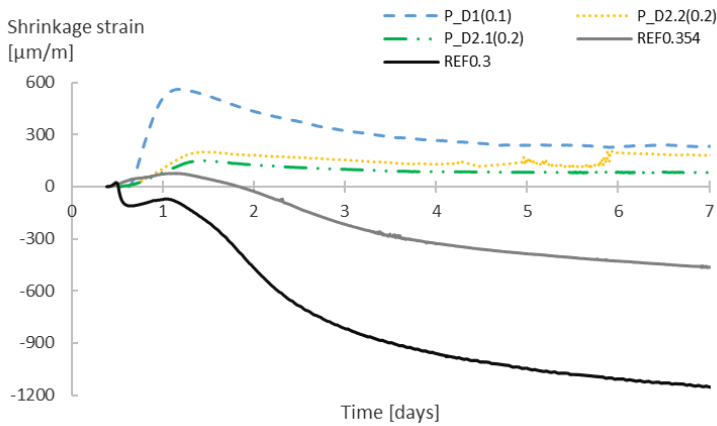


Figure 3.7 - Shrinkage strain of new cement pastes with sulfonate-based SAPs in comparison to the reference mixtures. The legend is organized from the highest (positive) strain to the lowest (negative) strain after 7 days. It should be read from left to right and from top to bottom.

In terms of kinetics, all three SAPs show a very similar behavior to the one depicted in Figure 3.6. There is still the indication that the SAPs are prematurely releasing their stored water at a very early age and at a high rate, especially SAPD1. However, with more water in the system, it is possible that some reabsorption is taking place after the initial release of the stored water in the SAPs. That would enable successive absorption and desorption by the SAPs, prolonging the effects of the internal curing.

### 3.4 Effects on the compressive strength

The compressive strength of the cement paste mixtures with and without SAPs was measured at the age of 28 days. For each mixture, three prisms (40 mm x 40 mm x 160 mm) were molded, demolded after 24 hours and cured in a room with controlled atmosphere ( $20 \pm 2^\circ\text{C}$  and  $\text{RH} > 95$ ) until the testing date. Each prism was initially split by means of three-point bending and each half was then tested for compressive strength using the testing machine Walter+Bai DB 250/15. The test was performed in accordance to the standard NBN EN 196-1 [30].

As a complementary method to better understand the influence of the SAPs on the compressive strength, the air content of the mixtures in the hardened state was also determined by means of an air void analysis with the RapidAir 457 device (Germann Instruments, Denmark) (Figure 3.8). The test was performed in accordance to the standard EN 480-11 [31]. In this test, small plate specimens (100 mm x 100 mm x 20 mm) obtained from cubic specimens (length of 100 mm) were used. The cubes were demolded after 24 h and cured for 28 days in a room with controlled atmosphere ( $20 \pm 2^\circ\text{C}$  and  $\text{RH} > 95$ ). One surface of each small plate was then polished, painted with black ink and dried for 24h in an oven at  $35^\circ\text{C}$ . Afterwards, a layer of white barium sulfate powder was applied on the polished and painted surface to fill in the voids.

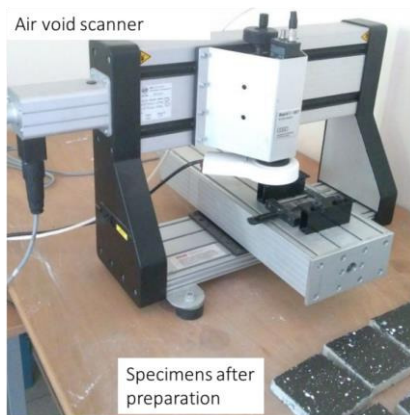


Figure 3.8 - Rapid Air system used for the air void analysis. The scanner is shown on the upper part of the figure. The prepared specimens are shown at the bottom.

The results of the compressive strength for the tested mixtures are shown in Figure 3.9. As expected, the increase of total water-to-cement ratio and the inclusion of SAPs in the mixtures caused a reduction in the compressive strength in comparison to the reference mixture with the lowest water content. The main source of such reduction has been reported in literature to be the macro-porosity formed by the SAP voids after release of the absorbed water [4, 12, 32].

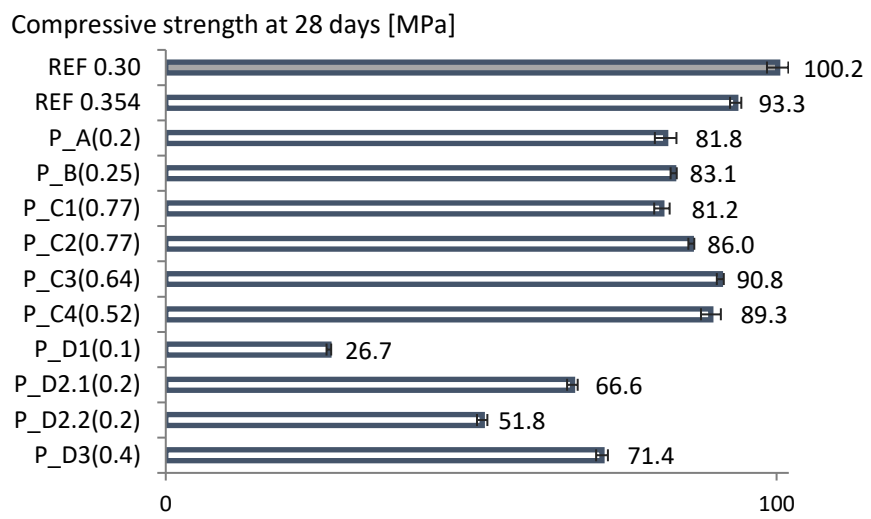


Figure 3.9 - Compressive strength of the tested cement pastes at 28 days of age.

The role of water in the development of strength of cementitious materials has been widely investigated and understood for quite some time now. As main rules, the so-called law of Abrams [33] and model of Powers [34] clearly state that the compressive strength of conventional concrete mixtures, for example, depends on the degree of hydration of the paste and the water-to-cement ratio (the higher the amount of water in the system, the lower the strength). It is also widely known and accepted that the amount of porosity, that can also be associated to the air void content in a determined material, can cause significant reduction in the mechanical strength. Powers [34], Ryshkewitch [35], and Hasselmann [36] presented models for that. However, given their ability to release water over time, the inclusion of SAPs in the cementitious materials adds on the already very dynamic process of cement hydration

and macro-pore formation in the cement matrix. The amount of water available for cement hydration changes over time with the inclusion of SAPs and that depends on the kinetics of water release by the different types of SAPs. The size, distribution and geometry of the macro-pores depend on the initial absorption capacity, the retentive capability, particle size distribution and shape of the SAPs.

Despite the fact that a general reduction trend is observed with an increase in the amount of water, different results were found for the mixtures containing the same amount of water but different SAPs (Figure 3.10). The addition of the entrained water in plain paste (REF0.354) caused a reduction in compressive strength of around 7% in comparison to REF0.3. As for the SAPs, in the mixtures with the total water-to-cement ratio of 0.354, different values were found. Those were 9% for P\_C3(0.64), 14% for P\_C2(0.77), 11% for P\_C4(0.52), 19% for P\_C1(0.77), 17% for P\_B(0.25), 18% for P\_A(0.2) and 29% for P\_D3(0.4). These values are in accordance with the findings from literature when 0.2–0.5 m% of SAPs are added [32, 37, 38]. For the mixtures P\_D2.1(0.2), P\_D2.2(0.2) and P\_D1(0.1), with higher water-to-cement ratio, the reductions were of 33%, 48% and 73% respectively.

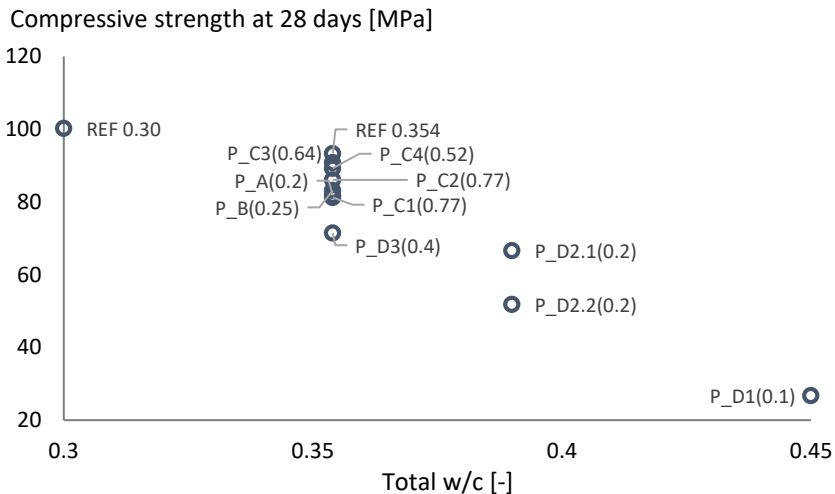


Figure 3.10 - Compressive strength of the cement paste mixtures as a function of the total water-to-cement ratio.

Amongst the SAP-containing mixtures with a total water-to-cement ratio of 0.354, the alginate-based SAPs promoted the lowest reduction. Especially for SAPs C2, C3 and C4, the reduction could be considered the same as the one observed for REF0.354, given the standard deviation values of the respective series. For the commercial SAPs, SAPA and SAPB had almost the same effect on the compressive strength of the mixtures. The addition of sulfonate-based SAPs (except for SAPD3) promoted the highest reductions in the compressive strength. However, the addition of such SAPs resulted in the production of the cement pastes with higher total water-to-cement ratio (0.39 for both P\_D2.1(0.2) and P\_D2.2(0.2), and 0.45 for P\_D1(0.1)).

Figure 3.11 shows the relation of the compressive strength with the air content of the mixtures in the hardened state. For most of the cases, it is clear that the increase in the air content is directly related to the reduction in compressive strength.

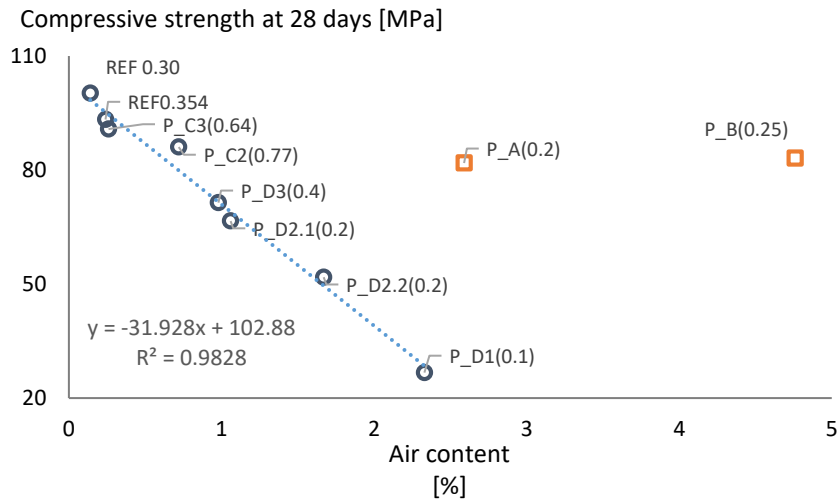


Figure 3.11 - Compressive strength of the cement paste mixtures as a function of the air content. The mixtures with SAPA and SAPB are indicated with a different marker to highlight the out-of-trend behavior observed in comparison to the other mixtures.

In general lines, the increase in the air content follows the absorption capacity of the SAPs in cement paste and the total amount of water in the mixture. For both SAPA and SAPB, a different trend is observed. Even

though the mixtures with both SAPs have the highest air content values, in terms of compressive strength both perform similar to SAPC2 (which paste had lower air content value in comparison to SAPs A and B). This could be related to the kinetics of water release by the SAPs and its impact on the internal curing and promotion of further hydration. As reported by Justs et al. [22], in a limited number of cases where SAPs were added to cementitious materials, an increase in strength was possible due to internal curing and enhanced cement hydration, also occurring in the macro-pores. In this study, no increase in strength was noticed, but it is possible that the effects of internal curing provoked a limited compensation of the strength reduction caused by the higher porosity.

Schrofl et al. in [4], reported that SAPs releasing their stored water prematurely cause a more noteworthy decrease in strength when compared to water-retentive SAPs, with a comparable amount of additional water. That was not observed in the mixtures studied here, the alginate-based SAPs, for example, performed slightly better than the commercial SAPs.

Depending on the time where the water release is taking place, the total volume of air due to the macro-pore formation might not be equivalent to the volume of entrained water added on the mixtures with SAPs. If the water release takes place before setting, it is possible that the macro-pore left by the SAP will not remain stable for long, because of the fluid state of the mixture before setting. That is evidenced by the differences found for the air content of all SAP-containing mixtures (Figure 3.11). Especially for the alginate-based SAPs, it was already discussed that said SAPs seemed to completely release their water earlier in comparison to the other SAPs and by analyzing the air content of the cement pastes in the hardened state, this might be confirmed. For the mixtures P\_C3(0.54) an air content of 0.26% was found, which is almost the same as the 0.24% found for REF0.354.

For the mixtures containing SAPs A and B, that seemed to have a more controlled of water release as it was observed in the shrinkage tests, air content values of 2.59% and 4.76% were obtained, respectively. In

contrast, the mixtures with sulfonate-based SAPs, to which a partial incontinent behavior was attributed, lower values were found.

To summarize the effects of the SAPs on the shrinkage strain and compressive strength of the different cement pastes, a relation between both properties is shown in Figure 3.12. In the figure it is clear noticeable that although most of the SAPs had a positive effect regarding the reduction of shrinkage, that came along with a reduced compressive strength. This highlights the importance of conducting a multi-strategy study when choosing the most appropriate SAP for a defined application.

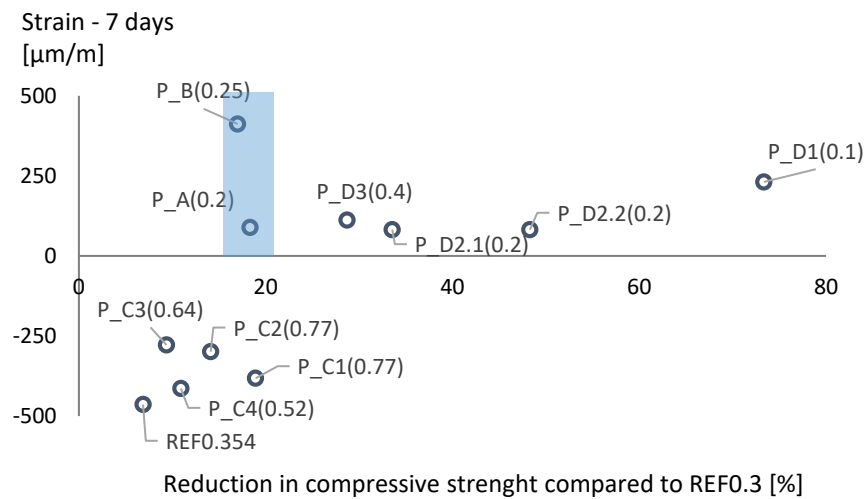


Figure 3.12 - Strain at 7 days and reduction in compressive strength of cement pastes at 28 days in comparison to REF0.3. The positive values of strain represent expansion and negatives ones represent shrinkage. The colored region represents the mixtures with the best performance, considering full mitigation of shrinkage with the lowest reduction in strength.

### 3.5 Desorption kinetics of SAPs and effects on the internal relative humidity (IRH) of cement pastes

From the mixtures studied in the previous section, five SAP-containing mixtures and the two reference mixtures without SAPs were chosen for the study of the relative humidity. Both commercial SAPs (SAPA and SAPB), the alginate-based SAPC3 and the sulfonate-based SAPD2.1 and SAPD3 were chosen.

The internal relative humidity levels of the cement pastes were monitored in duplicates, and during seven days, by two Rotronic hygroscopic DT RH sensors equipped with HC2-AW measuring cells (Figure 3.13). The same apparatus was used by Jensen and Hansen [39] and Huang and Ye [40]. The dimension of the sample container is 30 mm, the thickness of the testing specimen is less than 7 mm, and the distance between it and humidity sensor is less than 30 mm. The equipment was kept in a room with controlled atmosphere ( $20 \pm 2$  °C and  $60 \pm 5$  % RH) and the sample holder was immersed in bath with demineralized water at 20 °C during the test, using a temperature controlled unit and a circulating pump system.

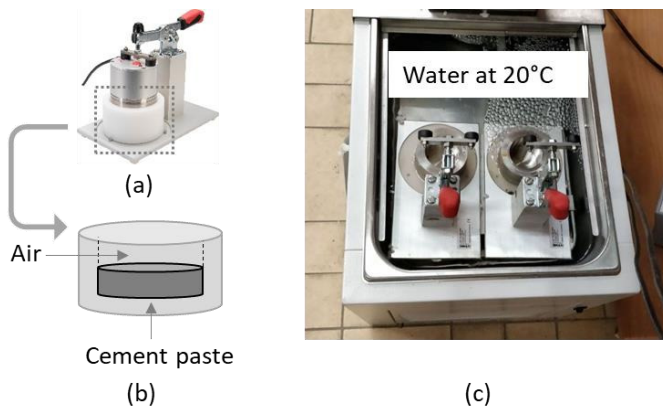


Figure 3.13 – Humidity sensor (a), detail of the testing specimen (b) and equipment used to keep a constant temperature around the specimen holder (c).

In order to reduce the effects of condensation on the humidity measurements in the very early stage (within one hour after mixing), the



specimen was sealed and put in the test room for 30 min to achieve temperature equilibrium after mixing. Then the specimen was moved and placed inside the sample holder. The lid sealing was removed and the humidity sensor was placed on top of the specimen container so that the measurements could initiate.

The results of the monitoring are shown in Figure 3.14. For REF0.3, the humidity levels start to drop even before the first 24 h of measurements and right after that it is already the lowest amongst all mixtures. At 24 h. In contrast, the humidity levels of REF0.354 only start to decrease after 48 h. For the SAP-containing pastes, higher humidity levels were found during the whole testing period in comparison to REF0.3 and different trends were observed.

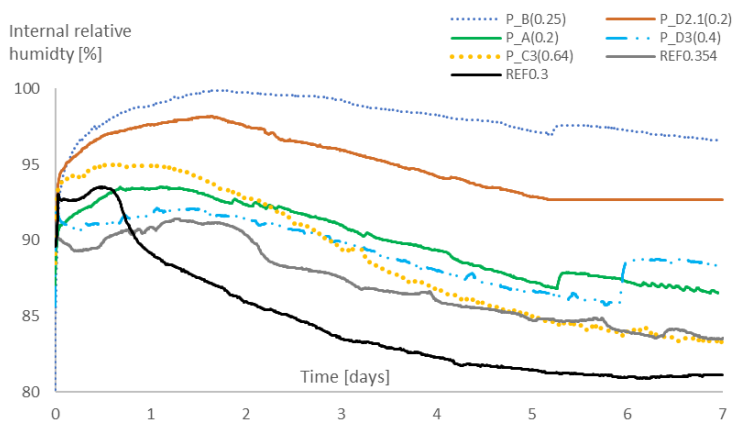


Figure 3.14 - Internal relative humidity levels of cement pastes with and without SAPs. The curves represent the average values of duplicates. The legend is organized from the highest to the lowest humidity value at 7 days.

Starting with the mixture P\_C3(0.64), a fast decrease in the humidity levels are noticed from day 2 onwards, and already by day 4 the mixture reaches the same humidity levels of REF0.354. The cement pastes containing SAPs A and D3 show a constant humidity level during the first two days of monitoring and a slight decrease starts to take place from that point on. However, by day 7 the values for these mixtures are higher than the references and between 85 and 90%. The mixtures with SAPB and

SAPD2.1 presented the highest values of internal relative humidity amongst all mixtures during the whole testing period.

In general, all SAP-containing mixtures showed a higher level of internal relative humidity when compared to the REF0.3 and REF0.354 (except for SAPC3 in that case), around or above 90% during the whole period of testing. This indicates that all SAPs are releasing the stored water at some point in time to maintain the IRH levels high due to internal curing.

Although it is not possible to quantify the water release, the monitoring of the humidity levels, despite some setbacks of the equipment, showed very interesting insights that provided further knowledge for the interpretation of results from the autogenous shrinkage linked to the kinetics of desorption by the SAPs and the internal curing effect. SAPB and SAPD2.1 seem to be releasing the water earlier in comparison to the other SAPs, which is indicated by higher initial levels of internal relative humidity.

The mixtures produced with SAPB and SAPD2.1 showed the highest expansion (Figure 3.4 and Figure 3.7) and that could be related to an earlier release of water to the hydrating paste. However, caution is advised when drawing this kind of conclusion from the relative humidity monitoring due to the geometry of the equipment and the size of the sample. As a matter of fact, a considerable distance remains in between the surface of the sensor and the top surface of the paste. In the event that a higher amount of water would be initially released from the SAPs, condensation could take place and mask the real values of humidity, since the sensors are only able to measure the humidity of the air layer above the sample. This could explain why there is such a difference in the amount of expansion observed for the paste with SAPD2.1 and the one with SAPB, while there is not much difference in the levels of humidity for these SAPs. The same can be extended to the mixture with SAPD3, its expansion in the shrinkage curve and the difference in the levels of humidity when compared to SAPB and SAPD2.1. In fact, considering the short-term strong absorption capacity and premature release of SAPD2.1, the high levels of IRH measured could also be related to bleeding caused by the intense water release from those SAPs in the small paste specimen

after the first 30 min of resting time used to avoid the condensation on top of the surface. In [41], the authors mention that concrete bleeding is strongly influenced by the type of SAP used, with retentive SAP reducing the bleeding, whereas it increases when SAP with only short-term absorption capacity is used.

The mixtures with SAPA and SAPD2.1 present a very similar development of shrinkage strain all over the test time, which is compatible with the trend observed for the humidity test. A SAP very similar to SAPA was studied by Snoeck et al. [21] in cement pastes with the same composition as the one used in this study. By means of nuclear magnetic resonance (NMR), the authors found that the SAP started releasing its water around 11 h (very close to setting time) and kept a gradual release until up to 30 h. This same SAP was also found to completely mitigate the autogenous shrinkage of the cement paste mixture.

For SAPC3, a higher level of relative humidity is observed from a very early moment, when compared to SAPA and SAPD3. With time, this level starts to drop and the humidity levels become very similar to the ones observed for the mixtures with the two other SAPs, but it keeps decreasing until it reaches the same levels of REF0.354. The fact that the humidity levels in the mixture with the alginate SAP are higher than those of REF0.3 at the end of test do show that water was released, but when observing the performance of the mixtures with SAPC3 during the autogenous shrinkage test (Figure 3.5) it is noted that this SAP is not effectively mitigating the shrinkage, which could indicate that the water was not being released at the appropriate time. The water release could be taking place either too early or after the setting of the mixtures. But none of the scenarios can be determined with the IRH test. However, by comparing the shrinkage curve of the mixtures containing the alginate-based SAPs with that of REF0.354, it is clear that the water release is actually taking place already from a very early moment, which is why all mixtures containing the alginate-based SAPs behave almost exactly as the REF0.354, which contains the same total water-to-cement ratio. As a summary, Figure 3.15 depicts the strain of the cement pastes in the shrinkage tests at 7 days and the corresponding internal relative humidity.

It is clear that a complete mitigation of shrinkage at that age could only be achieved in systems where the internal relative humidity was above 86%. This is in accordance with the findings reported by Snoeck et al. [21] and Ramon in [42] for SAPs similar to the commercial and sulfonate-based SAPs used in this research.

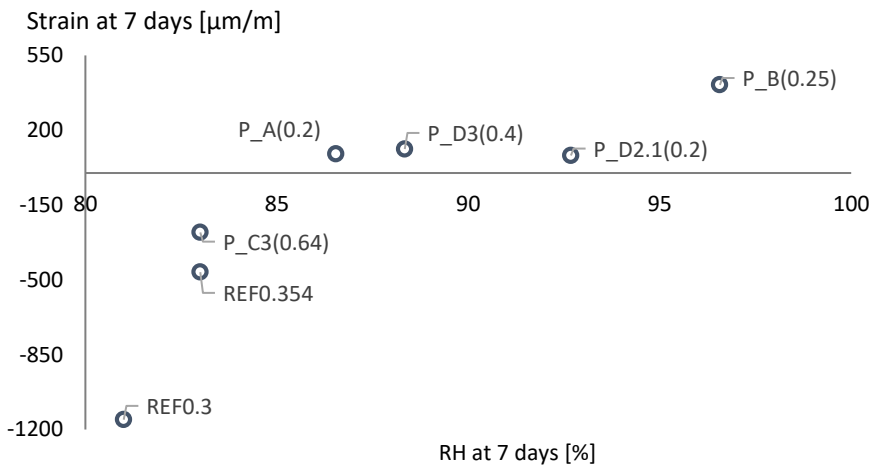


Figure 3.15 - Strain of cement pastes and internal relative humidity levels at 7 days.

To conclude, it is worth mentioning that an additional effect of internal curing with SAPs on hydration can play a role with regard to the final degree of hydration in mixtures with low water-to-cement ratios. Wyrzykowski and Lura [43] reported that the reduction of internal RH, in particular below 90%, strongly inhibits the hydration process. The authors state that by maintaining RH at higher levels, due to the effects of SAPs, a higher final degree of hydration can be expected. With a higher degree of hydration, higher compressive strength values could be reached, which could be associated to the distinguished behavior discussed in 3.4 for SAPB and its effect on the compressive strength.

### 3.6 Effects on the setting time and hardening of the cement pastes

The setting and hardening of the mixtures were studied by means of an electronic Vicat apparatus (Matest, Italy) in compliance with the standard EN 196–3 [44]. The specimen used for the Vicat was a truncated cone with a diameter of 80 mm at the base, 70 mm at the top and height of 40 mm. During the test, the specimens were exposed to the room environment ( $20 \pm 2^\circ\text{C}$  and  $60 \pm 5\% \text{ RH}$ ). The test was performed in duplicates.

An ultrasonic pulse velocity (UPV) method was also applied. The FreshCon equipment as described in by Reinhardt and Große in [45] was used, with compressive pulse waves. The measurements were automatically performed each 5 min during 24 h with an amplifying voltage of 450 V and a pulse signal with a width of 2.5  $\mu\text{s}$ . A U-shaped specimen with approximately 35  $\text{cm}^3$  of volume was used. The distance between the sender and receiver point was 22 mm. During the measurements, the specimen was covered by plastic foil connected to the mold by a thin layer of Vaseline to prevent drying shrinkage.

With both methods, the initial and final setting times were determined. With the Vicat apparatus, the initial setting time was taken at the moment where the distance between the testing needle and the base plate underneath the testing specimen was of  $6 \pm 3$  mm. The final setting time was determined as the first moment where the testing needle could not penetrate more than 0.5 mm in the testing specimen. With the UPV, the values were determined based on the rate of the velocity. The typical curve for the wave velocity, as it has been found in many studies [25, 45–52], is marked by two points where there is a sudden increase and then a reduction in the rate of the UPV. These points are very similar to the ones found during the transition of periods between the induction and acceleration phases of the cement hydration. They can be easily identified by plotting the first derivative of the UPV over time (Figure 3.16). The initial setting is taken as the point right before the sudden increase in the velocity rate. The final setting is determined as the moment where the variation of the UPV reaches a maximum value.

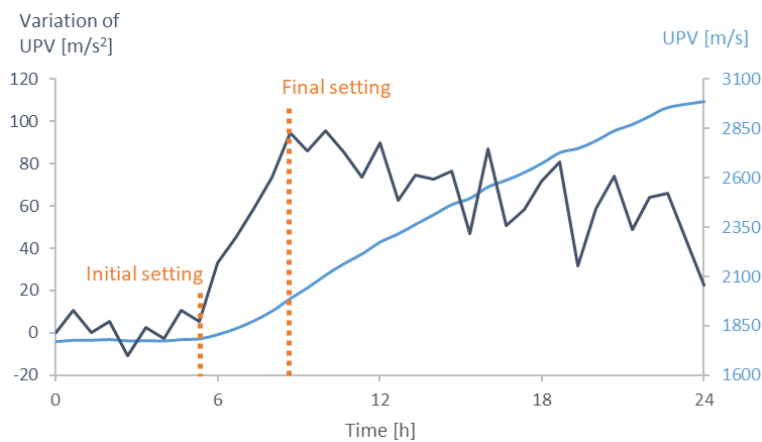


Figure 3.16 - Determining the initial and final setting point based on the rate of the UPV (REF0.3). In order to improve the visualization of the graph, values are averaged over 30 min.

The initial and final setting times as determined with the Vicat apparatus are shown in Figure 3.17. As expected, the addition of water in the mixtures tends to delay both the initial and final setting times of the mixtures and that occurs at different levels, depending on the amount of water.

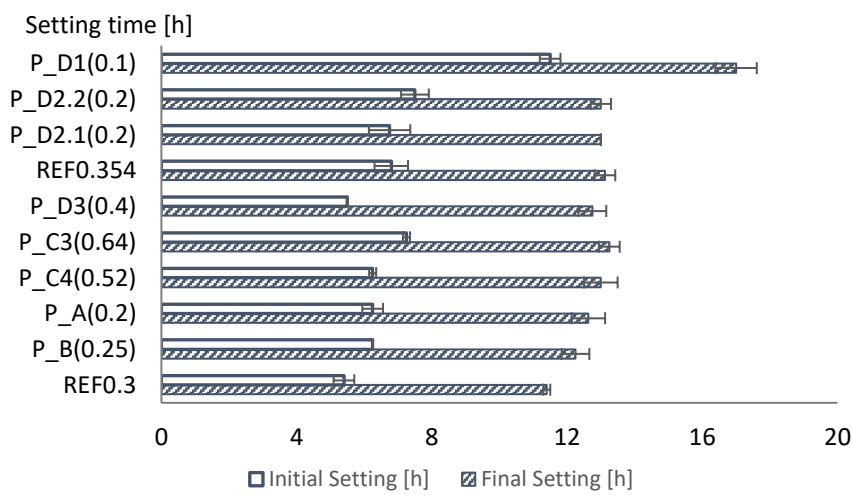


Figure 3.17 - Initial and final setting times of the studied cement mixtures determined with the Vicat apparatus. The mixtures are grouped based on the total water-to-cement ratio.

In comparison to REF0.3, the mixture REF0.354 presents a slight delay in the setting times. The initial and the final setting of REF0.354 occur 1.4 h and 1.72 h hours later than for REF0.3. The delaying effect is more pronounced for mixture P\_D1(0.1). With a total water-to-cement ratio of 0.45, this SAP-containing mixture starts to set only 5 h to 6 h later than both reference mixtures. The final setting time also occurs with a delay of 4h to 5 h in comparison to both reference mixtures. For all the other SAP-containing mixtures with a total water-to-cement ratio of 0.354 (or 0.39 for the mixtures containing SAPs D2.1 and D2.2), both setting times occur in between the reference mixtures. This can be explained by the gradual water release of the SAPs that puts the mixtures in an intermediate state with regards to water content before the final setting occurs. In literature, some studies also pointed out this delay in setting with the use of SAPs and additional water [37, 53, 54]. In [37], for example, De Meyst et al. found a delay of 2 h to 3 h in the final setting time of cement pastes produced with commercial SAPs and a total water-to-cement ratio of 0.354, in comparison to a reference mixture without SAPs and total water-to-cement ratio of 0.3. By increasing the total water-to-cement ratio up to 0.42 and using sulfonate-based SAPs, the authors observed a delay of around 5 h in the final setting time of the mixture. These findings corroborate with the results presented above.

The setting times determined with the UPV method are compatible with the ones found with the Vicat apparatus (Figure 3.18). The correlations between the amount of water and the presence of SAPs and the delay in the setting of the mixtures already discussed above can be extended here as well.

Considering the discussion presented in 3.3 and 3.5 regarding the possible earlier water release by some SAPs, not much could be seen as an influence of the kinetics of water release by the SAPs on the setting times. Mixtures with the same total water-to-cement ratio and different types and amount of SAPs, presented similar times of setting (both initial and final). As an attempt to try to investigate that, the curves corresponding to the evolution of the p-waves over time were analyzed (Figure 3.19).

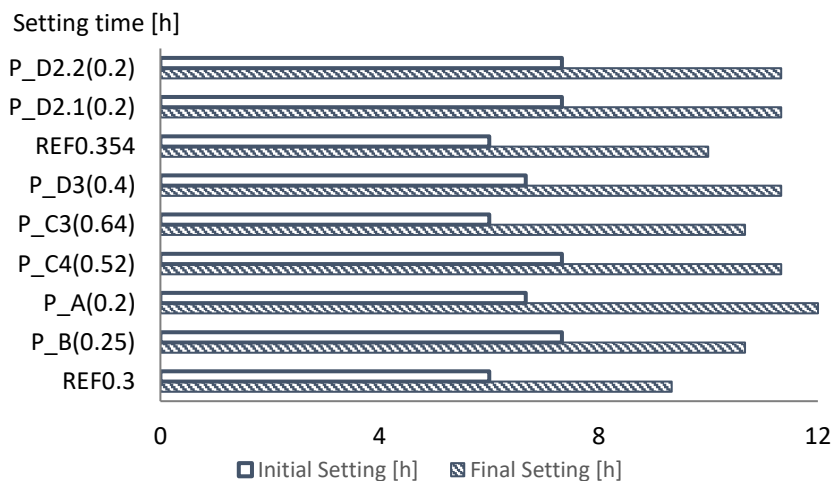


Figure 3.18 - Setting times of cement pastes as determined by the UPV method. The mixtures are grouped based on the total water-to-cement ratio.

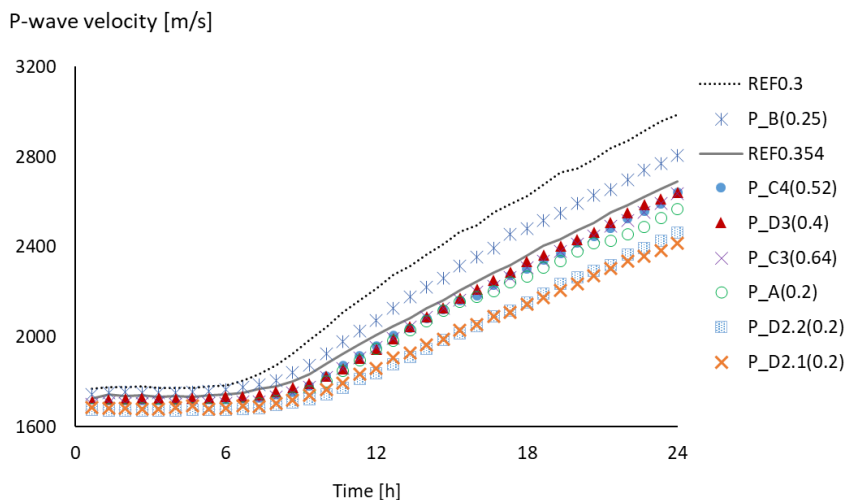


Figure 3.19 - Evolution of P-wave velocity for the studied cement pastes. A window from 6 h to 14 h is highlighted to showcase the delay in the initial setting and the rate of hardening of the mixtures. The legend is organized from the highest to the lowest values for the p-wave velocity at 24 h. It should be read from top to bottom.

All curves present the same general shape. 1) a dormant stage related to the first hours of hydration and where the cement paste is still very fluid; 2) A period of time where a path of connected hydrated particles starts to



form (the initial setting), identified by a sudden increase in the rate at which the velocity develops; 3) A period where the rate of velocity increase changes towards a more constant pace, indicating that a solid skeleton is formed all over the volume of the specimen (the final setting).

From the beginning, the curves already present a slight difference in the values of the wave velocity, which in time becomes more prominent. Since the waves travel faster in solid medium, the mixtures where lower velocities are being achieved could represent that more air or water is present [45, 52, 55]. That is well observed for REF0.3 in comparison to the all the other mixtures: with the lowest water content and the absence of SAPs, REF0.3 is expected to present the most compact volume with the least amount of air or free water. In comparison to REF0.354, all SAP-containing mixtures (except for P\_B(0.25)) present lower values of velocity in time. For the mixtures with a total water-to-cement ratio of 0.354 (with SAPs A, D3, C3 and C4) no clear difference is noted (the velocity develops at a very compatible rate and the final values are very similar to each other. For the pastes containing SAPs D2.1 and D2.2, a further decrease in the velocity values is observed, which can initially be associated to the increase in the total water-to-cement ratio up to 0.39.

For the specific case of the mixture P\_B(0.25), the velocity values are slightly higher than all other SAP-containing mixtures and REF0.354 itself. Although the UPV measurements were performed without duplicates and a small variation in the results could be possible, this could be related to a different water release by SAPB. As the SAPs release their stored water, the air voids left behind will contribute to the increased air content of the mixtures in the hardened state. The higher the air content, the lower the expected values of the p-wave velocity. But as already pointed out before, the water release by the SAPs constitutes a dynamic process. Hence, not only the water content, also the macro-pore formation due to water release will depend on the kinetics of desorption of each SAP. In that context, considering a case of two SAPs with different kinetics of water release (being an incontinent SAP, which releases its stored water at once, and the other a SAP with a “so-called” regulated water release over time), a different response can be expected in the way that the velocity curves

are shaped. As the first SAP releases its water at once and very early in time, the velocity values are expected to be lower than or very similar to the reference mixture with the same water content of the SAP mixture (depending if the complete water release happens after or before the initial setting). In contrast, for a SAP with a well regulated water release, the desorption might start at some point in time but only partially. In this way, the macro-pores will still be present, thus also reducing the end velocity value (Figure 3.19), but they will take longer to develop.

With that hypothesis, it is safe to state that regarding the kinetics of water desorption by the different SAPs studied, the fact that the mixture containing SAPB presents velocity values higher than the other SAP-containing mixtures with the same water content might be related to a more regulated water release by SAPB. That is directly linked to the results presented in section 3.3 and 3.5 that indicated a possible more regulated water release, reflected by an efficient mitigation of autogenous shrinkage and maintenance of high levels of internal relative humidity. In addition, some studies report on the assemblage of hydration products inside the SAP due to further hydration following internal curing, which could also change the response of the p-waves in a mixture. An example of that is the study developed by Esteves et al. [56]. The authors reported that for some SAPs higher amounts of calcium hydroxide can be formed, most likely due to their ability to bind  $\text{Ca}^{2+}$  ions. According to Mechtcherine et al. [57] if this were the case, one would expect also changes in stoichiometry of the C-S-H and other hydration products in the cement paste matrix.

To conclude, it is also important to highlight that the difference in the values of the velocity attributed to a higher or lower amount of air content could possibly change at later ages with the eventual complete water release by the SAPs, which could not be observed here given the duration of the experiment.

### 3.7 Conclusions

In this chapter, ten different superabsorbent polymers have been studied. Their effects on the properties of fresh and hardened cement pastes were investigated.

The absorption capacity of the SAPs in the cement paste was found to be different than the one measured in cement filtrate solution in most of the cases, depending on the chemical composition of the SAPs. For the commercial SAPs based on carboxylic acids, the effects of the strong ionic complexation with  $\text{Ca}^{2+}$  resulting in further crosslinking was reflected by a decrease in the water absorption in cement paste. On the other hand, the sulfonate-based SAPs showed a more stable behavior related to their kinetics of sorption in the cement paste mixtures. The exception for that was SAPD1 which presented a much unexpected behavior and a considerably high water absorption in cement paste. As for the alginate-based SAPs, only a slight reduction was observed in cement pastes when compared to the absorption in cement filtrate solution, which is related to the already relatively low absorption capacity of such SAPs.

The effects of SAPs in cementitious materials were found to be intimately related to the kinetics of sorption and desorption of the SAPs, which was observed in the mitigation of shrinkage, setting, hardening, development of strength and variation in the levels of internal relative humidity of the cement paste mixtures with SAPs. Related to their role as internal curing agents, only providing the correct amount of water was proven not to be enough for some SAPs. The additional entrained water aimed at internal curing must be provided to the mixture at the appropriate time (which is around the final setting time, when the self-desiccation starts to occur). This was evidenced in the results presented in this chapter where SAPs D1, D2.1, D2.2, C1-C4 were not able to efficiently mitigate autogenous shrinkage with the initially determined amount of water. Attention is once again drawn to SAPD3 and its innovative double crosslinking, which seemed to provide this SAP with a reabsorption capacity able to counteract the effects of an almost generalized faster water release from the sulfonate-based SAPs towards an efficient internal curing.

Although most SAPs presented a very positive result in terms of mitigation of shrinkage, they also promoted a negative impact on the compressive strength of the mixtures. Once again, that was found to be as dependent on the amount of added water as it is on the SAP chemistry and its properties. Incontinent SAPs can cause a reduction in strength depending on their absorption capacity and initial absorption (as it was observed for the alginate-based SAPs in contrast to the sulfonate-based SAPs D1, D2.1 and D2.2). As opposed to that, retentive SAPs and those with a more controlled water release (SAPA, SAPB) caused a more limited reduction of strength and evidence was found that for such SAPs, the strength reduction can be partially counteracted by the promotion of further hydration to a certain extent.

Moving forward to the next chapter, the main conclusion of the study so far points out to the need of knowing the SAPs properties and how they relate to their chemical composition. In addition, the advantages of fine-tuning the properties of in-house developed SAPs for the desired applications is of great advantage.

## References

1. Standardisation, N.-B.f., *NBN EN 1015-3:1999 - Methods of test for mortar for masonry - Part 3: Determination of consistence of fresh mortar (by flow table)*. 1999.
2. Mechtcherine, V., L. Dudziak, and S. Hempel. *Mitigating early age shrinkage of Ultra-High-Performance Concrete by using Super Absorbent Polymers (SAP)*. in *Creep, Shrinkage and Durability Mechanics of Concrete and Concrete Structures*. 2009. Ise-Shima, Japan: Taylor & Francis.
3. Monnig, S. and P. Lura, *Superabsorbent polymers - An additive to increase the freeze-thaw resistance of high strength concrete*. *Advances in Construction Materials 2007*, 2007: p. 351-358.
4. Schrófl, C., V. Mechtcherine, and M. Gorges, *Relation between the molecular structure and the efficiency of superabsorbent polymers (SAP) as concrete admixture to mitigate autogenous shrinkage*. *Cement and Concrete Research*, 2012. **42**(6): p. 865-873.
5. Snoeck, D., O.M. Jensen, and N. De Belie, *The influence of superabsorbent polymers on the autogenous shrinkage properties of cement pastes with supplementary cementitious materials*. *Cement and Concrete Research*, 2015. **74**: p. 59-67.
6. Jensen, O.M. and P.F. Hansen, *Water-entrained cement-based materials I. Principles and theoretical background*. *Cement and Concrete Research*, 2001. **31**(4): p. 647-654.
7. Yang, J., et al., *Early-state water migration characteristics of superabsorbent polymers in cement pastes*. *Cement and Concrete Research*, 2019. **118**: p. 25-37.
8. Kang, S.H., S.G. Hong, and J. Moon, *Importance of monovalent ions on water retention capacity of superabsorbent polymer in cement-based solutions*. *Cement & Concrete Composites*, 2018. **88**: p. 64-72.
9. Els Mannekens, G.D. *The development of SAPs for reducing autogenous shrinkage and accomplishing self-healing and self-sealing properties in concrete*. in *Durable Concrete for Infrastructure under Severe Conditions: Smart Admixtures, Self-responsiveness and Nano-additions 2019*. Ghent, Belgium: Magnel Laboratory for Concrete Research.
10. Schröfl, C., *Chemical design and synthesis of superabsorbent polymers*, in *Superabsorbent Polymers: Chemical Design, Processing and Applications*, S.V. Vlierberghe and A. Mignon, Editors. 2021, Walter de Gruyter GmbH. p. 182.
11. Snoeck, D., et al., *The effects of superabsorbent polymers on the microstructure of cementitious materials studied by means of sorption experiments*. *Cement and Concrete Research*, 2015. **77**: p. 26-35.

12. Snoeck, D., et al., *Effect of high amounts of superabsorbent polymers and additional water on the workability, microstructure and strength of mortars with a water-to-cement ratio of 0.50*. Construction and Building Materials, 2014. **72**: p. 148-157.
13. Wei, X.S. and Z.J. Li, *Early hydration process of Portland cement paste by electrical measurement*. Journal of Materials in Civil Engineering, 2006. **18**(1): p. 99-105.
14. Kang, S.H., S.G. Hong, and J. Moon, *Absorption kinetics of superabsorbent polymers (SAP) in various cement-based solutions*. Cement and Concrete Research, 2017. **97**: p. 73-83.
15. H.X.D. Lee, H.S.W., N.R. Buenfeld, *Effect of alkalinity and calcium concentration of pore solution on the swelling and ionic exchange of superabsorbent polymers in cement paste*. Cement and Concrete Composites, 2018. **88**: p. 150-164.
16. Tangkokiati, P., et al. *Characterization of Neutral Versus Anionic Superabsorbent Polymers (SAPs) in Ion-Rich Solutions for Their Use as Internal Curing Agents*. 2020. Cham: Springer International Publishing.
17. International, A., *ASTM C1698-09(2014), Standard Test Method for Autogenous Strain of Cement Paste and Mortar*. 2014: West Conshohocken.
18. Schroefl, C., et al., *Sorption kinetics of superabsorbent polymers (SAPs) in fresh Portland cement-based pastes visualized and quantified by neutron radiography and correlated to the progress of cement hydration*. Cement and Concrete Research, 2015. **75**: p. 1-13.
19. Mechtcherine, V., et al., *Effect of internal curing by using superabsorbent polymers (SAP) on autogenous shrinkage and other properties of a high-performance fine-grained concrete: results of a RILEM round-robin test*. Materials and Structures, 2014. **47**(3): p. 541-562.
20. Zhong, P.H., et al., *Internal curing with superabsorbent polymers of different chemical structures*. Cement and Concrete Research, 2019. **123**.
21. Snoeck, D., L. Pel, and N. De Belie, *The water kinetics of superabsorbent polymers during cement hydration and internal curing visualized and studied by NMR*. Scientific Reports, 2017. **7**.
22. Justs, J., et al., *Internal curing by superabsorbent polymers in ultra-high performance concrete*. Cement and Concrete Research, 2015. **76**: p. 82-90.
23. Dudziak, L.M., V, *Deliberations on Kinetics of Internal Curing Water Migration and Consumption Based on Experimental Studies on SAP-Enriched UHPC*, in *International RILEM Conference on Use of Superabsorbent Polymers and Other New Additives in Concrete*. 2010, RILEM: Lyngby, Denmark.

24. Trtik, P., et al., *Neutron Tomography Measurements of Water Release from Superabsorbent Polymers in Cement Paste*. International Rilem Conference on Material Science (Matsci), Vol Iii, 2010. **77**: p. 175-+.
25. Snoeck, D., *Self-Healing and Microstructure of Cementitious Materials with Microfibres and Superabsorbent Polymers*, in *Faculty of Architecture and Engineering*. 2015, Ghent University: Ghent, Belgium.
26. Sant, G., et al., *The origin of early age expansions induced in cementitious materials containing shrinkage reducing admixtures*. Cement and Concrete Research, 2011. **41**(3): p. 218-229.
27. Baroghel-Bouny, V., et al., *Autogenous deformations of cement pastes: Part II. W/C effects, micro-macro correlations, and threshold values*. Cement and Concrete Research, 2006. **36**(1): p. 123-136.
28. Smidsrød, O. and G. Skjåk-Bræk, *Alginate as immobilization matrix for cells*. Trends in Biotechnology, 1990. **8**: p. 71-78.
29. Jensen, O.M. and P.F. Hansen, *Water-entrained cement-based materials II. Experimental observations*. Cement and Concrete Research, 2002. **32**(6): p. 973-978.
30. Standardisation, N.-B.f., *NBN EN 196-1:2016 -Methods of testing cement - Part 1: Determination of strength*. 2016.
31. Standardisation, N.-B.f., *NBN EN 480-11:2005 - Admixtures for concrete, mortar and grout - Test methods - Part 11: Determination of air void characteristics in hardened concrete*. 2005.
32. Farzanian, K., et al., *The mechanical strength, degree of hydration, and electrical resistivity of cement pastes modified with superabsorbent polymers*. Construction and Building Materials, 2016. **109**: p. 156-165.
33. Abrams, D.A., *Design of Concrete Mixtures*. 1919: Structural Materials Research Laboratory, Lewis Institute.
34. Powers, T.C., *The Properties of Fresh Concrete*. 1968: Wiley.
35. RYSHKEWITCH, E., *Compression Strength of Porous Sintered Alumina and Zirconia*. Journal of the American Ceramic Society, 1953. **36**(2): p. 65-68.
36. HASSELMAN, D.P.H., *Relation Between Effects of Porosity on Strength and on Young's Modulus of Elasticity of Polycrystalline Materials*. Journal of the American Ceramic Society, 1963. **46**(11): p. 564-565.
37. De Meyst, L., et al., *Parameter Study of Superabsorbent Polymers (SAPs) for Use in Durable Concrete Structures*. Materials, 2019. **12**(9).
38. Ding, H., L. Zhang, and P. Zhang, *Factors Influencing Strength of Super Absorbent Polymer (SAP) Concrete*. Transactions of Tianjin University, 2017. **23**(3): p. 245-257.
39. Jensen, O.M. and P.F. Hansen, *Autogenous relative humidity change in silica fume-modified cement paste*. Advances in Cement Research, 1995. **7**(25): p. 33-38.

40. Huang, H. and G. Ye, *Examining the "time-zero" of autogenous shrinkage in high/ultra-high performance cement pastes*. Cement and Concrete Research, 2017. **97**: p. 107-114.
41. Boshoff, W., et al., *The effect of superabsorbent polymers on the mitigation of plastic shrinkage cracking of conventional concrete, results of an inter-laboratory test by RILEM TC 260-RSC*. Materials and Structures, 2020. **53**(4): p. 79.
42. Ramon, E., *Mitigating autogenous shrinkage of cementitious materials by means of superabsorbent polymers*, in *Department of Structural Engineering*. 2018, Ghent University: Ghent, Belgium. p. 127.
43. Wyrzykowski, M. and P. Lura, *Effect of relative humidity decrease due to self-desiccation on the hydration kinetics of cement*. Cement and Concrete Research, 2016. **85**: p. 75-81.
44. Standardisation, N.-B.f., *NBN EN 196-3:2016 - Methods of testing cement - Part 3: Determination of setting times and soundness*. 2016.
45. Reinhardt, H.W., C.U. Grosse, and A.T. Herb, *Ultrasonic monitoring of setting and hardening of cement mortar - A new device*. Materials and Structures, 2000. **33**(233): p. 581-583.
46. Darquennes, A., et al., *Effect of autogenous deformation on the cracking risk of slag cement concretes*. Cement & Concrete Composites, 2011. **33**(3): p. 368-379.
47. Kakuta, S. and T. Kojima, *Evaluation of Very Early Age Concrete Using a Wave-Propagation Method*. Quality Control of Concrete Structures, 1991. **14**: p. 163-172.
48. Lee, H.K., et al., *Ultrasonic in-situ monitoring of setting process of high-performance concrete*. Cement and Concrete Research, 2004. **34**(4): p. 631-640.
49. Keating, J., D.J. Hannant, and A.P. Hibbert, *Comparison of Shear Modulus and Pulse Velocity Techniques to Measure the Buildup of Structure in Fresh Cement Pastes Used in Oil Well Cementing*. Cement and Concrete Research, 1989. **19**(4): p. 554-566.
50. Sayers, C.M. and R.L. Grenfell, *Ultrasonic Propagation through Hydrating Cements*. Ultrasonics, 1993. **31**(3): p. 147-153.
51. Dangelo, R., et al., *Ultrasonic Measurements on Hydrating Cement Slurries - Onset of Shear-Wave Propagation*. Advanced Cement Based Materials, 1995. **2**(1): p. 8-14.
52. Robeyst, N., C.U. Grosse, and N. De Belie, *Measuring the change in ultrasonic p-wave energy transmitted in fresh mortar with additives to monitor the setting*. Cement and Concrete Research, 2009. **39**(10): p. 868-875.
53. Rizwan, S.A.M., S.; Ahmed, W, *Mitigation of Early Age Shrinkage in Self-Consolidating Paste Systems Using Superabsorbent Polymers*, in *Materials, System and Structures in Civil Engineering (MSSCE-2016)*. 2016: Lyngby, Denmark. p. 443-453.



54. Lyu, Y., *Autogenous Shrinkage of Cement-Based Materials: From the Fundamental Role of Self-Desiccation to Mitigation Strategies Based on Alternative Materials*, in *Faculty of Engineering and Architecture*. 2017, Ghent University: Ghent, Belgium.
55. Robeyst, N., et al., *Monitoring the effect of admixtures on early-age concrete behaviour by ultrasonic, calorimetric, strength and rheometer measurements*. Magazine of Concrete Research, 2011. **63**(10): p. 707-721.
56. Esteves, L.P., I. Lukosiute, and J. Cesniene, *Hydration of cement with superabsorbent polymers*. Journal of Thermal Analysis and Calorimetry, 2014. **118**(2): p. 1385-1393.
57. Mechtcherine, V., et al., *Application of super absorbent polymers (SAP) in concrete construction—update of RILEM state-of-the-art report*. Materials and Structures, 2021. **54**(2): p. 80.

Chapter 4. Investigation of different approaches to determine the time-zero as start for autogenous shrinkage measurements in cement pastes

This chapter was redrafted after:

Tenório Filho, J.R.; Pereira Gomes de Araújo, M.A.; Snoeck, D.; De Belie, N. Discussing Different Approaches for the Time-Zero as Start for Autogenous Shrinkage in Cement Pastes Containing Superabsorbent Polymers. *Materials* 2019, 12, 2962. <https://doi.org/10.3390/ma12182962>.

## 4.1 Time-zero in literature: definition and measurement methods

In cementitious materials, after the contact of water with the cement and during hydration, many changes take place in the material's structure. From that moment until the cementitious material reaches its final setting, chemical and physical processes result in expansion and shrinkage that can initiate cracking in the hardening material.

In the first moments of cement hydration, a large volume change is noticed mainly due to chemical shrinkage. Since it happens during a stage at which the cementitious material is still very fluid there are no major concerns regarding the risk of cracking. In this context, some authors suggest that the measurements of autogenous shrinkage should start at the moment where the material is able to resist the tensile stresses, which occur right after the transition of the material from a liquid to a solid state, i.e. setting [1-4]. This moment in time is referred to as time-zero.

While there is a certain agreement in the definition, there is still a lack of consensus on how to determine that point and many different techniques have been reported: the initial setting time by means of the Vicat test [5-7]; the final setting time by means of the Vicat test [3]; the final setting time by means of ultrasonic pulse velocity (UPV) [8-11]; the maximum negative rate of electric conductivity [2]; the knee point observed in autogenous shrinkage measurements by means of corrugated tubes [12]. In some codes and studies, even some arbitrary values of time are used. For example, in the case of ASTM C157 [13], an indication of 24 h is used. Regarding the use of the knee-point as mentioned in [12], Wyrzykowski et al. in [14] even highlight that different methods used to determine such point might lead to a considerably high deviation amongst measurements of different series. The authors highlight that the shape of the curve, which can be affected by external factors such as temperature and manual operation, might influence the precision of the choice of knee-point. In their study, a new approach is also proposed for the determination of the knee-point based on the time instant when the

scatter of the deformation rates of replicate samples reaches constant low level.

As it can be seen, a lot of different methods and techniques have been reported. However, not all of them represent the same phenomenon and some artefacts related to the test methods may hinder a comparative analysis, the choice of the best technique, and ultimately the study and conclusion on materials used to mitigate shrinkage.

Among the group of techniques based on the solidification of the material, the Vicat test seems to be the most used one given its simple approach. However, despite being simple to perform, the method is based on arbitrary thresholds to define the time of set. The ASTM C191 [15], for instance, defines the initial setting time as the time when a penetration of 25 mm is obtained, and the final setting time as the time when the needle does not sink visibly into the paste. The EN 196–3 [16], on the other hand, defines the initial setting time as the moment at which the distance between the needle and the base-plate is  $(6 \pm 3)$  mm and the final setting time as the moment at which the needle first penetrates only 0.5 mm into the specimen. Some standards also require the setup to be covered (NBN EN 13294 [17]), while others, as mentioned above, are exposed to the air, influencing the setting of the cementitious material due to increased drying. In this context, some authors [18, 19] refer to the use of the UPV method as being more accurate than the Vicat method, because it is more related to the development of the microstructure of the material.

As for the conductivity measurements, despite the fact that many studies have been developed in the field, it is still questionable if it is possible to identify the time-zero based on this method. While it might be useful to obtain information on the chemical processes during cement hydration, the method itself does not directly reflect the physical changes in the material and can be dependent on the water content of the mixture [20, 21].

Autogenous shrinkage is known to be related to a reduction in the internal relative humidity of the material (a consequence of the cement hydration) and associated to the development of the capillary pressure in the pore system due to the receding menisci [22-24]. Based on this understanding, some other approaches were established making use of different techniques, such as: the capillary pressure monitoring to assess the time-zero [25, 26]; the divergence point between the curves of chemical shrinkage and autogenous shrinkage strain [1, 27]; the drop in relative humidity [28, 29]; and the rate of autogenous shrinkage strain [1, 2, 30]. All those methods are more directly related to the physical mechanisms behind the autogenous shrinkage.

Being able to choose an appropriate time-zero value is of utmost importance since it might have a major impact on the interpretation of the shrinkage values which could lead to misinterpretations of results such as an underestimation of strain or overestimation of the effect of internal curing/shrinkage reducing agents.

When SAPs are incorporated in the mixture to promote internal curing, the importance of choosing a more appropriate time-zero becomes even more crucial. As the internal curing takes place and more water is provided to the system, the time for the start of the autogenous shrinkage is expected to change in comparison to mixtures without this feature. This also changes the behavior of the material when tested with the different methods cited above. A less appropriate choice of time-zero could lead to misinterpretation of the real effectiveness of the SAPs and inappropriate dosage.

## 4.2 Determination of the time-zero in this research

The experimental program was based on the measurement of the autogenous shrinkage deformation of cement pastes. The hardening of the mixtures was studied by means of the Vicat test and UPV. The build-up in the capillary pressure was monitored and the rate of deformation due to the autogenous strain was used to determine the transition point between the fluid and solid state of the mixtures. An air void analysis was also performed.

In total, four mixtures were studied, two without and two with SAPs. SAPs A and B, as described in Chapter 2, were used. All tests were performed in a room with controlled temperature ( $20 \pm 2$  °C) and relative humidity ( $60 \pm 5\%$ ).

### 4.2.1 Mixture compositions

All tests were performed on cement pastes produced with cement type CEM III-B 42.5N – LH/SR (CBR, Zeebrugge, Belgium); a polycarboxylate superplasticizer (at a constant dosage of 0.3 m% in relation to the cement mass; Glenium 51, 35% conc., BASF, Germany). The same mixing procedure as mentioned in Chapter 3 was adopted.

Information on the composition of the cement pastes can be found in Table 4.1. SAPs and superplasticizer are added as determined by mass of cement weight (m%). The amount of superplasticizer was kept constant, to minimize the effect on the setting of the materials with and without SAPs [31]. A water-to-cement ratio of 0.3 was chosen, as this REF0.3 mixture would show pronounced autogenous shrinkage [32]. REF0.354 was included based on the theory of Powers and Brownyard [33] which was adapted by Jensen and Hansen [24] for the case of internal curing. According to their study, an additional amount of water corresponding to an entrained water-to-cement ratio of 0.054 stored in the SAPs is enough for an effective internal curing in mixtures produced with ordinary Portland cement and a water-to-cement ratio of 0.3. The amount of SAPs for mixtures P\_SAPA and P\_SAPB was chosen as such that the additional

entrained water (0.054) would be absorbed based on their absorption capacity in cement paste, as determined in Chapter 3.

Table 4.1 - Composition of the cement pastes, showing the effective (–) and the entrained water-to-cement ratio (–), the amount of SAPs (m%), and the amount of superplasticizer (m%).

Mixture	Effective w/c	Additional w/c	Total w/c	SAPs (m%) <sup>1</sup>	Superplasticizer (m%) <sup>1</sup>
REF0.3	0.3	0	0.3	0	0.3
REF0.354	0.354	0	0.354	0	0.3
P_SAPA	0.3	0.054	0.354	0.20	0.3
P_SAPB	0.3	0.054	0.354	0.25	0.3

<sup>1</sup>m% versus cement

#### 4.2.2 Measuring the autogenous shrinkage and setting/hardening of the mixtures

The autogenous shrinkage was assessed according to the standard ASTM C1698–09 [34]. The setting and hardening of the mixtures were studied by means of an electronic Vicat apparatus in compliance with EN 196–3 [16], and ultrasonic pulse velocity (UPV) with a FreshCon equipment as described in by Reinhardt and Große in [9] with compressive pulse waves. The tests were performed using the same equipment and under the same environmental conditions as defined in Chapter 3.

#### 4.2.3 Build-up in the capillary pressure

A small pressure transducer (RVAP015GU, Sontatronics, Puchheim, Germany) registered the development of the capillary pressure every 10 min for 24 h. The custom-made test setup is shown in Figure 4.1. In the test, a 400 ml plastic cup is filled with cement paste. At a height of 37 mm from the bottom, a plastic tube of 50 mm length is inserted in the cup. At



the inner end of the tube, a piece of sponge is attached, while the other end is connected to the pressure transducer. Once water migrates from the cement paste to the tube, the transducer registers the variance in the voltage. The sponge acts as a preliminary filter that prevents the cementitious particles from coming into the tube. Right after filling, the cup was closed with a plastic lid to prevent drying shrinkage and exposure to the environment.

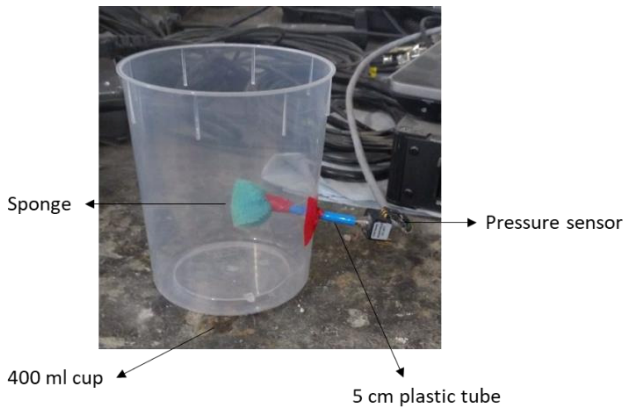


Figure 4.1 - Setup used for the capillary pressure monitoring.

#### 4.2.4 Air void analysis

The test was performed in accordance to the standard EN 480–11 [35]. Further description of the test method and specimen preparation is given in Chapter 3.

### 4.3 Results and discussion

In this part, the results will be discussed, first the setting time (4.3.1) will be investigated, followed by the transition point between fluid and solid state based on the rate of autogenous strain, determined with the corrugated tubes – the so-called knee-point approach – (4.3.2) and the development of capillary pressure (4.3.3). Following that, the autogenous strains for different time-zeros are presented (4.3.4) and the section is concluded with a discussion about practical issues of the different test methods (4.3.5).

#### 4.3.1 Setting time

The initial and final setting times determined using the Vicat apparatus and the FreshCon device are shown in Table 4.2. The values for both test methods were determined in the same way as described in Chapter 3.

Table 4.2 - Average values and standard deviation of the initial and final setting time determined by the Vicat test and UPV (n = 2).

Mixture	Initial Setting [h]		Final Setting [h]	
	Vicat	UPV	Vicat	UPV
REF0.3	5.34 ± 0.37	5.00 ± 0.33	11.38 ± 0.13	10.34 ± 0.33
REF0.354	6.88 ± 0.88	5.67 ± 0.33	13.13 ± 0.37	12.34 ± 0.33
P_SAPA	6.63 ± 0.37	6.67 ± 0.66	12.63 ± 0.88	11.67 ± 0.33
P_SAPB	6.25 ± 0.00	7.25 ± 0.92	12.25 ± 0.50	13.21 ± 0.46

Despite the differences between the test procedures, the specimens' size and the physical aspects of the test procedures, the results present considerable correspondence.

The increase in water-to-cement ratio for the mixture without SAPs (i.e., REF0.354) caused a small delay in both the initial and final setting time.

As for the mixtures containing SAPs, the initial setting times were somewhere in between the original reference (REF0.3) and the reference containing the same amount of total water as the mixtures with SAPs (REF0.354). This result can be explained by the gradual water release of the SAPs that put the mixtures in an intermediate state concerning water content before the final setting occurs.

It can be also noted that, for the mixture P\_SAPB, the final setting time determined by the UPV happens slightly later compared to the time measured for the reference mixtures and the mixture P\_SAPA, while this was not observed with the Vicat test. This indicates that the UPV method is more sensitive to the changes in the microstructure of the material than the Vicat method. Since SAPB has bigger particles than SAPA, a higher porosity can be expected. In fact, the air void analysis showed an amount of air content of 4.76% for P\_SAPB (with 1.57% for voids in the range between 505–1000 microns, 0.99% in the range between 1005–1500 microns, and 0.13% in the range between 1505–2000 microns) and 2.59% for P\_SAPA (with only 0.073% of voids in the range between 505–1000 microns, being this the highest void size range of the mixture).

#### 4.3.2 Transition point between fluid and solid state based on the rate of autogenous strain

The transition point between solid and fluid state was determined considering the moment where the rate of autogenous strain becomes zero. From that moment onwards, in the autogenous strain curve a change in the deformation of the material where the strain rate suddenly and temporarily shifts to a more constant behavior is noticed (Figure 4.2). The results for all the tested mixtures are presented in Table 4.3. When comparing with the results obtained with the Vicat and UPV methods, the knee-point occurs closer to the final setting for the mixtures.

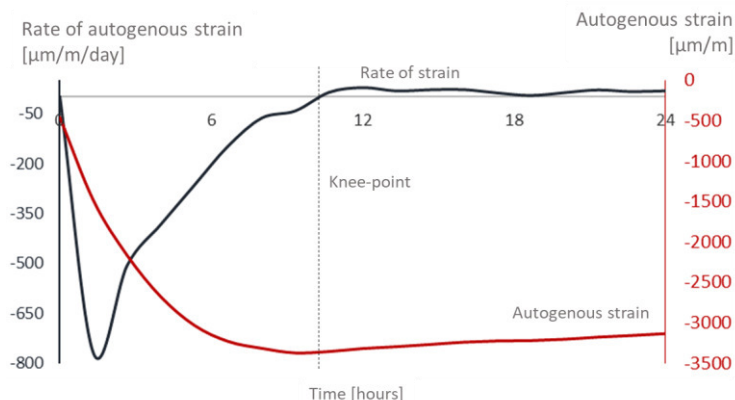


Figure 4.2 – Graphical description for the determination of the knee-point (mixture REF0.354).

Table 4.3 - Knee-point values for all mixtures (n = 2).

Mixture	Knee-Point (h)
REF0.3	9.85 ± 0.47
REF0.354	9.89 ± 0.46
P_SAPA	13.78 ± 0.21
P_SAPB	11.21 ± 0.57

Sant et al. [1] showed also a correlation between the final setting time determined by the Vicat apparatus and the divergence point between the chemical and autogenous shrinkage curves (occurring around the final setting time, as shown in Figure 4.3), also identified as the point where the rate of autogenous strain becomes closer to zero. According to the authors, while the Vicat test is relatively simple to perform, it uses an arbitrary method to define the time of setting and this should be taken into account when choosing a suitable method to determine the time-zero. In the same study, the authors also found a delay of 1.5–2 h in the final setting time determined by the Vicat method of cement paste mixtures containing shrinkage reducing admixtures (SRA) in relation to

reference mixtures without the SRA's. The same trend was observed when comparing the transition points of the autogenous strain curves.

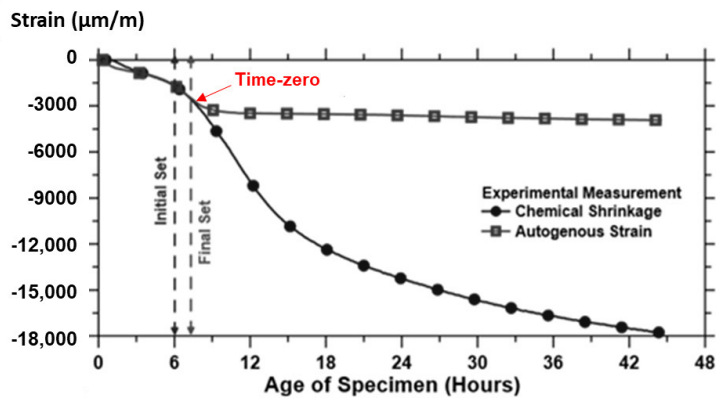


Figure 4.3 - Deviation between chemical shrinkage and autogenous strain as a procedure to determine time-zero. Adapted from [1].

#### 4.3.3 Development of capillary pressure

Figure 4.4 shows the capillary pressure values over time for all mixtures. In comparison with the mixture REF0.3, all the other mixtures present a small delay in the time for the highest build-up in the pressure. This points to the presence of more water (as in REF0.354) or to the gradual and continued water release by the SAPs for internal curing purposes.

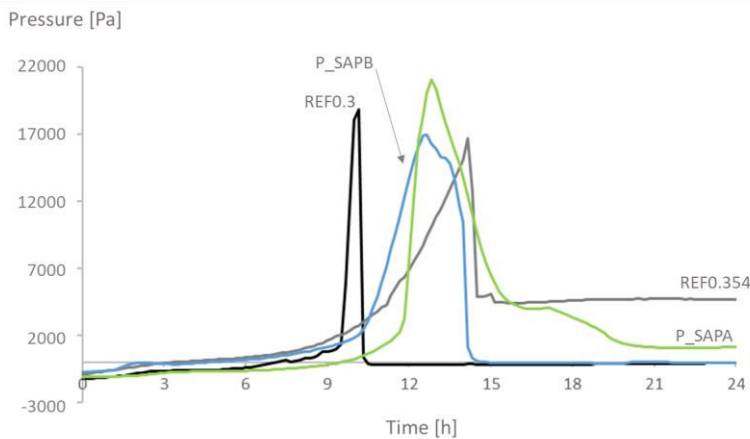


Figure 4.4 - Development of the capillary pressure over time for all mixtures.

According to Chang-Wen et al. [25], the structure of the capillary network at very early age should be mostly determined by the amount of water in the mixture. The authors state that inside the material, the water consumption is expected to occur first in the bigger pores and afterwards in the smaller ones. Since REF0.354 has the highest effective water-to-cement ratio among all mixtures, a higher volume of bigger pores in comparison to the other mixtures is expected.

The air void analysis showed that for the mixture REF0.3 the highest void size is in the range between 355–400 microns, while for the mixture REF0.354 this value is in the range between 455–500 microns. The water consumption in such pores is slower than in the smaller pores, which then leads to a delay in the pressure build-up. In addition, the higher amount of water might have led to a partial emptying of the pores right after the pressure breakdown, leading to a higher constant value of pressure for REF0.354 after 15 h, in comparison to the other mixtures.

By increasing the water-to-cement ratio in the mixture REF0.354 in comparison to the mixture REF0.3, a change in the maximum pressures is noticed. The higher water-to-cement ratio and the lower mechanical strength (see Chapter 3) reduces the value of the maximum pressure but at the same time delays the time when such value is reached. These findings are in accordance with those reported by Wittmann in [26]. In the mixtures P\_SAPA and P\_SAPB, since the water release by the SAPs starts to occur once the water is being consumed inside the pores of the material (and occurs gradually), the moment of pressure build-up is somewhere between REF0.3 and REF0.354. Duplicate specimens were tested for all the mixtures and the highest difference in the time for building-up in the capillary pressure was 1.17 h (for mixture P\_SAPA).

4.3.4 Autogenous strain for different time-zeros

Figure 4.5, Figure 4.6, Figure 4.7 and Figure 4.8 show the development of the capillary pressure for each mixture, with the indication of the initial and final setting time (determined by both the Vicat and UPV methods) and the transition time determined by the rate of autogenous strain.

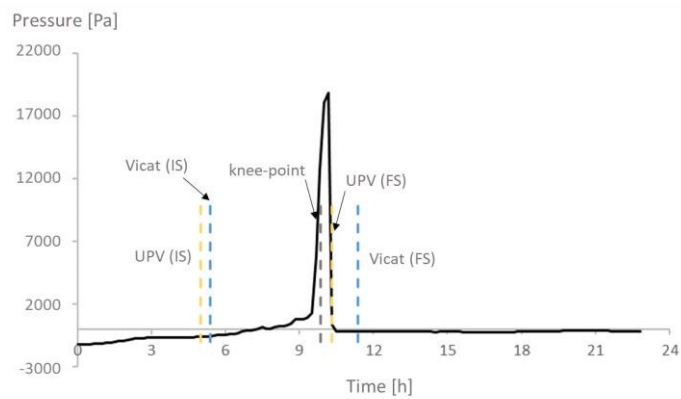


Figure 4.5 - Capillary pressure, setting times, and transition point of REF0.3. With IS referring to initial setting and FS referring to final setting.

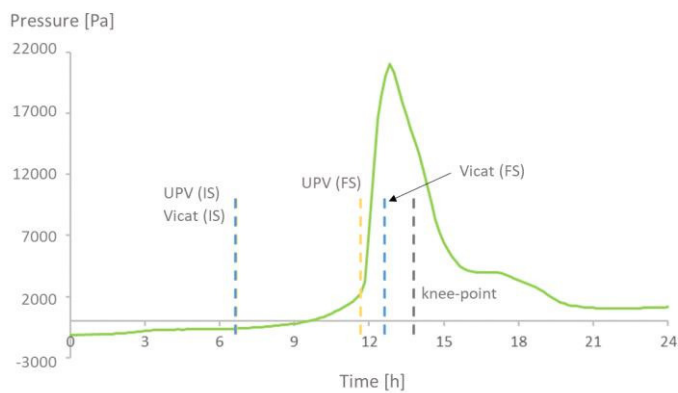


Figure 4.6 - Capillary pressure, setting times, and transition point of P\_SAPA. With IS referring to initial setting and FS referring to final setting.

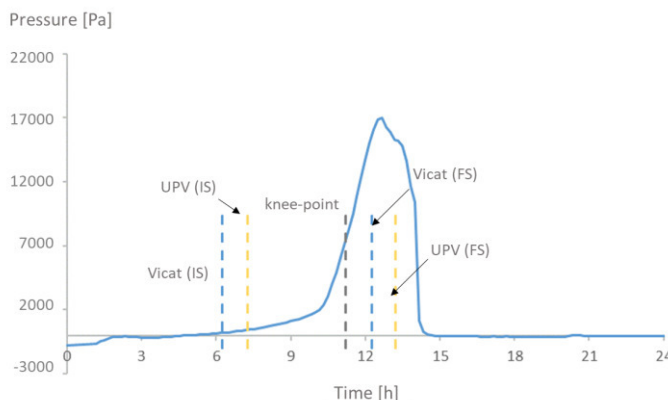


Figure 4.7 - Capillary pressure, setting times, and transition point of P\_SAPB. With IS referring to initial setting and FS referring to final setting.

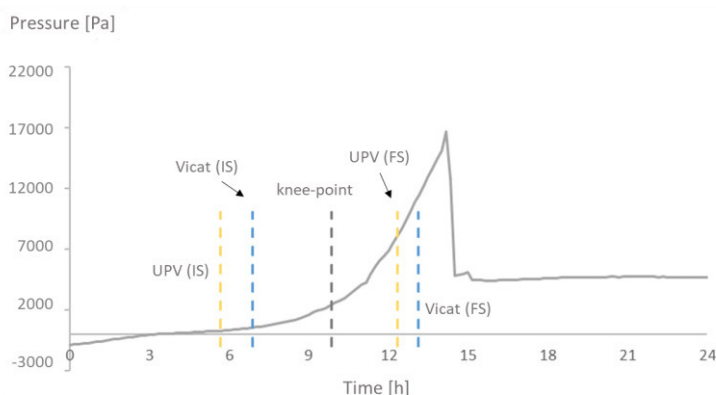


Figure 4.8 - Capillary pressure, setting times, and transition point of REF0.354. With IS referring to initial setting and FS referring to final setting.

For all mixtures, except for REF0.354, the build-up in capillary pressure occurs near the knee-point and the final setting time with a negligible difference considering the standard deviations (Table 4.2 and Table 4.3). This shows a correspondence between the moment where solidification starts to occur and the development of higher stresses inside the pores.

For the mixture REF0.354, the transition point occurs before the final setting time. The pressure starts to build-up around the knee-point and reaches its break-down after the final setting (Figure 4.8). In comparison



with the mixture REF0.3, due to the higher amount of water, the pores formed after the transition from liquid to solid state take longer to be emptied. Also, the formation of a stable solid skeleton is an essential condition for the self-desiccation, but it does not necessarily mean that this phenomenon will take place immediately after the formation of the skeleton [25]. This explains why the break-down in pressure occurs only a few hours after the knee-point.

As for the time-zero, for all mixtures, there is not much difference in the strains when choosing the knee-point or the final setting time as the time-zero. On the other hand, choosing the initial setting time would lead to higher values of strain (Figure 4.9, Figure 4.10, Figure 4.11 and Figure 4.12). Similar results were reported by Sant et al. [2] for cement paste mixtures with and without shrinkage-reducing admixtures. It is important to highlight that, given the nature of the progressive cement hydration, the transition from a fluid to a solid state does not occur in an specific (discrete) point in time, but over several hours, and the use of test methods applied in this study provide a time within this transition period.

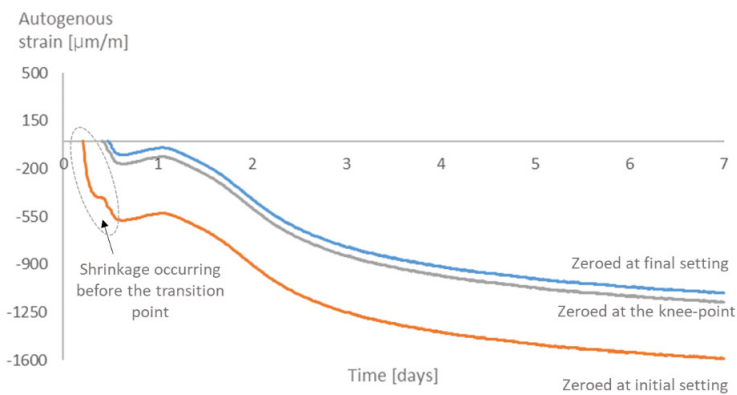


Figure 4.9 - Autogenous strain curves for different choices of time-zeros with REF0.3.

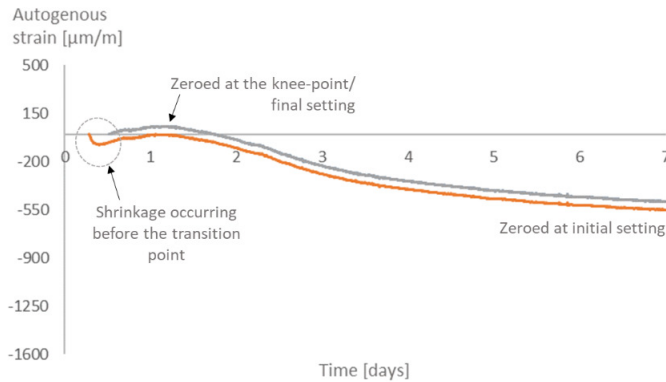


Figure 4.10 - Autogenous strain curves for different choices of time-zeros with REF0.354.

The initial setting time occurs before the knee-point, while the material is still more fluid than solid. At this moment, the shrinkage strain is still not dangerous to the material since there is not much development of stresses inside the pores. It is then reasonable to state that the choice of the initial setting time as time-zero leads to an overestimation of the effects of the shrinkage and an underestimation of the internal curing promoted by the SAPs.

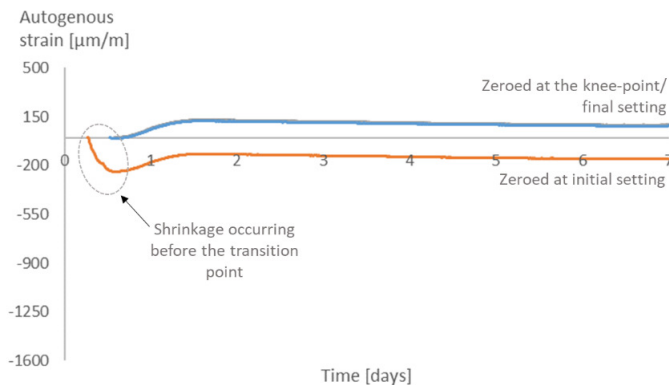


Figure 4.11 - Autogenous strain curves for different choices of time-zeros with mixture P\_SAPA.

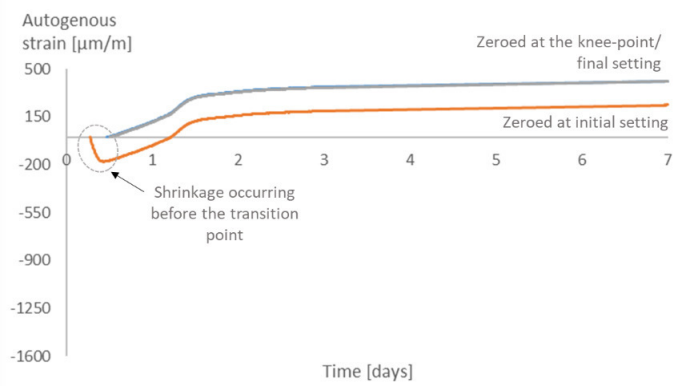


Figure 4.12 - Autogenous strain curves for different choices of time-zeros with mixture PSAPB.

## 4.4 Practical issues and conclusions

Even though a correlation was found between both techniques used to determine the final setting time (the Vicat method and the UPV) and no relevant difference was observed in the autogenous strain when choosing the final setting time or the knee-point as the time-zero, some practical issues should be taken into account when making a choice between those methods.

As stated before, both the Vicat method and the UPV are based on two different physical principles. While the first one relies on the development of the mechanical strength of the material to resist the penetration of the test needle, the UPV is more related to the development of the microstructure of the material.

The conditions of both tests (exposition to the environment, temperature, humidity and volume of the specimen) are different from each other, which at some point could lead to very different results. When using either of them to determine the time-zero, the conditions of the test should be as close as possible to the ones in the test method used to determine the autogenous strain. Not only that, the specimens should be prepared from the same mixture batch and the testing should start at the same time.

The measurements of autogenous shrinkage performed in accordance to the Standard ASTM C1698–09 relies on a specimen in a closed tube where no exchange of moisture is expected, which is impossible to be guaranteed with the automated Vicat apparatus, for example.

By relying only on the autogenous strain test method to determine the time-zero, not only time, but material can be saved, and the test executor can be assured that both the autogenous strain and the time-zero will be determined from a mixture under the same environmental conditions and geometric characteristics.

In addition to that, the following conclusion can be drawn:

- A transition point, representing the moment when the fluid material starts to develop a solid skeleton, can be easily determined based on the strain rate from the autogenous shrinkage test. This is the so-called knee-point.
- For the mixtures with effective water-to-cement ratio of 0.30, there is a correspondence between the transition marked by the knee-point and the highest build-up in the capillary pressure. As the effective water-to-cement ratio increases, the highest build-up in the capillary pressure occurs closer to the final setting time, which is later in time in comparison with the moment of transition marked by the knee-point.
- The addition of SAPs causes a delay in the moment of transition and build-up in capillary pressure, showing internal curing abilities and possible delay of the start of self-dessication.
- Choosing the time-zero as the initial setting time is not suitable and leads to an overestimation of the shrinkage strain and an underestimation of the internal curing effect promoted by the SAPs.
- There is not a relevant difference in choosing the time zero as the knee-point or the final setting time. However, choosing the knee-point seems more suitable since it can easily be determined from the results of the autogenous shrinkage test. No other additional test is then needed for determining the time-zero, which can save time and material.

## References

1. Sant, G., P. Lura, and J. Weiss. *A discussion of analysis approaches for determining 'time-zero' from chemical shrinkage and autogenous strain measurements in cement paste*. in *International RILEM conference on Volume Changes of Hardening Concrete: Testing and Mitigation*. 2006.
2. Sant, G., et al. *Examining time-zero and early age expansion in pastes containing shrinkage reducing admixtures (SRA's)*. in *2nd International RILEM Symposium on Advances in Concrete through Science and Engineering* 2006. RILEM Publications SARL.
3. Hammer, T.A. and Ø. Bjøntegaard. *Testing of autogenous deformation (AD) and thermal dilation (TD) of early age mortar and concrete-Recommended test procedure*. in *International RILEM Conference on volume changes of hardening concrete: testing and mitigation*. 2006. Lyngby, Denmark.
4. Boivin, S., et al. *Experimental Assessment of Chemical Shrinkage of Hydrating Cement Pastes*. in *Int. Workshop on Autogenous Shrinkage of Concrete*. 1998. Hiroshima, Japan: Japan Concrete Institute.
5. Aïtcin, P.C. *Autogenous shrinkage measurement*. in *Int. Workshop on Autogenous Shrinkage of Concrete (Autoshrink '98)*. 1999. London: Spon.
6. Tazawa, E. and S. Miyazawa, *Influence of Cement and Admixture on Autogenous Shrinkage of Cement Paste*. *Cement and Concrete Research*, 1995. **25**(2): p. 281-287.
7. Tazawa, E., et al., *Work of JCI committee on autogenous shrinkage*. *International Rilem Workshop on Shrinkage of Concrete*, Shrinkage 2000, Proceedings, 2000. **17**: p. 21-40.
8. Darquennes, A., et al., *Effect of autogenous deformation on the cracking risk of slag cement concretes*. *Cement & Concrete Composites*, 2011. **33**(3): p. 368-379.
9. Reinhardt, H.W., C.U. Grosse, and A.T. Herb, *Ultrasonic monitoring of setting and hardening of cement mortar - A new device*. *Materials and Structures*, 2000. **33**(233): p. 581-583.
10. Kakuta, S. and T. Kojima, *Evaluation of Very Early Age Concrete Using a Wave-Propagation Method*. *Quality Control of Concrete Structures*, 1991. **14**: p. 163-172.
11. Lee, H.K., et al., *Ultrasonic in-situ monitoring of setting process of high-performance concrete*. *Cement and Concrete Research*, 2004. **34**(4): p. 631-640.
12. Lyu, Y., *Autogenous Shrinkage of Cement-Based Materials: From the Fundamental Role of Self-Desiccation to Mitigation Strategies Based on*

- Alternative Materials*, in *Faculty of Engineering and Architecture*. 2017, Ghent University: Ghent, Belgium.
13. International, A., *ASTM C157 / C157M-17, Standard Test Method for Length Change of Hardened Hydraulic-Cement Mortar and Concrete*. 2017: West Conshohocken.
  14. Wyrzykowski, M., et al., *Corrugated tube protocol for autogenous shrinkage measurements: review and statistical assessment*. *Materials and Structures*, 2016. **50**(1): p. 57.
  15. International, A., *ASTM C191-18a, Standard Test Methods for Time of Setting of Hydraulic Cement by Vicat Needle*. 2018: West Conshohocken.
  16. Standardisation, N.-B.f., *NBN EN 196-3:2016 - Methods of testing cement - Part 3: Determination of setting times and soundness*. 2016.
  17. Standardisation, N.-B.f., *NBN EN 13294:2002 - Products and systems for the protection and repair of concrete structures - Test methods - Determination of stiffening time*. 2002.
  18. Darquennes, A., S. Staquet, and B. Espion, *Determination of time-zero and its effect on autogenous deformation evolution*. *European Journal of Environmental and Civil Engineering*, 2011. **15**(7): p. 1017-1029.
  19. Carette, J. and S. Staquet, *Monitoring the setting process of mortars by ultrasonic P and S-wave transmission velocity measurement*. *Construction and Building Materials*, 2015. **94**: p. 196-208.
  20. Weiss, J., *Experimental determination of the 'Time Zero', t<sub>0</sub> ('Maturity-Zero', M<sub>0</sub>)*, in *Early Age Cracking in Cementitious Systems*. 2003, RILEM. p. 195-206.
  21. Justnes, H., et al., *Correlating the deviation point between external and total chemical shrinkage with setting time and other characteristics of hydrating cement paste*. *International Rilem Workshop on Shrinkage of Concrete, Shrinkage 2000, Proceedings*, 2000. **17**: p. 57-73.
  22. Lura, P., *Autogenous Deformation and Internal Curing of Concrete*. 2003, Delft University of Technology: Delft, the Netherlands.
  23. Bentz, D.P. and O.M. Jensen, *Mitigation strategies for autogenous shrinkage cracking*. *Cement & Concrete Composites*, 2004. **26**(6): p. 677-685.
  24. Jensen, O.M. and P.F. Hansen, *Autogenous deformation and RH-change in perspective*. *Cement and Concrete Research*, 2001. **31**(12): p. 1859-1865.
  25. Chang-Wen, M., et al., *Water consumption of the early-age paste and the determination of "time-zero" of self-desiccation shrinkage*. *Cement and Concrete Research*, 2007. **37**(11): p. 1496-1501.
  26. Wittmann, F.H., *On the action of capillary pressure in fresh concrete*. *Cement and Concrete Research*, 1976. **6**(1): p. 49-56.

27. Hammer, T.A. *Test Methods for Linear Measurement of Autogenous Shrinkage before Setting*. in *Int. Workshop on Autogenous Shrinkage of Concrete*. 1998. Hiroshima, Japan: Japan Concrete Institute.
28. Snoeck, D., L. Pel, and N. De Belie, *The water kinetics of superabsorbent polymers during cement hydration and internal curing visualized and studied by NMR*. Scientific Reports, 2017. **7**.
29. Huang, H. and G. Ye, *Examining the "time-zero" of autogenous shrinkage in high/ultra-high performance cement pastes*. Cement and Concrete Research, 2017. **97**: p. 107-114.
30. Meddah, M.S. and A. Tagnit-Hamou, *Evaluation of Rate of Deformation for Early-Age Concrete Shrinkage Analysis and Time Zero Determination*. Journal of Materials in Civil Engineering, 2011. **23**(7): p. 1076-1086.
31. Snoeck, D. and N. De Belie, *Effect of superabsorbent polymers, superplasticizer and additional water on the setting of cementitious materials*. International Journal of 3R's, 2015. **5**(3): p. 721-729.
32. Snoeck, D., O.M. Jensen, and N. De Belie, *The influence of superabsorbent polymers on the autogenous shrinkage properties of cement pastes with supplementary cementitious materials*. Cement and Concrete Research, 2015. **74**: p. 59-67.
33. Powers, T.C. and T.L. Brownyard, *Studies of the Physical Properties of Hardened Portland Cement Paste*. Vol. 22. 1948, Chicago: Research Laboratories of the Portland Cement Association.
34. International, A., *ASTM C1698-09(2014), Standard Test Method for Autogenous Strain of Cement Paste and Mortar*. 2014: West Conshohocken.
35. Standardisation, N.-B.f., *NBN EN 480-11:2005 - Admixtures for concrete, mortar and grout - Test methods - Part 11: Determination of air void characteristics in hardened concrete*. 2005.





## Chapter 5. The effects of SAPs on concrete mixtures under laboratory conditions

This chapter was redrafted after:

Tenório Filho, J.R., Mannekens, E., Snoeck, D., De Belie, N. (2020). Salt-scaling resistance of SAP-modified concrete under freeze-thaw cycles. RILEM Spring Convention, University of Minho, Guimarães, Portugal, 9-10 March 2020.

Tenorio Filho, J. R., Mannekens, E., Van Tittelboom, K., Snoeck, D., & De Belie, N. (2020). Assessment of the potential of superabsorbent polymers as internal curing agents in concrete by means of optical fiber sensors. *Construction and Building Materials*, 238. 10.1016/j.conbuildmat.2019.117751.

Tenório Filho, J. R., Vermoesen, E., Mannekens, E., Van Tittelboom, K., Van Vlierberghe, S., De Belie, N., & Snoeck, D. (2021). Enhanced durability performance of cracked and uncracked concrete by means of smart in-house developed superabsorbent polymers with alkali-stable and -unstable crosslinkers. *Construction and Building Materials*, 297. 10.1016/j.conbuildmat.2021.123812

5.1 Introduction

Following the results of Chapter 3, where different SAPs were tested in cement pastes, four SAPs were chosen to be tested in concrete mixtures: the commercial SAPs A and B and the sulfonate-based SAPs D2.1 and D3. For the alginate-based SAPs, their low absorption capacity in demineralized water indicated that a considerably high amount of SAPs would be needed for the purpose of sealing/healing. The large-scale production of alginate-based SAPs was not a possibility for the industrial project partner responsible for the production of SAPs. Neither was it for the University laboratory that originally developed these SAPs for small-scale testing. Considering the unfeasibility of such upscaling during the large-scale stage of the research, the alginate-based SAPs were not further investigated and focus was given to the SAPs that could be produced for the large-scale testing stage of the research.

Initially, a reference mixture without the addition of SAPs was defined based on previous experience of InterBeton (Belgium), one industrial partner in the research. Such mixture had been used for the fabrication of tunnel elements, facing autogenous shrinkage problems and repair issues. Detailed information on the composition of the reference mixture is presented in Table 5.1.

Table 5.1 - Mix design of the reference mixture (REF0.46) and some properties.

Component	Amount [kg/m <sup>3</sup> ]	Property	Value
Cement	356	Slump [mm]	160
Sand 0/3	421	Air content <sup>1</sup> [%]	2
Sand 0/4	343	Compressive strength <sup>2</sup> [MPa]	53
Limestone	1086		
Superplasticizer	2.45	<sup>1</sup> determined in the fresh state	
Water	164	<sup>2</sup> determined at 28 days	

The cement used was a blast furnace slag cement type CEM III-B 42.5N – LH/SR, with a clinker content of 20%-34% (CBR, Belgium). The

superplasticizer was Tixo (25% conc.) from Sika (Belgium). Sea sand and limestone were used as fine and coarse aggregate, respectively. Their properties were determined by the industrial partner and are listed in Table 5.2 and in

Table 5.3. The granulometry is presented in Figure 5.1 and Figure 5.2.

Table 5.2 - Properties of the fine aggregates in accordance to the standard EN 12620:2008 (A1) [1].

<b>Aggregate</b>	<b>Fineness modulus</b>	<b>Fines content [%]</b>	<b>Sulfate content [%]</b>	<b>Chloride content [%]</b>
Sand 0/3	2.00	0.5	<0.1	0.061
Sand 0/4	2.63	1.4	<0.1	0.041

Table 5.3 - Properties of the coarse aggregate aggregates in accordance to the standard EN 12620:2008 (A1) [1].

<b>Aggregate</b>	<b>Fines content [%]</b>	<b>Crushing resistance [-]</b>	<b>Abrasion resistance [-]</b>	<b>Conventional organic matter [%]<sup>1</sup></b>
Limestone 4/20	0.8	17	17	0.1

<sup>1</sup> determined according to the standard NBN B 11-256:2016 [2].

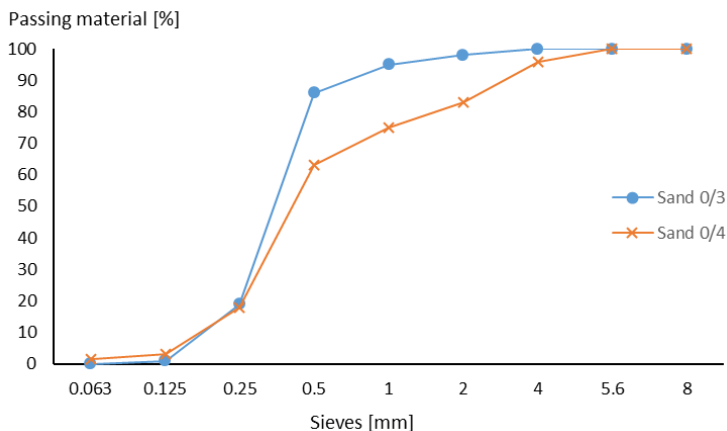


Figure 5.1 - Granulometry of the fine aggregates.

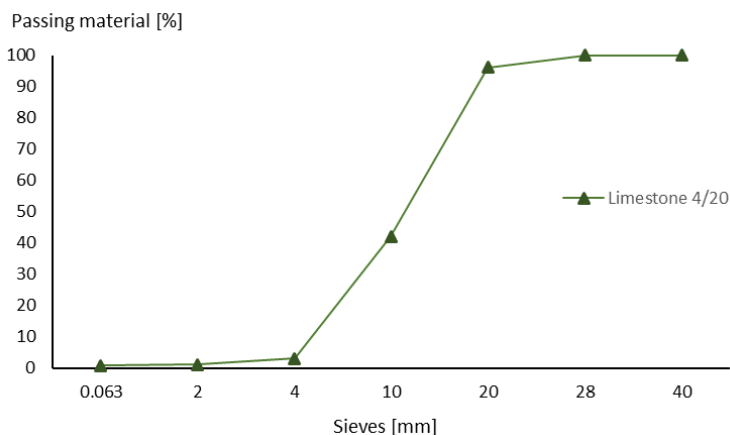


Figure 5.2 - Granulometry of the coarse aggregates.

Based on this reference mixture, the concrete mixtures with the addition of SAPs in targeted the following criteria:

- workability compatible with the consistency class S3 after saturation of the SAPs (considered 10 min after the first contact with water);
- class C35/C45 for the compressive strength (to be obtained after 28 days or at a later age);

- limited interference in the protocols for mixing and transportation at industrial scale;
- in case shrinkage induced cracking is not completely mitigated, there should still be a crack sealing/healing so that water permeability in the low pressure water permeability test (Aldea) shows reduction with factor of 1000;
- amount of scaled material below the threshold of  $1.5 \text{ kg/m}^2$  after 28 freeze-thaw cycles with deicing salts.

As it was done for the cement pastes in Chapter 3, the addition of the SAPs in the concrete mixtures followed a preliminary testing with posterior optimization of the mix design. Initially, a certain dosage of SAPs was defined and their effects were studied on the workability, compressive strength, autogenous/drying shrinkage and scaling resistance under freeze-thaw cycles with de-icing salts.

## 5.2 Preliminary mix-design

### 5.2.1 Production of the reference mixture

First, the reference mixture provided by the industrial partner was produced and tested under laboratory conditions to verify if the targeted properties could be achieved under the current mixing protocols. The same materials described in 5.1 were used. The mixing procedure was adopted as described below, using a planetary mixer with vertical axis and capacity of 50 L:

- Dry materials were mixed for 1 minute;
- The mixing water + superplasticizer were added and everything was mixed for 2 minutes;

The materials were stored in sealed plastic bags inside plastic buckets. One day before mixing the materials were taken out of the bags and left to dry at room temperature. In order to achieve the same workability class of the original mixture without affecting the water-to-cement ratio, the amount of superplasticizer changed from 0.69 m% to 1.8 m% with respect to the cement content. The workability and the air content of the fresh mixture were determined 10 min after the contact of water with the dry materials in the mixing. The workability was measured by means of a slump test in accordance to the standard EN 12350-2: 2019 [3]. The air content was determined following the pressure gauge method described in the standard EN 12350-7: 1999 [4]. The compressive strength of the reference concrete was also tested with cubic specimens (length of 150 mm) at the age of 28 days. The results of the preliminary testing are shown in Table 5.4.

Table 5.4 - Properties in the fresh and hardened state of the reference concrete (REF0.46) produced in the laboratory (n=3).

Slump [mm]	Air content in the fresh state [%]	Compressive strength at 28 days [MPa]
154 ± 12	2.1 ± 0.3	56.9 ± 0.6

The results obtained from the batches produced in the laboratory were found in accordance with those provided by the industrial partner (Table



5.1). This reference mixture will from now on be referred to as REF0.46, with 0.46 being the total water-to-cement ratio.

#### 5.2.2 Production of the SAP-containing mixtures and water absorption of SAPs in concrete

In a broader context, the amount of SAPs in cementitious materials will always be determined based on an iterative process where the positive and negative effects of the SAPs on the properties of the mixture should be balanced. For the purpose of internal curing and mitigation of autogenous shrinkage, Jensen and Hansen [5, 6] proposed a theoretical approach to determine the amount of entrained water for complete mitigation of autogenous shrinkage of cement pastes with water-to-cement ratio below 0.36. Wyrzykowski et al. [7] recommend an approach based on the amount of internal curing water that should compensate for the volume of chemical shrinkage.

In this study, the fixed amounts of 0.5 m% for SAPs A, B and D2.1 and 1 m% for SAPD3 were chosen to first assess the absorption capacity of the SAPs in concrete and gain initial insights about the effects of SAPs on other properties of the concrete mixtures. Most of the studies that have made use of synthetic and commercially available SAPs showed that a dosage of SAPs in the range of 0.2-0.6% with respect to the cement mass should be enough to considerably reduce or completely mitigate the deformation due to autogenous shrinkage at mortar or paste level [8-16] and in high performance concrete compositions (HPC) [17-20]. In the case of SAPD3, given its lower absorption capacity and the experience with the cement pastes it was decided to start with the dosage of 1 m% so that the mixture with SAPD3 could have a total water-to-cement ratio similar to the mixtures with SAPs A and B.

Following the same procedure presented in Chapter 3 for the cement pastes, the absorption capacity in the concrete mixtures was evaluated by means of comparison of workability. SAPs were added in a concrete mixture equal to the reference concrete presented in 5.2.1 and additional water was provided to the mixture until a compatible workability (measured by means of the slump test) was achieved. The mixing

procedure was similar to the one described in 5.2.1 and is presented below.

- Dry materials (including SAPs) are mixed for 1 minute;
- The mixing water + superplasticizer are added and everything is mixed for 2 minutes;
- The additional water is added and everything is mixed for 2 minutes;

The workability expressed by means of slump, the absorption of the SAPs and the water-to-cement ratio of the concrete mixtures are presented in Table 5.5. To facilitate the identification of the mixtures, the following code was chosen: C\_X(m), where C designates concrete mixture, X indicates the SAP that was used, and m represents the dosage of the SAP in relation to the mass of cement (m%).

The slump values obtained for the SAP-containing mixtures were very compatible to that of the reference mixture. The absorption capacity of the SAP was determined considering the amount of additional water needed to reach the reference slump and the amount of SAPs in the mixture. After the determination of the absorption capacity of each SAP, each mixture was produced again with the total amount of water being added at the same time to the mixture as mixing water. The slump test was performed again and no significant difference was found with the slump measured when using the original mixing procedure. A second reference with total water-to-cement ratio of 0.57 was also produced to investigate the effects of only adding extra water without SAPs. For this mixture, the dosage of superplasticizer was reduced to 0.3 m% to avoid segregation. From now on, this mixture will be referred to as REF0.57. The final mix designs are presented in Table 5.5 and Table 5.6.

Table 5.5 - Information about the SAP-containing mixtures. The slump, water-to-cement ratio and absorption capacity of SAPs in both cement paste and concrete are presented.

SAP	Slump [mm]	Air content [%]	Absorption [g/g]		w/c <sub>add</sub> <sup>1</sup>	w/c <sub>total</sub> <sup>2</sup>
			Paste	Concrete		
C_A(0.5)	160	2	27	24	0.12	0.58
C_B(0.5)	140	2.5	21	22	0.10	0.56
C_D2.1(0.5)	150	2.8	45	51	0.26	0.72
C_D3(1)	165	2	14	11	0.11	0.57

<sup>1</sup>w/c<sub>add</sub> represents the additional water-to-cement ratio included to compensate the mixing water absorbed by the SAPs.

<sup>2</sup> w/c<sub>total</sub> represents the total water-to-cement ratio of the mixture and corresponds to the water-to-cement ratio of the reference (0.46) plus the additional water-to-cement ratio.

Table 5.6 – Mix design of the concrete mixtures with SAPs and the reference mixtures. Values shown in kg/m<sup>3</sup>.

Mixture	Cement	Sand 0/3	Sand 0/4	Limestone 4/20	Water		Superplasticizer	SAP
					Mixing	Entrained		
REF0.46	356	421	343	1086	164	0	6.41	0
REF0.57	342	405	330	1044	195	0	1.03	0
C_A(0.5)	341	403	329	1040	157	41	6.14	1.70
C_B(0.5)	342	405	330	1044	157	38	6.16	1.71
C_D2.1(0.5)	326	385	314	993	150	84	5.85	1.63
C_D3(1)	342	405	330	1044	157	38	6.16	3.42

## 5.3 Effects of SAPs on the shrinkage of concrete mixtures

### 5.3.1 Manual measurements

The shrinkage strain of the concrete mixtures was measured on prismatic specimens (100 mm x 100 mm x 400 mm) with a demountable mechanical strain gauge (DEMEC). For each mixture, six specimens were cast and cured for 23 h in a room with controlled atmosphere of  $20 \pm 2$  °C and RH > 95%. Right after casting, the free surface of the specimens was covered with a layer of plastic foil, attached to the mold with a thin layer of Vaseline to improve the adhesion and prevent drying. After the curing period, the specimens were demolded and half of them were wrapped with aluminum tape to avoid moisture exchange with the environment, thus reducing the effects of drying shrinkage. All specimens (covered and non-covered) were left in a room with a controlled atmosphere of  $20 \pm 2$  °C and  $60 \pm 5\%$  RH. Two measuring points were glued to the surfaces of the specimens (except for the troweled surface due to the fact of shape irregularities that could hinder the measurements), placed 200 mm apart on the central line of the specimens' surface (Figure 5.3). The measurements started 24 h after the first contact of cement with the mixing water.

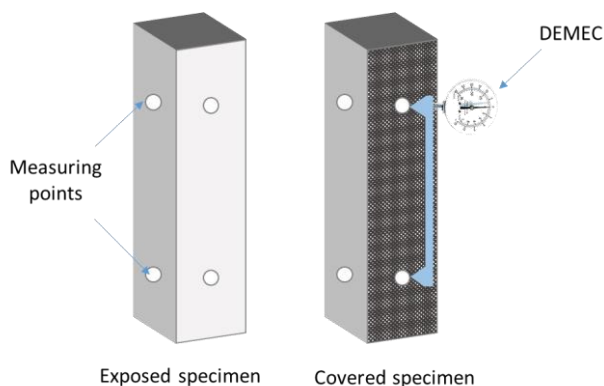


Figure 5.3 – Schematic representation of the DEMEC setup for shrinkage measurements. Measuring points positioned in the central line of the surface, 200 mm apart from each other.

The results of the measurements over time are shown in Figure 5.4 for the covered specimens and in Figure 5.5 for the exposed specimens.

The addition of water in the mixtures promoted a reduction in the autogenous shrinkage. In comparison to REF0.46, all mixtures presented a lower value of shrinkage (or even expansion) during the whole testing time. At the age of 28 days, the reference mixture with higher water-to-cement ratio presented a 28% reduction in strain compared to the original reference mixture.

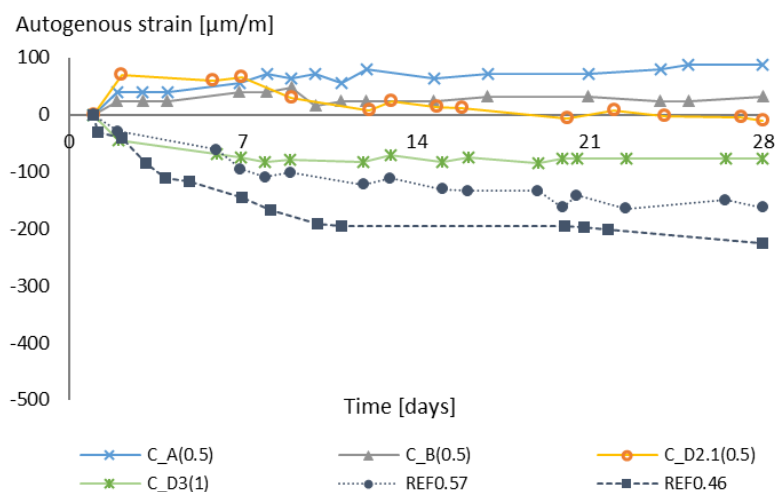


Figure 5.4 – Autogenous strain of the concrete mixtures (measured on the specimens wrapped in aluminum tape).

The use of SAPs, however, promoted a more expressive reduction and even complete mitigation in some cases. The addition of SAPD3 promoted a reduction of 66% and 53% in strain in comparison to REF046 and REF0.57 at 28 days. After 7 days, the mixture C\_D3(1) presented a very stable behavior, with a very low rate of shrinkage (around 2  $\mu\text{m}/\text{m}/\text{day}$  between 7 and 14 days, and almost none from 14 days until 28 days). For both reference mixtures a considerably higher rate was noticed: REF0.46 shrank at a rate of approximately 39  $\mu\text{m}/\text{m}/\text{day}$  during the first 4 days, 12  $\mu\text{m}/\text{m}/\text{day}$  from there up to 11 days, and continued in a shrinking trend until 28 days. REF0.57 presented a very similar behavior, but with a rate

58% lower during the first 4 days and 65% lower from there up to 11 days. For SAPs A and B a complete mitigation of shrinkage was found up to 28 days, while for SAPD2.1 it lasted up to 16 days.

In comparison to the cement pastes some similarities are observed regarding the kinetics of the SAPs, even though different amount of SAPs and water were used. SAPs A and B presented a very stable expansion trend. In contrast to that, SAPD2.1 showed an initial expansion to the same level of the commercial SAPs but then the measured strain started to decrease right after 48 h, moving towards a shrinkage trend, which took place around day 20.

As for mixture C\_D3(1), despite the fact that it was produced with the same amount of additional water as mixtures C\_A(0.5) and C\_B(0.5) some shrinkage was still recorded. Following the approach presented by Wyrzykowski et al. [7], an entrained water-to-cement ratio of 0.1 should be enough for a complete mitigation of autogenous shrinkage in concrete produced with cement type CEM III (based on the value of  $0.1 \text{ cm}^3/\text{g}$  of binder for the chemical shrinkage at 28 days of cement pastes produced with cement type CEM III and water-to-cement ratio of 0.4 [21, 22]). That resulted in a total water-to-cement ratio of 0.56 for the SAP-containing mixtures, which is around the same value used for C\_A(0.5), C\_B(0.5) and C\_D3(1).

As it was discussed in Chapter 3, a successful mitigation of autogenous shrinkage based on internal curing is as related to the provision of the right amount of water to the cement matrix, as it is to the moment when the water is made available to the mixture. As pointed out before, this is strongly related to the kinetics of water retention and release by the SAPs. In fact, in the study with cement pastes a possible premature and intense water release from all sulfonate-based SAPs was discussed (reflected by a peak of expansion followed by a considerable reduction in the expansion values and increase of shrinkage over time), with SAPD2.1 possibly releasing all its stored water and SAPD3 possibly reabsorbing part of the water with its increasing absorption capacity over time.

When subjected to drying, a completely different behavior was found and no mitigation or substantial reduction of shrinkage was observed. The total shrinkage strain measured for all mixtures at 28 days was very similar for all specimens (Figure 5.5).

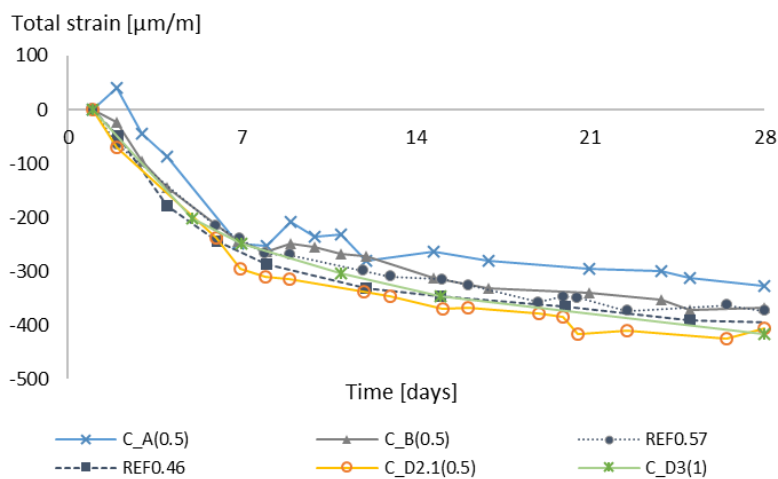


Figure 5.5 – Total strain of the concrete mixtures (measured on the specimens exposed to the air).

The strain due to drying was calculated by subtracting the autogenous strain from the total strain and the values are depicted in Figure 5.6. As expected, a more severe drying was observed for the mixtures with a higher water content, especially the ones containing SAPs. For both reference mixtures, a lower rate of drying is observed from 7 days until up to 28 days (around  $2.7 \mu\text{m/m/day}$ ). The sudden change in the rate of drying for these mixtures represents the absence of free water in the system, which limits the rate of drying. In the mixture C\_D2.1(0.5), a very similar behavior is noticed. A much higher strain was observed for this mixture at 7 days, as a result of the increased water-to-cement ratio (0.72), but the rate of drying becomes even lower than that of the reference mixtures (around  $1.5 \mu\text{m/m/day}$ ) after 7 days. This confirms what was already observed for this SAPD2.1 as a strong and almost complete water release at a very early age (only now enhanced by the drying effect). The effects of drying are very similar in the mixtures with

commercial SAPs, and as it happened with SAPD2.1, a higher strain was observed for both C\_A(0.5) and C\_B(0.5) in comparison to the reference mixtures, even at early ages. The rate of drying for these two SAP mixtures after 7 days (around 5.5  $\mu\text{m}/\text{m}/\text{day}$ ) shows that there is still water in the system, enough to keep a higher internal relative humidity which is reflected by further drying.

As for SAPD3, during the first 7 days of measurements, the drying occurs at a very similar rate in comparison to REF0.57. From that moment on, while there is a very limited drying occurring in the reference mixture, the one containing SAPD3 keeps presenting drying, which occurs at a rate of around 8  $\mu\text{m}/\text{m}/\text{day}$ . In comparison to the other SAPs, the drying pattern of the mixture containing SAPD3 was the closest to REF0.57 during the first 7 days of measurements and the most intense after 7 days. That can be related to the already discussed possible prematurely release and reabsorption of water.

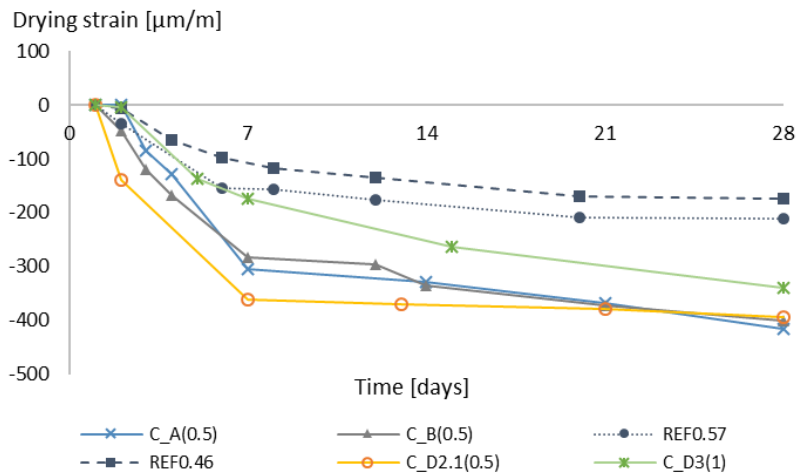


Figure 5.6 – Drying shrinkage strain of the concrete mixtures.

In literature, a few studies report on the effects of SAPs on drying shrinkage of cementitious materials. Assmann and Reinhardt in [23] performed a study on concrete mixtures with and without SAPs. The authors produced two reference mixtures without SAPs and water-to-cement ratios of 0.36 and 0.42, and an additional mixture containing an



acrylamide/acrylic acid SAP at a dosage of 0.25 m% with a total water-to-cement ratio of 0.42 (effective water-to-cement ratio of 0.36 and entrained water-to-cement-ratio of 0.06). The authors measured the shrinkage in prismatic specimens under different conditions: 1) completed sealed with aluminum tape to prevent drying and moisture exchange, to measure only autogenous shrinkage; 2) specimens wrapped in polyethylene foil that would allow a gentle drying (this approach should simulate a thick walled structure which can only dry slowly); and 3) specimens completely exposed to the air (completely subjected to drying). In terms of shrinkage, the authors found that upon exposure to more severe drying from the start, REF0.42 and the SAP(0.36+0.06) mixture presented a higher shrinkage strain when compared to REF0.36. That was not the case here and the concrete composition might provide a possible explanation for that. In their study, Assmann and Reinhardt kept the cement constant for all mixtures and reduced the volume of aggregates to compensate the increase in the volume of water. In this thesis, the volume of the mixture and the proportion amongst dry materials was kept constant. In the second approach, the addition of water will reduce the amount of cement per  $\text{m}^3$  and the resulting volume of paste will eventually be lower compared to the first one which in turn could contribute to a less pronounced shrinkage [24, 25]. As a matter of fact, the volume of paste for REF0.46 is around 29%, while for REF0.57 it is around 30%, which is a small difference

Jensen and Hansen [6] studied the drying of cement pastes with and without SAPs. They initially measured the autogenous shrinkage of the mixtures under sealed conditions for 4.5 months and exposed them to drying under atmosphere conditions similar to the ones used in this research. The authors found that SAP containing mixtures were subjected to a more severe drying in comparison to the reference paste without SAPs. After 18 months of monitoring the residual strain for the SAP mixtures was 72% higher than for the reference. However, the total strain of the SAP mixtures was still considerably lower than the reference, thanks to the internal curing effect on the self-desiccation. A very similar conclusion was also reported by Mechtcherine et al. [26] and [27] where

the authors also observed that drying would be more severe for SAP-modified concrete if the drying were to take place at earlier ages.

As a general conclusion, the overall effect of internal curing with SAP on total shrinkage will depend upon the total water-to-cement of the mixture and the iRH during drying and, hence, upon the proportion between the reduced autogenous and the enhanced drying shrinkage.

Concerning the measurements and preliminary conclusions so far, it is important to bring attention to the fact that the time-zero for the start of the measurements in this case was 24 h and as discussed in Chapter 4 this can play an important role in the interpretation of the results. It was still possible to make a reasonable comparison of the different mixtures regarding shrinkage, however, the missing part of the curve in between the “knee-point” and the 24 h could also lead to a different conclusion, especially considering a possible expansion stage in the mixture C\_D3(1) where the specimens were covered.

Given the consistent expansion stage observed in the mixtures containing commercial SAPs during the monitoring of the autogenous shrinkage, two new mixtures were produced with a reduced amount of SAPs and additional water. A lower SAP dosage (with also reduced amount of additional water) could result in mixtures with a lower reduction in compressive strength (as it will be further discussed in section 5.4) while still mitigating or considerably reducing the autogenous shrinkage. The measured autogenous strains for the new mixtures are shown in Figure 5.7, together with both REF0.46 and REF0.57. Even though the total water-to-cement ratio of the new SAP-mixtures is slightly lower than in REF0.57, this reference was still used as a comparison to highlight the positive effects of having SAPs and not only additional water for reduction of autogenous shrinkage.

A complete mitigation of autogenous shrinkage was not achieved, however, only a very limited shrinkage strain was observed. The maximum shrinkage strain measured was of  $-32 \mu\text{m}/\text{m}$  at 28 days. As mentioned before, by starting the measurements only at 24 h, an important stage of the curves is not considered in the results presented

above. Given the nature of the kinetics of SAPs A and B and the previous results observed with the cement pastes, it can be expected that some expansion would also occur, but it is not taken into account in the curves. That expansion would probably be enough to shift the curves slightly upwards, representing a complete mitigation of the shrinkage.

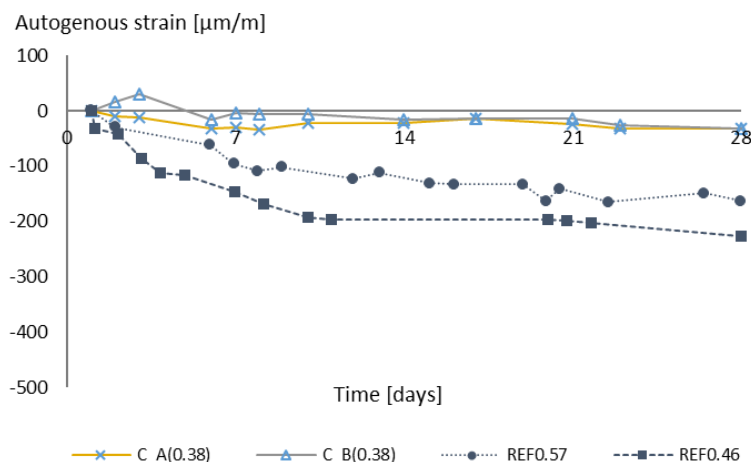


Figure 5.7 - Autogenous strain of the concrete mixtures with lower dosage of commercial SAPs (measured on the specimens wrapped in aluminum tape).

### 5.3.2 Monitoring the deformation of concrete specimens with optical fiber (SOFO) sensors

In this part of the text, the use of optical fiber sensors for monitoring of shrinkage deformation will be discussed. This served as a preliminary study to investigate the feasibility of the use of such sensors in the large-scale demonstrator built to validate the results of the research under realistic conditions, as it will be presented and discussed in Chapter 6.

Up to now, most of the studies described in the literature investigating the deformation due to autogenous shrinkage of concrete have relied on test methods based either on volumetric or linear measurements. The latter have been performed with the use of length transducers placed on the top surface of prismatic specimens, with the measurements starting at different times (6 h, 9 h or 24 h), following the prescription of the ASTM

C157/C157M-17 (24 h) [28] or the final setting time of the mixtures [17, 18, 29, 30]. This means that different shrinkage values are reported and part of the shrinkage is neglected when the measurements are started too late, i.e. after setting. As intensively discussed in Chapter 4, being able to choose an appropriate time-zero value is of utmost importance since it might have a major impact on the interpretation of the shrinkage values which could lead to misinterpretations of results such as an underestimation of strain or overestimation of the effect of internal curing/shrinkage reducing agents.

Although some solid conclusions could be drawn from the manual measurements of shrinkage/expansion strain, such method might represent a higher workload on site, considering the monitoring of a real-size structure. Additionally, the techniques applied to monitor shrinkage of concrete might lead to different responses at different locations due to crack formation or due to the presence of internal voids and discontinuities. For that reason, the use of long-gauge deformation sensors can allow a more global and precise understanding of the material/structure under investigation compared to the traditional methods, as the DEMEC used in this research.

Studies using optical fiber sensors to monitor real concrete structures have been reported since the 90's, especially with regard to displacement monitoring in bridges, decks, dams and railway infrastructure [31-39]. These sensors allowed the monitoring of the strain development in concrete structures under different environmental conditions since the moment of casting, which can be of great interest to study the effect of shrinkage in concrete at very early age.

The sensors used here, from now on referred to as SOFO (produced by SMARTEC, Switzerland), are transducers that transform a distance variation into a change in the path unbalance between two optical fibers that can be measured with a reading unit connected to a computer. They are composed of an active part, responsible for measuring the deformation, and a passive part, responsible for transmitting the data to a reading unit (Figure 5.8). The sensors used in this study have an active length of 250 mm and a passive length of 10 m. The specimens used for

the measurements with the sensors had the same dimensions as those mentioned used for manual measurements (100 mm x 100 mm x 400 mm). At the middle height of the mold, a steel bar with a diameter of  $\varnothing$  6 mm and length of 440 mm was placed to ensure a correct position of the sensors (Figure 5.9). After casting, the specimens were covered with plastic foil, attached to the molds with a thin layer of Vaseline to prevent drying.

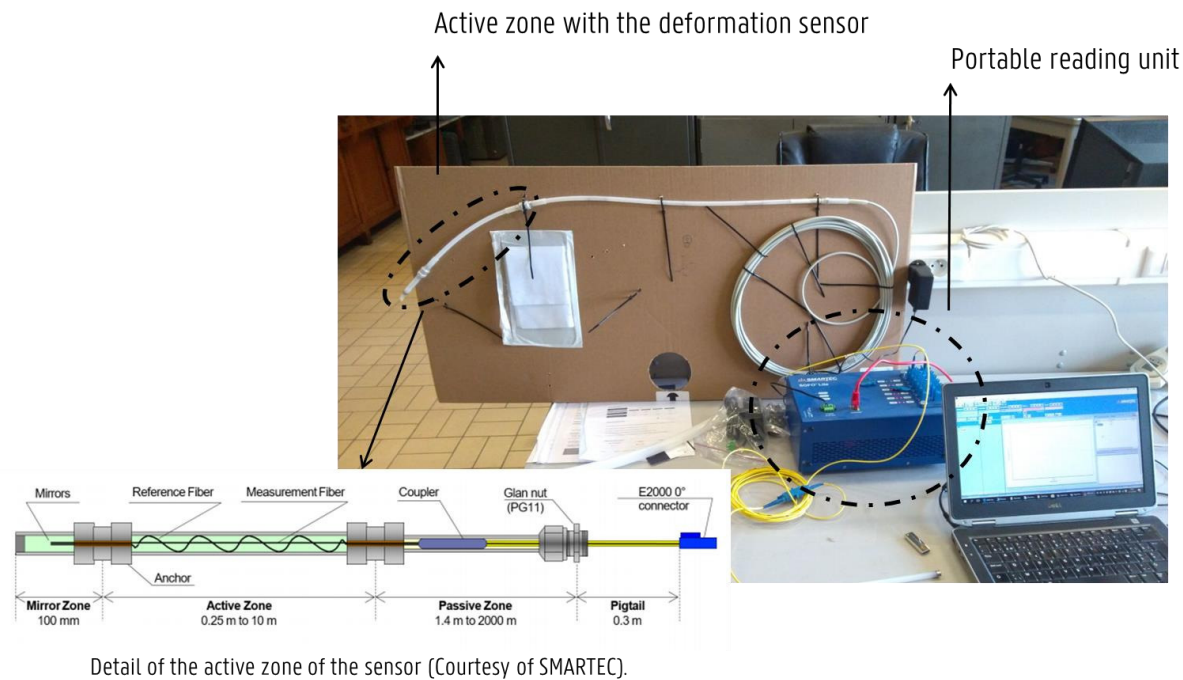


Figure 5.8 - Details of the SOFO sensor and portable reading unit.

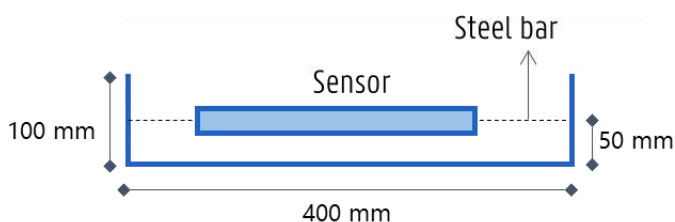


Figure 5.9 - Setup used for the measurements: wood prismatic mold with embedded sensor (attached to a steel bar).

The sensors were attached to the rebar with plastic rings and remained embedded in the concrete during the test. After casting, the specimens were immediately transferred to a room with a controlled atmosphere of  $20 \pm 2^\circ\text{C}$  and  $60 \pm 5\% \text{ RH}$ , where the measurements were performed. The measurements were performed automatically, every 10 min for 28 days, starting 30 min after concrete mixing. Given the costs and availability of the sensors, for this preliminary test three mixtures were chosen: REF0.46, C\_B(0.5) and C\_D2.1(0.5). One specimen per mixture was tested. The deformation curves are shown in Figure 5.10.

The values of strain were zeroed at the knee point (as discussed in Chapter 4), corresponding to 10.73 h for REF0.46, 12.48 h for C\_B(0.5), and 12.24 h for C\_D2.1(0.5). With the measurements starting 12-14h earlier in comparison to the manual method a slight expansion was observed for REF0.46 at the very early age. Apart from that, very similar results were obtained.

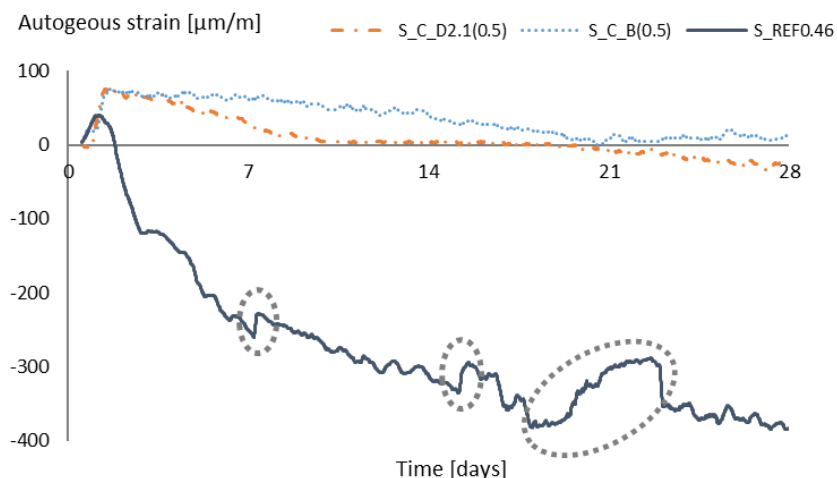


Figure 5.10 - Autogenous strain curves of the tested concrete mixtures.

For both SAP mixtures a complete mitigation of autogenous shrinkage was achieved. The shapes of the curves presented here are very compatible with the ones presented in Figure 5.4. For SAP D2.1 an intense decrease in the expansion trend is noticed already after 24 h. For all mixtures a higher tendency of shrinkage was found in comparison to the specimens monitored with the DEMEC. One of the reasons for that can be the loss of humidity during the test. The specimens used in the manual measurements were completely wrapped with aluminum tape whereas the SOFO beams were covered with plastic foil. That covering might not have been as efficient as the aluminum tape to prevent drying and loss of humidity.

Another interesting feature can also be observed in the curve for the reference mixture. At around 7, 14 and 20 days some “jumps” were recorded. In a shrinkage strain curve, these vertical jumps upwards could represent an immediate elongation of the sensor. In this case, it is observed that the jumps are almost immediately surpassed and the curve goes back to a shrinking trend. A possible reason for this elongation, followed by further shrinking, is the presence of micro-cracks developing in the concrete matrix surrounding the sensors.



The fact that this particularity was only observed for the reference mixture, where no internal curing is taking place, added to the fact that there are some restraints in the system provided by the steel bar offer some support for such theory. To verify that, after the measurements were finished, the specimens were demolded and cut in half to expose the region nearby the sensors. Initially, no de-bonding was noticed between the cement matrix and the steel bar or between the bar and the sensor. Furthermore, for the reference mixture, micro-cracks up to 50  $\mu\text{m}$  were found within 1 cm from the location of the sensor and along the complete active length (Figure 5.11 and Figure 5.12). The width of those micro-cracks is compatible with the value of the jumps noticed in the shrinkage curve.

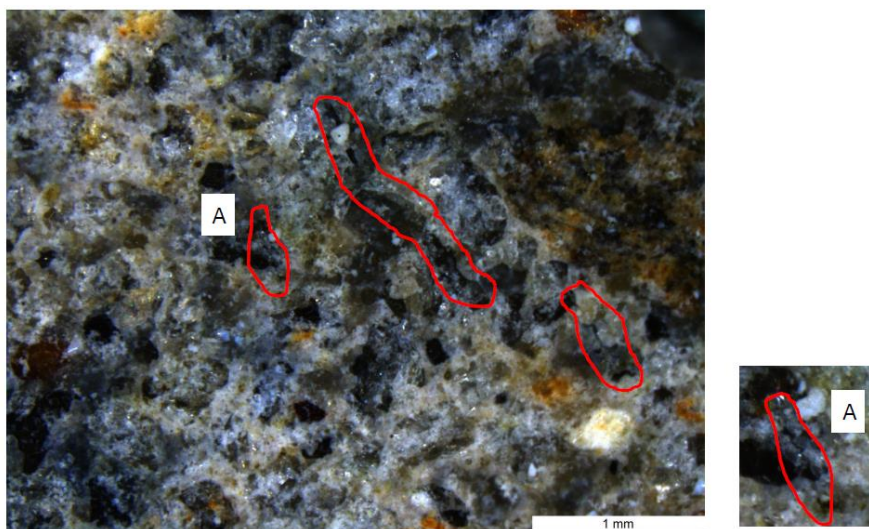


Figure 5.11 - Micro-cracks identified in the cement matrix in the surroundings of the sensor.

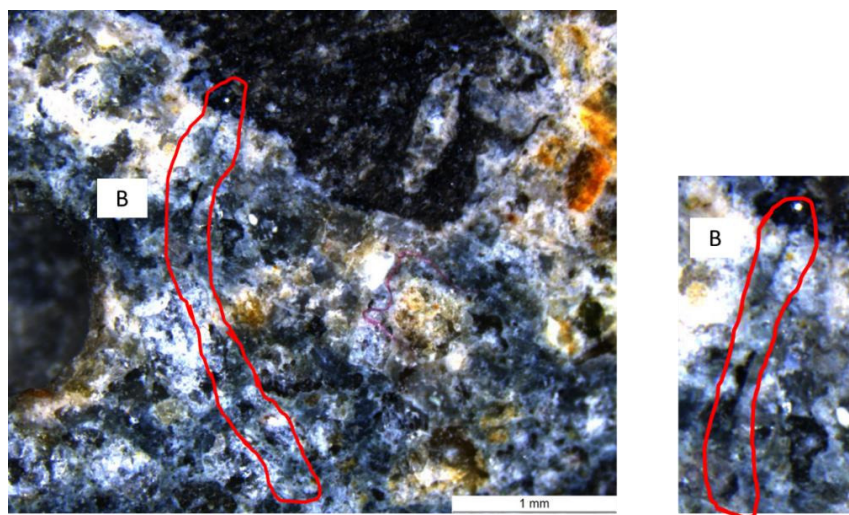


Figure 5.12 – Micro-crack identified in the cement matrix in the surroundings of the sensor.

## 5.4 Effects of SAPs on the compressive strength of concrete

As general rule so far, the addition of SAPs in cementitious mixtures has been found to promote a reduction in compressive strength, mainly due to the effect of the macro-pore formation after water release by the SAPs. The severity of such reduction will depend on the amount and type of SAPs, the testing age, curing conditions before testing, the amount of additional water (if used) and the water-to-cement ratio of the system.

Specifically for concrete, Craeye et al. [17] reported reductions of up to 31% in the compressive strength of a concrete produced with a dosage of 0.081 m% of SAPs at the age of 28 days. In their work, though, the authors seemed to have overestimated the absorption capacity of the SAPs, using an amount of additional water superior to what was actually needed for the absorption of the SAPs [40]. Lam and Hooton in [41] found a reduction of more than 50% compared to a control mixture without SAPs. In this case, the authors also seemed to overestimate the absorption capacity of the SAPs, in a way that the final water content of the mixture is higher. By increasing the amount of SAPs keeping the same amount of additional water, the authors found that the strength of the SAP mixture was approximately equal to the strength of a reference mixture without SAPs and same total water-to-cement ratio. The same was reported by Piérard et al. [18], Snoeck [9], Dudziak and Mechtcherine [42], and Mechtcherine et al. [26].

What most studies mentioned above also show is that, normally, the highest reduction of strength caused by the addition of SAPs is found to happen at early ages. As hydration proceeds and further hydration becomes possible with the internal curing provided by the SAPs, the reduction of strength at later ages is not that prominent. A very similar trend has been found with the use of other types of internal curing agents, such as lightweight aggregates and chemical admixtures, as reported by Lura et al. [43].

In this research, the tests were conducted in triplicates, using cubes with side of 150 mm. The specimens were cured in a room with controlled

atmosphere (of  $20 \pm 2$  °C and RH > 95%) and tested after 7, 28 and 56 days. As expected, the addition of SAPs and water caused a reduction in strength in comparison to the reference mixture with less water (REF0.46). The reduction was noticed for all tested ages, but to a different extent (Figure 5.13).

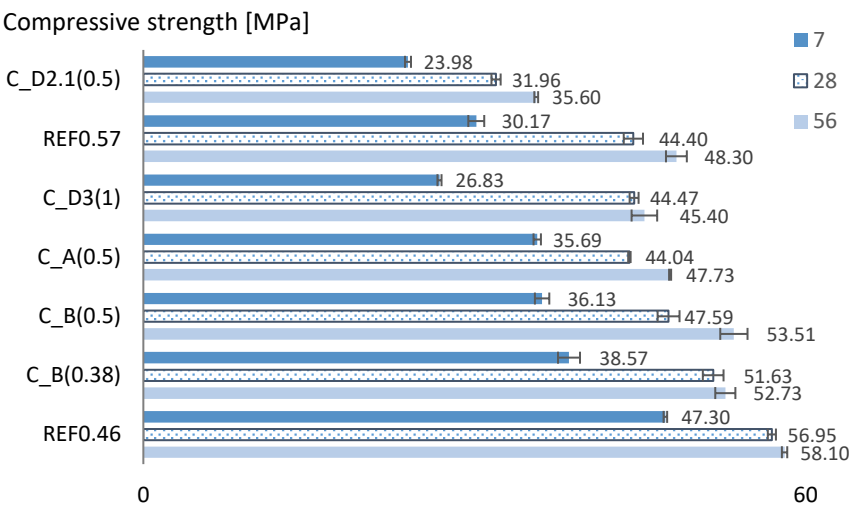


Figure 5.13 – Average compressive strength and standard error of all tested concrete mixtures at the ages of 7, 28 and 56 days.

At the age of 7 days the reduction ranged from 16% to 48%, being the lowest reduction for the mixtures containing commercial SAPs, and the highest in the mixtures containing sulfonate SAPs (37% for SAPD3 and 58% for SAPD2.1), followed by the reference with extra water and no SAP (34%). After 28 days, the reduction was in the range of 18% to 48%, being the maximum reduction found for mixture C\_D2.1(0.5). For this age, the same strength was found for the mixtures with SAPD3, A and REF0.57. In contrast, all mixtures with SAPB presented a reduction below 23%. At the later age of 56 days, the range of reduction was the lowest, going from 16% to 44%. The lowest reductions were again observed for the mixtures with SAPB.

The highest reduction in strength caused by the addition of SAPs and additional water was found at the age of 7 days, in good accordance with the reports from literature discussed before. In terms of composition, the

SAP mixtures that were produced with a total water-to-cement ratio of 0.57 (except for SAPB) performed in a way very similar to REF0.57 after 28 and 56 days. At the age of 7 days, the commercial SAP mixtures performed better than REF0.57, which suggest a positive effect of a more controlled water release by the SAPs and even due to the mitigation of shrinkage and reduction of possible micro-cracks. At later ages, the impact of these positive effects is reduced as more empty voids are formed. At the ages of 28 and 56 days, C\_B(0.5) performed better than C\_A(0.5). Considering that in both mixtures there is the same amount of water, the same dosage of SAPs and mitigation of shrinkage to the same level, this difference might be related to the particle size of the SAPs. With a  $d_{50}$  of 40  $\mu\text{m}$  for SAPA and 360  $\mu\text{m}$  for SAPB a higher number of particles from SAPA is expected in the concrete mixture in comparison to SAPB. A higher number of particles means a higher number of air voids acting as flaws inside the hardened cement paste, which might lead to micro-cracks upon loading and weakening of the matrix.

The effects of the SAPs on the compressive strength, can be associated to this balance between the formation of macro-pores, promotion of internal curing and possible further hydration. Thus, a direct relation between the compressive strength and air voids or amount of water cannot be derived that straightforward for all ages. Figure 5.14 illustrates that for the water-to-cement ratio. All trend lines are power functions, chosen as the ones with the best fit.

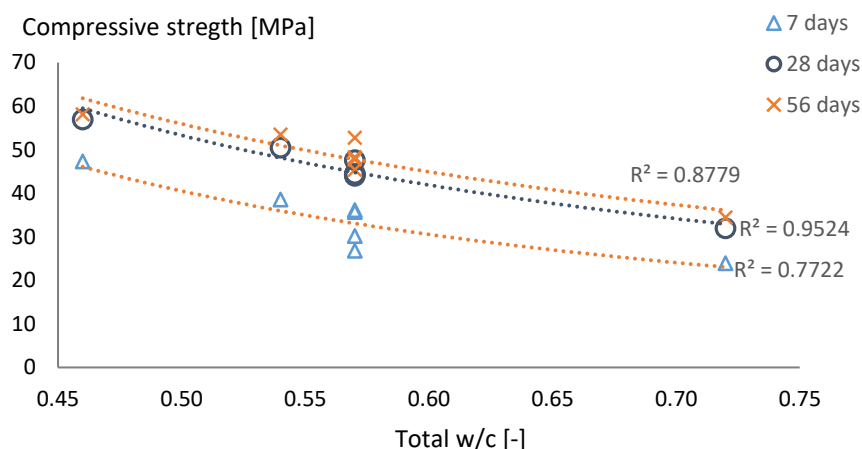


Figure 5.14 - Compressive strength of all tested mixtures at different ages as a function of the total water-to-cement ratio

For all tested ages there is somewhat a relation between the compressive strength and the amount of water in the mixtures. The higher the amount of water, the lower the strength. For the total water-to-cement ratio of 0.57, the existence of mixtures with and without SAPs allows for a better understanding of that.

At the age of 7 days, the largest difference is observed between the SAP containing mixtures and the reference mixture without SAPs. C\_SAPD3(0.5) has the value closest to REF0.57, but still lower, whereas C\_A(0.5) and C\_B(0.5) have a strength that is equal or slightly higher than this reference. In terms of kinetics, it has already been established that SAPD3 possess a small incontinent behavior in comparison to the commercial SAPs. As the water is released earlier, at this stage, the mixture produced with this SAP is more similar to REF0.57 than all the others (compressive strength and shrinkage). At 28 and 56 days, the difference in strength amongst SAP mixtures and REF0.57 is considerably reduced and the power function relating the compressive strength and the water-to-cement ratio presents a better fit. Furthermore, the increase in strength between 28 and 56 days is larger for the SAP mixtures than for REF0.46.

Regarding structural applications of SAP modified concrete, it would be of value to be able to predict the development of strength at different ages,

as it is commonly done with concrete mixtures for common applications. For that matter, the strength development of the SAP mixtures presented in this chapter was predicted using the formulation described in the Eurocode 2 [44] as presented below.

$$f_{cm}(t) = f_{cm} * \exp \left\{ s * \left[ 1 - \left( \frac{28}{t} \right)^{\frac{1}{2}} \right] \right\} \quad (5.1)$$

Where  $f_{cm}(t)$  is the mean concrete compressive strength at an age of  $t$  days (in MPa),  $f_{cm}$  was adopted as the compressive strength of the concrete mixture at the age of 28 days (in MPa),  $t$  is the age of the concrete (in days), and  $s = 0.25$  (corresponding to a cement of strength class CEM 42.5 N).

The calculated values for the SAP mixtures were found to be in good accordance with the tested values for both 7 and 56 days, except for C\_D3(1), with a difference of less than 4% (Table 5.7). This shows evidence that even with the all the dynamic behavior that the inclusion of SAP might bring to the concrete mixture, the usual prediction method can still be applied with good accuracy.

Table 5.7 - Comparison of tested and calculated values (Eurocode 2) of compressive strength.

Mixture	$f_{cm}$ [MPa]	Compressive strength at 7 days [MPa]		$ \Delta ^2$ [%]	Compressive strength at 56 days [MPa]		$ \Delta ^2$ [%]
		Tested	EC2 <sup>1</sup>		Tested	EC2 <sup>1</sup>	
C_A(0.5)	44.04	35.69	34.30	3.9%	47.73	47.39	0.7%
C_B(0.38)	50.44	38.57	39.28	1.8%	53.51	54.27	1.4%
C_B(0.5)	47.59	36.13	37.06	2.6%	52.73	51.21	2.9%
C_D2.1(0.5)	31.96	23.98	24.89	3.8%	34.48	34.39	0.3%
C_D3(1)	44.47	26.83	34.63	29.1%	45.40	47.85	5.4%

<sup>1</sup>EC2 stands for Eurocode 2.

<sup>2</sup> $|\Delta|$  represents the absolute percentage value of the difference between the calculated and tested value.

## 5.5 Effects of SAPs on the scaling resistance of concrete under freeze-thawing with de-icing salts

One of the most important problems regarding durability of cement-based materials is deterioration by frost action [45]. Concrete in roads, bridges, tunnels or other applications in the northern hemisphere is often exposed to freezing temperatures during winter and could be then exposed to de-icing salts that are eventually used to clear the ice. Repairing or replacing infrastructure and concrete structures results in heavy expenditures [46]. In the Flemish Region of Belgium for example, as Belgium is a busy transit country in Europe, yearly investments of 350 million euros are made for road construction and its maintenance [47]. Freeze-thaw damage can take multiple forms, but the most common one is damage due to surface spalling under cyclic freeze-thaw load [45, 48]. Surface spalling implicates the loss of small aggregates under the surface and loss of flakes of binder from the surface (Figure 5.15).



Figure 5.15 - Surface of a concrete specimen (REF0.46) before (left) and after (right) 28 freeze-thaw cycles with de-icing salts (3% NaCl solution).

Powers in [49] described early on why air entrainment was effective in reducing the frost action in cement paste as well as the mechanism of frost action itself. As water freezes in pore spaces and transforms from a liquid to a solid, an expansion of up to 9% is caused, resulting in expansion pressures. When water in a capillary cavity freezes, the amount of excess water needs to be able to leave or a dilatation of the cavity of 9% of the



volume of the frozen water is needed, in order not to have an increasing hydraulic pressure. This hydraulic pressure thus develops if the pore space is filled by the formation of ice, which by volume expansion forces the liquid out. This development occurs unless all capillary cavities are not farther than approximately 750-1000  $\mu\text{m}$  from the nearest boundary to escape. Powers also stated that an osmotic pressure could accumulate the hydraulic pressure. As water in the capillaries is not pure and contains soluble substances, a difference in local salt concentrations between different capillary cavities could be the source of osmotic pressure. In addition to that, cryo-suction pressure due to the stability criterion for the triple-phase condition of water in the cement paste [50] and the crystallization pressure due to the confined pores being penetrated by ice [51] also induces internal frost damage. If an appropriate air void system is developed and air-entraining agents are incorporated in the cement paste during mixing, relief can be provided for these pressures and the deterioration from freeze-thaw cycles and scaling progression can be mitigated.

Regarding the effects of SAPs, upon de-swelling as a consequence of water release, the SAP voids form a system of close-spaced voids in the cement paste, resembling the pore system obtained by air entrainment [52, 53]. Although the void system obtained by the use of SAPs resembles that of a pore system obtained by air entrainment agents, the use of SAPs does include some advantages in comparison to the use of air entraining admixtures (AEA). A decrease in tendency to coalesce and segregate leads to a stable void system, which can be designed due to the addition of SAPs regarding the total amount, size and even shape of the individual voids [52]. The effect of SAPs on the freeze-thaw resistance of concrete was broadly investigated by testing mass loss after freeze-thaw cycles in a RILEM inter-laboratory study [54]. Two commercially available SAPs were tested regarding their effect on the freeze-thaw resistance (with and without deicing salt) by 13 international laboratories spread across the world. Concrete mixtures were produced with local materials and water-to-cement ratio of 0.45 and 0.50. The addition of SAP did not result in an increased air content in the tested fresh mixtures, therefore the resulted

resistance can be explained solely by the performance of the SAP. Similar results to AEA incorporation were obtained in some cases without addition of extra water, but in most cases the AEA performed significantly better. Although the performance of the mixtures with SAPs, in terms of scaled material, was overall lower than the mixtures with an AEA, the mechanical properties were reduced less by the addition of a SAP and additional water, than by air entrainment.

In this research, five concrete mixtures were studied under freeze-thaw cycles with de-icing salts: REF0.46, C\_A(0.5), C\_B(0.50), C\_D2.1(0.5) and C\_D3(1).

The scaling test followed the recommendations of the standard EN 12390-9 [55] with the temperature cycle as shown in Figure 5.16. The freezing medium used was a 3% NaCl solution (prepared with demineralized water), corresponding to a thin layer of 3 mm poured on the top surface of the specimens (25 ml of solution for each specimen, in this case).

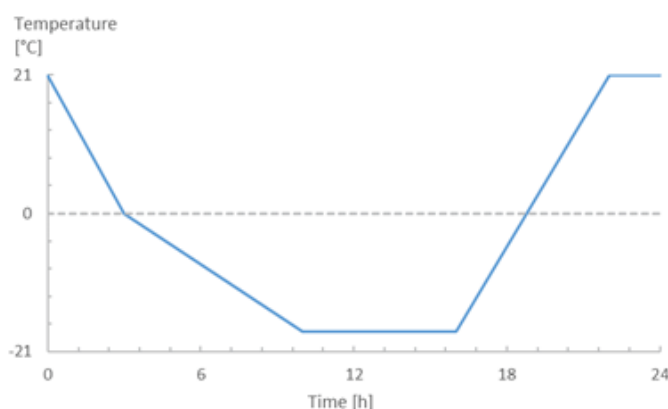


Figure 5.16 - Temperature cycles used in the freezing chamber during the test.

For each concrete mixture, a cylinder with a diameter of 10 cm and a height of 20 cm was cast. After 25 days, each cylinder was cut in three smaller cylinders with a diameter of 10 cm and a height of 5 cm. They were then placed into a PVC tube with an inner diameter of 10 cm and a height of 7 cm. A thin layer of epoxy was applied at the sides to prevent any leakage of the freezing fluid from the top of the surface. From the

26th till the 28th day, a thin layer of 3 mm of demineralized water was poured on the top surface of the specimens to verify the existence of any leakage Figure 5.17. On the 28th day, the specimens were placed inside an insulating recipient, the freezing medium was poured on them and the specimens were put inside the freezing chamber. The scaled material was measured after 7, 14, 21 and 28 cycles. The filters used to collect the scaled material were dried in the oven under 100 °C after the collection of the material. Additionally, the air void analyses previously described in Chapter 3 were performed at 28 days to determine the spacing factor of the mixtures. Both the salt scaling and air void analysis were performed in triplicates.



Figure 5.17 - Preparation of specimens for the freeze-thaw cycles. The molds filled with epoxy are shown on the left and the sealed specimens after receiving the saline solution on the right.

The cumulative scaled material of the concrete specimens is shown in Figure 5.18. Except for SAPD2.1, all SAPs promoted a considerable reduction in the amount of scaled material in comparison with the reference mixture without SAPs. After 28 cycles, the reduction was around 49%, 33% and 55% for SAPs A, B and D3, respectively. The results are in compliance with the findings of Kusayama et al. in [56] and Mechtcherine et al. in [54]. In literature, some failure thresholds are usually mentioned regarding the amount of scaled material. In [54] and [57] a value of 1.5 kg/m<sup>2</sup> is cited, while the Belgian standard for concrete paving flags [58] mentions a limit of 1.0 kg/m<sup>2</sup>, both after conducting 28 freeze-thaw cycles. The mixtures containing SAPs A, B and D3 comply with

both the thresholds cited up to 28 freeze-thaw cycles. In contrast, the reference mixture presented a scaling higher than  $1.0 \text{ kg/m}^2$  after 14 cycles and a value higher than 1.5 between the 21<sup>st</sup> and 28<sup>th</sup> cycle. As for the mixture produced with SAPD2.1, a higher scaling during the whole testing period in comparison to all the other mixtures was found (almost four times higher than the reference already after 7 cycles after 28 cycles).

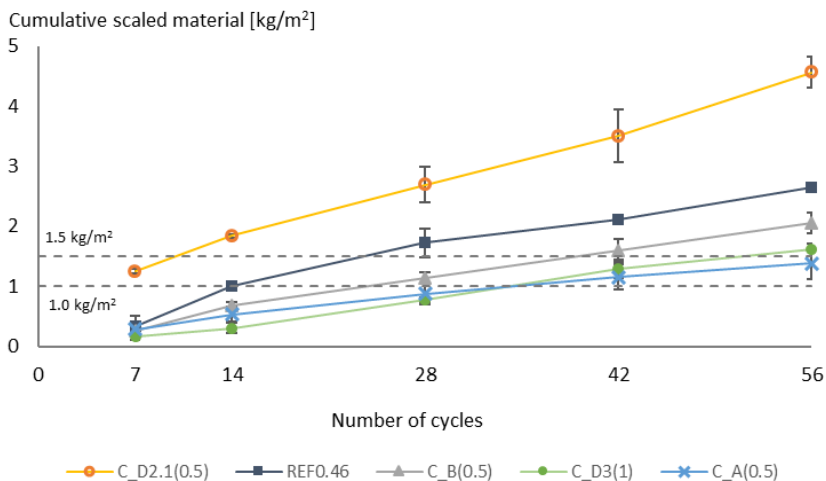


Figure 5.18 – Average cumulative scaled material and standard error of the concrete mixtures under freeze-thaw cycles with de-icing salts. Each point represents the average of three tested specimens.

In the air void analysis, the spacing factor ( $L$ , in mm) of each mixture was calculated using Equation 5.2, proposed by Powers in [49], for a ratio of  $p/A \geq 4.342$ . In the equation,  $S$  is the specific surface of the air voids (as determined by the automated air void analyzer and measured in  $\text{mm}^{-1}$ ),  $p$  represents the paste content as a percentage of concrete volume (in %), and  $A$  stands for the air content in the hardened state (as determined by the automated air void analyzer, measured in %). All parameters used for the calculations and the respective spacing factor values for all mixtures are shown in Table 5.8.

$$L = \frac{3}{S} * \left( 1.4 * \left( \frac{p}{A} + 1 \right)^{1/3} - 1 \right) \quad (5.2)$$

Table 5.8 - Air void parameters for the calculation of the spacing factor.

Mixture	Air content [%]	Paste content [%]	Specific surface [mm <sup>-1</sup> ]	Spacing factor [mm]
REF0.46	2.37	28	15.51	0.44
C_A(0.5)	3.35	28	20.80	0.28
C_B(0.5)	4.2	28	16.48	0.32
C_D2.1(0.5)	1.64	28	14.12	0.57
C_D3(1)	3.53	28	21.28	0.27

A good correspondence was found between the amount of scaled material after 28 cycles and the spacing factor of the concrete mixtures (Figure 5.19).

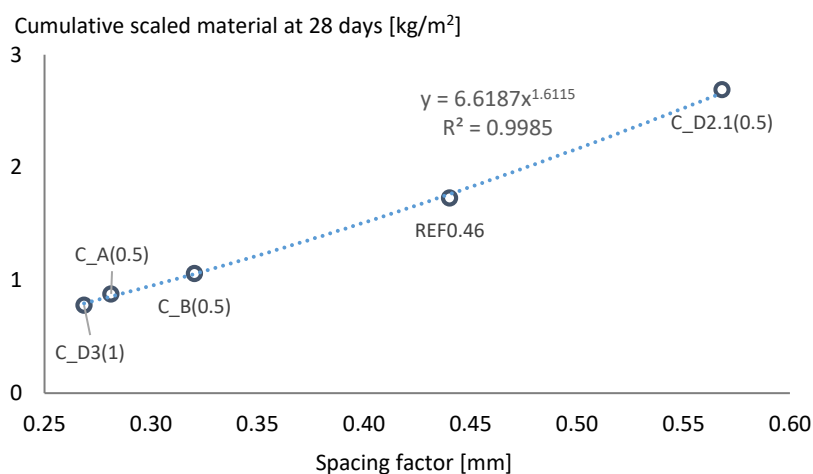


Figure 5.19 - Amount of scaled material after 28 cycles as a function of the spacing factor.

The increased scaling resistance observed for the concrete mixtures containing SAPs A, B and D3 seems to be associated to an efficient air void system built in the mixtures due to the addition of SAPs. For all three mixtures (C\_A(0.5), C\_B(0.5) and C\_D3(1)) a reduction in spacing factor was found, indicating that for these mixtures there is a shorter distance between the capillary pores and the air voids left by the SAPs. In the opposite way, the mixture containing SAPD2.1 presented the highest

spacing factor amongst all mixtures, leading to the lowest scaling resistance. Here, once more, the kinetics of water release by the SAPs play an important role in the performance of the concrete. The air content value of C\_D2.1(0.5) could once again indicate the premature water release by SAPD2.1. Upon such release at an early time, it is possible that the air voids left by the SAPs after de-swelling cannot remain stable enough in the still fluid/plastic mixture. That would not only cause a reduction in the size, but in the number of air voids in the cement paste, reducing the spacing factor and the scaling resistance. In addition to that, it is important to mention the higher total water-to-cement ratio and reduced compressive strength of C\_D2.1(0.5).

## 5.6 Promotion of immediate sealing in cracked concrete

Cracked specimens were used to assess the effects of the SAPs on the immediate sealing of cracks upon swelling. The mixtures REF0.46, C\_B(0.5) and C\_D3(1) were used. For SAPD3, two mean particle sizes were tested: 100  $\mu\text{m}$  and 300  $\mu\text{m}$ . The composition of the mixtures is the same as presented in Table 5.1 and in Table 5.6.

The water permeability setup proposed by Aldea [59] was used. In this setup, a cylindrical specimen with a diameter of 80 mm and thickness of 20 mm is placed in between two water-filled containers. On the top of the upper container, a thinner glass tube with a diameter of 12 mm is installed to monitor the level of water going through the crack. During the test, the amount of time that it takes for a water column with height of 280 mm to pass through the cracked specimen is recorded. The water exit point is at the same level as the bottom surface of the specimen. A schematic overview of the setup is shown in Figure 5.20.

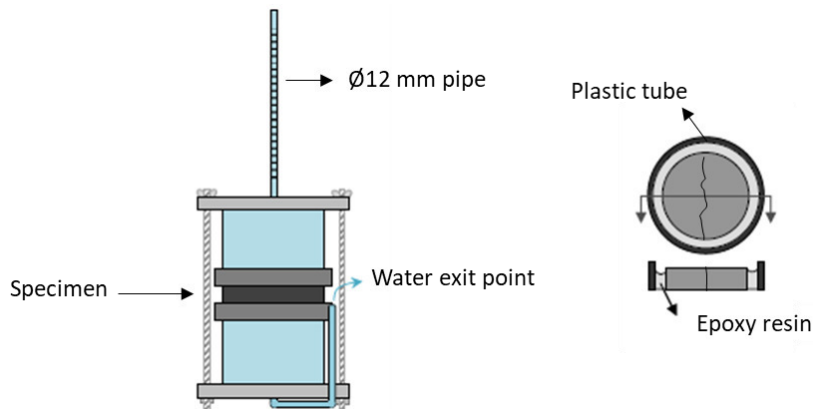


Figure 5.20 - Overview of the test set up with detail of the specimen on the right. Adapted from Snoeck [9].

During the preparation of the specimens, cylinders with a diameter of 100 mm and height of 200 mm were first cut into cylinders with a diameter of 80 mm and height of 20 mm. They were then cracked (in order to obtain a crack width upon unloading of 200-250  $\mu\text{m}$ ) by means of a Brazilian

splitting test at the age of 28 days. During the splitting, the specimens were externally reinforced with a screw clamp to avoid total rupture. Once a crack going through the specimen was achieved, the specimens were carefully taken to a microscope to measure the crack width. When needed, the specimens were re-submitted to splitting until the crack observed under the microscope achieved the targeted width. After cracking, the specimens were placed inside a PVC mold with a diameter of 100 mm and the gap between the specimen and the mold was filled with epoxy resin. Care was taken that no resin filled the crack by means of taping the samples. The epoxy (Figure 5.20, right side) also guaranteed unidirectional flow during water permeability testing. Once the resin hardened, the specimens were vacuum saturated for 24h with demineralized water. After that, the specimens were placed in the testing setup for the measurements of immediate sealing. To account for possible unsteady flow due to the presence of air bubbles or loose particles inside the crack, the water flow was recorded for five consecutive days. In order to assess a possible healing of the cracks over time, the specimens were removed from the permeability set up and subjected to wet dry cycles after the five-days testing for the immediate sealing to stimulate healing. The cycles consisted of 12 h of immersion in demineralized water and 12 h of exposure of the specimens to air for a period of 28 days.

The water permeability coefficient of each series (before and after healing) was then calculated considering the average flow of the five days. For that, Darcy's law was used:

$$k = \frac{a_f \cdot T_s}{A \cdot t_f} \cdot \ln \left( \frac{h_0}{h_f} \right) \quad (5.3)$$

With,  $a_f$  = cross-sectional area of the fluid column [ $\text{m}^2$ ];  $T_s$  = specimen thickness [m];  $A$  = surface area of the sample subjected to the flow [ $\text{m}^2$ ];  $t_f$  = measured time [s];  $h_0$  = initial pressure head [m];  $h_f$  = remaining pressure head [m] and  $k$  = coefficient of water permeability [m/s].



During the course of the measuring time of five days, no significant differences were found for the water flow of the different specimens. In order to compare the difference in the efficiency of the SAPs, the average value of the coefficient of water permeability over the five days was considered as representative for each series. Results are shown in Figure 5.21.

Both SAPs B and D3 showed a reduction in water permeability of the cracked specimens, but different rates of reduction were found. SAPB promoted a reduction of 45% while for SAPD3 of 72% and 65% was obtained for the  $d_{50}$  of 100  $\mu\text{m}$  and 300  $\mu\text{m}$ , respectively.

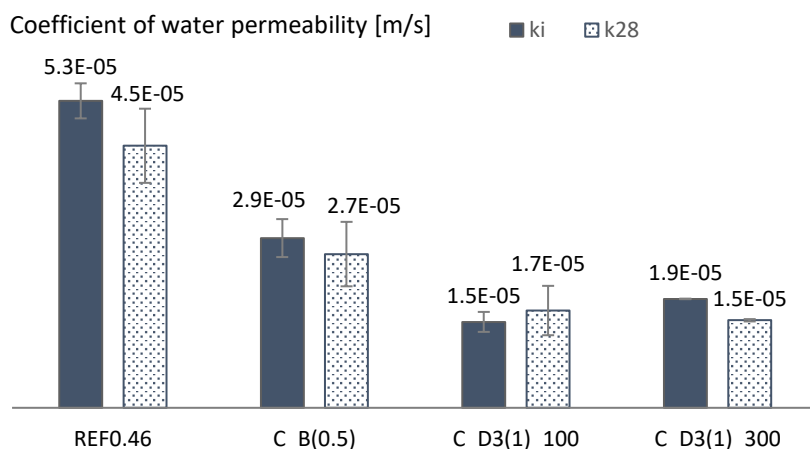


Figure 5.21 – Average coefficient of water permeability and standard error for the tested concrete mixtures before (ki) and after healing cycles (k28).

Comparing the properties of the SAPs and the concrete compositions, the dosage of SAPD3 was double the dosage of SAPB which means more particles of SAPD3 are present in the concrete mixture and the probability of more SAPs being distributed along the crack is higher for the concrete made with SAPD3.

The coefficient of variation for the different series was up to 22% before healing and as high as 44% after the healing regime. This variation can be directly related to the geometry of the cracks. The cracking method adopted does not provide a uniform crack width over the length of the

crack since it simulates a realistic crack. In addition to that, the measurements of the crack width were performed at the crack mouth, on both sides of the specimens, but they might not reflect the internal geometry and tortuosity of the crack. According to Van Mullem et al. [60], the internal geometry of the crack (which cannot be controlled, regardless of the chosen cracking technique) can cause a difference of more than 25% in the permeability of specimens with an identical nominal surface crack width.

No significant healing was noted for any of the series, which can be explained on the one hand by the relatively high water-to-cement ratio of the concrete mixtures and on the other hand by the type of cement used (CEM III-B 42.5N – LH/SR). The high amount of water used in the mixing process and the reduced amount of clinker present in the cement are not ideal for healing purposes given the reduced amount of anhydrate binder particles available for further hydration, which is one of the main mechanisms of healing.

With regards to the compressive strength, all SAP-containing mixtures presented a reduction in comparison to the reference mixture without SAPs (Figure 5.22), as already discussed in 5.4. The reduction varied in the range of 16% (C\_B(0.5)) to 22% (C\_D3(1)\_300).

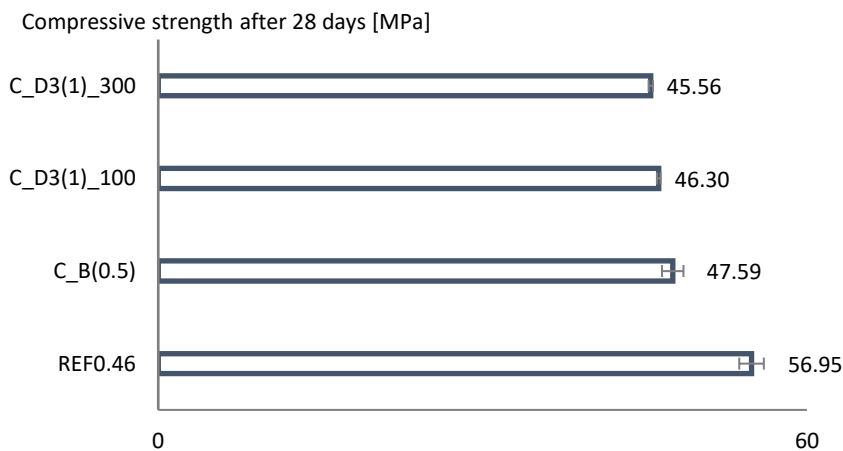


Figure 5.22 - Compressive strength of the studied concrete mixtures at 28 days.

Considering that the dosage of SAPD3 was twice the one used for SAPB, the fact that it causes the same reduction in strength but with the considerable reduction in water permeability of cracked specimens is very promising, also when compared to results reported in literature. In [61], Lee et al. tested two different SAPs (all based on acrylic acid chemistry) with mean particle size in the range of 200 to 300  $\mu\text{m}$  and absorption capacity around 20 g/g in cement filtrate solution and around 200 g/g in demineralized water (similar to SAPB). The authors reported that a reduction of 95% to 98% in the total water flow of cracked concrete specimens with average crack width of 300  $\mu\text{m}$  was obtained, respectively, for dosages of SAPs of 8% and 13% over the mass of cement. This reduced flow was observed around 13 h after the start of the test, where the specimens had not been submitted to any healing regime. However, given the considerably higher amount of SAPs, a reduction of 87% was found for the compressive strength of the SAP specimens with 13% of SAPs, in comparison to the reference without SAPs. Hong and Choi [62] tested the immediate sealing promoted by SAPs and its effect on the water permeability of cracked specimens with a crack width in the range of 250 to 350  $\mu\text{m}$ . The authors reported a reduction in the range of 34-52% and 52-72% in the water flow for a dosage of SAPs of 0.5% and 1%, respectively, over the binder weight. The authors used a polyacrylate-co-acrylamide spherical SAP. A reduction of 21% and 44% was found for the compressive strength at 28 days for the dosages of 0.5 m% and 1 m%, respectively, in comparison to the reference without SAPs.

## 5.7 Conclusions

In this chapter, the effects of SAPs on different properties of concrete mixtures were discussed.

The absorption capacity of SAPs in the concrete mixtures was found to be very similar to the one found for cement pastes. Even with different water-to-cement ratios, dosage and type of superplasticizer being used in concrete. Additionally, by providing the correct amount of water for the absorption of the SAPs, no significant differences were observed in the workability of the mixtures with and without SAPs. All these suggest that the preliminary study with cement pastes is a valuable tool to gain initial insights on the behavior of SAPs in concrete mixtures, especially regarding water absorption and workability. By working with cement pastes, the scale of test is smaller, as is the consumption of materials.

During the shrinkage tests, once more it was observed that only providing the correct amount of water to counteract the deformations caused by autogenous shrinkage might not be enough for a successful outcome. As it was already observed with the study of cement pastes in Chapter 3, the kinetics of water release by the SAPs played a decisive role in the mitigation of shrinkage in the concrete mixtures. For the commercial SAPs, that previously had shown a more retentive behavior with controlled water release, the provision of the theoretical amount of water was enough to ensure a complete mitigation of autogenous strain during a period of 28 days. The same amount of water was not enough when provided to the sulfonate SAPs, previously described as SAPs with an incontinent behavior. This same amount of water, when used in the mixture containing SAPD3 promoted only a partial reduction of the autogenous strain (still quite relevant, above 50% when compared to both reference mixtures without SAPs). For SAPD2.1, an amount of water more than two times higher than the amount provided for the other SAPs had to be used for a complete mitigation of shrinkage. The reason for that, was the intense water release by this SAP at a very early age. The total shrinkage of the SAP mixtures in drying conditions was found to be almost the same as for the reference mixtures without SAPs. The main reason for

that is associated with drying. Upon exposure to the air, the higher water content of the SAP mixtures promoted a more intense drying. Evidence was found that for SAPs A, B and D3, entrained water was still available in the mixture after the age of 7 days.

The manual measurement with the demountable strain gauge (DEMEC) presented itself as a valid method for the monitoring of the autogenous and total strain of the concrete specimens. Solid conclusions could be drawn in a comparative way for all mixtures. The method is very simple to apply, but demands a higher workload with manual preparation of the specimens and regular monitoring. A possible downside of the method was indicated as the start of the measurements normally takes place only after the fluid-solid transition of the mixture, which in some cases might lead to an under/overestimation of strain, especially when SAP mixtures are studied. Alternatively, the use of the advanced optical fiber sensors for monitoring of the shrinkage/expansion deformation allowed to start the measurements immediately after testing, reducing. The results obtained with the method were found to be in very good accordance with the ones obtained with the DEMEC method. Additionally, new possibilities were observed, as it was the case for identification of micro-cracks.

Besides mitigating the autogenous shrinkage by means of internal curing, the addition of SAPs promoted other benefits. When subjected to freeze-thaw cycles with de-icing salts, the mixtures containing SAPs A, B and D3 presented a considerable higher resistance to scaling when compared to the reference mixtures. This was reflected by a reduced amount of scaled material throughout the testing period, complying with thresholds widely reported in literature and used in practical applications. Still considering durability aspects, the addition of SAPs was also found to reduce to a high extent the water permeability (under low pressure) of cracked specimens. Special attention was given to SAPD3 and its double crosslinking feature, which enabled the use of a higher amount of SAPs in comparison to a commercial alternative, still promoting a better reduction of water permeability with a comparable reduction in strength.

In contrast to all these benefits obtained from the addition of SAPs in the concrete mixtures, a negative impact on the compressive strength was observed. This was the result of a complex balance amongst the formation of macro-pores after the water release by the SAPs, the kinetics of water release, particle size of the SAPs and internal curing (more specifically, its effects on mitigation of shrinkage and promotion of possible further hydration). This reduction was found to be more intense at earlier ages. Still, for all tested mixtures the mixtures with commercial SAPs performed slightly better than a reference with the same amount of water. When compared to the reference mixture with the lower water content, such impact was reduced at later ages, limited to less than 20% at the age of 28 days. From a practical perspective, the prediction of strength at different ages by using the current Eurocode 2 was found to also be valid for SAP-containing mixtures.

Considering all outcomes from this chapter and balancing the negative and positive effects of SAPs in the concrete mixtures, two SAPs were chosen for continuation of the studied and application in the large scale tests described in the next chapter. SAPB was selected to be used as internal curing agent for autogenous shrinkage mitigation and SAPD3 to promote immediate-sealing if cracks were to occur. A third mixture combining both SAP will also be investigated. This would be considered as the mixture for the ideal structure, with the combined features of internal curing and self-sealing.

## References

1. Standardisation, N.-B.f., *NBN EN 12620+A1:2008 - Aggregates for concrete*. 2008.
2. Standardisation, N.-B.f., *NBN B 11-256 : 2016 - Granulaten en bodems - Bepaling van het conventionele gehalte aan organische stoffen - Testmethode met waterstofperoxide*. 2016.
3. Standardisation, N.-B.f., *NBN EN 12350-2 : 2009 - Testing fresh concrete - Part 2: Slump test* 2009.
4. Standardisation, N.-B.f., *NBN EN 12350-7 : 2009 - Testing fresh concrete - Part 7: Air content - Pressure methods*. 2009.
5. Jensen, O.M. and P.F. Hansen, *Water-entrained cement-based materials I. Principles and theoretical background*. Cement and Concrete Research, 2001. **31**(4): p. 647-654.
6. Jensen, O.M. and P.F. Hansen, *Water-entrained cement-based materials II. Experimental observations*. Cement and Concrete Research, 2002. **32**(6): p. 973-978.
7. Wyrzykowski, M., et al., *Recommendation of RILEM TC 260-RSC: using superabsorbent polymers (SAP) to mitigate autogenous shrinkage*. Materials and Structures, 2018. **51**(5): p. 135.
8. Jensen, O.M., *Use of Superabsorbent Polymers in Construction Materials*. Microstructure Related Durability of Cementitious Composites, Vols 1 and 2, 2008. **61**: p. 757-764.
9. Snoeck, D., *Self-Healing and Microstructure of Cementitious Materials with Microfibres and Superabsorbent Polymers*, in *Faculty of Architecture and Engineering*. 2015, Ghent University: Ghent, Belgium.
10. Snoeck, D., O.M. Jensen, and N. De Belie, *The influence of superabsorbent polymers on the autogenous shrinkage properties of cement pastes with supplementary cementitious materials*. Cement and Concrete Research, 2015. **74**: p. 59-67.
11. Snoeck, D. and N. De Belie, *Effect of superabsorbent polymers, superplasticizer and additional water on the setting of cementitious materials*. International Journal of 3R's, 2015. **5**(3): p. 721-729.
12. Snoeck, D., L. Pel, and N. De Belie, *The water kinetics of superabsorbent polymers during cement hydration and internal curing visualized and studied by NMR*. Scientific Reports, 2017. **7**.
13. Tenório Filho, J.R., D. Snoeck, and N. De Belie. *The effect of superabsorbent polymers on the cracking behavior due to autogenous shrinkage of cement-based materials*. in *60th Brazilian Concrete Conference*. 2018. Foz do Iguaçu, Brazil: Brazilian Concrete Institute.
14. De Meyst, L., et al., *Parameter Study of Superabsorbent Polymers (SAPs) for Use in Durable Concrete Structures*. Materials, 2019. **12**(9).

15. Snoeck, D., L. Pel, and N. De Belie, *Superabsorbent polymers to mitigate plastic drying shrinkage in a cement paste as studied by NMR*. Cement & Concrete Composites, 2018. **93**: p. 54-62.
16. Geiker, M.R., D.P. Bentz, and O.M. Jensen, *Mitigating autogenous shrinkage by internal curing*. High-Performance Structural Lightweight Concrete, 2004. **218**: p. 143-154.
17. Craeye, B., M. Geirnaert, and G. De Schutter, *Super absorbing polymers as an internal curing agent for mitigation of early-age cracking of high-performance concrete bridge decks*. Construction and Building Materials, 2011. **25**(1): p. 1-13.
18. J. Piérard, V. Pollet, and N. Cauberg. *Mitigating autogenous shrinkage in HPC by internal curing using superabsorbent polymers*. in *International RILEM Conference on Volume Changes of Hardening Concrete: Testing and Mitigation*. 2006. Lyngby, Denmark: RILEM Publications SARL.
19. Jiang, C.H., et al., *Autogenous shrinkage of high performance concrete containing mineral admixtures under different curing temperatures*. Construction and Building Materials, 2014. **61**: p. 260-269.
20. Wu, L.M., et al., *Autogenous shrinkage of high performance concrete: A review*. Construction and Building Materials, 2017. **149**: p. 62-75.
21. Kheir, J., et al., *Chemical Shrinkage of Low Water to Cement (w/c) Ratio CEM I and CEM III Cement Pastes Incorporating Silica Fume and Filler*. Materials, 2021. **14**(5): p. 1164.
22. Lu, T., Z. Li, and H. Huang, *Effect of Supplementary Materials on the Autogenous Shrinkage of Cement Paste*. Materials, 2020. **13**(15): p. 3367.
23. Assmann, A. and H.W. Reinhardt, *Tensile creep and shrinkage of SAP modified concrete*. Cement and Concrete Research, 2014. **58**: p. 179-185.
24. Rozière, E., et al., *Influence of paste volume on shrinkage cracking and fracture properties of self-compacting concrete*. Cement and Concrete Composites, 2007. **29**(8): p. 626-636.
25. Bissonnette, B.t., P. Pierre, and M. Pigeon, *Influence of key parameters on drying shrinkage of cementitious materials*. Cement and Concrete Research, 1999. **29**(10): p. 1655-1662.
26. Mechtcherine, V., L. Dudziak, and S. Hempel. *Mitigating early age shrinkage of Ultra-High-Performance Concrete by using Super Absorbent Polymers (SAP)*. in *Creep, Shrinkage and Durability Mechanics of Concrete and Concrete Structures*. 2009. Ise-Shima, Japan: Taylor & Francis.
27. Dudziak, L.M., V, *Deliberations on Kinetics of Internal Curing Water Migration and Consumption Based on Experimental Studies on SAP-Enriched UHPC*, in *International RILEM Conference on Use of*



- Superabsorbent Polymers and Other New Additives in Concrete*. 2010, RILEM: Lyngby, Denmark.
28. International, A., *ASTM C157 / C157M-17, Standard Test Method for Length Change of Hardened Hydraulic-Cement Mortar and Concrete*. 2017: West Conshohocken.
  29. Sven Mönnig and H.-W. Reinhardt. *Results of a comparative study of the shrinkage behaviour of concrete and mortar mixtures with different internal water sources*. in *International RILEM Conference on Volume Changes of Hardening Concrete: Testing and Mitigation*. 2006. Lyngby, Denmark: RILEM Publications SARL.
  30. Barcelo, L., M. Moranville, and B. Clavaud, *Autogenous shrinkage of concrete: a balance between autogenous swelling and self-desiccation*. Cement and Concrete Research, 2005. **35**(1): p. 177-183.
  31. Vulliet, L., et al., *Development and laboratory tests of deformation fiber optic sensors for civil engineering applications*. Optical Inspection and Micromasurements, 1996. **2782**: p. 97-108.
  32. Kawano, Y., T. Mikami, and K. Ikushima, *A Suggestion of Health Monitoring for the Road Bridge Floor with Fiber Optic Sensor*. Structural Health Monitoring 2015: System Reliability for Verification and Implementation, Vols. 1 and 2, 2015: p. 240-246.
  33. Kawano, Y., T. Mikami, and F. Katsuki, *Health Monitoring of a Railway Bridge by Fiber Optic Sensor (SOFO)*. Structural Health Monitoring 2010, 2010: p. 1319-1324.
  34. Zonta, D., et al., *Design and laboratory validation of a structural element instrumented with multiplexed interferometric fiber optic sensors*. Sensors and Smart Structures Technologies for Civil, Mechanical, and Aerospace Systems 2008, Pts 1 and 2, 2008. **6932**.
  35. Inaudi, D., A. Elamari, and S. Vurpillot, *Low Coherence Interferometry for the Monitoring of Civil Engineering Structures*. Second European Conference on Smart Structures and Materials, 1994. **2361**: p. 216-219.
  36. Inaudi, D., S. Vurpillot, and N. Casanova, *Bridge monitoring by interferometric deformation sensors*. Fiber Optic Sensors V, 1996. **2895**: p. 34-45.
  37. Inaudi, D., et al., *Development and field test of deformation sensors for concrete embedding*. Industrial and Commercial Applications of Smart Structures Technologies - Smart Structures and Materials 1996, 1996. **2721**: p. 138-148.
  38. Inaudi, D., S. Vurpillot, and E. Udd, *Long-gage structural monitoring for civil structures*. Fourth Pacific Northwest Fiber Optic Sensor Workshop, 1998. **3489**: p. 93-100.

39. Kronenberg, P., et al., *Dam monitoring with fiber optics deformation sensors*. Smart Systems for Bridges, Structures, and Highways - Smart Structures and Materials 1997, 1997. **3043**: p. 2-11.
40. Hasholt, M.T., et al., *Can superabsorbent polymers mitigate autogenous shrinkage of internally cured concrete without compromising the strength?* Construction and Building Materials, 2012. **31**: p. 226-230.
41. Lam H. and R.D. Hooton. *Effects of internal curing methods on restrained shrinkage and permeability*. in *4th int. sem. on self-desiccation and its importance in concrete technology*. 2005. Lund, Sweden.
42. Dudziak L, M.V. *Mitigation of volume changes of ultra-high performance concrete (UHPC) by using super absorbent polymers*. in *Ultra High Perform Concr Second Int Symp Ultra High Perform Concr*. 2008.
43. Lura P, Jensen O, and I. S, *Chapter 6: Experimental methods to study internal water curing*, in *RILEM Report 41 Internal Curing of Concrete*, Kovler K and J. OM, Editors. 2007, RILEM Publications SARL. p. 57-69.
44. STANDARDIZATION, E.C.F., *Eurocode 2: Design of concrete structures - Part 1-1: General rules and rules for buildings*, in *SECTION 3 MATERIALS* 2004.
45. Wang, Z., et al., *Relative humidity and deterioration of concrete under freeze-thaw load*. Construction and Building Materials, 2014. **62**: p. 18-27.
46. Tang, S.W., et al., *Recent durability studies on concrete structure*. Cement and Concrete Research, 2015. **78**: p. 143-154.
47. Craeye, B., G. Cockaerts, and P. Kara De Maeijer, *Improving Freeze-Thaw Resistance of Concrete Road Infrastructure by Means of Superabsorbent Polymers*. Infrastructures, 2018. **3**(1): p. 4.
48. P. Kumar Mehta, P.D. and P.D. Paulo J. M. Monteiro, *Durability*. 2014, McGraw-Hill Education: New York.
49. Powers, T.C. and T.F. Willis. *The air requirement of frost-resistant concrete*. in *Twenty-Ninth Annual Meeting of the Highway Research Board* 1949. Washington, D.C, USA: Highway Research Board.
50. Setzer, M.J., *Micro-Ice-Lens Formation in Porous Solid*. Journal of Colloid and Interface Science, 2001. **243**(1): p. 193-201.
51. Scherer, G.W., *Crystallization in pores*. Cement and Concrete Research, 1999. **29**(8): p. 1347-1358.
52. Laustsen, S., M.T. Hasholt, and O.M. Jensen, *Void structure of concrete with superabsorbent polymers and its relation to frost resistance of concrete*. Materials and Structures, 2015. **48**(1-2): p. 357-368.
53. Monnig, S. and P. Lura, *Superabsorbent polymers - An additive to increase the freeze-thaw resistance of high strength concrete*. Advances in Construction Materials 2007, 2007: p. 351-358.

54. Mechtcherine, V., et al., *Effect of superabsorbent polymers (SAP) on the freeze-thaw resistance of concrete: results of a RILEM interlaboratory study*. Materials and Structures, 2017. **50**(1).
55. Standardisation, N.-B.f., *CEN/TS 12390-9 : 2016 - Testing hardened concrete - Part 9: Freeze-thaw resistance with de-icing salts - Scaling*. 2016.
56. Kusayama S, Kuwabara H, and I. S-I. *Comparison of salt scaling resistance of concretes with different types of superabsorbent polymers*. in *Application of Superabsorbent Polymers and Other New Admixtures in Concrete Construction*. 2014. RILEM Publications S.A.R.L.
57. Romero H.L, et al. *Study of the damage evolution of concrete under freeze-thaw cycles using traditional and non-traditional techniques*. in *XIII international conference on cement chemistry*. 2011. Madrid.
58. Standardisation, N.-B.f., *NBN EN 1339 - Concrete paving flags - Requirements and test methods*. 2003.
59. Aldea, C.M., S.P. Shah, and A. Karr, *Effect of cracking on water and chloride permeability of concrete*. Journal of Materials in Civil Engineering, 1999. **11**(3): p. 181-187.
60. Van Mullem, T., et al., *Novel active crack width control technique to reduce the variation on water permeability results for self-healing concrete*. Construction and Building Materials, 2019. **203**: p. 541-551.
61. Lee, H.X.D., H.S. Wong, and N.R. Buenfeld, *Self-sealing of cracks in concrete using superabsorbent polymers*. Cement and Concrete Research, 2016. **79**: p. 194-208.
62. Hong, G. and S. Choi, *Rapid self-sealing of cracks in cementitious materials incorporating superabsorbent polymers*. Construction and Building Materials, 2017. **143**: p. 366-375.

Chapter 6. The use of SAPs for the construction of crack-free large-scale structures under realistic conditions

This chapter was redrafted after:

Tenório Filho, José Roberto; Snoeck, Didie; De Belie, Nele. Mixing protocols for plant-scale production of concrete with superabsorbent polymers. *Structural Concrete*. 2020; 21: 983– 991. <https://doi.org/10.1002/suco.201900443>

Tenório Filho, José Roberto; Mannekens, Els; Van Tittelboom, Kim; Van Vlierberghe, Sandra; De Belie, Nele; Snoeck, Didier. Innovative SuperAbsorbent Polymers (SAPs) to construct crack-free reinforced concrete walls: an in-field large-scale testing campaign. *Journal of Building Engineering*. 2021. <https://doi.org/10.1016/j.jobbe.2021.102639>

## 6.1 Introduction

Although SAPs have been widely recognized as a potential new admixture for concrete structures, their use has been so far restricted to small-scale research, with only a few large-scale applications being reported in literature. Van Tittelboom et al. [1] used SAPs to improve the autogenous crack healing of real-scale concrete beams (150 mm × 250 mm × 3000 mm). In [2], Dudziak describes the use of SAPs to construct a pavilion designed as a thin-walled structure with no conventional reinforcements and with very slim columns built in 2006 for the FIFA World Cup. De Meyst et al. [3] used SAPs to reduce the autogenous shrinkage strain in small ultra-high performance concrete walls under laboratory conditions. In China, SAPs have been used in real life applications: Zhu et al. [4] reported that SAPs have been successfully used as internal curing agent in a railway slab; in [5], Liu et al. describe the use of SAPs in the construction of the China Zun tower, where a reduction of 46% in shrinkage was achieved. Also in China, Shi et al. [6] reported on the successful use of SAPs to suppress the so called “rubber particle up-floating phenomenon” during the construction of a bridge deck (80 m long) with crumb rubber concrete.

In this chapter, SAP\_B and SAP\_D3.1, previously described in Chapter 2 and optimized for application as internal curing agent and self-sealing, are used for the construction of large-scale reinforced concrete walls with the goal of building real life structures that would possess the features of shrinkage reduction by means of internal curing and immediate sealing of cracks that would happen to occur. Five walls, corresponding to 154 m<sup>3</sup> of concrete, were built and monitored in real time. A total of 230 kg of “in-house” developed SAPs were produced specifically for the study. An extensive laboratory testing campaign was also carried out to fully characterize the concrete mixtures and provide scientific input for the interpretation of results obtained with the monitoring of the walls. This chapter will be divided in two parts. The first is dedicated to a preliminary study investigating mixing protocols for plant-scale production of concrete with superabsorbent polymers. The second will describe the construction and monitoring of the large-scale demonstrator, under realistic conditions.

## 6.2 Mixing SAPs in concrete: from laboratory scale to the concrete plant

In all of the studies cited in Chapter 2, the production of the cementitious mixtures containing SAPs was restricted to laboratory conditions and the SAP particles were inserted in the mixture together with the dry materials at the beginning of the mixing procedure. For taking such new concrete compositions from the laboratory to the practical applications of industry, i.e. large-scale production in the concrete plant, a few aspects should be taken into account to make sure that the properties and performance achieved under laboratory conditions can be reproduced on site. The swelling time of the SAPs and the mixing time should be in accordance, so that the water absorption has occurred the most prior of transportation and casting, the power of the mixers and the moment of adding the SAPs to the concrete mixtures must ensure a sufficient and homogeneous distribution of the SAP particles in the system.

To tackle that, a preliminary study was developed to compare the performance of concrete specimens produced under laboratory conditions and mixing protocols, and specimens produced after large-volume mixing of concrete in a concrete plant. During the mixing at the concrete plant, two possibilities were investigated for the addition of SAPs in the mixture: 1) SAPs pre-mixed with the dry materials and 2) SAPs added directly at the concrete truck after the initial mixing.

The experimental program was based on the determination of workability by means of a slump test; shrinkage measurement of concrete specimens by use of a demountable mechanical strain gauges (DEMEC); the evolution of compressive strength at 7, 28 and 56 days (using cubic specimens with 150 mm dimensions); and the distribution of air voids by means of an air void analyzer (as described in Chapter 3).

### 6.2.1 Concrete mixtures produced in the laboratory

Two concrete mixtures were initially produced in the laboratory. One reference mixture and a SAP-containing mixture. Both concrete mixtures were produced with cement type CEM III-B 42.5N – LH/SR; a polycarboxylate superplasticizer (25% conc., at a constant dosage of 1.8

m% in relation to the cement mass); sea sand 0/4 (absorption of 0.4% in mass); sea sand 0/3 (absorption of 0.3% in mass); limestone 2/20 (absorption of 0.5% in mass) and a commercial superabsorbent polymer (at a dosage of 0.25% over the mass of cement). SAP\_B, as described in Chapter 2 was used. More details about the components of the concrete are given in Chapter 5. REF0.46, as described in Chapter 5 was used. For the SAP mixture, a dosage of 0.25 m% of SAPB was used. Since the intent of this preliminary study was to study the mixing protocols for the addition of SAPs in large-scale production of concrete, the amount of SAPs used was lower than the one determined in Chapter 5 when the aim was to achieve complete mitigation of autogenous shrinkage. More information on the composition of the mixtures first studied in the laboratory are shown in Table 6.1 and Table 6.2. The amount of additional water used in the mixture was based on the absorption capacity of SAP\_B, as determined in Chapter 5. The indication (L) used in the name of the mixtures means that they were produced in the laboratory.

All mixtures were produced in a mixer with a vertical axis, in batches of 50 L. In the mixing procedure, the dry materials were first mixed for 1 min (including SAPs, when present), then the mixing water and superplasticizer were added and mixed for additional 2 min. When SAPs were present, the additional entrained water was added at the third minute and the mixing proceeded for additional 2 min. The total mixing time was 3 min for the reference mixture and 5 min for the SAP-containing mixture.



Table 6.1 - Composition of the studied concrete mixtures produced in the laboratory, values in kg/m<sup>3</sup>.

Mixture	Cement	Sand 0/3	Sand 0/4	Limestone 2/20	Superplasticizer	SAP	Additional water	w/c <sub>(total)</sub> [-]
REF0.46(L)	356	421	343	1086	6.40	0	0	0.46
C_B(0.25)(L)	348	412	336	1062	6.26	0.89	18.27	0.52 <sup>1</sup>

<sup>1</sup>For the SAP mixture the effective water-to-cement ratio is 0.46.

Table 6.2 - Properties of the concrete mixtures produced in the laboratory.

Mixture	Compressive Strength [MPa] at 28 days (n=3)	Air content in the fresh state (%)	Slump [mm]
REF0.46(L)	56.95 ± 0.64	2.1	154
C_B(0.25)(L)	50.44 ± 1.52	1.9	155

### 6.2.2 Mixtures compositions produced in the concrete plant

The reference and the mixture containing SAPs presented in Table 6.1 were reproduced in the concrete plant. Two mixtures were produced with SAPs, one with the SAPs added after the mixing of the other materials (including water) and the other with the SAPs added together with the dry materials. First, small batches of 30 L were mixed in a regular site mixer (planetary mixer with horizontal axis) and adjustments were made in the water content to achieve the specified slump. The same mixing procedure used under laboratory conditions was used for this smaller batch at the concrete plant. After that, the three concrete mixtures (the reference and the two SAP-containing mixtures) were produced in batches of 2 m<sup>3</sup>, mixed with the concrete-plant mixer and transported in a concrete truck. From these batches, specimens were cast for testing in the hardened state. The mixing procedures were the following:

For SAPs added at the end of the mixing procedure:

- All materials are mixed for 25 s in the plant-mixer;
- SAPs and additional water are added in the concrete truck and everything is mixed continuously during transportation for a maximum of 10 min.

For SAPs added at the beginning of the mixing procedure:

- The SAPs inside water-soluble bags (1 or 2 kg of SAPs per bag) are included on the transporting belt (Figure 6.1) with the other dry material and everything is mixed for 120 s in the plant-mixer;
- Water (mixing water and additional water for the SAPs) and superplasticizer are added in the plant-mixer and everything is mixed for 25 s.



Figure 6.1 - View from the materials belt. SAPs in a water-soluble bag are shown on the right.

Given the nature of the SAPs (a powder in the dry state) and the design of the materials belt, a few possible problems were highlighted with the method, i.e. the material being carried away by the wind or being subjected to an early saturation in case of rain during the transportation of the materials on high ambient relative humidity. To tackle that, the SAPs were inserted into water-soluble bags, commonly used for the transportation of pigment powders. During the mixing of the dry materials the water-soluble bags will be destroyed, releasing the SAPs amongst the dry materials and allowing them to be properly dispersed before they are exposed to water and swelling takes place. The remaining pieces of the water-soluble bags are then dissolved upon contact with water. Complete dissolution occurs within 2 min of contact with water (Figure 6.2).

When mixing the reference mixture in the small mixer (volume of 30 L), a total water-to-cement ratio of 0.52 was needed to achieve the required slump, instead of 0.46. The SAP-containing mixtures were then produced with the new water-to-cement ratio of 0.52 and the additional water required for the SAPs absorption was added on top of that (additional water-to-cement ratio of 0.05). The resulting total water-to-cement ratio for the SAP-containing mixtures was 0.57. The resulting mixtures

presented an air content in the fresh state of 1.5% and 2.3% (for the SAPs added on the materials belt and in the truck, respectively). The composition of the adjusted mixtures produced at the concrete plant are shown in Table 6.3. The designation (P) is used to indicate production at the plant.

Table 6.3 - Composition of the adjusted mixtures produced at the concrete plant. Values in kg/m<sup>3</sup>.

Mixture	Cement	Sand 0/3	Sand 0/4	Limestone 2/20	SAP	w/C <sub>(total)</sub> [-]
REF0.52(P)	348	412	336	1062	0	0.52
C_B(0.25)(P)	342	405	330	1044	0.86	0.57

This adjustment in the water content of the laboratory compared to the plant-scale reference mixtures might be related to the conditions of use of the aggregates. In the laboratory, the aggregates were used after drying, exposed to the air for at least 24 h. At the plant site, the aggregates are stored outside, thus being considered to be already saturated and are directly used as such.

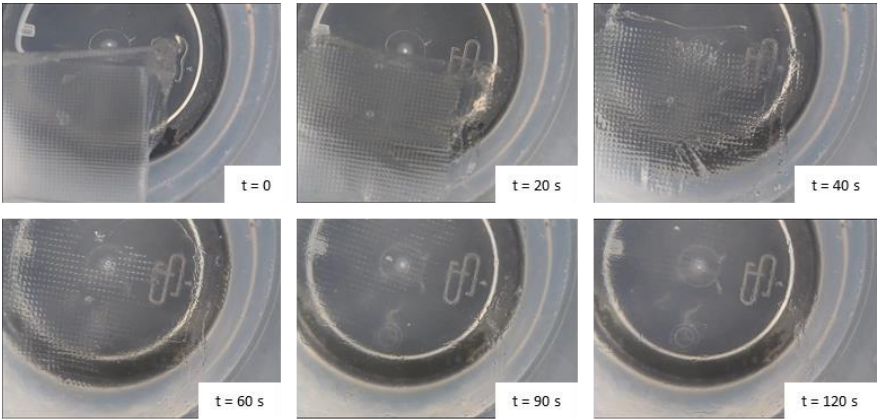


Figure 6.2 - Dissolution of a water-soluble bag in demineralized water over time.

### 6.2.3 Shrinkage measurements

For each mixture (produced at the laboratory and at the plant site), prismatic specimens (100 mm x 100 mm x 400 mm) were cast and cured for 23 h in a room with controlled atmosphere of  $20 \pm 2$  °C and RH > 95%. Right after casting, the free surface of the specimens was covered with a layer of plastic foil, attached to the mold with a thin layer of Vaseline to improve the adhesion and prevent further drying.

After the curing period, the specimens were demolded and prepared for testing. At the laboratory, the specimens were wrapped with aluminum tape to avoid moisture exchange with the environment, thus reducing the effects of drying shrinkage. All specimens were left in a room with a controlled atmosphere of  $20 \pm 2$  °C and  $60 \pm 5\%$  RH. Two measuring points were glued to the side surfaces of the specimens (except for the troweled surface due to the fact of shape irregularities that could hinder the measurements), placed 200 mm apart on the central line of the specimens' surface. The measurements were performed once per day for 28 days and started 24 h after the first contact of cement with the mixing water.

The autogenous strain curves over time for all specimens are shown in Figure 6.3. For the SAP-specimens produced at the concrete plant, the designations (SB) and (T) refer to the addition of SAPs at the beginning with the water-soluble bags and in the truck at end of the mixing procedure, respectively.

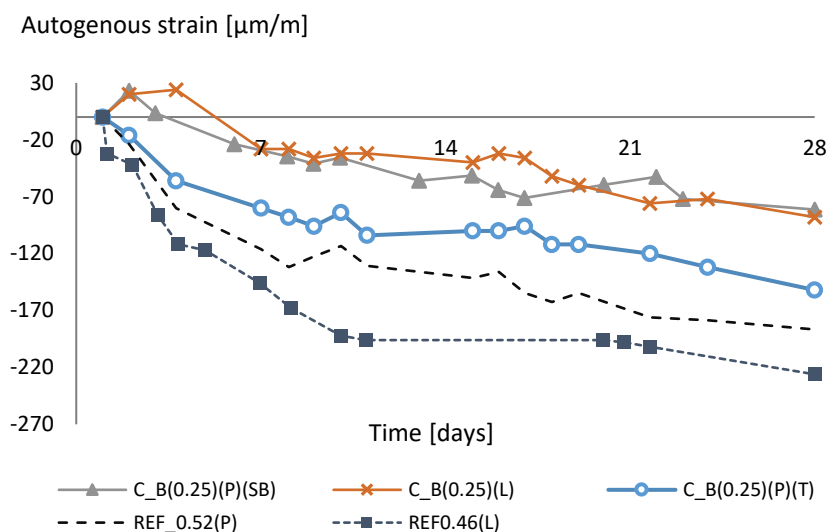


Figure 6.3 – Autogenous strain of the concrete specimens cast at the plant site and laboratory.

A reduction in the shrinkage strain is noticed for both SAP-containing mixtures in comparison to the reference specimen. For the specimen where SAPs were dry mixed at the beginning (C\_B(0.25)(P)(SB)) a shrinkage reduction of around 56% occurs. On the other hand, for the case where the SAPs were added in the truck (C\_B(0.25)(P)(T)) the reduction was only 18%. Considering that in both cases, the same amount of materials (under the same conditions) and the same equipment was used during the mixing, the lower efficiency in shrinkage reduction for C\_B(0.25)(P)(T) might be related to an agglomeration of the SAPs particles when added in an already wet mixture, which compromises a more uniform distribution of the SAPs in the concrete mass. Because of that, internal curing water is not available to cover the same volume as it is in the C\_B(0.25)(P)(SB) mixture. A numerical study developed by Wyrzykowski et al. [7] based on the experimental work performed by Trtik et al. [8] showed that water from SAP can readily be transported away from the SAP over distances as large as about 2-3 mm in the early stages of hydration. Based on that concept, it could be expected that a poor distribution of SAPs (that could be the case for example, by agglomeration

of SAP particles) could hinder the efficiency of the internal curing, even when the same amount of SAPs are used.

In terms of mixing protocols and conditions, the SAP-mixtures produced in the laboratory and in the concrete plant (with SAPs added at the beginning of the mixing) presented a very similar trend of autogenous deformation. Between the reference mixtures, the one produced in the concrete plant was found to have a lower shrinkage compared to the produced in the laboratory. That is mainly due to the slight increase in the amount of mixing water.

#### 6.2.4 Air void analysis

Specimens of 100 mm x 100 mm x 20 mm were used for the verification of the air void content and distribution in the specimens according to the standard EN-480 [9], as described in Chapter 3. The specimens were polished after cutting, and then painted with black ink, and after drying for 24 h at 35 °C a layer of barium sulfate (powder) was applied to the painted surface, filling the voids. The test was performed in triplicates.

Based on the absorption capacity of the SAPs in concrete, an estimation of the expected particle sizes of the SAPs after swelling was performed with the use of equation 6.1, where  $V$  is the volume of the swollen particle ( $\text{cm}^3$ ),  $v$  is the volume of the dry SAP particle ( $\text{cm}^3$ ),  $Abs$  is the absorption capacity of the SAP in concrete and  $d$  is the bulk density of the SAP (in this case,  $0.85 \text{ g/cm}^3$ ). The assumption was made that all SAPs have spherical shapes in both dry and saturated state. As the SAPs are made by bulk polymerization, this is not valid due to their irregular nature. However, this assumption allows comparing the formed macro porosity when using SAPs in concrete [10-12]. The result was then compared with the air void analysis.

$$V = v \times [(Abs \times d) + 1] \quad (6.1)$$

Figure 6.4, Figure 6.5 Figure 6.6 show the air void distribution for the concrete mixtures C\_B(0.25)(L), C\_B(0.25)(P)(SB) and C\_B(0.25)(P)(T), respectively.

A difference of 40% is noticed in the total air content in the hardened state of the mixtures when comparing the mixtures where the SAPs were dry mixed (in the laboratory and at the plant site) with the mixture where the SAPs were added after mixing in the plant while the concrete was transported in the truck. Even though the mixtures C\_B(0.25)(L) and C\_B(0.25)(P)(SB) presented a very similar total air content (3.37% and 3.45%, respectively), the air void distribution presents a small difference. For the mixture C\_B(0.25)(L), the peak in the air void content occurs for a void diameter in the range of 505 to 1000  $\mu\text{m}$ . For the mixture C\_B(0.25)(P)(SB) the highest peak occurs in the range of 1005 to 2000  $\mu\text{m}$  and a second peak in the range of 505 to 1000  $\mu\text{m}$ . In contrast, for the mixture C\_B(0.25)(P)(T), the second peak in the range of 505 to 1000  $\mu\text{m}$  is still present but there is also an almost uniform distribution between 1005 and 3000  $\mu\text{m}$  with the highest peak reaching 4000  $\mu\text{m}$  (the maximum range captured by the equipment). Microscopic analysis even showed the formation of bigger pores, due to the agglomeration effect when adding dry SAPs to the fresh mixture in the truck.

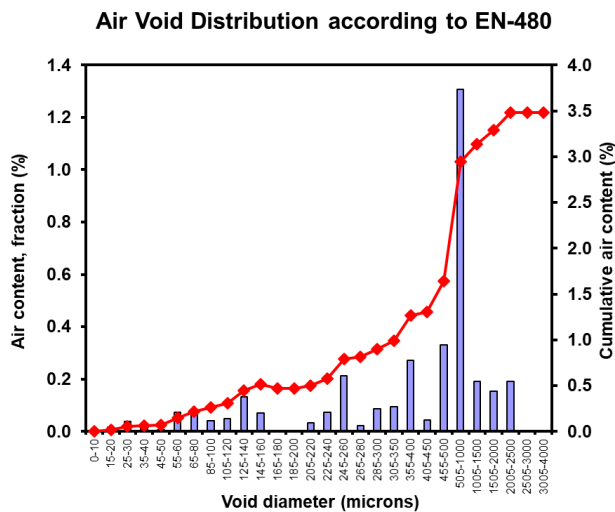


Figure 6.4 - Air void distribution in the concrete with dry mixed SAPs in the laboratory (C\_B(0.25)(L)).



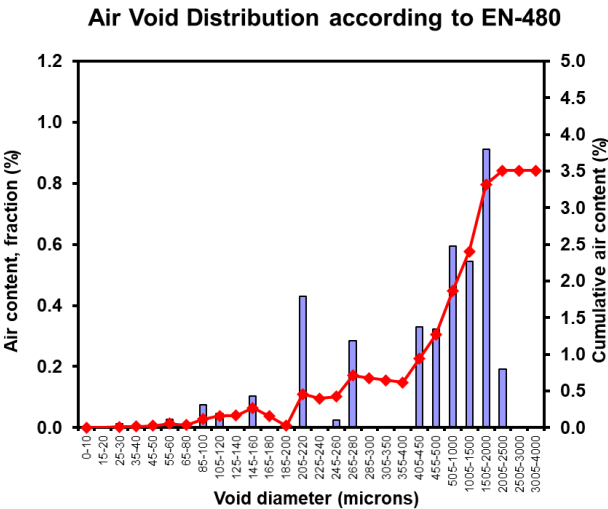


Figure 6.5 - Air void distribution in the concrete produced in the plant with SAPs added at the beginning of the mixing (C\_B(0.25)(P)(SB)).

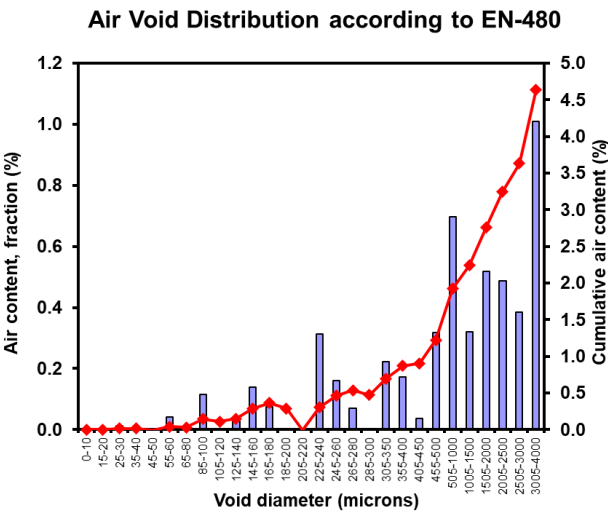


Figure 6.6 - Air void distribution in the concrete produced in the plant with SAPs added at the end of the mixing (C\_B(0.25)(P)(T)).

By applying Equation 6.1, the range of 505 to 1000  $\mu\text{m}$  is compatible with the expected size of swollen SAP particles with a size in dry conditions being in the range of 180 to 350  $\mu\text{m}$ . For the range of 1005 to 2000  $\mu\text{m}$ , the expected dry sizes are in the range of 370 to 710  $\mu\text{m}$ . Considering that the value of  $d_{90}$  is 460  $\mu\text{m}$  and that the biggest single particle size for this SAP would be smaller than 500  $\mu\text{m}$  that could be an indication of a limited agglomeration happening in the mixture C\_B(0.25)(P)(SB).

Figure 6.7, Figure 6.8 and Figure 6.9 show the voids and respective sizes as measured on the specimens used for the air void analysis for the mixtures C\_B(0.25)(L), C\_B(0.25)(P)(SB) and C\_B(0.25)(P)(T).

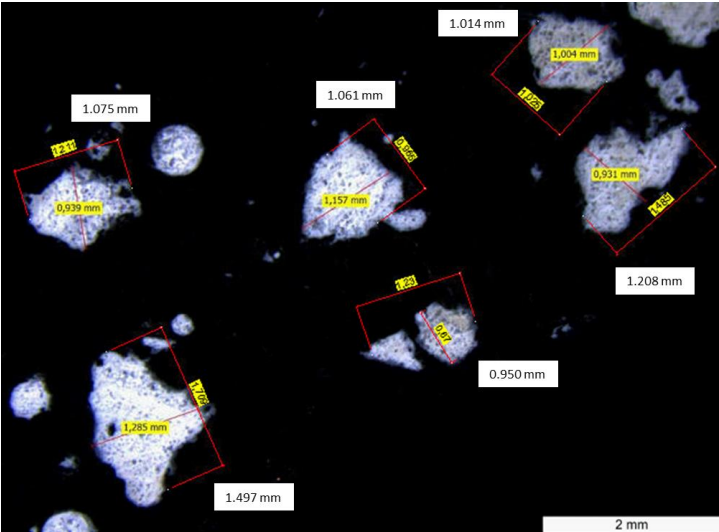


Figure 6.7 - Voids left after the water release of SAP particles in the mixture C\_B(0.25)(L). The size of the voids is presented as the average between two measurements in different directions.

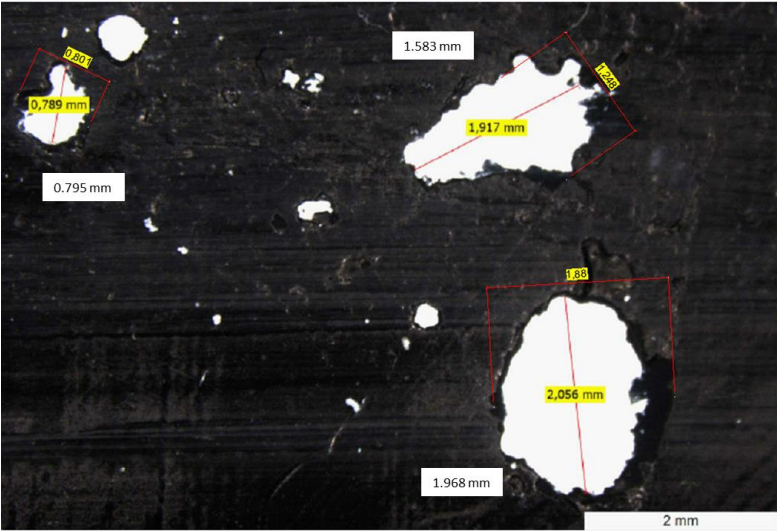


Figure 6.8 - Voids left after the water release of SAP particles in the mixture C\_B(0.25)(P)(SB). The size of the voids is presented as the average between two measurements in different directions.

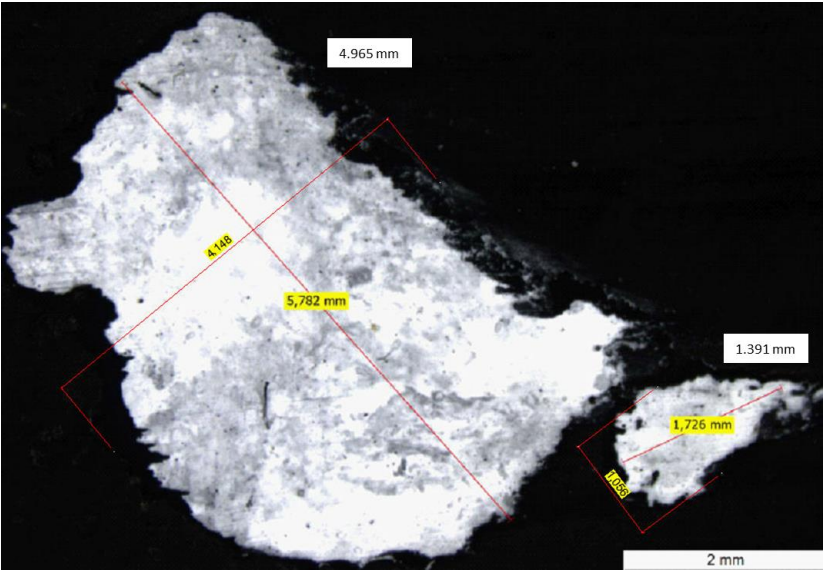


Figure 6.9 - Voids left after the water release of SAP particles in the mixture C\_B(0.25)(P)(T). The size of the voids is presented as the average between two measurements in different directions.

The dimensions measured are in accordance with the values calculated with Equation 6.1 and the predictions made based on the air void distribution presented in Figure 6.4, Figure 6.5 and Figure 6.6. These values confirm that no agglomeration happened for the mixture C\_B(0.25)(L) and some might have occurred for the mixture C\_B(0.25)(P)(SB), but to a minor extent. The dimensions shown in Figure 6.9 correspond to dry particle sizes in the range of 615  $\mu\text{m}$  to 2 mm even which are out of the particle size distribution of the SAP used. For that case, it is clear that there is an agglomeration of particles for the addition of the SAPs only in the truck.

#### 6.2.5 Compressive strength

The compressive strength test was performed on cubes with 150 mm dimensions (the results are shown in Figure 6.10). The test was performed at 28 days in triplicates and the specimens were cured in a room with controlled atmosphere (of  $20 \pm 2$  °C and RH > 95%) until the day of testing. The specimens produced under laboratory conditions and the ones produced at the concrete plant performed in a very similar way. For the second case, a reduction of 8% was found for C\_B(0.25)(P)(SB) in comparison to the reference mixture, while for C\_B(0.25)(P)(T) this reduction was around 12%. The slightly larger reduction in strength for the mixture C\_B(0.25)(P)(T) could be related to the agglomeration of SAP particles and the formation of even bigger macropores, as the one shown in Figure 6.9.

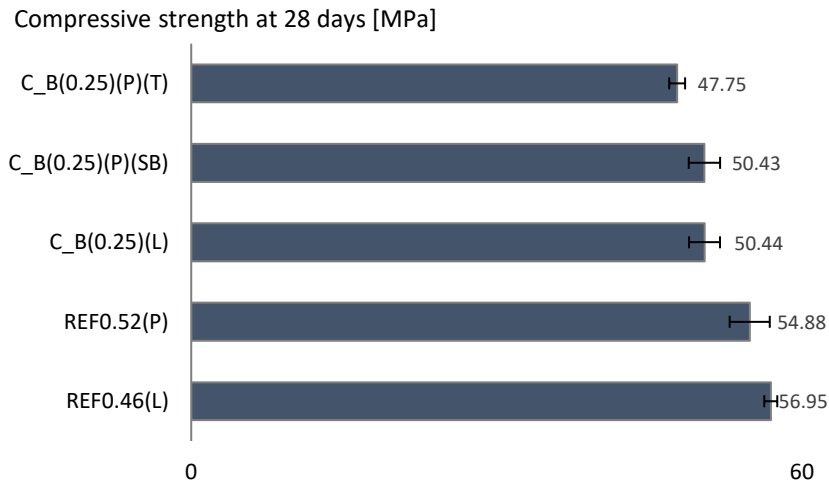


Figure 6.10 - Compressive strength days of the tested mixtures at 28 days.

### 6.2.6 Final remarks

The option of adding the SAPs directly in the truck after all the materials were already mixed might seem more practical in the daily application but it has a considerable negative impact on the reduction of autogenous shrinkage by means of internal curing. When it comes to the effects of the SAPs on the total shrinkage (considering the pronounced drying effects) or the compressive strength, no significant difference was found, but attention should be paid when extending this statement to concrete compositions with a higher dosage of SAPs, since the agglomeration effect might be more pronounced, leading to a higher change in the microstructure of the material once the SAPs are completely empty of entrapped water.

The addition of the SAPs together with the dry materials seemed more promising given the results presented and the use of water-soluble bags presented itself as an interesting alternative to avoid that SAP particles are carried out by the wind or initiate the swelling process prior to the mixing. This approach was then chosen to be used for the production of the large-scale demonstrator, as it will be described in the following sections.

As a final recommendation, not only the mixing parameters are important, but also the state of the materials, especially considering the aggregates and their water absorption. Depending on their storage condition and humidity during concrete production, it could represent an important effect on the workability of the concrete and thus hinder the interpretation of the water absorption by the SAPs done by means of slump tests.

### 6.3 Construction and monitoring of the large-scale demonstrator

In total, five walls were built with dimensions 14 m x 2.75 m x 0.80 m. Two walls were used as references (REF1 and REF2) with no SAPs added. Three walls were produced with the addition of SAPs: a wall built with SAP\_B (W\_SAP1) with the purpose of mitigating autogenous shrinkage, a wall built with SAP\_D3.1 (W\_SAP2) designed to promote sealing of cracks and to partially reduce autogenous shrinkage, and a wall with both SAP\_B and SAP\_D3.1 (W\_SAP1+2) combined representing the ideal wall with the ability to mitigate autogenous shrinkage and to promote self-sealing of cracks. The walls were demolded 48 h after casting. Upon demolding, half of each wall received a surface treatment with an external curing agent, often used as a countermeasure to mitigate shrinkage in tunnel applications partially. The walls were cast in the last week of August and first two weeks of September with average minimum and maximum temperatures between 10.9 and 19.2 °C.

The testing campaign was divided into two parts: 1) on-site monitoring of the walls and 2) characterization of the concrete in laboratory conditions. The characterization of the concrete started with the measurement of the fresh concrete properties right after mixing and the preparation of test specimens. Optical fiber sensors, as described in Chapter 5, were included to monitor the shrinkage in the two main walls (being the reference wall with water-to-cement ratio of 0.44 and the wall with the combination of SAPs). In addition, the manual monitoring on-site started 48 h after casting, right after the removal of the formwork from the walls. The casting of the wall took place between the last week of August and the second week of September. During the first month of monitoring, the maximum and minimum average temperatures were  $19 \pm 4$  °C and  $10 \pm 2$  °C, respectively. More details on each stage of the testing campaign and a description of the testing methods are given in this section. Different stages from the testing campaign, from the casting of the slabs until the monitoring of the walls, are depicted in Figure 6.11.



Figure 6.11 - Different stages of the testing campaign: from the casting of the slab until the monitoring of the walls.



### 6.3.1 Mixture composition and details of the walls

The wall REF1 was produced with a total water-to-cement ratio of 0.44. The wall REF2 was produced with a total water-to-cement ratio of 0.52. This amount of 0.52 corresponds to the total water-to-cement ratio of the wall produced with SAP1 including the free water and the entrained water in the SAPs (the amount of entrained water was determined based on the absorption capacity of the SAP, as mentioned in section 2.1). REF2 was therefore included in order to highlight the advantages of using SAPs as internal curing agents in contrast with only using additional water and no SAPs in the mixture. The amounts are based on prior research on laboratory scale as described in Chapter 5.

In terms of composition, the wall REF1 was built with a concrete having a strength class C35/45. The crack width was designed and limited to 0.3 mm with reinforcement of diameter 16 mm every 9.6 cm. The other four walls were built with a concrete having a strength class C30/37. The crack width was limited to 0.3 mm with reinforcement of diameter 16 mm every 10.7 cm (Figure 6.1). The slabs on which the walls were constructed were made with the same concrete as wall REF1. The slabs were constructed at least three months in advance to the walls.

All walls were produced with concrete having a consistency class S4. All concrete mixtures were produced with cement type CEM III-B 42.5N – LH/SR (CBR, Belgium); a polycarboxylate superplasticizer (Tixo, 25% conc., BASF, Belgium); a modified polycarboxylate superplasticizer (Sika-Viscoflow 26, Sika, Belgium); sea sand 0/4 (absorption of 0.4% in mass); and limestone 2/20 (absorption of 0.5% in mass). The concrete for the wall REF2 had a lower dosage of superplasticizers in comparison to the other concrete mixtures given the higher effective water-to-cement ratio. The mixture design of the concrete produced for each wall is given in Table 6.1.

For each wall, 32 m<sup>3</sup> of concrete was produced. This amount was split into two trucks of 11 m<sup>3</sup> and one truck of 10 m<sup>3</sup>.

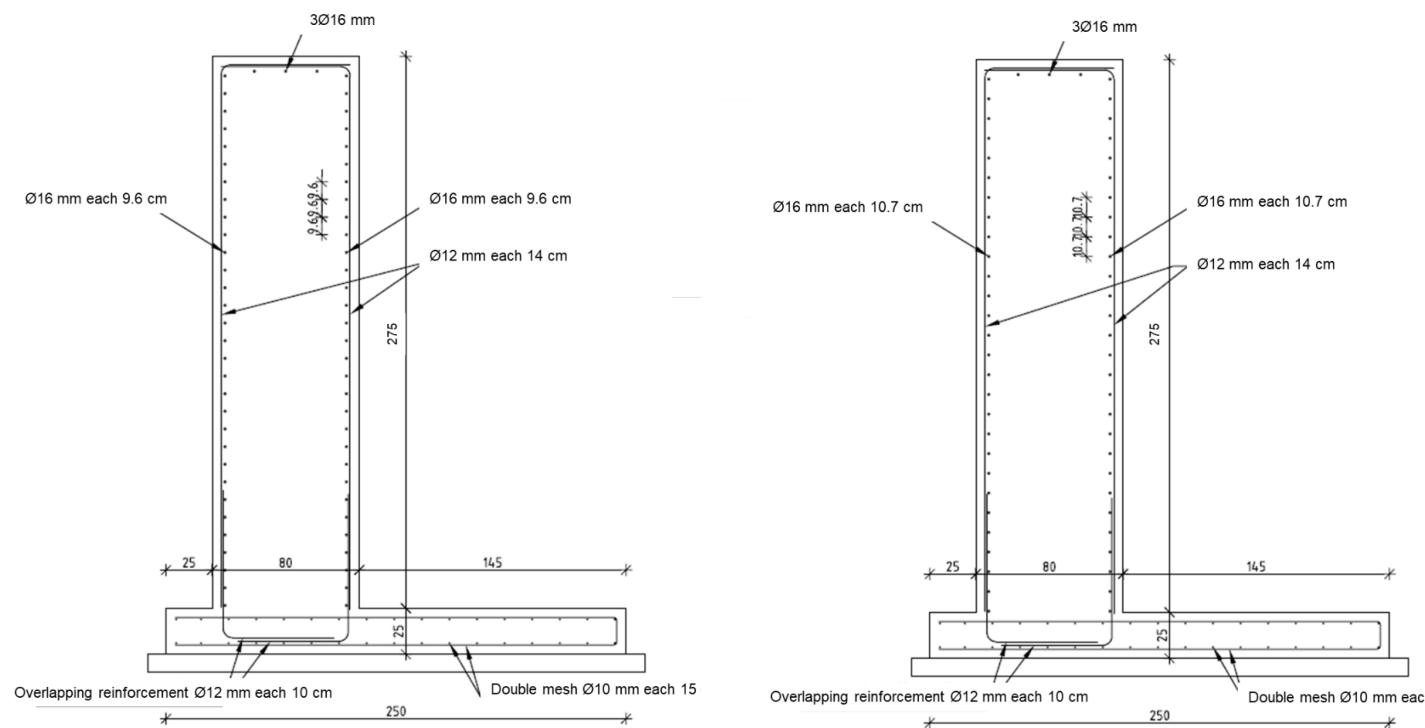


Figure 6.12 - Reinforcement details of the wall REF1 (on the left) and the other walls (on the right).

Table 6.4 - Composition of the studied concrete mixtures, values in kg/m<sup>3</sup>.

Mixture	Cement	Sea sand 0/4	Limestone 2/20	Tixo	Sika Viscoflow-26	SAP1	SAP2	w/C <sub>tot</sub>	w/C <sub>eff</sub>
REF1	360	736	1116	2.42	1.56	0	0	0.44	0.44
REF2	360	695	1054	0.95	0	0	0	0.52	0.52
W_SAP1	360	702	1078	2.42	1.56	1.37	0	0.52	0.44
W_SAP2	360	702	1078	2.42	1.56	0	3.6	0.54	0.44
W_SAP1+2	360	702	1078	2.42	1.56	1.37	3.6	0.62	0.44

The effective water-to-cement ratio (w/ceff) refers to the amount of mixing water without considering the additional entrained water in the SAPs.

The total water-to-cement ratio (w/ctot) refers to the amount of mixing water plus the additional entrained water in the SAPs.

### 6.3.2 Characterization of the concrete mixtures

For each truck of concrete produced, a series of tests were carried out to characterize and affirm the uniformity of the concrete batches. For the fresh state that meant: determining the workability by means of a slump test right after mixing and 30 min after that (in order to assess any loss in workability that could have been caused by the absorption of water by the SAPs in time) following EN 12350-2 [13]; the air content (EN 12350-7 [14]); the setting by means of a Voton probe (NEN 2734 [15]) and by means of ultrasound pulse velocity measurements with a FreshCon system [16] (the FreshCon was only used for one concrete truck from each wall and the test was performed for 24 h). In the hardened state, all batches were characterized in terms of compressive strength (at 7, 28 and 56 days) on cubic specimens with a dimension of 150 mm. The air void distribution and air content in the hardened state was studied in compliance with the standard EN 480-11 [9] using polished specimens (dimensions of 100 mm x 100 mm x 20 mm) and the automated air void analyzer RapidAir-3000 (Germann Instruments, Denmark). The free shrinkage was investigated using prismatic specimens (100 mm x 100 mm x 400 mm) and the restrained shrinkage with steel rings in accordance with the ASTM C157 [17] (the test method was applied for one concrete truck from each wall and the test was performed for 28 days). Except for the ultrasound pulse velocity and the restrained shrinkage, all other tests were performed in triplicates.

The specimens prepared for mechanical strength tests were cured in a room with controlled atmosphere of  $20 \pm 2$  °C and a RH > 95%. The setting time with the Voton probe, the setting with the FreshCon device and the restrained shrinkage with the steel rings were performed in a room with controlled atmosphere of  $20 \pm 2$  °C and  $60 \pm 5\%$  RH. The samples used for FreshCon measurements and the restrained shrinkage tests were covered with plastic foil during the complete measurement period to exclude evaporation of mixing water and to have sealed conditions.

To monitor free shrinkage, the specimens were cured in a room with controlled atmosphere of  $20 \pm 2$  °C and  $60 \pm 5\%$  RH for the first 24 h. Right after casting, the free surface of the specimens was covered with a layer

of plastic foil to prevent drying. After demolding, half of the specimens were wrapped with aluminum tape to avoid moisture exchange with the environment and simulate the conditions for autogenous shrinkage. The other half was left with the specimens exposed to the atmosphere to simulate the drying shrinkage. Two measuring points were glued to the side surfaces of the specimens (except for the troweled surface due to the shape irregularities that could hinder the measurements), placed 200 mm apart on the central line of the specimens' surface. The measurements were performed using a demountable mechanical strain gauge (DEMEC), once per day for 28 days and started 24 h after the first contact of cement with the mixing water right after demolding. The measurements were performed in a room with a controlled atmosphere of  $20 \pm 2$  °C and  $60 \pm 5\%$  RH where the specimens were kept during the complete testing period.

### 6.3.3 Monitoring of the walls

#### 6.3.3.1 *Shrinkage and cracking formation*

The shrinkage and crack formation of the walls were manually monitored right after demolding (48 h after casting) with the manual measurement of the shrinkage strain on the surface of the walls and the visual monitoring of the development of cracks. To measure the shrinkage, measuring pair-points (200 mm apart) were placed on the surfaces of the walls right after demolding, on both sides of the wall. On each surface (exposed to the environment and protected with the external curing agent), a segment with length of 5 m was created and two layers of measuring points were placed respectively at 0.50 m and at 1.80 m from the bottom of the walls. In total, 40 measuring pair-points were placed on each wall. A schematic representation of the measuring locations is shown in Figure 6.13.

Specifically for the REF1 wall and SAP1+2 combination wall, the optical fiber sensors described in Chapter 5 were also used to monitor the shrinkage. The sensors were embedded in the concrete, attached to the reinforcement (Figure 6.14), on both sides of the walls (exposed and

externally cured side) in two locations, at 0.5 m and at 1.80 m from the bottom (the same location as the measuring points shown in Figure 6.13).

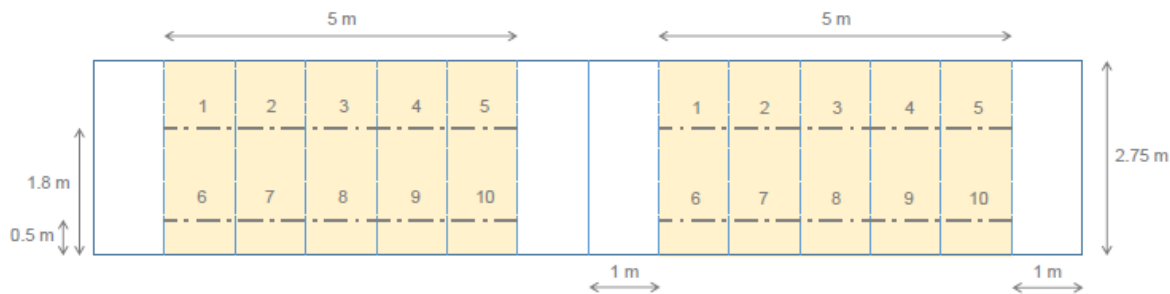


Figure 6.13 - Mapping of measuring points for the manual monitoring of shrinkage strain on the walls. The dash-dot lines represent the position where the measuring points were placed. The right side of the wall was treated with an external curing agent.

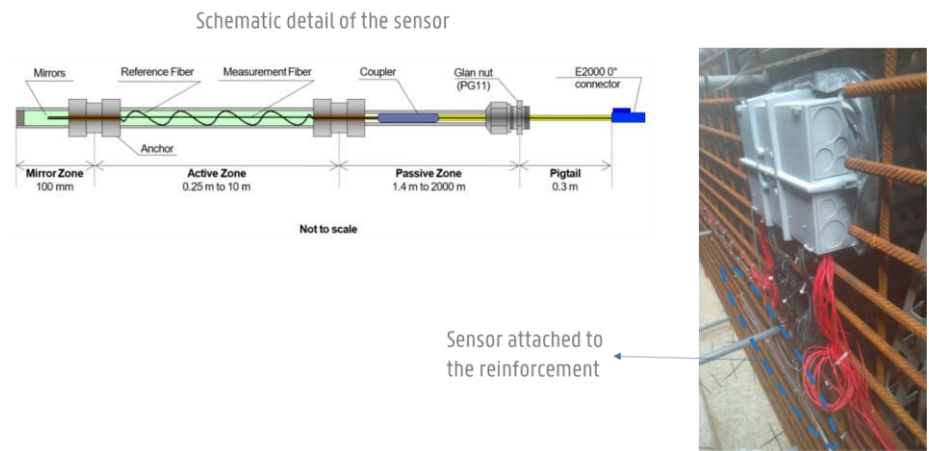


Figure 6.14 - Schematic detail of the sensor attached to the reinforcement. The drawing of the sensor is a courtesy of SMARTEC.

### 6.3.3.2 Monitoring of corrosion potential by means of multi-reference electrodes (MuRE)

For the monitoring of corrosion potential in both REF1 and W\_SAP1+2 nickel based multi-reference electrodes developed by Cescor (Italy) were used. The electrodes were embedded in the concrete, attached to the reinforcement (Figure 6.15). For the monitoring, the electrodes were connected to a measuring unit that enabled the monitoring of up to eight electrodes at a time. This unit was placed in an access box inside the wall, with an opening to the outside from where the active electrodes could be changed if needed (Figure 6.16). The measuring unit was connected to the Smartmote.NET system (Smartmote, Germany) which allowed wireless and real time monitoring, with all data stored online.

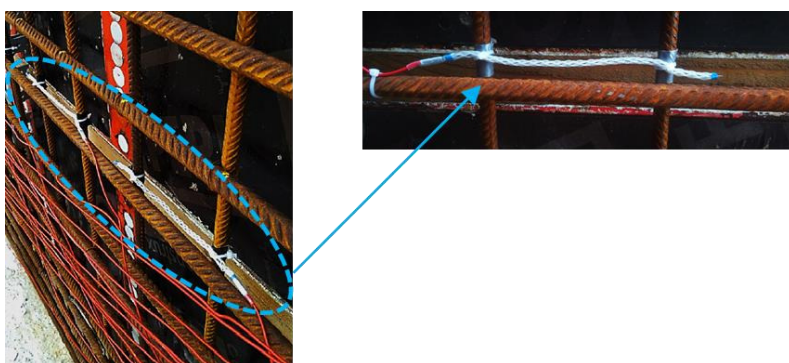


Figure 6.15 - Nickel electrodes attached to the reinforcement steel of the wall.



Figure 6.16 - Access box where the electrodes could be connected to the measuring unit.



The electrodes were numbered sequentially and their approximate location was mapped in order to facilitate the choice of electrodes to be monitored depending on the location of cracks (Figure 6.17).

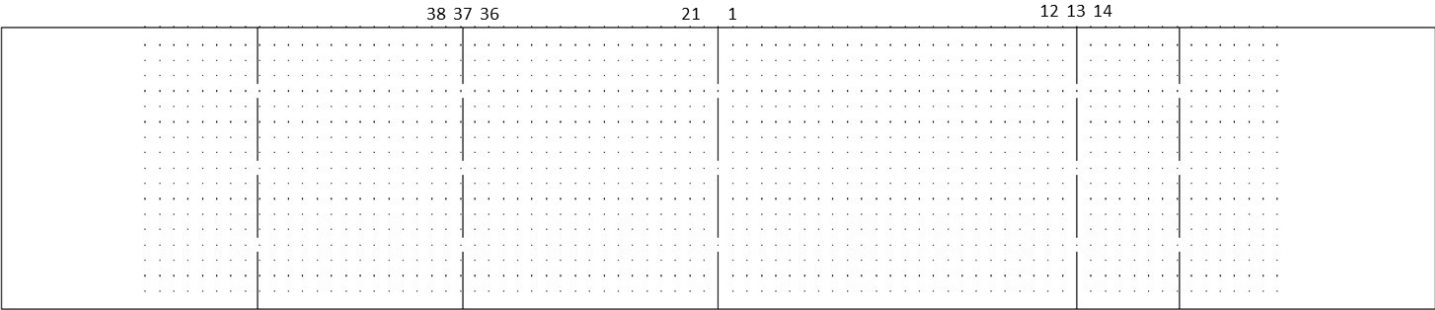


Figure 6.17 - Mapping of the location of the electrodes. The numbers at the top correspond to the location of the electrodes represented in the results section. The vertical dashed lines represent the cracks.

#### 6.3.3.3 Water permeability of cracked areas

The water permeability of wall REF1 upon the appearance of cracks was assessed by means of a water permeability test performed on site. After 75 days from the casting of the reference wall, once the crack dimensions became stable, a water container with dimensions (0.15 m x 0.30 m x 1.5 m) was installed on one side of the wall, on top of a crack (Figure 6.18).



Figure 6.18 - Water contained placed on the cracked wall REF1.

After installation, the connection between the wall and the container was checked for the existence of leaking. The water basin was then filled with tap water and no flow was recorded for a period of 3 days, until the wall could be considered saturated. The water basin was refilled and covered to avoid evaporation, and the water levels were recorded for 30 days.

#### 6.3.4 Results and discussion

##### 6.3.4.1 Properties in the fresh state

The results of the slump test, air content in the fresh state and setting time with the Voton probe are shown in Table 6.5. Values are shown per truck and the average value is presented.

In terms of workability, it can be noticed that for each mixture, there was no significant difference amongst the different concrete batches for each wall, represented by each truck. All concrete mixtures were designed to achieve a consistency class S4, meaning a slump value in the range of 160-210 mm (with a maximum of 230 mm) [13]. The addition of the SAPs did not result in any significant changes in the workability of the mixtures compared to REF1. All the additional water used can then be considered to have been properly absorbed by the SAPs during the mixing process. The slump measured 30 minutes after the first determination did not show any change, meaning that the absorption of the SAPs was stable during that time and significant release of water had not taken place.

For the air content, uniform values were seen amongst the different trucks for the five different concrete mixtures. In between the two reference mixtures, the extra water did not promote any changes for air in the fresh state. However, upon the addition of the SAPs, a significant difference has been found in all SAP mixtures compared to both reference mixtures without SAPs. When added to the cementitious materials, the SAPs will absorb a certain amount of the water and become water-filled inclusions, which should not account for an increase in the air content while the mixture is in its fresh state. With the hardening taking place and water being released by the SAPs, the previously water-filled inclusions become air-filled pores and only then, the SAPs could be related to an increase in the amount of air in the mixture. However, some cases have been reported in literature where an unexpected amount of air entrainment in the fresh state has been noticed for mixtures containing SAPs.

Table 6.5 - Overview of properties of the concrete mixtures in the fresh state.

Parameter	REF1				REF2				W_SAP1				W_SAP2				W_SAP1+2			
	T1	T2	T3	Av.	T1	T2	T3	Av.	T1	T2	T3	Av.	T1	T2	T3	Av.	T1	T2	T3	Av.
Slump [mm]	200	190	190	193	200	210	190	200	210	220	230	220	210	200	220	210	210	190	200	200
Air content [%]	1.7	1.5	1.3	1.5	1.4	1.3	1.9	1.5	2.4	2.8	3	2.7	2	2.2	2.1	2.1	2.3	2.6	2.3	2.4
Setting time: Voton [h]	4.1	4	4	4.0	3.9	4.3	4	4.1	8.4	8.1	7.8	8.1	7.8	8.1	7.9	7.9	7.8	7.9	8.1	7.9
Setting time: p-wave [h]	5.7	-	-	5.7	2.7	-	-	2.7	7.3	-	-	7.3	7	-	-	7	7	-	-	7
Setting time: s-wave [h]	6.3	-	-	6.3	5	-	-	5	8	-	-	8	9	-	-	9	9	-	-	9

T stands for truck.

Av. stands for average

Monnig and Lura [18] found that the air content measured in the fresh concrete was 1.7% for the reference mixture and 5.2% for the SAP mixture. Reinhardt et al. [19] noticed that one of the SAPs studied caused extra air in the fresh concrete. The air content in the SAP mixture was 4-5.4% whereas it was only 0.5-1% for mixtures with another type of SAP, which was at the same level as the reference mixtures without an air-entraining admixture. In [20], Assmann observed during mixing that the addition of SAPs was associated with extra air entrainment. The measured air content in fresh concrete containing SAPs was 4.5%. In the air void analysis in the hardened state, an air void content of 6.5% was reported, whereas, a value of less than 3.5% was expected based on the volume of the added SAPs.

Hasholt et al. [21] state that this effect could be directly related to the production process of the SAPs. The authors found evidence that, especially for SAPs produced by suspension polymerization, the existence of surfactant residue can have an air entraining effect. While this might be more often observed in studies where such type of SAPs have been used, the authors also point out that it is not possible to completely rule out that also bulk polymerized SAPs can carry components with air-entraining effects, such as traces of monomer or extractable pieces of polymers (i.e. sol fraction of the SAP), in particular when crushing of the solid gel has led to cleavage of crosslinks.

As for the setting time, the results from the Voton probe showed that no retarding effect took place with the addition of extra water without SAPs, when comparing the setting times from REF1 and REF2. Nevertheless, caution should be taken when comparing these two mixtures, since different types and dosage of superplasticizer have been used for both mixtures (refer to Table 6.4). When it comes to the effects of the addition of SAPs, a comparison can be made amongst the SAP-containing mixtures and REF1. The addition of SAPs and extra water resulted in a delay of around 4 h in the setting of the mixtures, regardless the type of SAPs. Considering that W\_SAP1 and W\_SAP2 were both produced with a different dosage and different types of SAPs, only having in common the total water-to-cement ratio, that effect could be related to the additional

water. A delay in the setting time for mixtures containing SAPs and extra water has also been reported by [22-25].

However, since the kinetics of water release from the SAPs might differ, further analysis is needed. In addition, the use of the Voton probe can be considered slightly subjective and a scatter is present due to user/operator variability. During a Voton probe test, the sample remained uncovered and, as the mixture with SAPs was humid for a longer period [26], the surface of REF specimens may have started to dry out more quickly compared to the surfaces of the SAP specimens. The evolution of hardening as studied by the ultrasonic pulse velocity method using P- and S-waves provided a better understanding (Figure 6.19 and Figure 6.20) and led to more solid conclusions on the bulk hardening.

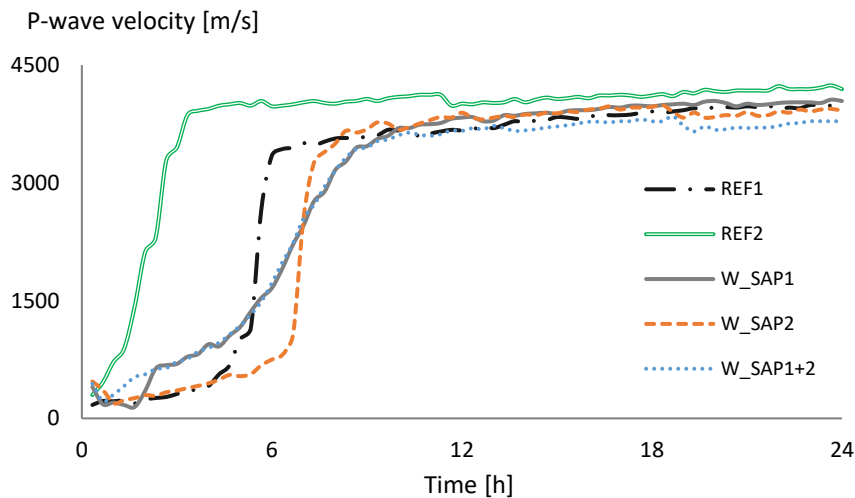


Figure 6.19 - Evolution of P-wave velocity over time.

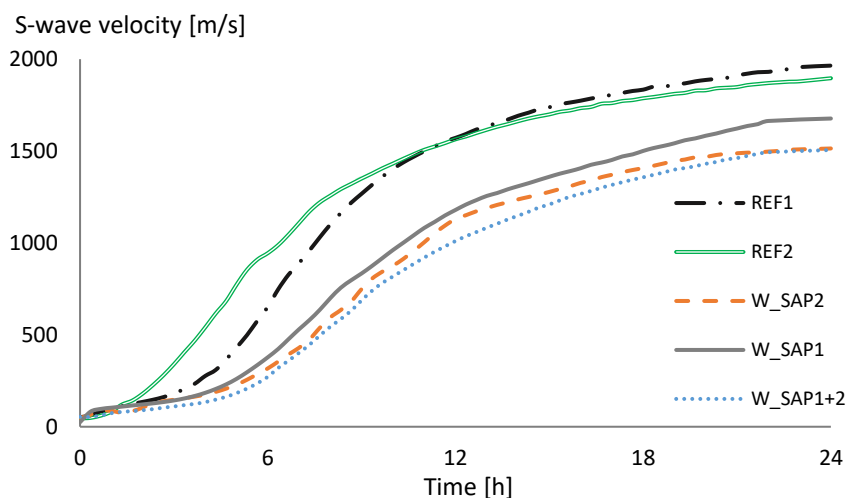


Figure 6.20 - Evolution of S-wave velocity over time

The mixture produced for the wall REF2 shows the fastest setting amongst all the studied mixtures, which can be explained by the difference in the dosage of superplasticizer. While REF2 was produced with only the superplasticizer Tixo, all other concrete mixtures were produced with a dosage of the Tixo superplasticizer 62% higher than REF2 and an additional dosage of Sikaflow superplasticizer.

In the analysis of the P-waves (Figure 6.19), when comparing the SAP-containing mixtures with REF1, two different behaviors are identified, which can be related to the two different types of SAPs used. First, for the mixture containing SAP\_D3.1, the hardening curve presents a pattern very similar to the one observed for both reference mixtures REF1 and REF2, with a sudden increase in the P-wave velocity right after the initial setting stage. This could be related to the kinetics of water release from this SAP, indicating that a slower or even later release of water is taking place, as discussed in chapters 3 and 5. On the other hand, both mixtures produced with the addition of SAP\_B (W\_SAP1 and W\_SAP1+2) present a different pattern in the development of the hardening when compared to REF1. For those mixtures, the increase in the P-wave velocity happens slower in time, until a final setting stage is reached. This could indicate a



more gradual water release by SAP\_B, occurring earlier and slower in time.

From the curves obtained with the S-waves (Figure 6.20) it can also be seen that all SAP-mixtures present a delayed setting in comparison with both reference mixtures and that REF2 hardens faster than REF1, as already discussed above. Since the S-waves do not travel in fluid media, in this case water, the curves do not indicate a particular behavior regarding the water release by the SAPs as it was possible with the P-waves. On the other hand, once the mixtures hardened, the S-wave curves showed a more distinct variation on the final velocity values. Both reference mixtures presented higher values of velocity at later stages of the hardening process. Since the S-waves can only propagate in solid media this reflects the differences in the air void content in the mixtures at the hardened state. As already expected, after hardening of the concrete the SAPs would have released their stored water leaving behind macropores filled with air. When comparing amongst the SAP mixtures it can be noticed that the wall produced with only SAP\_D3.1 presents a possible higher amount of air voids in comparison to the walls produced with SAP\_B and the combination of both SAPs. Even though the amount of additional water was the same for the mixtures produced with SAP\_B and SAP\_D3.1, individually, and higher for the mixture produced with the combination of both, the higher air void content for the mixture with SAP\_D3.1 could be an indication that the macropores left behind by SAP\_B are being filled over time with hydration products [12, 27, 28].

From the curves of the P-wave and S-wave velocity, a final setting time could also be picked, for comparison with the results from the Voton probe (Table 6.5). The point corresponding to the final setting time was chosen based on the maximum of the derivative curve of the wave velocity, as described in chapter 4. Even though both techniques are based on different physical principles, both provided a logical trend of behavior for comparison amongst the different mixtures, regarding the effects of the SAPs on the setting time. Specifically for the case of REF2, the P-waves indicate the earliest setting time in comparison to the other methods. Since the determination was based on the shape of the curves,

this could be explained by the fact that P-waves propagate in solid and fluid media. The high amount of mixing water used in the production of REF2 could interfere in the propagation of the wave at the beginning of the test, which is reflected in the shape of the curve.

6.3.4.2 Properties in the hardened state

The air content in the hardened state is shown in Figure 6.21. In terms of variability of results, it can be considered that no significant difference has been found amongst different trucks for each mixture. The standard deviations of the results (0.75% for REF1, 0.26% for REF2, 0.75% for W\_SAP1, 0.45% for W\_SAP2 and 0.53% for W\_SAP1+2) are in accordance with those also found in literature (up to 0.62%) [29, 30]. When comparing the SAP mixtures to the reference mixtures without SAPs, an expected increased air content was found, especially for the mixtures containing SAP\_B.

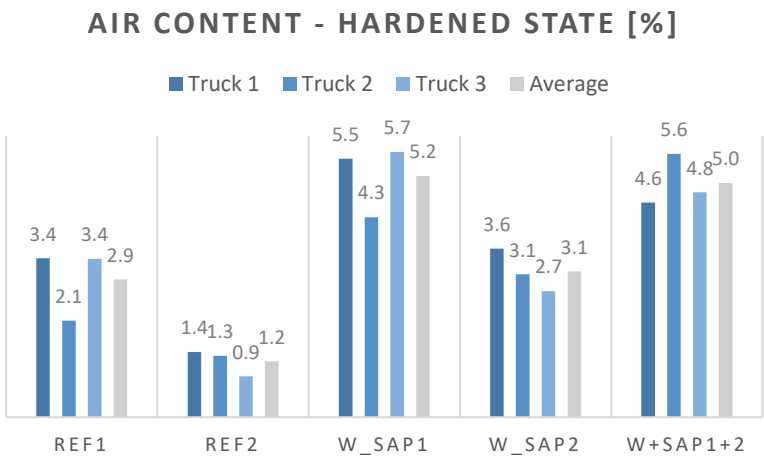


Figure 6.21 - Air content in the hardened state per truck per mixture.

Considering that the SAPs completely absorbed the extra water added on top of each of the SAP mixtures, the difference in air content caused by the formation of macropores due to the water release from the swollen SAPs is expected to be in good correspondence with the volume of extra water added, based on obtaining the same workability for each mixture.

For mixture W\_SAP1, this volume corresponds to 2.8% of the total volume of the mixture, which is not that distant from the difference in the average air content between REF1 and W\_SAP1 (around  $2.1 \pm 0.8\%$ ). For the mixture W\_SAP2, no significant difference has been found compared to REF1. In addition, considering that the amount of additional water was the same for both W\_SAP1 and W\_SAP2 and given that all the water would have been absorbed by the SAPs, it was expected that the amount of air in the hardened states of both mixtures W\_SAP1 and W\_SAP2 were to be at the same level. However, given the lower absorption capacity of SAP\_D3.1 in comparison to SAP\_B (11 g/g for SAP\_D3.1 and 21 g/g for SAP\_B) the macropores formed by SAP\_D3.1 would be smaller in comparison to those formed by SAP\_B. Since the test method itself is based on the visual mapping of pores on the surface of the specimen, not all pores of smaller SAP\_D3.1 particles might have been detected by the scanner, which could explain the reduced air content of W\_SAP2 in comparison to W\_SAP1. Furthermore, due to internal curing, part of the macro pores will be filled by hydration products, thus slightly decreasing the total porosity observed [28].

In the previous section, it was discussed that the difference in values of S-waves was an indication that the mixture W\_SAP2 presented a higher air content than the mixtures produced with SAP\_B. That was not the indication of the air-void analysis. Considering both test methods, the analysis of the air voids and determination of the air content as performed by [9] depends on the filling of the air voids with a powder (in this study, barium sulfate was used). In the previous section, the possibility was stated of the air voids left by SAPs being partially filled with hydration products. During the execution of the air-void analysis, only the surface of the specimens is scanned, meaning that even if the macropores were partially filled with hydration products, that could not totally reflect a significant difference in porosity. As hydration products are formed, they are mostly found near the boundary of the SAP void. However, the deposition of the material in the void is low thus, the difference in porosity is not that significant, especially in the concrete mixtures studied (given the high amount of water and the type of binder that was used) [12].

On the other hand, the S-waves method is based on the propagation of ultrasound waves through the material, which is far more sensitive to volumetric changes inside the macropores.

Figure 6.22 shows the void range distribution for all mixtures. For both W\_SAP1 and W\_SAP2, the air void distribution seems to be in accordance with the expected swollen sizes of the SAP particles. For W\_SAP2, most voids were found in the range of 450 – 1000  $\mu\text{m}$ . For W\_SAP1 that range comprised the voids within 505-1500  $\mu\text{m}$ . Considering the dimensions of the dry particles of both SAPs, their absorption capacity and assumed spherical shape, the calculated expected size after swelling is around 1200  $\mu\text{m}$  for SAP\_B and 620  $\mu\text{m}$  for SAP\_D3.1, which is in accordance with the measured void sizes. This proves again that SAPs are present throughout the mixture and possess the expected sizes, meaning that the SAPs absorbed the correct amount of mixing water at final setting.

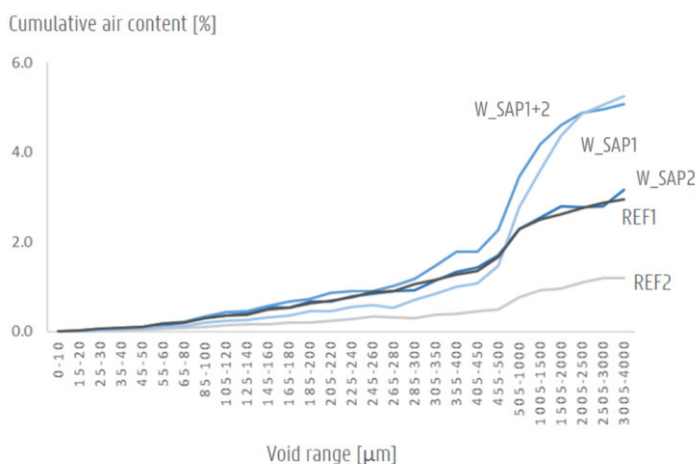


Figure 6.22 - Air void distribution per mixture (average results shown).

Regarding the mechanical properties of the different mixtures, in terms of compressive strength all walls have achieved the design strength class (Figure 6.23). As for the difference amongst mixtures, the addition of water (regardless of the presence of SAPs) promoted a reduction in the compressive strength for all mixtures in comparison with REF1. REF2,

W\_SAP1 and W\_SAP2 all were produced with the same total water-to-cement ratio. However, W\_SAP1 presented a higher compressive strength value while W\_SAP2 presented almost the same result as REF2.

Although all three mixtures have been produced with the same amount of water, the difference in the kinetics of water release and subsequent internal curing of both SAPs would be the cause of this difference. The results shown in Figure 6.19 pointed out a difference in the water release by the SAPs (with SAP\_B probably releasing its stored water earlier than SAP\_D3.1) and to a possible formation of hydration products in the voids left by SAP\_B (to a higher extent than the ones left by SAP\_D3.1). The earlier water release by SAP\_B can be acting in favor of further hydration at early ages [28], which in time can counteract the reduction in strength caused by the macro-pore effect.

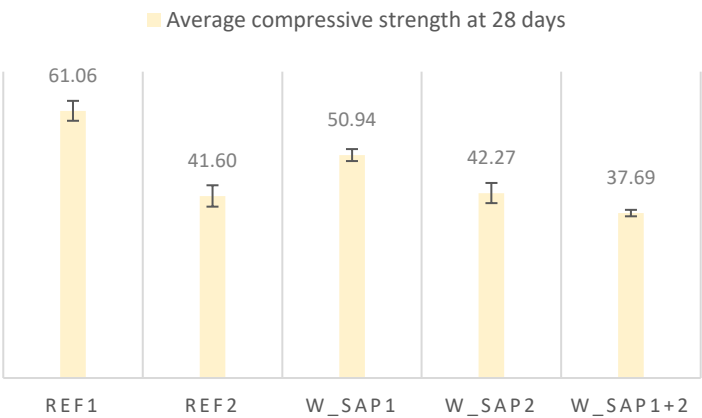


Figure 6.23 - Average compressive strength of each mixture at 28 days.

The evolution in strength over time (Figure 6.24) shows that indeed the values of W\_SAP1 for the compressive strength are higher than for the other SAP mixtures and REF2, already from 7 days onwards. After 28 days, the increase in strength is less pronounced which indicates that the possible gains due to further hydration at early ages are not that prominent at the later ages of the concrete (at 56 days), as internal curing

decreases over time due to a decreasing release of entrained water over time.

The relation between the development of strength, amount of water and type of SAPs used can also be further discussed and some insights can be highlighted. When the development of strength is compared to the total water-to-cement ratio of the mixtures, it can be noticed that at the age of 7 days the correlation between the parameters presents its lower value (Figure 6.25). Furthermore, the kinetics of the SAPs might have a stronger effect, especially at earlier ages due to the release of stored entrained water to mitigate self-desiccation.

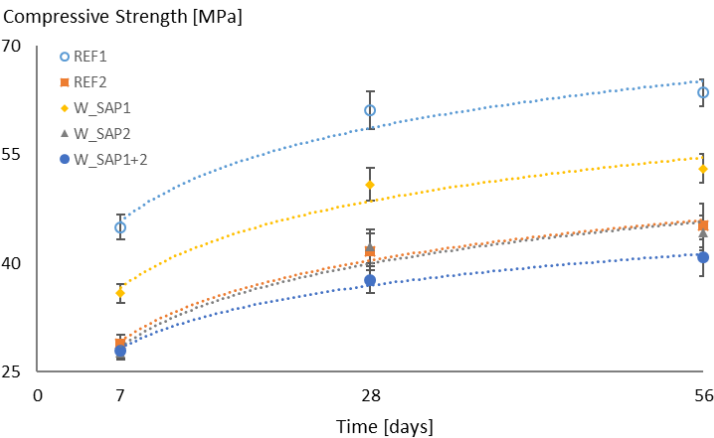


Figure 6.24 - Evolution of strength over time. The average values are shown.

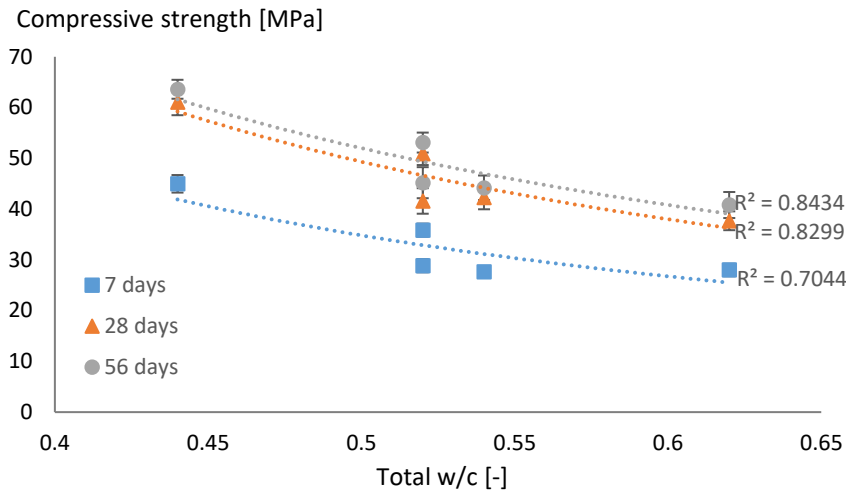


Figure 6.25 - Compressive strength at different ages as a function of the total water-to-cement ratio for all mixtures. The average values are shown.

6.3.4.3 Monitoring of shrinkage with laboratory specimens

The results of the shrinkage with laboratory specimens showed a very distinct behavior for the SAP-containing mixtures and the references without SAPs, as already mentioned in Chapter 5. No significant difference was found amongst specimens from different trucks for each of the mixtures.

For the specimens covered with aluminum tape, in order to reduce the effects of drying, all SAP-containing mixtures presented a considerable reduction in shrinkage strain in comparison to REF1 (Figure 6.26). The mixtures containing SAP\_B performed better in comparison to the one containing only SAP\_D3.1, with an average strain value of  $-25 \mu\text{m}/\text{m}$  ( $n = 9$ ) at 28 days and even some expansion strain for W\_SAP1+2, which can be considered as a complete mitigation of the (autogenous) shrinkage strain.

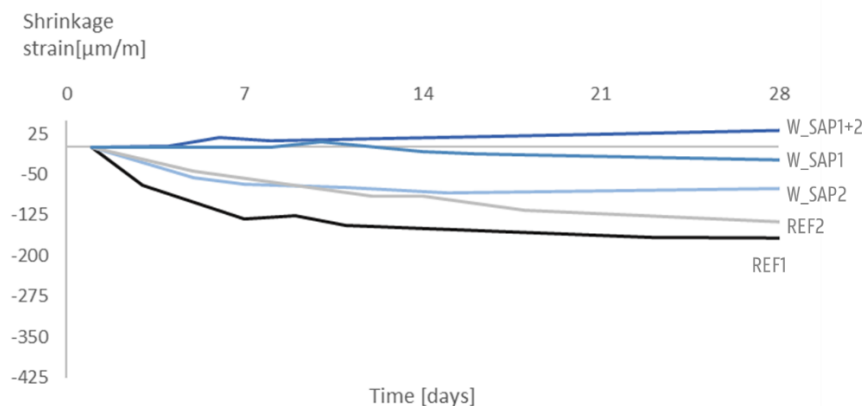


Figure 6.26 - Shrinkage strain of laboratory specimens covered with aluminum tape.

When comparing W\_SAP2 to REF2, it was noticed that during the first 7 days of measurements both mixtures present the same trend. However, from that moment on, the mixture containing SAP\_D3.1 reaches a constant value in terms of shrinkage strain, which is maintained for the remaining testing time. On the other hand, REF2 continues to shrink and the shrinkage strain values continue to increase in the negative branch of the graph. Although the mixture W\_SAP2 was not able to promote a complete mitigation of the (autogenous) shrinkage strain, a significant reduction was found, especially in comparison to REF1. Such reduction could already be enough to prevent the occurrence of shrinkage cracking, especially at earlier ages (during the first days).

The differences in behavior of the specimens containing the different SAPs could be explained by the differences in the kinetics of water desorption from both SAP\_B and SAP\_D3.1 as discussed before with the P-waves results (Figure 6.19). An earlier water release by SAP\_B could be responsible for the expressive reduction in shrinkage strain already after setting. On the other hand, a slower and later water release by SAP\_D3.1 could explain why the more expressive reduction of shrinkage strain would only occur later in time [31].

For the mixture W\_SAP1+2, the slightly better performance in comparison to W\_SAP1 could be due to the combined effect of both SAPs.



SAP\_B significantly reduces the shrinkage during the first days whereas SAP\_D3.1 acts by keeping the internal humidity levels for a longer time, which is the main factor linked to the reduction of the shrinkage strain.

In all cases, the addition of SAPs has shown to be very effective in the reduction/complete mitigation of the shrinkage strain. In terms of variability of the results, no significant difference was found amongst the different trucks from each mixture, with the highest standard deviation corresponding to 32  $\mu\text{m}/\text{m}$ . Furthermore, all sets of specimens (3 per truck) showed the same trend.

For the case where the specimens were not covered with aluminum tape, thus being exposed to the effects of drying, all specimens (with and without SAPs) performed in a very similar way (Figure 6.27). In here, the addition of SAPs seemed not beneficial to reduce shrinkage near the surface of the specimens. With the exposure to the air and the increased drying effect, it is reasonable to say that the SAP-containing mixtures behave as if they were mixtures produced only with additional water (as in REF2). This behavior could be linked to the fact that upon drying conditions the water stored in the SAPs is released very prematurely in time and would not contribute to the internal curing, as discussed in chapter 5. In [32], the authors describe the effects of SAPs on the total shrinkage of concrete mixtures drying at 65% RH (similar conditions as in this study) and point out that the overall effect of internal curing with SAPs on total shrinkage will depend on the total water-to-cement ratio of the mixture and the relative humidity of the environment during drying, and hence upon the proportion between the (reduced) autogenous and the (enhanced) drying shrinkage.

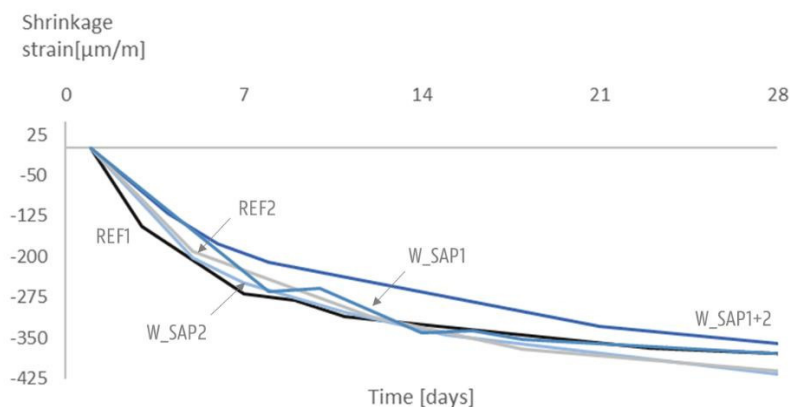


Figure 6.27 - Shrinkage strain of laboratory specimens exposed to the air.

In terms of suitability of the method for the measurement of the shrinkage, it is important to highlight that the use of the DEMECs has some limitations. The first relates to the measurements starting only after demolding of the specimens, which occurred 24 h after mixing of the concrete. Part of the early-age shrinkage, which is occurring around the time of setting is then not being recorded. An in depth discussion of the importance of choosing the correct time for starting of the measurements regarding autogenous shrinkage was presented in Chapter 4. Another limitation of the method is related to the position of the measuring points only on the surface of the material. As the free drying more dominantly occurs near the surface, in time all water from the SAPs near the surface will have evaporated, leaving no room for more internal curing at this location. The internal curing that could possibly still be occurring inside the specimen is not being recorded. Despite those limitations, the method can still provide important and reliable results and give important insights for a comparative study of the effect of different types of SAPs in the mitigation of shrinkage.

As a way of expanding the possibilities of analysis in our study, the use of embedded optical fiber sensors was used for the monitoring of shrinkage on site inside the wall, which will be discussed in the following sections.

#### 6.3.4.4 *Cracking of the walls and monitoring of shrinkage on site*

During eight months of monitoring, some cracks have been found on both reference walls, while the SAP-containing walls remained crack-free. The first through-going crack on wall REF1 was noticed 5 days after casting, while for the wall REF2 it happened 9 days after casting. The cracking pattern of both reference walls is shown in Figure 6.28 and Figure 6.29. The values of the crack width represent the average width over the length of the crack (measured every 10 cm). The denominations side A and side B are used to indicate the two sides of the walls.

For the wall REF1, the cracks started at the center of the wall and then appeared about every 2 m. Most of the cracks propagated through the thickness of the wall. No significant difference was found in the cracking pattern of the portion of the wall that received the external curing agent. The cracks on the side A of the wall presented the largest widths, which might be related to the orientation of the walls in relation to the sun light. The side A is turned to the east and side B is turned to the west. Side A is exposed to the sun during the hours of increasing external temperature while side B only gets direct exposure during the afternoon, when the external temperature reaches its peak and starts to cool down.

In comparison to REF1, the wall REF2 cracked less. Even though REF2 was produced with around 10% less reinforcement, it was also produced with a higher water-to-cement ratio and less cracks were thus expected.

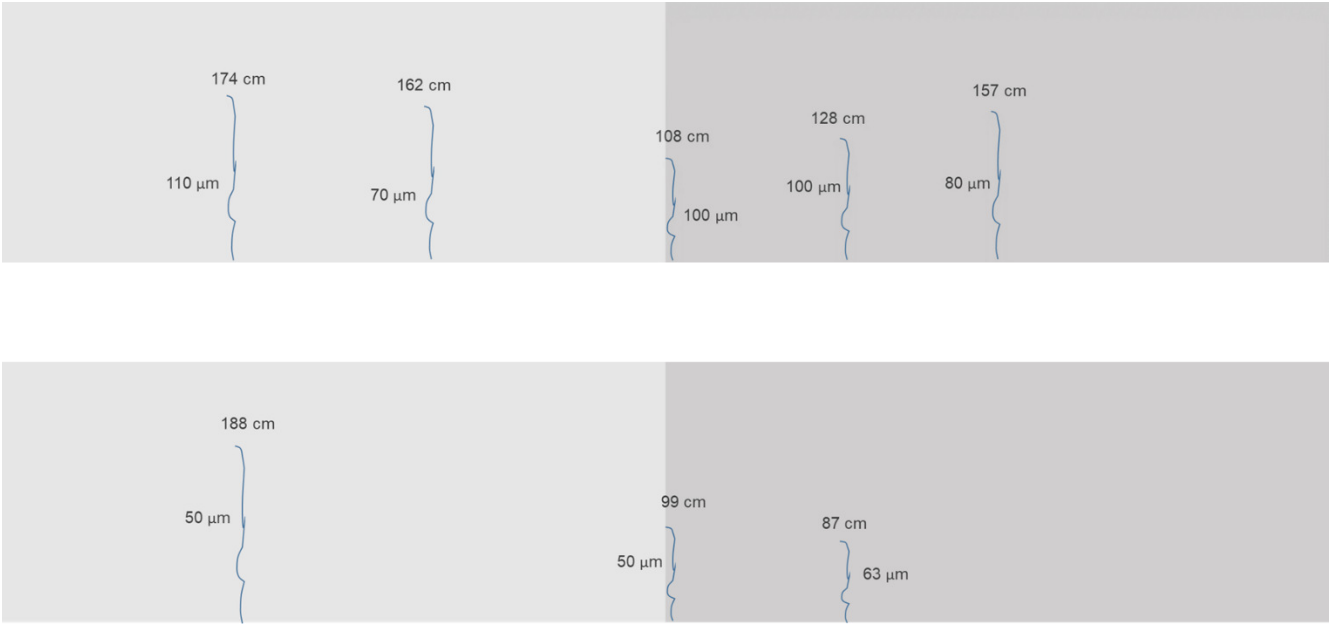


Figure 6.28 - Cracking pattern of wall REF1, showing the total height of the crack measured from the bottom [cm] and the average width [ $\mu\text{m}$ ]. The upper part of the figure represents the side A and the bottom part of the figure represents the side B of the wall. The darker grey area had been treated with external curing agent. For a better comparison, one of the images is mirrored.

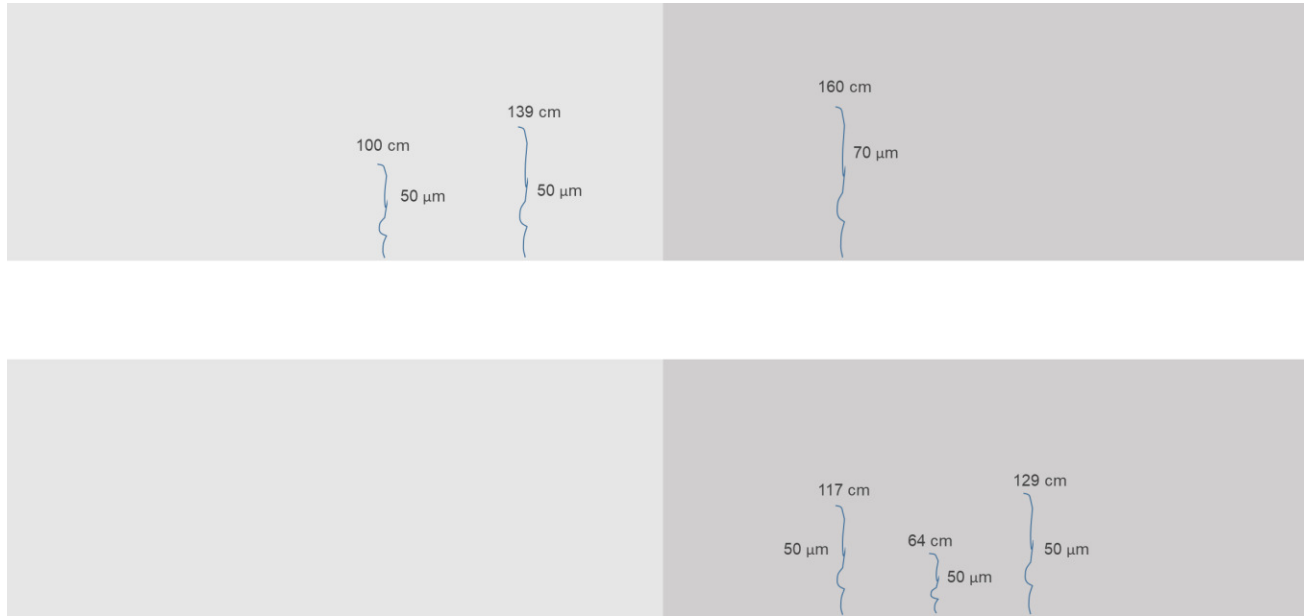


Figure 6.29 - Cracking pattern of wall REF2, showing the total height of the crack measured from the bottom [cm] and the average width [ $\mu\text{m}$ ]. The upper part of the figure represents the side A and the bottom part of the figure represents the side B of the wall. The darker grey area had been treated with external curing agent. For a better comparison, one of the images is mirrored.

The cracking time for the concrete mixtures used to construct the walls was also monitored under restrained shrinkage by means of steel rings, while being covered with plastic foil to exclude evaporation. Even though the specimens used for the test were different to the walls in terms of dimensions and presence of reinforcement, plus there were differences in the curing conditions, the test was still able to showcase the difference in the cracking time of the different concrete mixtures and to highlight the potential in terms of autogenous shrinkage mitigation by the inclusion of SAPs (Figure 6.30).

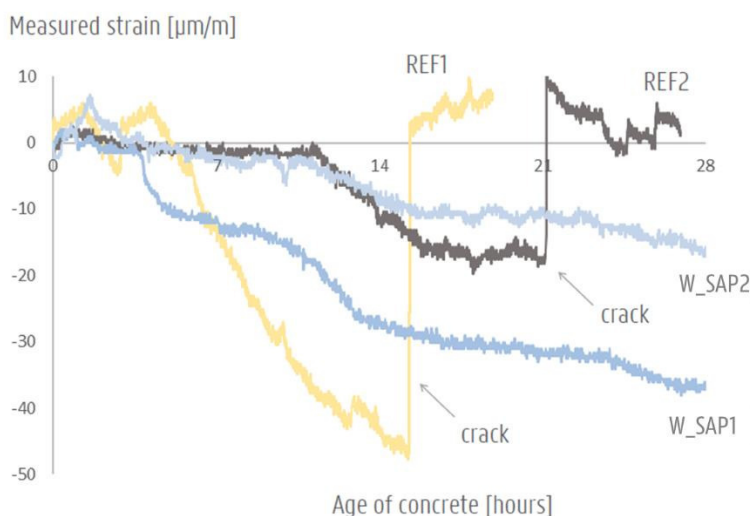


Figure 6.30 - Strain measured in the ring tests.

According to the sudden increase in the strain values of the rings, cracks appeared after 14 days and 21 days for the mixtures REF1 and REF2, respectively. The existence of the cracks was also confirmed visually on the specimens. No cracks developed in the specimens produced with SAPs. Due to a faulty sensor, no data was recorded for the mixture W\_SAP1+2. However, no visual cracks were seen in the ring, after 28 days of testing. The results highlight the fact that the use of additional water without SAPs can delay the cracking time, but it is not enough to avoid cracking completely, which was only achieved upon use of SAPs and extra water. The times of cracking occur later in the ring test than in the walls

due to the difference in setup and sample size, limiting the effects of thermal shrinkage, even though the formwork was removed after 48 h from the large-scale walls.

The average shrinkage strain at the bottom layer of the walls (on the surface without external curing, side A) as measured by means of the DEMECs is shown in Figure 6.31. The measurements started 48 h after casting, right after the removal of the formwork from the walls. There is a clear difference in the strain levels at early and late stages when comparing the walls with and without SAPs. The wall REF1 presents the highest shrinkage strain values, while the wall with the combination of SAPs presents the lowest ones. The walls W\_SAP1 and W\_SAP2 performed in a very similar way along the whole testing time. Both presented strain values very similar to REF2 from 10 days until the completion of the testing.

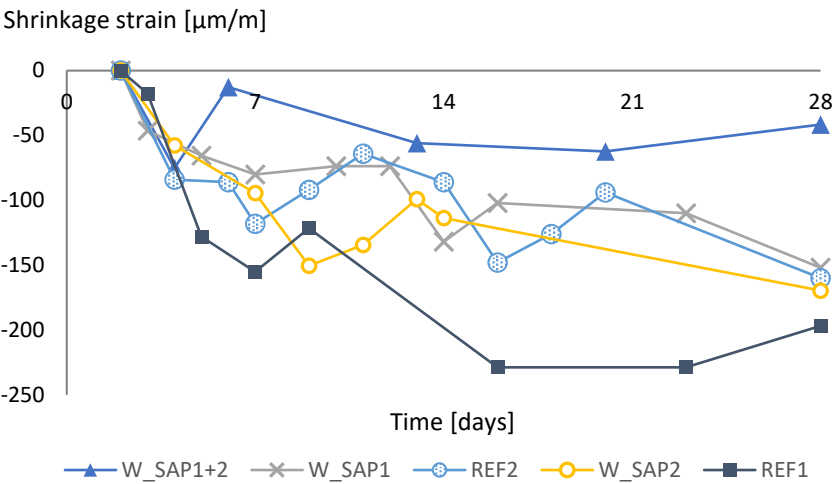


Figure 6.31 - Shrinkage strain at the bottom layer of the walls (no external curing).

In terms of strain level and occurrence of cracks, it can be noted that for the SAP specimens, the level of strain found in the wall REF1 by the time the first cracks were noticed ( $-128 \mu\text{m/m}$ , around 5 days) is only reached after 14 days. During the first 7 days, the maximum strain recorded for the SAP walls was considerably lower than in the wall REF1: 90% lower in

W\_SAP1+2, 49% lower in W\_SAP1 and 55% lower in W\_SAP2. The fact that the SAP walls did not present any cracks indicates that the reduction in strain level during the early ages, when the concrete is still developing its strength, was the limiting factor for the development of cracks in the SAP walls, showing the benefit of internal curing by SAPs.

Figure 6.32 shows the shrinkage strain at the bottom of the wall on the side with the external curing agent. The use of the external curing agent promoted a further reduction in the strain levels of the walls where SAPs were added. A reduction of 64% was found for W\_SAP1 and W\_SAP2, respectively, compared to REF1 at the age of 7 days and around 45% at the age of 28 days. In contrast, where the external curing was not applied the reduction was around 50% for both W\_SAP1 and W\_SAP2 at the age of 7 days, and around 45% at the age of 28 days. The use of the external curing agent could be reducing the effects of the external temperature on the drying of the surface, which in turn will reduce the early water release by the SAPs. With that, the SAPs can maintain higher levels of internal humidity for a longer period, which is translated into lower levels of shrinkage strain in comparison to the case where no external curing agent was used.

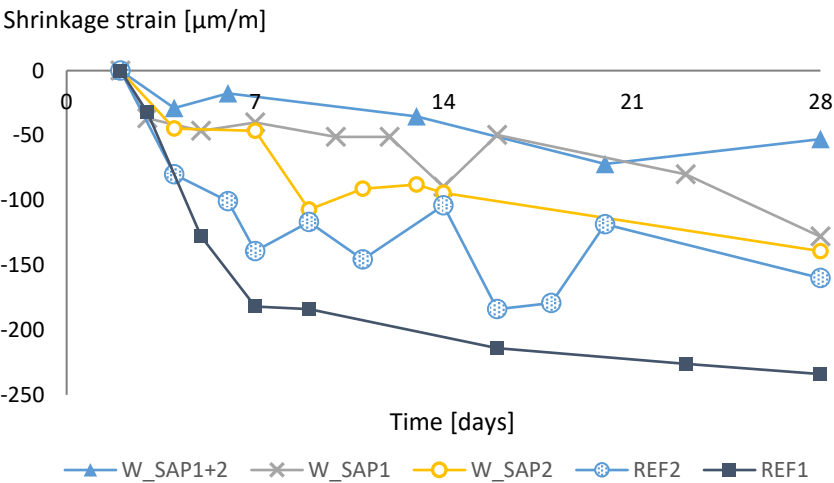


Figure 6.32 - Shrinkage strain at the bottom layer of the walls (with external curing).



The measurements performed on the top layer of the walls showed increased strain levels in comparison to the bottom layer. This increase was noticed to be more prominent at later ages and for the concrete with the highest total water-to-cement ratio (W\_SAP1+2): up to 53%. The higher values were already expected given the lower density of the steel reinforcement at the top layer of the walls in comparison to the bottom and the distance to the non-deforming plate, which in turn allows the top layer to shrink with less restriction. The strain curves for the top layer of the walls are depicted in Figure 6.33 and Figure 6.34.

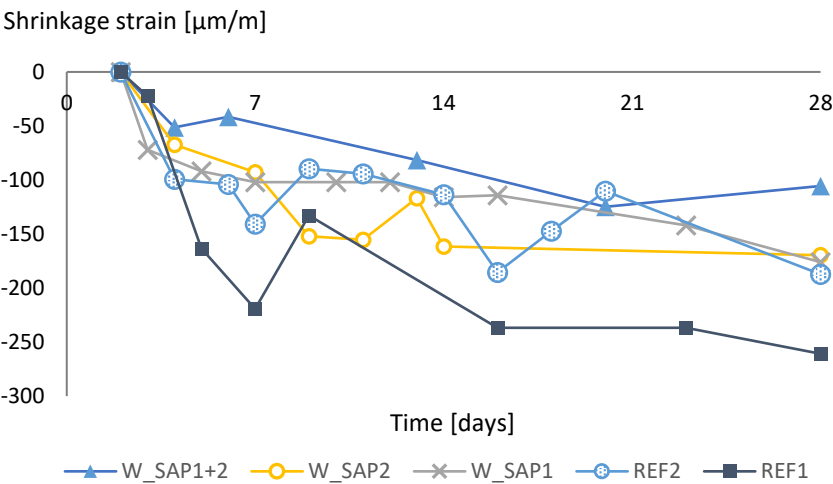


Figure 6.33 - Shrinkage strain at the top layer of the walls (no external curing).

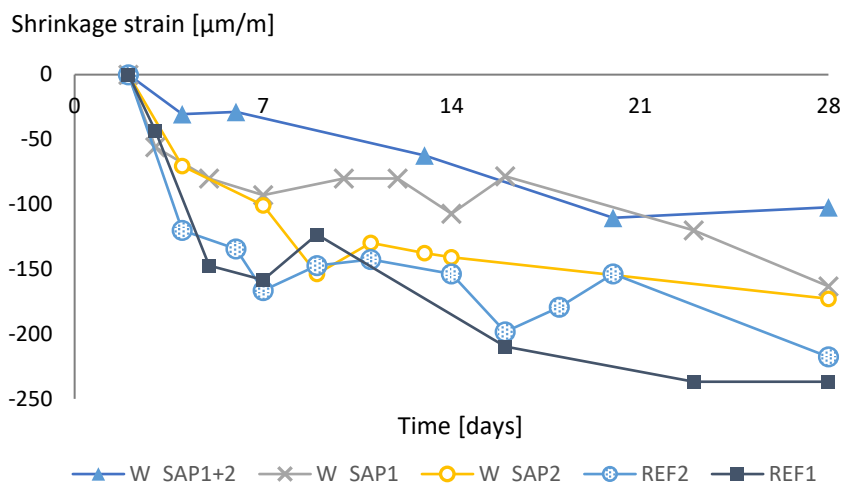


Figure 6.34 - Shrinkage strain at the top layer of the walls (with external curing).

In comparison to the specimens tested in the laboratory, the shrinkage strain measured on the walls was higher than for the laboratory specimens covered with aluminum foil (Figure 6.26) and lower than for the laboratory specimens that were exposed to the air (Figure 6.27). As expected, the concrete in the walls is not only exposed to autogenous shrinkage but is also exposed to the effect of drying shrinkage and the strain measured on the surface on the walls is the result of a combined effect of different types of shrinkage. The dimensions of the walls are far larger than the ones of the laboratory specimens and the volume of concrete in both can influence the shrinkage. The bulk effect of the volume of concrete in the wall might work as a restraint for the total shrinkage along with the steel reinforcement that is not present in the laboratory specimen. That combined effect might explain why the shrinkage strain measured on the surface of the walls is in between the values measured for the laboratory specimens. Assmann and Reinhardt [32] measured the shrinkage in prismatic specimens made of concrete under different conditions. 1) completed sealed with aluminum tape to prevent drying and moisture exchange, to measure only autogenous shrinkage; 2) specimens wrapped in polyethylene foil that would allow a gently dry; 3) specimens completely exposed to drying. The authors found that the specimens in the second group presented a shrinkage strain that

was in between groups 1 and 2. In their discussion, the authors suggest that the partial prevention of drying could be used as to simulate a thick walled structure that can only dry slowly. Which was the case in this study.

Additionally, by comparing the curves for the shrinkage strain of the walls as measured by the DEMEC with the ones from the laboratory specimens (Figure 6.26 and Figure 6.27), it can be noted that the measurements on the walls present a considerable amount of “jumps” in the measurements that are sometimes out of the observed general trend of the curves. This might be the effect of the thermal expansion and shrinkage on the surface of the wall caused by the constant temperature changes as the temperature on the surface of the wall warms up and cools down during the day. Such effect could not be entirely avoided since it was not always possible to perform the measurements always on the same period of the day.

The shrinkage of the walls as monitored by the optical fiber sensors showed the same trend for both the conditions without (Figure 6.35) and with external curing agent (Figure 6.36). The measurements were zeroed at the knee-point of the shrinkage strain curve for each mixture. The method is described in Chapter 4.

For the case where no external curing agent was used, a reduction of 55% in the strain levels at 7 days of the SAP mixture was found in comparison to the reference mixture. This reduction was only 18% at 28 days, which as stated before did not promote the appearance of cracks on the SAP walls. With the use of the external curing agent, the strain reduction at 7 days was 63%. The same 18% reduction was obtained at 28 days. The optical fiber sensors placed at the top layer of the wall showed larger strain values. Figure 6.37 shows the curves from the top layer of the side of the walls externally cured. The sensors positioned on the top layer of the wall on the side without external curing was damaged during the casting of the concrete and no data could be recorded.

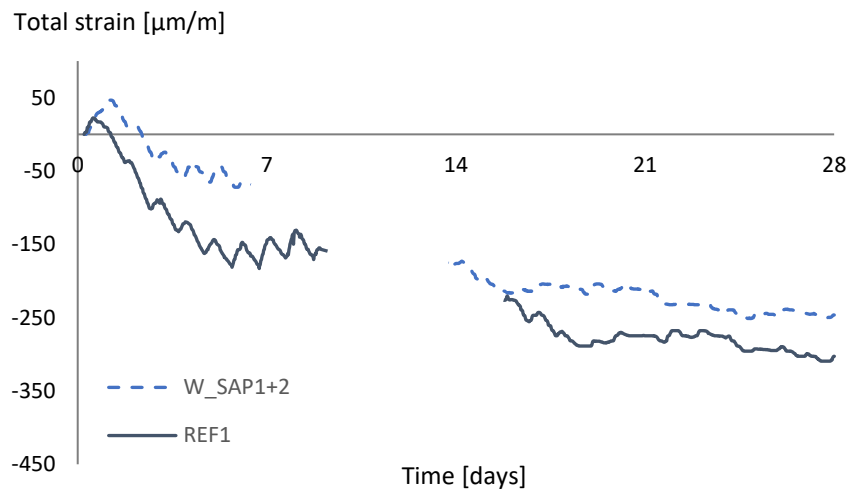


Figure 6.35 - Shrinkage strain of the wall REF1 and wall W\_SAP1+2 measured with the optical fiber sensors. Results from the bottom layer without external curing. The interruption in both curves represents a momentous cut in the power supply of the measuring unit.

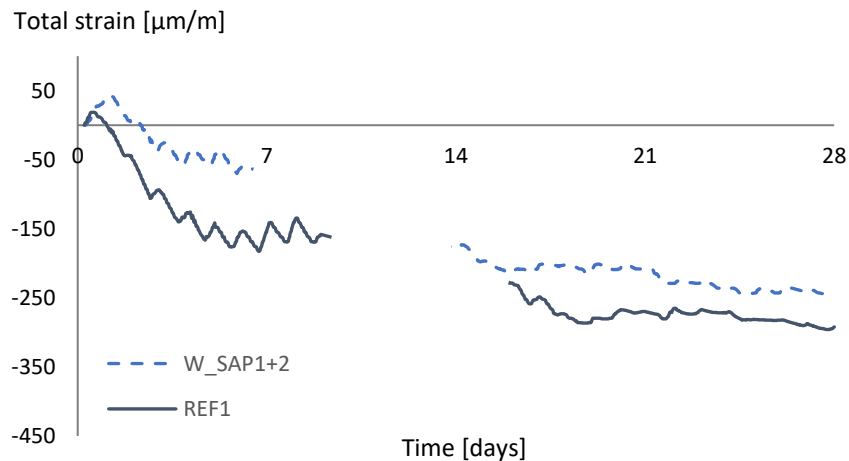


Figure 6.36 - Shrinkage strain of the wall REF1 and wall W\_SAP1+2 measured with the optical fiber sensors. Results from the bottom layer with external curing. The interruption in both curves represents a momentous cut in the power supply of the measuring unit.

In comparison to the curves from the bottom layers, a larger expansion was noticed on the curves from the sensors placed on the top layer of

both walls. That also reflects the lower restrain effect at the portions of the wall further from the baseplate.

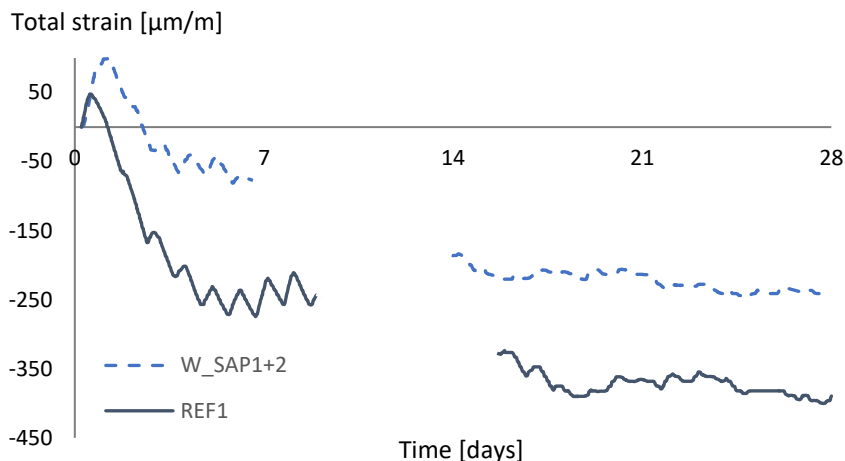


Figure 6.37 - Shrinkage strain of the wall REF1 and wall W\_SAP1+2 measured with the optical fiber sensors. Results from the top layer with external curing. The interruption in both curves represents a momentous cut in the power supply of the measuring unit.

Both monitoring methods, the optical fiber sensors and the DEMECs were able to reflect the differences in the shrinkage behavior of the different mixtures and very similar conclusions could be drawn from the results. In terms of comparison, the levels of strain registered for the reference wall were very comparable for both methods. In contrast, a considerable difference was found for the SAPs walls (regardless the use of external curing agent or the position of the sensors). This is shown in Figure 6.38 and Figure 6.39 where the measurements with the SOFO sensors were zeroed at 48 h to coincide with the starting time of the DEMECs. In both cases, the curves of the SAP wall register levels of strain quite similar to the reference wall after the first 7 days of monitoring. This is related to the moment of initiating the measurements. The curves of the SAP wall present a considerable expansion stage during the first day of measurements, which is when the SAPs start to release the water and promote internal curing. By starting the measurements after that

moment, not all the expansion stage is considered and the effects of internal curing are not registered.

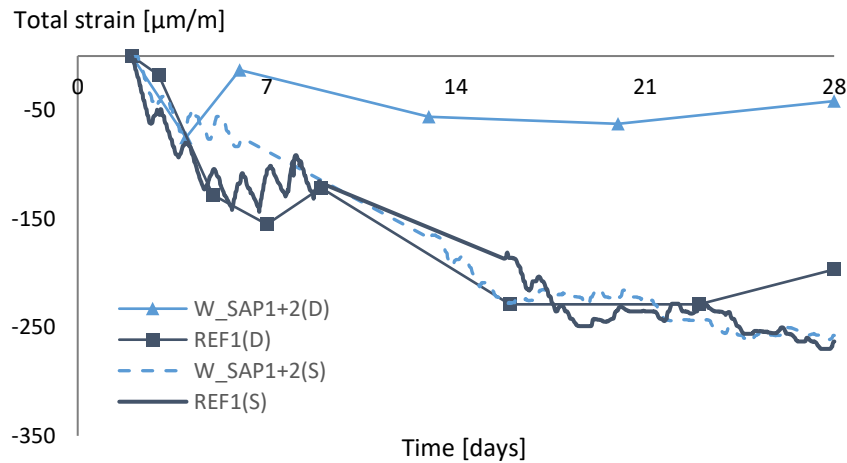


Figure 6.38 - Comparison of strain levels measured with the DEMEC and SOFO sensors at the bottom layer of the walls on the side without external curing.

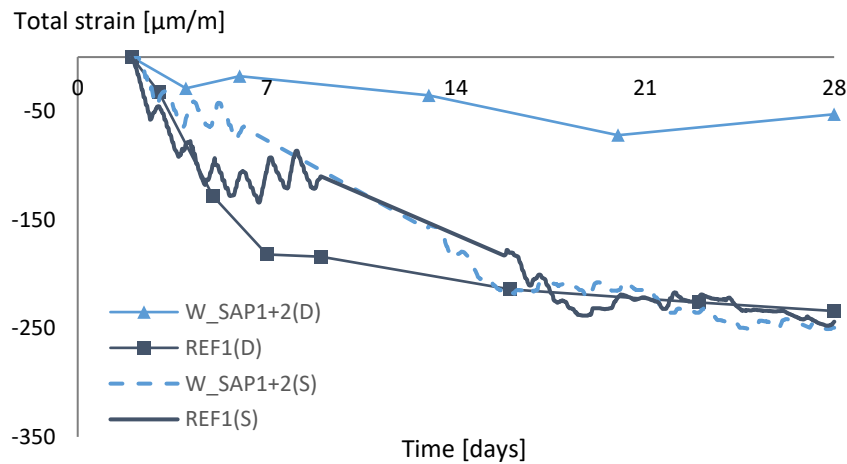


Figure 6.39 - Comparison of strain levels measured with the DEMEC and SOFO sensors at the bottom layer of the walls on the side with external curing.

Despite these differences, both methods were suitable for the monitoring of the shrinkage of the walls, but caution is advised when comparing them directly. Pros and cons may be weighted in terms of costs and availability

for both monitoring methods. The costs per sensor in the dimensions used in this study can reach up to 800 Euros. On the other hand, the labor work can amount to 1 h for the monitoring of one wall with the use of the DEMEC, while with the use of the sensors the measurements are performed automatically by a recording unit installed on site.

#### 6.3.4.5 Water permeability of the cracked wall REF1

Three months after the last recording of the first round of the test, healing started to be observed on the portion of the crack with width below  $50\ \mu\text{m}$  on the opposite side of the wall (Figure 6.40).

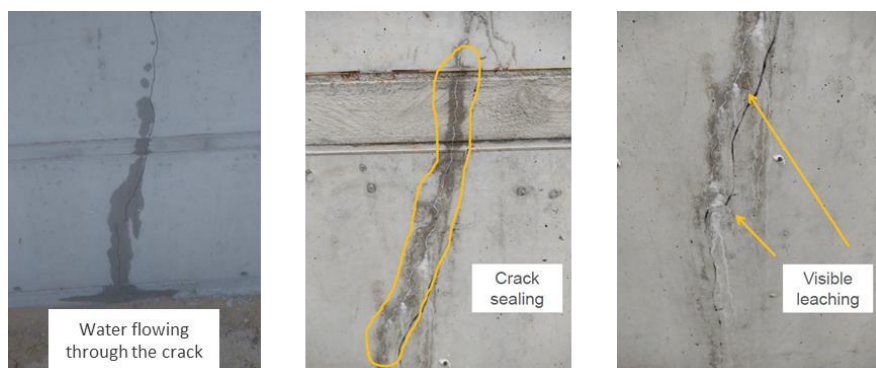


Figure 6.40 - Crack on the opposite side of the wall during the water permeability tests and healing period.

To assess the influence of the healing on the water permeability, the water container was refilled and the test was performed again during 20 days. The results are shown in Figure 6.41.

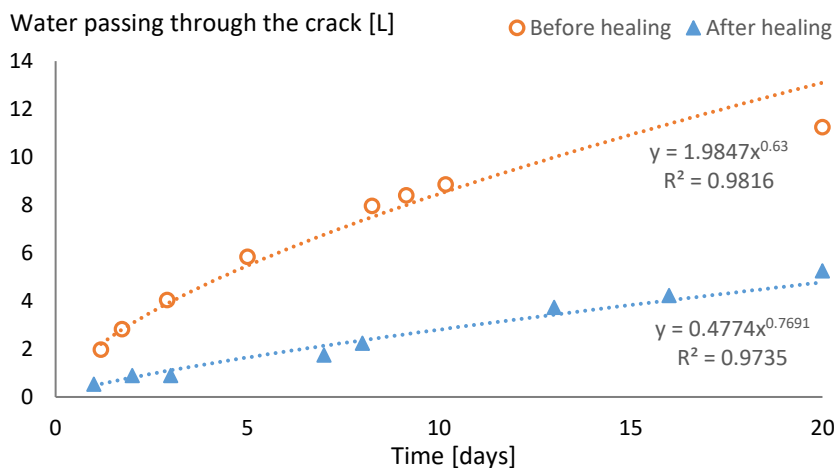


Figure 6.41 - Water permeability of the crack surface of wall REF1.

There is a significant reduction in the water permeability, expressed as the amount of water passing through the crack as a function of time. During the first 10 days of monitoring, the flow rate (in L/day) after the healing was 66% lower than before the healing. At 20 days, the amount of water that had passed through the crack after the healing was equivalent to the amount passing through the same crack (before healing) only 5 days after the start of the measurements. Even though no cracks had been observed in none of the SAP walls, it could be expected that a similar healing effect could take place for cracks subjected to wet dry cycles, as it was the case for the reference wall. Furthermore, due to the presence of SAPs and their swelling potential, immediate sealing could also be expected (as discussed in Chapter 5) further reducing the water permeability.

#### 6.3.4.6 Monitoring of corrosion potential by means of multi-reference electrodes (MuRE)

Initially, eight electrodes nearby the access box were connected just to make sure the system was working properly. The potential was then measured for approximately one month. Two months after the casting of the walls, different electrodes in wall REF1 were connected to the



measuring unit, following the appearance of cracks. The location of such electrodes is indicated in Figure 6.17.

The measurements of potential are shown in Figure 6.42. In the graph, a dashed line marks the characteristic corrosion potential for nickel (-257 mV), indicating the most likely passive and active region for the corrosion process. For approximately 4 months, the potential values were quite stable in all the locations. At around 6 months after the casting of the walls, a sudden decrease in the value of the potential was noticed for the sensors located at the points 37 and 38, near one of the cracks. The values observed for those electrodes are positioned in the active region, indicating that some localized corrosion process might have started.

For wall W\_SAP1+2, since no cracks developed, the electrodes that were initially active after the casting of the wall remained connected to the measuring unit. Due to a malfunctioning regarding the communication between the reading unit in this wall and wireless station on site, only a limited dataset is available. Despite of that, all electrodes recorded potential values in the passive region, indicating that no corrosion started (Figure 6.43).

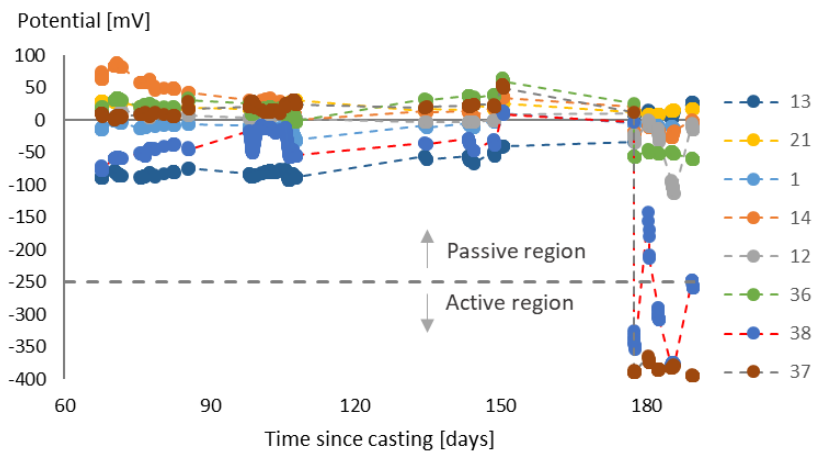


Figure 6.42 - Potential measured near some cracked locations of wall REF1. The dashed lines represent the moment where the measuring unit was not recording.

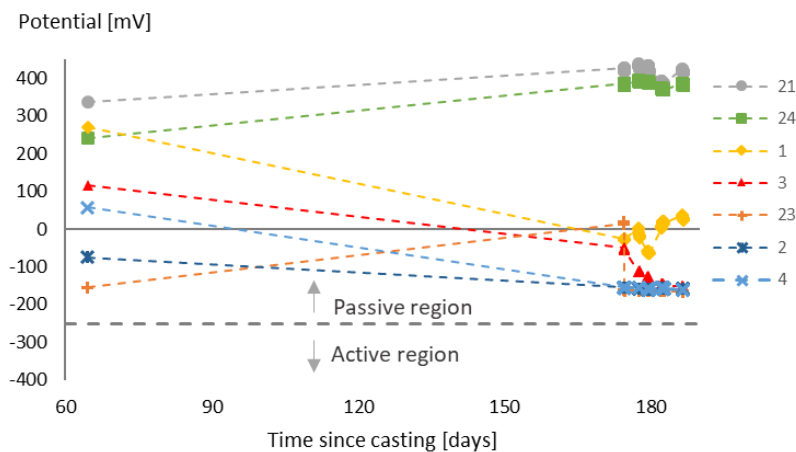


Figure 6.43 - Potential measured at different locations of wall W\_SAP1+2. The dashed lines represent the moment where the measuring unit was not recording.

6.3.4.7 Preliminary cost analysis

In terms of costs, the addition of both types of SAPs enabled the production of crack free massive concrete walls with 10% less reinforcement than a reference wall without SAPs that presented going-through cracks only five days after casting. This reduction of reinforcement still is not only appealing for economic reasons but can also represent a very positive impact regarding the reduction of environmental damage related to the production of steel rebars by the construction industry.

Table 6.6 shows a summary of the costs for the construction of the walls REF1 and W\_SAP1. The calculation of costs for the vertical reinforcement considers the costs for transportation (0.68 euros/kg of steel) and for placement (0.27 euros/kg of steel). The costs of the concrete correspond to 78.7 euros/m<sup>3</sup> and 75 euros/m<sup>3</sup> for the concrete mixtures in the strength class C35/45 and C30/37, respectively. The costs to produce the “in-house” developed SAPs were not considered. The production process of such SAPs in this project is still not totally scaled up to an industrial production level, which means that the current costs are considerably higher. Nevertheless, upon scaling up of the production process at industrial scale, the production costs of SAP\_D3.1 are expect to be comparable with those for SAP\_B (€5-10/kg of SAP).

Table 6.6 - Costs to produce wall REF1 and wall W\_SAP1.

Item	Costs (euros)	
	Wall C35/45	Wall C30/37 (SAP1)
Vertical reinforcement	535.33	480.29
Concrete	2423.96	2310
Commercial SAPs	0	204.77
Total	2959.29	2995.06

For the construction of the walls alone, the inclusion of the commercial SAPs represents an increase of 1.21% in the costs, compared to the construction of the wall without SAPs. In terms of long-term performance, given the fact that the SAP walls presented no cracks this increase in the costs might be eliminated considering the savings with maintenance due to repair of cracks. Regarding the maintenance of a cracked tunnel wall, constructed by one of the industrial partners in our study, with similar dimensions and concrete composition to the walls presented in this paper, a cost of approximately 240 euros/m of crack was presented. This cost covers the injection of cracks with a polyurethane resin.

Applying these costs related to a possible injection for the cracks in the wall REF1 (as shown in Figure 6.28) would lead to an additional cost of approximately 1749.60 euros. This would represent a total cost of 4708.89 for the wall REF1, 57% more than the cost for the construction of the wall W\_SAP1.

## 6.4 Conclusions

In this study, superabsorbent polymers have been used in the largest testing campaign to date in Europe. One commercially available SAP and an “in-house” developed SAP constituted with different alkali-(un)stable crosslinkers were studied.

The use of the commercial SAP was intended to promote internal curing in the concrete structure, thus reducing the cracking potential due to early-age shrinkage. The “in-house” developed SAP was initially designed for the promotion of instant sealing of cracks with later enhancement of the self-healing potential of the concrete. The combination of both SAPs was foreseen as the way to build the ideal concrete wall, which would not only possess an internal curing agent for mitigation of shrinkage but also an internal system to enhance the self-sealing/healing of possible occurring cracks.

Throughout the large-scale testing and monitoring campaign, both SAPs have been found to eliminate the cracking potential due to early-age shrinkage in the concrete walls successfully. Those results have been confirmed by monitoring shrinkage in lab specimens. The monitoring revealed that the effects of SAPs are significantly influenced by dimensions of the testing specimen and the external environment, especially when the drying of the concrete surface is more pronounced. The values of shrinkage strain for the SAP-walls were higher than the values of the covered laboratory specimens and lower than the exposed laboratory specimens, but still no cracks occurred. The effect of the environmental conditions could be counteracted with the bulk effect of the large-scale walls, when compared to the small laboratory specimens.

For the large-scale testing, some practical problems had to be tackled. The introduction of SAPs in water-soluble bags on the transportation belt for the solid components towards the mixer showed that the materials could be successfully used without the need for drastic changes in the production process.

With the conclusion of the study, the SAPs (commercially or “in-house” developed) were proven a very promising new admixture for cementitious materials, not only under laboratory conditions, but also in a large-scale real demonstrator case. The inclusion of SAPs promoted a reduction of up to 75% in the shrinkage strain in comparison with a reference mixture without SAPs. That reflected in SAP walls that presented no cracks after eight months of monitoring, while the reference walls without SAPs presented through-going cracks in the first seven days after casting. Even though the potential for self-sealing/healing could not be verified in the SAP walls, this could be considered as the most positive result in our campaign, since the addition of the SAPs eliminated the occurrence of the expected cracks.

## References

1. Van Tittelboom, K., et al., *Comparison of different approaches for self-healing concrete in a large-scale lab test*. Construction and Building Materials, 2016. **107**: p. 125-137.
2. Dudziak L, M.V. *Mitigation of volume changes of ultra-high performance concrete (UHPC) by using super absorbent polymers*. in *Ultra High Perform Concr Second Int Symp Ultra High Perform Concr*. 2008.
3. De Meyst, L., et al., *The Use of Superabsorbent Polymers in High Performance Concrete to Mitigate Autogenous Shrinkage in a Large-Scale Demonstrator*. Sustainability, 2020. **12**(11): p. 4741.
4. C. Zhu, X.L., Y. Xie. *Influence of SAP on the Performance of Concrete and its Application in Chinese Railway Construction*. in *Application of superabsorbent polymers and other new admixtures in concrete construction*. 2014. RILEM Publications.
5. J. Liu, C.Y., X. Shu, Q. Ran, Y. Yang. *Recent advance of chemical admixtures in concrete*. in *15th International Congress on the Chemistry of Cement*. 2019. Prague.
6. Shi, W.-w., et al., *Case study of a SAP-CRC bridge deck in Lu-shan County, Henan, China*. Structural Concrete. **n/a**(n/a).
7. Wyrzykowski, M., et al., *Modeling of water migration during internal curing with superabsorbent polymers*. ASCE Journal of Materials in Civil Engineering, 2012. **24**(8): p. 1006-1016.
8. Trtik, P., et al., *Neutron tomography investigation of water release from superabsorbent polymers in cement paste*, in *International Conference on Material Science*. 2010: Aachen, Germany.
9. Standardisation, N.-B.f., *NBN EN 480-11:2005 - Admixtures for concrete, mortar and grout - Test methods - Part 11: Determination of air void characteristics in hardened concrete*. 2005.
10. Snoeck, D., et al., *X-ray computed microtomography to study autogenous healing of cementitious materials promoted by superabsorbent polymers*. Cement & Concrete Composites, 2016. **65**: p. 83-93.
11. Snoeck, D., L. Pel, and N. De Belie, *Comparison of different techniques to study the nanostructure and the microstructure of cementitious materials with and without superabsorbent polymers*. Construction and Building Materials, 2019. **223**: p. 244-253.
12. Snoeck, D., et al., *Effect of high amounts of superabsorbent polymers and additional water on the workability, microstructure and strength of mortars with a water-to-cement ratio of 0.50*. Construction and Building Materials, 2014. **72**: p. 148-157.
13. Standardisation, N.-B.f., *NBN EN 12350-2 : 2009 - Testing fresh concrete - Part 2: Slump test* 2009.

14. Standardisation, N.-B.f., *NBN EN 12350-7 : 2009 - Testing fresh concrete - Part 7: Air content - Pressure methods*. 2009.
15. Institute, N.-R.N.S., *In-situ floorings - Quality and execution of monolithic screeds and paving*. 2003, NEN - Royal Netherlands Standardization Institute. p. 24.
16. Reinhardt, H.W., C.U. Grosse, and A.T. Herb, *Ultrasonic monitoring of setting and hardening of cement mortar - A new device*. *Materials and Structures*, 2000. **33**(233): p. 581-583.
17. International, A., *ASTM C157 / C157M-17, Standard Test Method for Length Change of Hardened Hydraulic-Cement Mortar and Concrete*. 2017: West Conshohocken.
18. Monnig, S. and P. Lura, *Superabsorbent polymers - An additive to increase the freeze-thaw resistance of high strength concrete*. *Advances in Construction Materials* 2007, 2007: p. 351-358.
19. Reinhardt, H.W., A. Assmann, and S. Monig, *Superabsorbent Polymers (Saps) - an Admixture to Increase the Durability of Concrete*. *Microstructure Related Durability of Cementitious Composites*, Vols 1 and 2, 2008. **61**: p. 313-322.
20. Assmann, A., *Physical properties of concrete modified with superabsorbent polymers*. 2013, University of Stuttgart.
21. Hasholt, M.T., O.M. Jensen, and S. Laustsen, *Superabsorbent Polymers as a Means of Improving Frost Resistance of Concrete*. *Advances in Civil Engineering Materials*, 2015. **4**(1): p. 237-256.
22. J. Piérard, V. Pollet, and N. Cauberg, *Mitigating autogenous shrinkage in HPC by internal curing using superabsorbent polymers*. in *International RILEM Conference on Volume Changes of Hardening Concrete: Testing and Mitigation*. 2006. Lyngby, Denmark: RILEM Publications SARL.
23. Dudziak, L.M., V, *Deliberations on Kinetics of Internal Curing Water Migration and Consumption Based on Experimental Studies on SAP-Enriched UHPC*, in *International RILEM Conference on Use of Superabsorbent Polymers and Other New Additives in Concrete*. 2010, RILEM: Lyngby, Denmark.
24. Rizwan, S.A.M., S.; Ahmed, W, *Mitigation of Early Age Shrinkage in Self-Consolidating Paste Systems Using Superabsorbent Polymers*, in *Materials, System and Structures in Civil Engineering (MSSCE-2016)*. 2016: Lyngby, Denmark. p. 443-453.
25. De Meyst, L., et al., *Parameter Study of Superabsorbent Polymers (SAPs) for Use in Durable Concrete Structures*. *Materials*, 2019. **12**(9).
26. Snoeck, D., L. Pel, and N. De Belie, *Superabsorbent polymers to mitigate plastic drying shrinkage in a cement paste as studied by NMR*. *Cement & Concrete Composites*, 2018. **93**: p. 54-62.



27. Ma, X., et al., *Effects of SAP on the properties and pore structure of high performance cement-based materials*. Construction and Building Materials, 2017. **131**: p. 476-484.
28. Justs, J., et al., *Internal curing by superabsorbent polymers in ultra-high performance concrete*. Cement and Concrete Research, 2015. **76**: p. 82-90.
29. Snoeck, D., et al., *In-situ crosslinking of superabsorbent polymers as external curing layer compared to internal curing to mitigate plastic shrinkage*. Construction and Building Materials, 2020. **262**.
30. Jakobsen, U.H., et al., *Automated air void analysis of hardened concrete - a Round Robin study*. Cement and Concrete Research, 2006. **36**(8): p. 1444-1452.
31. Zhong, P.H., et al., *Internal curing with superabsorbent polymers of different chemical structures*. Cement and Concrete Research, 2019. **123**.
32. Assmann, A. and H.W. Reinhardt, *Tensile creep and shrinkage of SAP modified concrete*. Cement and Concrete Research, 2014. **58**: p. 179-185.

## Chapter 7. Final remarks and recommendations for future research

## 7.1 General conclusions

In this research, different types of superabsorbent polymers were developed and studied aiming at a successful mitigation of shrinkage cracking in concrete mixtures to be used in real-life structures. Four “in-house” developed SAPs based on modified alginates and four also house” developed SAPs based on sulfonates were investigated and their performance in both cement pastes and concrete mixtures were compared to two commercial SAPs based on acrylic-acid. The results of the research program carried out in the laboratory, allowed to select SAPs for the production of five large-scale reinforced concrete walls under realistic conditions. Three of the walls, where SAPs were included in the mixtures, remained crack-free for the complete period of more than eight months. In contrast, in the walls where no SAPs were added, crack formation was identified already five days after casting. From the first characterization of the SAPs in laboratory until their application in the large-scale structures, important advances were achieved. The general conclusions of the research and the contribution to the state-of-the-art of the topic were summarized as answers to following questions:

1. *What was the effect of the chemical composition of SAPs on the shrinkage mitigation, sealing and healing properties of the studied mixtures?*
2. *Is it possible to bring SAPs to real-life applications?*
3. *What are the main advantages of the use of SAPs for cracking control in real-life structures?*

*1. What was the effect of the chemical composition of SAPs on the shrinkage mitigation, sealing and healing properties of the studied mixtures?*

In this research, three different types of SAPs regarding their chemical composition were studied: acrylic acid-, sulfonate- and alginate-based SAPs. The different chemical basis of the SAPs reflected directly in their kinetics of sorption and desorption, which had a clear effect on the various properties of cement pastes and concrete mixtures produced with the SAPs.

Acrylic acid-based SAPs presented an absorption capacity between 20-25 g of mixing water per g of SAP when inserted in cement paste and concrete. This relatively low absorption capacity reduced the absorption of  $\text{Ca}^{2+}$  ions by the SAPs, which is well known to cause the so-called charge-screening effect and strong complexation effect in acrylic acid-based SAPs. The latter results in ionic crosslinking and sudden reduction of the absorption capacity of the SAP, reflected by an intense water release at an early period if a first free swelling occurred. In terms of desorption, these SAPs were found to release the entrained water in a controlled way, around the final setting of the mixtures. The combination of low absorption capacity and controlled water release resulted in a complete mitigation of autogenous shrinkage in both cement pastes and concrete mixtures tested under laboratory conditions, with a limited negative impact on the compressive strength of the mixtures. At the age of 28 days, up to 20% reduction was found in comparison to a reference mixture with the same effective water-to-cement ratio, and no reduction or even a slight increase of 7% in compressive strength in comparison to a reference mixture with the same total water-to-cement ratio.

Four SAPs based on sulfonate-chemistry were investigated: 1) a combination of the co-monomers NaAMPS (2-acrylamido-2-methyl-1-propanesulfonic acid sodium salt) and SVS (sodium vinyl sulfonate); 2) and 3) mainly consisting of co-monomer NaAMPS, 'diluted' with different amounts of a non-charged or neutral monomer ACMO (acryloyl morpholino acrylate); 4) a SAP solely composed of monomer NaAMPS. The modification of the latter, however, is defined by the use of a second alkali-unstable crosslinker. One of the main differences between this group of SAPs and the acrylic acid-based SAPs is that sulfonate-based SAPs are less influenced by complexation with  $\text{Ca}^{2+}$ , which means that they are

less susceptible to further crosslinking. In addition, both co-monomers (NaAMPS and SVS) contain the sodium salt form of a sulfonic acid group, which leads to a very densely charged hydrogel with great osmotic power for absorbing water. This was reflected by a considerable high absorption capacity of types 1), 2) and 3) both in cement paste and concrete (up to 180 g/g of mixing water for type 1 and 50 g/g of mixing water for types 2 and 3). For the specific case of type 4, a much lower initial swelling degree was obtained (up to 13 g/g of mixing water in cement paste and concrete, and 40 g/g in demineralized water), which was achieved thanks to the presence of the second and alkali-unstable crosslinker. However, once the compound has been put in the alkali environment of the cementitious materials for a few hours/days, the crosslinks that are constituted by the second crosslinker are hydrolyzed and the swelling potential of the SAP becomes much greater again *in situ* (values up to 135 g/g in demineralized water were obtained after a exposure of 72 h in cement filtrate solution).

Despite some differences in initial absorption capacity, all sulfonate-based SAPs showed an intense water release. When added to cement pastes and concrete, that resulted in need of a higher dosage of SAPs and additional water to promote a complete mitigation of shrinkage, which caused large reduction in compressive strength. At the age of 28 days, up to 43% reduction was found, for example, for SAP type 2 compared to a reference with the same effective water-to-cement ratio. In the case of the type 4 SAP, even though a complete mitigation of autogenous shrinkage was not achieved in laboratory specimens, an expressive and consistent reduction of strain was obtained, which was found to be enough to avoid shrinkage cracks in the testing walls, as will be pointed out in the next topics. The low initial absorption capacity of this SAP with a further increase upon the hydrolysis of the alkali-unstable crosslinker enabled the use of a higher amount of these SAPs with the same amount of additional water as for other mixtures with commercial SAPs. That resulted in a very similar impact on the compressive strength of the concrete mixtures. At 28 days, a reduction of around 20% in comparison to the reference concrete strength was found with the same effective water-to-cement ratio, and no reduction compared to the reference concrete with the same total water-to-cement ratio. Additionally, when used for the sealing of cracked specimens, this SAP promoted a reduction

of 72% in the water permeability in comparison to a cracked reference concrete without SAPs. In contrast, one of the commercial SAPs promoted a reduction of only 45% in the water flow through the cracked surface, when compared to the control mixture. In terms of impact on the strength, the two SAPs promoted the same level of reduction in compressive strength in comparison to the reference. To increase the sealing effect of the mixture with the commercial SAP, a higher amount of SAPs would be required. If additional water would be also added to compensate for the loss in workability caused by the addition of SAPs, a further reduction on strength would follow. That highlights the main advantages of the innovative sulfonate-based SAP with the double crosslinking.

As for the alginate-based SAPs, four different compositions were tested. The amount of gel fraction and the ratio between modified alginates and acrylic acid were varied. None of the variations was found to promote significant changes in the performance of the SAPs. The use of modified alginates is reported in literature as an alternative to the use of other types of SAPs due to a less intense impact on the mechanical properties of the mixtures. That was indeed observed in this research when alginate-based SAPs were used in cement pastes. A reduction of around 10% in the compressive strength at 28 days was found in comparison to a reference mixture with the same effective water-to-cement ratio. Comparatively, the use of commercial SAPs in cement pastes with the same total water-to-cement ratio as the ones with alginate-based SAPs promoted a reduction of 20% in the compressive strength of the mixtures at 28 days. That lower reduction is mainly associated with the significantly lower absorption capacity of the alginate-based SAPs. In cement pastes, values between 7-10 g/g of mixing water were obtained, in comparison to up to 20 g/g of mixing water for the commercial SAPs, and even 180 g/g of mixing water for one of the sulfonate-based SAPs. In contrast, the weak retention capacity of these SAPs was found to be not beneficial for the mitigation of autogenous shrinkage. All mixtures produced with these SAPs behaved almost in the same way as a reference mixture without SAPs and same amount of water. In demineralized water, the absorption capacity of the alginate SAPs was 30 g/g. That amount of absorption also represents a limiting factor for the use of this type of SAP for sealing, since

the particle size of the swollen SAPs would also be considerably limited. Depending on the particle size distribution chosen in the dry state of the SAP, a high dosage would be required for an efficient sealing of a certain crack width range.

## *2. Is it possible to bring SAPs to real-life applications?*

Based on the laboratory tests, optimum dosages of SAPs were found considering complete mitigation of autogenous shrinkage and maximum sealing effect, in combination with a minimum impact on the compressive strength. One of the commercial SAPs and the double crosslinked sulfonate-based SAPs were chosen to be applied in the construction of the large-scale walls. The first question raised referred to how to insert the SAPs in a large-scale concrete-plant mixer. That had to be executed without significant changes to the mixing protocols adopted by the ready-mix factory. Additionally, the SAPs should be protected from external moisture to avoid swelling before a proper dispersion of the SAP particles in the mixture occurred. The solution for that was found with the use of water soluble-bags. The SAPs were divided in limited portions amounting to 2 kg per bag and transported together with the aggregates on a moving belt. That approach was found to promote a better dispersion of the SAP particles in the mixture, which resulted in a better promotion of internal curing, in comparison to the inclusion of the SAPs in the concrete truck after the initial mixing.

Once the walls were constructed, the monitoring of shrinkage deformations represented another practical challenge. A manual method using demountable strain gauges (DEMEC) was used to monitor the shrinkage between reference points glued on the surface of the walls. Additionally, optical fiber sensors were embedded in the concrete, attached to the steel reinforcement. Both methods showed a very similar trend for the performance of the mixtures: where SAPs were added, a considerably lower shrinkage strain was recorded, especially during the first 7 days. Even though a mitigation of the total shrinkage was not obtained, the reduction of autogenous shrinkage was enough to limit the strain in the concrete at early ages. That resulted in the absence of cracks in the SAP-modified walls over the complete monitoring period of eight months, while both walls where no SAPs were added started to crack already five days after casting. The use of the DEMECs was proven to be quite easy and straightforward, and also resulted in a reliable method to

describe the evolution of shrinkage strain in a comparative way amongst the different concrete mixtures. However, the execution of the method can be quite time consuming and more affected by thermal effects on the surface of the structure due to ambient sunlight directly on the walls. Alternatively, with the use of the optical fiber sensors a considerable amount of time can be saved, since the measurements are performed, stored automatically by a reading unit located on site which led to a continuous monitoring of the walls. With the embedded sensors, the monitoring of the deformation can start as soon as the concrete is poured and that allows a more precise interpretation of the results, following the moment when the autogenous strain starts to be measured.

Another important factor with practical implications that needs to be highlighted is the compliance of SAP-modified concrete with existing models for prediction of strength. In this research, even with a very complex system for the development of strength in SAP-modified concrete, that is highly dependable on the kinetics of water release and a balance between internal curing and formation of macro pores, the concrete mixtures produced with the addition of SAPs were found to comply to a high extent with the model proposed in the Eurocode2 for prediction of strength at different ages based on the characteristic strength of the concrete at 28 days of age.

### *3. What are the main advantages of the use of SAPs for cracking control in real-life structures?*

Throughout the research, the SAPs were found to be very versatile materials, which is something not commonly found for the current admixtures commercially available for the cement/concrete industry. Besides promoting internal curing and reducing the risk of cracking due to shrinkage, the SAPs in this research were found to also promote significant sealing and increase in the resistance against salt scaling under freeze-thawing cycles with deicing salts. All of those features were achieved with a limited negative impact on the mechanical properties of the concrete mixtures.

Two other very important benefits were obtained as a consequence of the shrinkage reduction promoted by the SAPs: 1) with no cracks developing in the period up to eight months, no indication of corrosion was identified in the SAP-modified wall monitored with multi-reference electrodes embedded in the concrete. In contrast, a corrosion potential



was measured in two locations near a crack in the reference wall, approximately six months after casting; 2) the walls where SAPs were added were constructed with 10% less reinforcement, used as shrinkage reinforcement, than the reference wall without SAPs. Still, no cracks were formed. This already represents a reduction of costs and environmental impacts related to the production of steel, next to the durability-related advantages of using the SAP mixture. One of the objectives of this study was to use SAPs to reduce the observed cracking in the walls by 50%. Instead, 100% was achieved. That is an encouraging evidence that a further reduction in the shrinkage reinforcement could be possible.

In terms of costs, the production of the SAP-modified walls represented an increase of 1.2% in comparison to a wall without SAPs. This cost is mainly due to the production of the SAPs (which amounts to 5-8 €/kg for commercial SAPs). However, by considering the cost for repairing future repair of cracks, saving of up to 58% could be achieved with the use of SAPs. This was estimated considering a specific repair based on the injection of cracks with a polyurethane resin and currently prevailing prices in Belgium.

To conclude, this research presented solid evidence that SAPs are suitable for the production of large-scale structural elements under realistic conditions in order to mitigate autogenous shrinkage and to show a subsequent possibility for sealing and healing of occurring cracks. A multitude of benefits can be achieved in terms of performance of the concrete mixture with a limited and controllable range of negative effects. The results presented in the thesis represent an important contribution to pave the way of SAPs towards the market. Additionally, they highlight the possibilities that can be achieved with fine-tuning of properties of in-house developed SAPs, that can be designed for very specific applications.

## 7.2 Prospects for future research

A few important aspects of the development of concrete mixtures with SAPs were not reported in this thesis. Three of them can be highlighted:

1. The impact of SAPs on the service life of concrete regarding carbonation and chloride ingress is currently under study in the framework of the iSAP project and should provide a valuable contribution to the current state-of-the-art. Not many studies have been developed on this topic and the few that are found in literature indicate that the addition of SAPs might increase the ingress of chlorides and the rate of carbonation, mainly due to a higher porosity caused by the macro-pore formation after water release by the SAPs;
2. The quantification of environmental impact of the use of SAPs in the production of concrete mixtures for structural application is currently being investigated in the framework of another project (SMARTINCS – Smart, Multi-functional, Advanced Repair Technologies In Cementitious Systems) by means of a life-cycle assessment of the walls studied in the iSAP project.
3. The effects of SAPs on the development of strength of concrete mixtures deserves special attention. In that regard, future research is needed correlating the water release by different types of SAPs and its effects on the degree of hydration and the formation of macro-porosity linked to strength development of the cementitious matrix. This could provide knowledge for the modification of current prediction models, enabling a more accurate prediction of strength at different ages and limitation of negative effects on strength. This is a key-factor to facilitate the acceptance of SAP-modified concrete by the industry.



## Curriculum vitae

### Personal Information

---

Name	José Roberto Tenório Filho
Date of birth	March 10 <sup>th</sup> 1992
Place of birth	Arapiraca – Alagoas – Brazil
Nationality	Brazilian
Contact	Roberto.Tenorio@UGent.be (jr.roberto@hotmail.com)

### Education

---

2018 – 2021	<p>Doctorate (PhD) in Civil Engineering Faculty of Engineering and Architecture at Ghent University</p> <p>Thesis: Innovative superabsorbent polymers (iSAP) for crack mitigation of concrete structures: from laboratory to construction site</p>
2011 – 2017	<p>Bachelor in Civil Engineering Technology Center at Federal University of Alagoas</p> <p><i>Exchange Student (2015-2016) – Science without Borders Program Faculty of Engineering and Architecture at Ghent University</i></p> <p>Thesis: Rheological characterization of cement pastes and mortars containing waste of marble and granite</p>
2007 – 2010	<p>Technical degree in Buildings Construction Federal Institute for Education, Science and Technology</p> <p>Final project: Topographic survey for road renovation with asphalt paving</p>

**Scientific prizes**

---

- 2020      Best Pitch Presentation - RILEM PhD Workshop
- 2017      Best paper of the category “scientific work with technological innovation” – VIII Alagoano Symposium of Civil Engineering
- 2014      Best paper of the category “Civil construction and building materials” – VIII Conference of Engineering, Science and Technology
- 2012      Best paper of the category “Civil construction and building materials” – VI Conference of Engineering, Science and Technology
- Best paper of the category “Scientific work with technological innovation” – VIII Alagoano Symposium of Civil Engineering
- Academic excellence award in the category “Civil Engineering” - Program for junior researchers (PIBIC) of the Federal University of Alagoas

**Scientific publications**

---

*A1 publications*

- Tenório Filho, J. R., Vermoesen, E., Mannekens, E., Van Tittelboom, K., Van Vlierberghe, S., De Belie, N., & Snoeck, D. (2021). Enhanced durability performance of cracked and uncracked concrete by means of smart in-house developed superabsorbent polymers with alkali-stable and -unstable crosslinkers. *Construction and Building Materials*, p. 123812.
- Tenório Filho, J. R.; Mannekens, E. ; Tittelboom, K. V. ; Vlierberghe, S. V.; De Belie, Nele ; Snoeck, Didier. Innovative SuperAbsorbent Polymers (iSAPs) to construct crack-free reinforced concrete walls: an in-field large-scale testing campaign. *Journal of Building Engineering*, p. 102639, 2021.
- Mechtcherine, V.; Wyrzykowski, M.; Schrofl, C.; Snoeck, D.; Lura, P.; Belie, N.; Mignon, A.; Vlierberghe, S. V.; Klemm, A. J.; Almeida, F.; Tenório Filho, José R.; Boshoff, W. P.; Reinhardt, H.; Igarashi, S. Application of super absorbent polymers (SAP) in concrete construction update

of RILEM state-of-the-art report. *Materials and Structures (ONLINE)*, v. 54, p. 80, 2021.

Tenório Filho, José Roberto; Mannekens, E.; Tittelboom, K. V.; Snoeck, D.; De Belie, N. Assessment of the potential of superabsorbent polymers as internal curing agents in concrete by means of optical fiber sensors. *Construction and Building Materials*, v. 238, p. 117751, 2020.

Tenório Filho, José R.; Snoeck, Didier; De Belie, Nele. Mixing protocols for plant-scale production of concrete with superabsorbent polymers. *Structural Concrete (London. Online)*, v. 21, p. suco.201900443, 2020.

Meyst, L.; Kheir, J.; Tenório Filho, José R.; Tittelboom, K. V.; Belie, N. The Use of Superabsorbent Polymers in High Performance Concrete to Mitigate Autogenous Shrinkage in a Large-Scale Demonstrator. *Sustainability*, v. 12, p. 4741, 2020.

Tenório Filho, José R.; Miranda, L. R. M.; Melo, Karoline A.; Gomes, P. C. C.; Uchoa, S. B. B. Development of a novel viscosity modifier agent for cementitious materials: preliminary study. *Journal of Materials in Civil Engineering*, v. 33, p. 06021001, 2020.

Tenório Filho, José Roberto; Araujo, M. A. P. G.; Snoeck, D.; De Belie, N. Discussing Different Approaches for the Time-Zero as Start for Autogenous Shrinkage in Cement Pastes Containing Superabsorbent Polymers. *Materials*, v. 12, p. 2962, 2019.

#### *A2 publications*

Tenório Filho, J. R.; Lima, S. F. C. Construções penais e o diálogo com a cidade: a (não) política de implantação de equipamentos penais no meio urbano. *URBE. Revista Brasileira de Gestão Urbana*, v. -, p. ---, 2018.

Tenório Filho, J. R.; Melo, Karoline A. Brazilian waste: an alternative in the production of self-compacting concrete (SCC). *BFT INTERNATIONAL Concrete Plant Precast Technology*, v. 48, p. 61-65, 2017.

*Publications in Conferences*

- Tenório Filho, J. R., Snoeck, D., & De Belie, N. Superabsorbent polymers for smart and durable concrete structures. In 2nd SARCOS PhD & ECI Meeting, Abstracts. Guimaraes, Portugal. 2020
- Tenório Filho, J. R., Mannekens, E., Snoeck, D., & De Belie, N. Salt-scaling resistance of SAP-modified concrete under freeze-thaw cycles. Presented at the RILEM Spring Convention, Guimarães, Portugal. 2020
- Tenório Filho, J. R., Snoeck, D., & De Belie, N. Monitoring the early-age shrinkage cracking of concrete with superabsorbent polymers by means of optical fiber (SOFO) sensors. XV International Conference on Durability of Building Materials and Components, (DBMC 2020), Barcelona, Spain. 2020
- Tenório Filho, J. R., Pereira Gomes de Araújo, M. A., Snoeck, D., Mannekens, E., & De Belie, N. Exploring different choices of “time zero” in the autogenous shrinkage deformation of cement pastes containing superabsorbent polymers. 3rd International Conference on the Application of Superabsorbent Polymers (SAP) and Other New Admixtures Towards Smart Concrete. Skukuza, South Africa. 2019
- Tenório Filho, J. R., Mannekens, E., Snoeck, D., & De Belie, N. Investigating the efficiency of “in-house” produced hydrogels as internal curing agents in cement pastes. 2nd International Conference on Sustainable Building Materials. Eindhoven, The Netherlands. 2019
- Kheir, J., De Meyst, L., Tenório Filho, J. R., Hammer, T. A., Klausen, A., Hilloulou, B., De Belie, N. Impact of super absorbent polymers on early age behavior of ultra-high performance concrete walls. Durable Concrete for Infrastructure under Severe Conditions: Smart Admixtures, self-responsiveness and nano-additions. Ghent, Belgium. 2019.
- Holanda, L. M. A. P. ; Tenório Filho, José Roberto; Weber, A. O. S. Desempenho acústico de diferentes técnicas construtivas de sistemas de vedação vertical interna de edificações habitacionais ? estudo de caso. In: XVII Encontro Nacional de Tecnologia do Ambiente Construído, 2018, Foz do Iguaçu.

- Tenório Filho, José Roberto; Snoeck, D.; Belie, N. The effect of superabsorbent polymers on the cracking behavior due to autogenous shrinkage of cement-based materials. In: 60 Congresso Brasileiro do Concreto, 2018, Foz do Iguaçu, Brazil. 2018.
- Lima, M. P.; Tenório Filho, José Roberto. Previsão probabilística com uso do software COMREL para vida útil de estruturas de concreto armado submetidas a carbonatação. Anais do XI Congresso de Engenharia, Ciência e Tecnologia - CONECTE, 2018.
- Lima, M. P.; Tenório Filho, José Roberto. A qualidade do controle tecnológico do concreto em obras de maceió: avaliação a partir dos resultados de rompimento de corpos de prova. Anais do XI Congresso de Engenharia, Ciência e Tecnologia - CONECTE, 2018.
- Tenório Filho, J. R.; Carvalho, B. I. S.; Tenorio, J. R. P.; Marques, G. B. Desempenho ambiental de uma estrutura de concreto com diferentes composições - avaliação de ciclo de vida com o software SIMAPRO. VIII Simpósio Alagoano de Engenharia Civil, SAEC 2017.
- Tenório Filho, J. R.; Mendes, E. L. S.; Melo, Karoline A. Study of mix design parameters for self- compacting concrete based on the rheological characterization of cement based mortars. Proceedings of the 25th Conference on Rheology of Building Materials. Hamburg: Tredition GmbH, 2016. p. 329-338.
- Tenório Filho, J. R.; Cavalcante, A. F. ; Menezes, G. C. B. ; Silva, L. Y. L. ; Amorim, R. P. ; Weber, A. O. S. Considerações sobre Durabilidade e Manutenção de Edificações no Campus A. C. Simões. In: IX Congresso de Engenharia, Ciência e Tecnologia - CONECTE 2015, Maceió.
- Tenório Filho, J. R.; Lima, S. F. C. Utilização de sistema pré-fabricado em concreto para construção de estabelecimentos penais. Anais do VIII Congresso de Engenharia, Ciência e Tecnologia - CONECTE, 2014.
- Tenório Filho, J. R.; Melo, Karoline A. Estudo de parâmetros de dosagens para concretos autoadensáveis a partir da definição de parâmetros reológicos de pastas e argamassas. Anais do VIII Congresso de Engenharia, Ciência e Tecnologia - CONECTE, 2014.



Tenório Filho, J. R.; Mendes, E. L. S.; Melo, Karoline A.; Gomes, P. C. C. Avaliação de propriedades reológicas de pastas cimentíceas contendo metacaulim visando a produção de concretos com diferentes consistências. Anais do VII Congresso de Engenharia, Ciência e Tecnologia - CONECTE, 2013.

Lopes, J. F. B.; Tenório Filho, J. R.; Miranda, L. R. M.; Uchoa, S. B. B.; Tonholo, J. Caracterização reológica de pastas e argamassas com a presença de uma composição polimérica usada como modificadora de viscosidade. Anais do VII Congresso de Engenharia, Ciência e Tecnologia - CONECTE, 2013.

Tenório Filho, J. R.; Melo, Karoline A. . Produção de concretos com adição de resíduo de beneficiamento de mármore e granito a partir de parâmetros reológicos de pastas e argamassas. In: VI Congresso de Engenharia, Ciência e Tecnologia - CONECTE, 2012, Maceió.

Tenório Filho, J. R.; Souza, J. R. F ; Melo, Karoline A. . Definição de Parâmetros Reológicos de Pastas e Argamassas. In: 54° Congresso Brasileiro do Concreto, 2012, Maceió. Anais do 54° Congresso Brasileiro do Concreto, 2012.

#### *Patent registration*

Uchoa, S. B. B.; Tonholo, J.; Gomes, P. C. C.; Melo, Karoline A.; Lisboa, E. M.; Miranda, L. R. M.; Tenório Filho, J. R. Composição para concreto auto-adensável e agente modificador de viscosidade. (2015). Registrado no INPI – Instituto Nacional de Propriedade Industrial. BR102015011030. Tipo de patente: privilégio de inovação. Pedido depositado em 27/04/2015.





Crack-free reinforced concrete walls built with superabsorbent polymers.